UNIVERSITAT DE BARCELONA

Epigenetic Mechanisms in Monocyte-Associated Differentation and Inflammation Processes

Roser Vento Tormo

UNIVERSITAT DE BARCELONA

EPIGENETIC MECHANISMS IN MONOCYTE-ASSOCIATED DIFFERENTIATION AND INFLAMMATION PROCESSES

PhD Thesis

Roser Vento Tormo

IDIBELL
Institut d'Investigació Biomèdica de Bellvitge

PEBC
Cancer Epigenetics and Biology Program
Programa d'Epigenètica i Biologia del Càncer
Programa de Epigenética y Biología del Cáncer

UNIVERSITAT DE BARCELONA

EPIGENETIC MECHANISMS IN MONOCYTE-ASSOCIATED DIFFERENTIATION AND INFLAMMATION PROCESSES

Memoria presentada por Roser Vento Tormo para optar al grado de Doctor en Biomedicina por la Universidad de Barcelona

UNIVERSIDAD DE BARCELONA – FACULTAD DE MEDICINA

PROGRAMA DE DOCTORADO EN BIOMEDICINA

Este trabajo ha sido realizado en el Grupo de Cromatina y Enfermedad del Programa de Epigenética y Biología del Cáncer (PEBC) del Institut d' Investigaciò Biomédica de Bellvitge (IDIBELL)

Dr. Esteban Ballestar
Director

Roser Vento Tormo
Doctoranda

"Perquè viure és combatre la peresa
de cada instant i restablir la fonda
dimensió de tota cosa dita,
podem amb cada gest guanyar nous àmbits
i amb cada mot acréixer l'esperança."

Miquel Martí i Pol.
(Primer llibre de Bloomsbury)

A casa sempre ens han ensenyat a ser agraïts a les oportunitats que ens dóna la vida, perquè tot allò que vivim ens fa aprendre i créixer. En aquest cas, a més he tingut la fortuna de conviure amb gent magnífica i viure experiències increïbles, així que en més raó estic molt agraïda a tot el que ha envoltat aquesta tesi doctoral.

En primer lloc voldria donar-li les gràcies a **l'Esteban** per haver-me donat l'oportunitat de formar part del seu equip de treball. Li agraïsc el vot de confiança que ha depositat amb mi a nivell científic, fent possible abordar projectes en els quals hem gaudit i après moltíssim. Així mateix li estic molt agraïda en l'àmbit personal per la seua disponibilitat a l'hora de dedicar temps i esforços en ajudar a resoldre assumptes que queden una mica més allunyats de l'àmbit professional. L'Esteban a més té la capacitat de saber formar molts bons equips de treball i li estic molt agraïda pel fet que m'haja assignat la Damiana com la meua companya de treball.

La **Damiana** per mi ha significat molt més que una guia científica, ja que he après tant d'ella que podria dir-se que ha imprintat en mi la seua forma de fer ciència, de discutir-la i inclús de llegir i escriure-la. La curiositat amb què et comenta els projectes et desperta la motivació, i la serenitat amb què rep les teues paraules la creativitat. He de dir que he tingut la sort que totes les qualitats que té de científica les té també com a amiga. Gràcies.

I si alguna cosa significa Barcelona per mi és el **Javi**. Ambdós plegats hem rigut, plorat, espantat i gaudit junts però sobretot hem après a viure disfrutant del plaer de les petites coses. I el que més em sorprèn és que per molt que passe el temps, cada dia aprenc alguna cosa nova d'ell. A més de ser una persona immillorable el Javi és un científic increïble. No puc evitar recordar l'època on Javi era l'únic post-doc del laboratori i cuidava de tots els que començàvem de nou. Sempre treia per tots nosaltres una estoneta per discutir del nostre projecte, veient un blanc on nosaltres veiem negre, i fent-nos preguntes i aportacions perquè arribarem a ser bones científiques.

A la resta del grup també li estic molt agraïda, ja que fan possible que cada dia siga millor que l'anterior. **Al Lluís, l'autor de la portada,** al qual jo sempre he admirat la seua creativitat i coneixement. No tinc cap dubte que pot arribar on es propose, i ànims en tot bonic. Al **Nono** qui a més de ser l'eficiència personificada, sempre està disposat a tirar-te una maneta. Malgrat que fa poc de temps que viu a Barcelona, ja s'ha fet tan important a la nostra vida, que els caps de setmana que està fora, sempre notes que et falta alguna cosa. A la **Laura** amb la qui ha sigut un plaer poder haver coincidit des de que vaig començar la tesi. És d'aquestes persones essencials als laboratoris i que tenim la sort de tindre al PEBC7: organitzada, alegre, pendent de tot el que ens falta als altres i sempre contenta de poder ajudar els altres. A la **Natalia,** que és

una persona super endreçada, constant i treballadora, i estic segura que li anirà molt bé en el seu futur. Al **Xec**, del qui no només he tingut la sort de seure al costat de la bancada durant un temps, sinó que a més a més m'ha ensenyat Menorca per primera vegada. I ja per fi a la **Tian**, amb la qual sols he pogut coincidir unes poques setmanes, però que han sigut suficients per veure que li anirà genial al lab.

M'agradaria també agrair de forma àmplia a tota aquella gent que ha format part del laboratori i que he tingut la sort de poder coincidir amb ells. A la **Virgi,** qui durant molt de temps va ser la persona amb la qui vaig seure al costat de la bancada, la qual cosa em va permetre conèixer molt millor les virtuós que la caracteritzaven: eficient, alegre, organitzada,... Li estic especialment agraïda perquè malgrat que esta super ocupada, durant aquest temps, m'ha ajudat moltíssim amb tots els tràmits i formats de la tesis. Al **Loren** (qui estic segura que també somnia amb els burritos de la Virgi..) i qui va ser durant gran part de la tesis company d'ordinador, la qual cosa ens va permetre establir una relació super propera que encara mantenim. Ha segut clau en aquesta tesis, puix encara recorde les seues paraules d'ànim "de predoc a predoc" que et feien no baixar la guardia en temps difícils, i els dinars plens de rises d'eixos que et fan botar les llàgrimes. Tampoc m'oblide de l'**Henar**, qui va ser la meua primera mestra al lab i la qual em va cuidar moltíssim durant els meus inicis tant dins com a fora del lab. Et trobem en falta! La **Biola**, amb la qui vaig coincidir amb el meu inici just quan ella acabava, però que sempre ha estat i segueix estant disposada a ajudar-me en tot. I per últim la **Marina** amb la qual vaig coincidir molt poc però que em va semblar una molt bona persona.

A l'**Olga**, la **Maribel**, l'**Alba** i el **Quim**, amb els qui tenim el plaer de compartir l'espai del PEBC7 amb ells, i els quals sempre estan disposats a tirar-nos una maneta i a compartir un somriure amb nosaltres. Amb l'**Olga**, així com la **Lidia** i la **Bruna**, vaig poder tindre la sort de compartir la seua amistat fora del laboratori, i recorde amb molta alegria les excursions a la muntanya que solíem fer així com els sopars que fèiem tots junts.

I com el laboratori no acaba en el PEBC7 voldria aprofitar per agrair a totes les persones que formen el PEBC en general. Molt especialment a **la Vicky**, la qual és d'aquestes persones que a poc a poc es van fent essencials en la teua vida i en les que saps que estant elles mai et sentiras sola. També als currantes i fixos de plantilla del cap de setmana, l'**Humberto**, l'**Adrià**, l'**Angel**, el **Miguel**, la **Laia**,... els quals fan que inclou els caps de setmana siga divertit treballar al PEBC.

Aprofite també per donar les gràcies a l'**Alex**, qui junt amb la Virgi, m'han fet el favor d'actuar com a infermers per poder recuperar mostres, i sempre sempre amb bona cara. Alex, que la "pipiolilla" presenta la tesis! Com passà el temps... I pensant en el temps passat voldria també agrair al **Salva**. Amb ell vaig aprendre a superar els meus propis límits i pors, van ser uns anys molt divertits, els quals compartits amb **Jose, Ainara** i **Carlos** els van convertir amb excepcionals.

A la gent del PEBC3 i del PEBC4 (**Laia, Anna, Núria, Esther, Manu**,...) també els hi tinc molta estima, amb moltes persones dels quals he tingut l'oportunitat de disfrutar de la meravella de la natura. I a la **Paloma** i a la **Laura B.** que encara que ja no estan al laboratori sempre recordaré les seues festes de disfresses, la seua disponibilitat a l'hora de regalar-te el seu temps i el seu somriure sempre pegat a la cara.

Molt especialment també voldria agrair al **Fer**, que és el rei del clonatge i de cultius, i del qual he tingut el plaer de compartir la seua saviesa i bona voluntat per tot, siga l'hora i la situació que siga. També a la **Paula**, la **Càtia,** la **Raquel** i l'**Anna**, amb l'alegria que les caracteritza i la bondat per ajudar-te. El mateix dic per al **Sebas** i per a **Toni,** l'ajuda bioinformàtica/genòmica dels quals ha sigut imprescindible al llarg d'aquesta tesis. I el **Mario** i la **Rut**, amb els qui vaig tindre la sort de compartir uns meravellosos dies en el darrer congrés a Cambridge.

A **Carmen** que per mi, per la seua energia , força de voluntat i alegria, sempre serà un exemple a seguir. I al **Carles**, l'expert de les pyros que tenim la sort de tindre al costat del laboratori.

A més del PEBC, he tingut la sort de tindre els millors companys de pis que mai hi haguera imaginat. Així "la Cueva" va ser més que una casa, va significar un conjunt d'experiències i diversions irrepetibles, a casa tothom era benvingut. Recorde les festes dels dissabtes nits plens de gent que sempre acabaven en una timbrada dels veïns i amb els quals l'**Amanda** amb el seu somriure ens enlluernava a tots, els dinars del mon dels diumenges en els que **Bea** ens ensenyava a cuinar o els moments sofà amb els que l'**Helena** ens cosia els calcetins. Molt especialment agraïsc a la **Carla** tots aquests anys compartits juntes. Amb ella he compartit aficions, maneres de pensar, i sobretot molts somriures. Moltes gràcies per estar present en els moments més complicats, i ànims bonica, tu eres la pròxima! També al **Javi L**., el qual era una alegria tindre'l a casa i com amic, perque sempre era capaç de furtar-te un somriure fóra quin fóra el teu estat.

També agraÏsc a la **Dani**, perquè “no és més gran qui més ocupa sinó qui més buit deixa quan se’n va”. Que agust vam estar juntes i quina llàstima que vas haver de tornar a Costa-Rica. Espere que pogam coincidir prompte de nou. I al **Couso**, el qual tinc la sort de poder veure amb freqüència pel barri, i quedar amb ell sempre alegra.

A la **Núria**, sense les nostres converses la tesis haguera sigut molt més complicada. Gràcies per ensenyar-me a viure. I l’ **Andrew**, el qual em recorda el que a vegades oblidem “la vida és curta i cal aprofitar el moment”

A les **meues amigues del poble**. Perquè per moltes voltes que donen les situacions, i sent que cada una estem repartides per una part del món al final tot comença acaba amb elles, i així ha segut a la tesi. Tot va començar amb una festa sorpresa de comiat plena de llàgrimes (puix totes sabíem que ja mai més podríem quedar per un cervesa ràpida després d’un dia fatal) i acabarà en un cap de setmana genial de festa de tesis a Barcelona.

I deixe pel final les persones que segurament més s’ho mereixen a la meua família i el meu company. A la **mare** i al **pare**, no hi ha dia que passe que no pense en vosaltres, i si alguna cosa és dura per mi en la recerca és això, no tindre-us a prop. Vosaltres meu ensenyat a potenciar totes les meues virtuds que he necessitat amb aquesta tesis: la perceverança quan un resultat no surt, la paciència de l’espera, la sol.lidaritat amb els companys per ajudar i deixar-se ajudar, i la passió pel coneixement. Al meu “tete” **Miquel**, al qui per mi és un exemple a seguir per la seua bondat, intel·ligència i alegria. Gràcies per dedicar-me tantes hores en tot el que t’he anat demanat i per la teua empatia. I a la meua **tia** Dolo, a qui dedique aquesta tesi i esforç. És admirable la força i positivis-me que tens, tenim molt que aprendre de tu. Molts ànims, estic segura que amb aquesta actitud tot anirà de categoria, i més peque ací estem tots per donar-te suport, igual que fas tu constantment amb nosaltres.

Al **Carles** amb el qui tinc la sort de compartir aquest camí. Sense cap dubte estar amb tu és la decisió més encertada que he pogut prendre mai. T’estic molt agraïda per la teua paciència durant aquests mesos d’incertesa, perquè sempre facilites les coses i m’ajudes amb tot el que està al teu abast. I perquè ara entenc que voler és inclús més bonic que ser volgut. I res, ara sols queda preparar amb il·lusió el nostre viatge. Gràcies de tot cor perquè amb tu res és impossible

INDEX

FIGURE INDEX

SUMMARY

Innate immune responses represent the first barrier of defence when a pathogen enters the organism. Innate immune cells are crucial in the inflammatory response as they are able to destroy pathogens by themselves, as well as attract and activate a specific and tailored adaptive response. The most abundant type of innate immune cells is the mononuclear phagocyte system, which is comprised of monocytes (MOs), macrophages (MACs), dendritic cells (DCs) and their progenitors. MACs are tissue resident cells with high phagocytic capacity, whereas DCs are cells with elevated mobility and ability to stimulate and prime naïve T cells. During inflammation, MOs represent an extra source of DCs and MACs, which guarantees defence against external and internal insults. MOs not only have a role as a reservoir of cells, but they also have an exclusive function in innate immunity as shown by their own capacity to secrete autoinflammatory cytokines.

The identity of diverse cells of the immune system relies on different transcriptional programs triggered by the activation of a broad diversity of transcription factors and the epigenetic landscape. The sets of transcription factors and upstream signalling pathways implicated in MO-to-DC and -MAC differentiation have been studied in depth. However, little is known about the mechanisms that dictate the acquisition of epigenetic changes during differentiation in these cell types. Terminal differentiation from MOs-to-DCs, MO-to-MACs, and other related cell types like osteoclasts (OCs), constitutes ideal biological models employed to investigate the mechanisms by which extracellular stimulation is translated into nuclear epigenetic control.

This doctoral thesis focuses on the study of the epigenetic mechanisms involved in different MO-associated differentiation and inflammation processes. We have described the molecular sequential events that lead to changes in the pattern of DNA methylation, as well as their significance in the context of inflammation.

Firstly, we have performed high-throughput DNA methylation in MO-to-DC and MO-to-MAC differentiation and in DC and MAC maturation following bacterial lipopolysaccharide (LPS) stimulation. Extensive loss of DNA methylation occurs in both MO-to-MAC and MO-to-DC differentiation processes, whereas only few genes vary their methylation status following LPS treatment (maturation level). More interestingly, genes that are essential for cell identity were differentially methylated between MO-to-DC and MO-to-MAC differentiation, in turn, indicating a possible role of methylation in cell fate determination. Since DC and MAC differentiation differ

from each other by the addition of IL-4 in the former, we tracked the JAK3-STAT6 pathway downstream to IL-4. We proved that JAK3/STAT6 axis was the main pathway responsible for orchestrating changes in genes exclusively DNA demethylated in one of the differentiation process via a mechanism dependent of TET2 (the enzyme involved in active DNA methylation). All of these results demonstrate for the first time the cytokine-mediated downstream sequence of events leading to direct gene-specific demethylation in differentiation of innate immune cells.

Detailed analysis of function of the demethylated genes in MO-to-MAC differentiation revealed the presence of a subset of genes related to inflammasome function, an essential cellular complex during inflammation. In our work, we have demonstrated that DNA demethylation of several inflammasome-related genes takes place during MO-to-MAC differentiation and MO activation, and that in both cases, DNA methylation is controlled by the Nuclear Factor Kappa B (NF-kB) pathway. Our study also shows increased DNA demethylation of those inflammasome-related genes *in vitro* activated or differentiated MOs from autoinflammatory disease patients (CAPS and FMF). Overall, these results reveal a potential, new mechanism by which the regulation of inflammasome function is altered in those CAPS and FMF patients.

Despite the fact that MO-to-DC and MO-to-MAC differentiation are mainly associated with DNA demethylation, we have identified the acquisition of *de novo* DNA methylation in a few genes in both MO differentiation processes. We have demonstrated that for such genes, gene expression occurs before gain of DNA methylation; and inhibition of DNMT3b, an enzyme involved in *de novo* DNA methylation, does not have effects on gene expression. However, DNMT3b inhibition causes a loss of surface DC markers, which highlights a role of *de novo* DNA methylation in gene expression stabilization needed for a proper phenotype acquisition.

Finally, in order to gain insight into alternative epigenetic regulatory mechanisms underlying myeloid differentiation, we have characterised miRNA changes in MO-to- DC, MO-to-MAC, and MO-to-OC differentiation. We have demonstrated that two miRNAs clusters become upregulated in an NF-kB dependent manner, specifically the miR-212/132 and miR99b/let-7e/125a clusters. The miRNAs in these clusters are able to cause the specific downregulation of lineage inappropriate genes, and such inhibition is essential for proper differentiation process for MACs,DCs and OCs.

ABBREVIATIONS

5-aza-dC	5-aza-2'-deoxycytidine
5caC	5-carboxylcytosine
5fC	5-formylcytosine
5hmC	5-hydroxymethylcytosine
5hmU	5-hydroxymethyluracil
5mC	5-methylcytosine
AD	Active Demethylation
AD-AR	Active Demethylation Active Restoration
AD-PD	Active Demethylation Passive Dilution
AGO	Argonaute
AIM2	Absent in melanoma 2
ALR	AIM2-like receptor
ASC	Apoptosis-associated speck-like protein, also called PYCARD
BM	Bone Marrow
BP	Base pair
BS	Bisulphite
C/EBP	CCAAT/enhancer binding protein
CAPS	Cryopirin-associated periodic syndromes
CARD	Caspase activation and recruitment domain
CASP-1	Caspase-1
cDC	Classical Dendritic Cell
CDP	Common DC Progenitor
CGI	CpG Island
ChIP	Chromatin immunoprecipitation
CINCA/NOMID	Multisystem inflammatory disease
CLP	Common Lymphoid Progenitor
cMoP	Committed Monocyte Progenitor
CMP	Common Myeloid Progenitor
DAMP	Damage Associated Molecular Pattern
DBD	DNA-binding domain
DC	Dendritic cell
DNMT	DNA methyltransferase

ERK	Extracellular signal regulated kinase
FCAS	Familial cold-induced autoinflammatory syndrome
FMF	Familial Mediterranean fever
GATA1	GATA-binding protein 1
GFI1	Growth-factor independent 1
GM-CSF	Granulocyte-Macrophage Colony-Stimulating factor
GMP	Granulocyte Macrophage Progenitor
HAT	Histone acetyltransferase
HDAC	Histone deacetylase
HDM	Histone demethylase
HMT	Histone methyltransferase
HSC	Haematopoietic Stem Cells
IL	Interleukin
JAK	Janus Kinase
JMJD3	Jumonji domain-containing 3
JNK	c Jun N terminal kinase
LC	Langerhans cells
LPS	Lypopolysaccharide
M1	Classically Activated Macrophages
M2	Alternatively Activated Macrophages
MAC	Macrophages
MAPK	Ras-mitogen-associated protein kinase
M-CSF	Macrophage Colony-Stimulating Factor 1
MDP	Common Macrophage Dendritic Cell Progenitor
MHC	Major Histocompatibility Complex
miRNA	microRNA
MO	Monocyte
MPP	Multipotent Progenitor
MWS	Muckle-Wells syndrome
NF-kB	Nuclear Factor Kappa B
NLR	NOD-like receptor
OC	Osteoclast
PAMP	Pathogen-Associated Molecular Patterns
pDCs	Plasmacytoid dendritic cells

PI3K	Phophoinositol 3-kinase
PRR	Pattern Recognition Receptors
RANKL	Receptor activator of nuclear factor kappa-B ligand
RISC	RNA-induced silencing complex
RUNX1	Runt-related transcription factor 1
TAL1	Stem-cell leukemia factor
TF	Transcription factor
TLRs	Toll-Like Receptors
TNF	Tumour necrosis factor
TSS	Transcription Start Site
Tyr	Tyrosine
UTR	Untranslated region

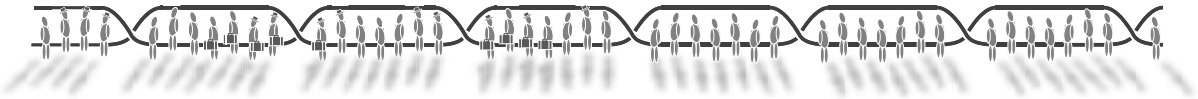

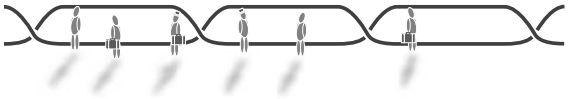

INTRODUCTION

1 INTRODUCTION

1.1 The Hematopoietic System

Haematopoiesis is the formation of blood cells, including all cellular components of the immune system and is dynamic both in time and space during vertebrate development. A first wave of haematopoiesis occurs during embryonic development, creating primitive nucleated red blood cells that are able to provide oxygen to the embryo. However, not all different adult blood populations are generated during this first developmental stage, and a second independent hematopoietic wave appears within the formation of the embryo. During this second definitive haematopoiesis, which is maintained in the bone marrow during its entire life, haematopoietic stem cells (HSCs) are able to create the different blood cell types. [1]

HSCs are multipotent cells with self-renewal capacity that are sustained at nearly constant levels in an adult. HSCs are a heterogeneous cell population, and distinct subpopulations of HSCs have recently been described to be located in different specialised niches in the bone marrow (BM). Those niches supply the environmental conditions for the proper development of particular kinds of stem cell and progenitors. [2]

To produce mature blood cells, HSCs progress into sequential steps where they lose pluripotency and self-renewal capacity as they gain in specialisation. In the first stage, HSCs differentiate into multipotent progenitors (MPPs) that retain the pluripotency of HSCs but diminish their self-renewal characteristics. Secondly, committed progenitors with decreasing pluripotency appear, dividing the immune system into two main branches: the lymphoid and the myeloid lineage. Lymphoid cells, such as B and T lymphocytes, come from a common lymphoid progenitor (CLP), whereas the majority of myeloid cells (including monocytes (MOs) and macrophages (MACs)) are derived from a common myeloid progenitor (CMP). A third progenitor that is able to produce different populations of dendritic cells (DCs) has also been characterised (CDP from common DC progenitor) [3]

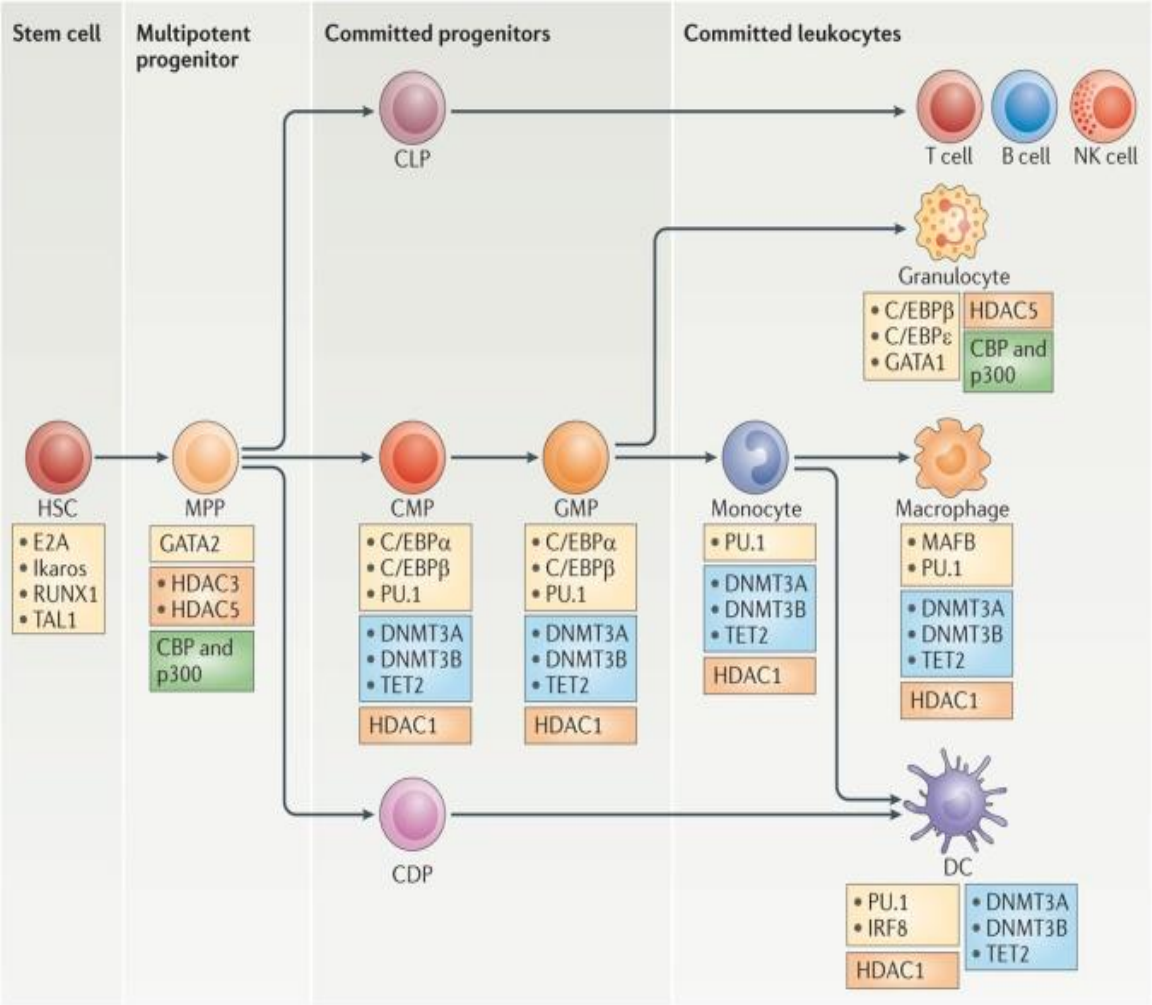

Figure 1-1 Transcription factors and epigenetic regulators of hematopoietic cell differentiation. This figure shows the main stages of hematopoietic differentiation, with special emphasis in the myeloid branch (in the central horizontal axis), indicating the key transcription factors (yellow boxes) and epigenetic enzymes that could be involved at each stage. Enzymes that participate in DNA demethyation events are shown in blue boxes, histone deacetylases are shown in orange boxes, and histone acetyltransferases are shown in green boxes.

1.1.1 The Innate and Adaptive immune response

The coordinated action of lineage-determining transcription factors (TF) together with the epigenetic machinery, allows the establishment of highly differentiated hematopoietic lineages that orchestrate immune responses. The myeloid branch comprises cells such as MOs, MACs or granulocytes mainly involved in the innate immune responses, whereas, the lymphoid branch includes lymphocytes that undergo clonal expansion and are responsible for adaptive immunity.

The innate immune system assumes the first cellular response against pathogens once chemical and physical barriers are exceeded. There are three scenarios in which the innate immune system is triggered, all of which are identified in terms of recognition: recognition of "microbial nonself", recognition of "missing self" and recognition of "induced or altered self".

The "microbial nonself" strategy consists of the host's ability to recognise conserved molecular patterns that are essential products of microbial physiology and that are not produced by the host. These prototype structures are referred to as pathogen-associated molecular patterns (PAMPs). We need to bear in mind that in spite of their name, these structures are also present in non-pathogenic microorganisms. The innate immune cells sensors for such structures are called pattern recognition receptors (PRR) and can be secreted, transmembrane and cytosolic. A good illustration of the innate immune system specific recognition machinery is the Toll-like receptors family (TLRs) [4,5]. TLRs are a family of transmembrane PRRs activated by different external signals that switch on several internal signalling pathways of the host cell, including those pathways that activate TF like CREB or Nuclear Factor Kappa B (NF-Kb). On the other hand, the "missing self" approach relies on the detection of markers of normal cells that are able to inhibit the activation of the immune response. For example, natural killer cells eliminate cells expressing low quantity of Major Histocompatibility Complec (MHC)-I due to viral infection or cancer transformation, functioning as a signal of cell lysis under these circumstances [6]. The last recognition approach is the "recognition of induced self", which comprises the elimination of the cells by the recognition of markers of abnormal self that are induced upon infection and cellular transformation. Endogenous stress signals detected as risk alarm are called damage-associated molecular patterns (DAMPs). An example of DAMP is the ATP when is located in the extracellular space due to a catastrophic disruption of the cell [7]

Once the insult is recognized by the innate immune system, innate immune effector cells are activated. Innate immune effector cells involved in different responses with a high range of specificity are found: from cells able to destroy pathogens by phagocytosis (such as neutrophils or MACs) to cells like basophils, involved in the facilitation of the transmigration of immune cells by affecting vascular cells. Natural killer and MACs are specialized in secreting cytokines with the capacity to attract other immune cell types and to stimulate the cellular immune innate response. Plasmatic proteins (also known as acute phase proteins) are mainly produced in the liver and attracted to the inflammation site. These molecules include complement proteins and single antimicrobial molecules (such as the C-reactive protein), that are activated by interaction with microbes and are able to turn on immune innate effector cells. This inflammatory environment also triggers the activation of the adaptive immune system by DCs in the majority of cases. DCs are cells of the innate immune system attracted to areas of inflammation and specialized in the phagocytosis of the pathogen and their presentation and subsequent activation of the lymphocytes. DCs bridge both the innate and adaptive immune

system, as they are cells from the innate immune system able to activate the most specialized, antigen specific and effective responses mediated by the adaptive immune system.

In order to present antigens to the adaptive immune system, DCs evolve from immature antigen-capturing cells to mature antigen-presenting cells. During DC maturation, DCs convert antigens into immunogens to be presented, and express molecules such as cytokines, chemokines, costimulatory molecules, and proteases needed to initiate the adaptive immune response. As DCs mature, they acquire the properties necessary to form and transport peptide-loaded MHC class II complexes to the cell surface[8], a process which coincides with increased expression of costimulatory molecules, such as B7-1/CD80 and B7-2/CD86. Mature DCs also have the capacity to present antigens through MHC-I, a phenomena called cross-presentation.

The adaptive immune response includes the production of antibodies by B lymphocytes and the generation of specific T cell clones, which are responsible for the direct destruction of cells infected by the antigen and the activation of cells involved in this purpose. The required diversity of B lymphocytes and T cell clones is produced during lymphocyte maturation. The ability to display antigen-specific responses depends on the process of somatic recombination, which is also known as V(D)J recombination [9]. Somatic recombination refers to the process of DNA recombination whereby the functional genes that encode for each antigen-specific receptor are built (BCR and TCR for B and T cells, respectively). This rearrangement generates a high repertoire of B and T clones with unique antigen-receptor that are able to react specifically to a wide variety of insults. In subsequent steps of B and T cell maturation, only those lymphocytes whose receptors bind to high affinity to the major histocompatibility complex (MHC) will remain through positive selection; in addition, potentially autoreactive lymphocyte clones will be removed by negative selection. In B cells, the affinity and specificity is improved after the contact of the insult via the processes of Class Switch Recombination (CSR) and Somatic Hypermutation (SHM).

B and T cells present immunological memory, which means that an initial response to a specific pathogen brings about an enhanced response in subsequent encounters with the same insult. The adaptive memory is created due to the production and expansion of specific B and T cells clones after antigen recognition by specific T and B cell receptors in an adequate context. These cell clones are called B and T memory cells and are stored in the body until a future contact with the aggressor, triggering a faster and more efficient response. Adaptive memory guarantees lifelong protection to re-infection with the same pathogen due to a rapid clonal expansion of the memory T and/or B cells. [10]

Adaptive immunity involves strong, highly specific and long-term responses, and their activation must be finely regulated. To ensure the action of adaptive responses only when they are strictly necessary, antigen presentation by DCs needs to occur in the context of inflammation, as only in those conditions the costimulatory molecules are expressed. Conversely, when antigen presentation is achieved in the steady-state conditions, DCs remain inactive (without expressing costimulatory molecules) which might lead to T cell anergy and tolerance [11].

To ensure the action of adaptive responses only when they are strictly necessary, a complex network of TFs act together at different stages. Decisions depend on the context where they are taken, so the contribution of epigenetic factors acquire more relevance.

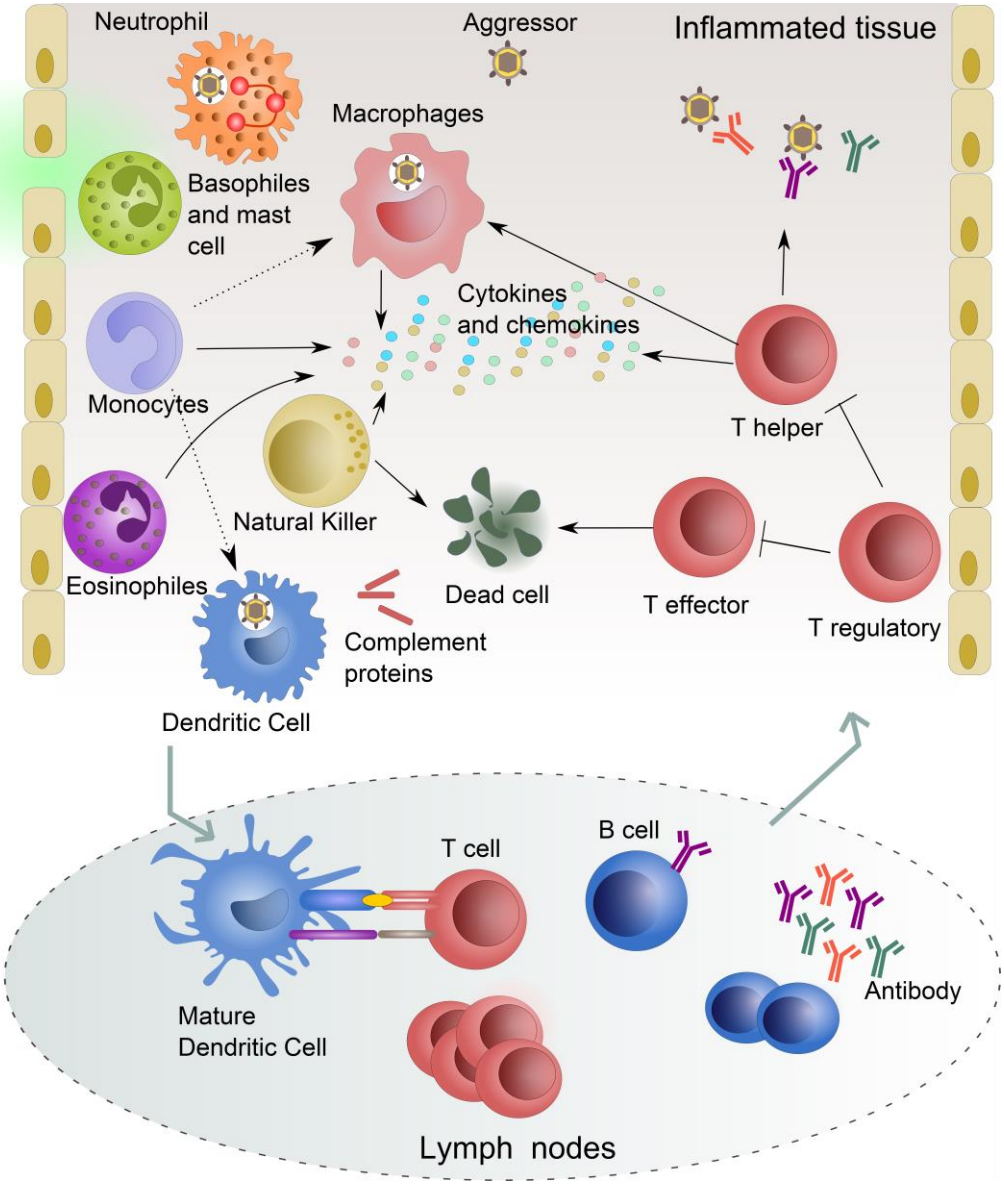

Figure 1-2 Response of the Immune System against pathogen infection
Innate immune responses are the first barrier against an insult. Innate effector cells are able to phagocyte the antigen, eliminate dysfunctional cells, and secrete cytokines and chemokines, which attract and activate other innate immune cells. In this way, inflammation is initiated (left panel) and plasmatic components such as complement proteins are activated. DCs activated in the inflammatory context are able to migrate to lymph nodes where they present the antigen to the B and T lymphoid cells, triggering the specific adaptive responses mediated by them (middle panel). B lymphocytes are responsible for producing antibodies that bind and neutralise the antigen. In turn, T lymphocytes bind in a specific way to the antigen and are in charge for orchestrating the immune responses by activating other cells of the immune system (T helper) or to direct killing of infected or damaged cells (T effector). Another subset, the regulatory T-cells, are able to maintain immune homeostasis via inhibition of differentiation and activity of pro-inflammatory T helper cells (right panel).

1.1.2 The mononuclear phagocyte system

The myeloid lineage comprises innate immune cells such as mast cells, MOs, phagocytes (MACs, neutrophils and DCs), basophils and eosinophils. A very dynamic and plastic group of cells in this lineage is represented by the mononuclear phagocyte system, which includes MOs, DCs and MACs.

1.1.2.1 Monocytes

MOs represent 10% of the nucleated cells in blood, with considerable marginal pools in the spleen and lungs that can be mobilised on demand [12,13]. Blood MOs (especially the classical subset of $CD14^+$ cells) present a short half-life of approximately 20 hours[14] and have been considered for years as a transient precursor reservoir for tissue-resident mononuclear phagocytes. Investigations into mononuclear phagocytes over the last decade have allowed us to see MOs not only as a source of MACs and DCs, but also as cells that present functional diversity and play a critical role in pathogen defence and inflammatory diseases.

As part of the granulocyte-MAC lineage, MOs originate from bone marrow CMPs that are able to differentiate afterwards into the granulocyte MAC progenitor (GMP). They subsequently differentiate into the common MAC DC progenitor (MDP) and ultimately turn into the committed MO progenitor (cMOP). [15] Under inflammatory conditions, an extra-source of MOs might be needed and, in this case, the spleen is the organ responsible for supplying MO precursors. [16]

Although several transitional states of MOs have been reported [17], human MOs have been divided classically into two main subpopulations: $CD14^+$ MOs (which can be further subdivided into distinct populations differentiated by the expression of CD16) and $CD14^{low}CD16^+$ MOs. Human $CD14^+$ cells represent “classical MOs”, that migrate to sites of inflammation where they act as a precursors to peripheral mononuclear phagocytes [17]. Human $CD14^+$ cells resemble $Ly6C^{hi}$ inflammatory murine MOs [18]. By contrast, “patrolling MOs” defined in mice as $Ly6C^{low}$ are

equivalent to human $CD14^{low}CD16^{+}$ MOs and are involved in surveying endothelial integrity [19,20]. The origin of $CD14^{low}$ cells in steady state conditions seems to be the $CD14^{+}$ MOs, which under several environmental signals differentiate from classical to patrolling MOs. Indeed, there are some authors who consider $CD14^{low}$ cells as terminally differentiated blood-resident MACs rather than bona fide MOs [21].

Under inflammatory conditions, an extra supply of MOs is needed for a proper response, with elevated MO egress from the BM into the circulation, in a way that is dependent on the binding of the CC-chemokine receptor 2 (CCR2) to their ligands (CCL2, CCL7 and CCL8) [22]. Once in circulation, the function of inflammatory MOs remains poorly defined but is probably related to their high phagocytic capacity, as well as their ability to readily access all organism and tissues.

MOs are able to detect the microbial-derived products and respond by expressing microbicide molecules, and to secrete proinflammatory cytokines (in particular tumor necrosis factor (TNF)-alpha, IL-1, IL-18, IL-12) and chemokines (CCL3, CXCL9) that swiftly activate innate immune responses [23]. Moreover, in inflamed tissues, MOs orchestrate the host's antimicrobial protective responses through the differentiation into MACs and DCs [23].

1.1.2.2 Dendritic Cells

DCs are BM-derived cells specialized in antigen presentation that are found in the blood, lymphoid, interstitial, and epithelial tissues. DCs express the machinery necessary to detect potential pathogenic molecules and process them into short pieces called antigens that fit the MHC cleft and could then be presented to lymphocytes to establish an Ag-specific response. DCs bridge the initial recognition of antigens with the specific cell- and antibody mediated clearance, hence being able to direct the type, magnitude, and specificity of the immune response.

DCs were originally identified by Steinman and Cohn for their unique stellate morphology, their capacity to attach to surfaces, and their superior capacity to prime naïve T lymphocytes, which is what distinguished them from MACs[24,25]. Nowadays, DCs are still defined by their great capacity to migrate from non-lymphoid organs and to activate naïve T cell response, as well as for their high expression of MHCII and the integrin CD11c[26]. In the majority of cases, this definition is appropriate to define DCs as a new lineage. Nevertheless, some cells acquire characteristics from other lineages during inflammation, which makes immunologists reconsider the exclusive identity of the DC[27]. For example, the function of DCs is very heterogeneous and not limited to presenting antigens to T cells, as DCs can also activate adaptive responses by releasing cytokines, such as IL-12[28,29].

To solve the problem of DC classification, some researchers support the hypothesis that DCs, together with MACs and MOs, should be classified according to their ontogeny, since exclusive precursors for each cell type have been defined [30–32]. As established by the classical DC development diagram, MOs and DCs are generated by the MDP progenitor that give rise to common DC progenitors that are restricted to the production of the main DCs subsets [named classical DCs (cDCs) and plasmacytoid DCs (pDCs)]. cDCs arise from intermediate progenitors, which exist in the BM and migrate through the blood towards peripheral tissues where they complete differentiation, whereas pDCs terminally differentiate in the BM.

The cDCs are short half-lived (approximately 3-5 days) cells with an enhanced ability to sense tissue injuries, capture environmental- and cell-associated antigens, process them, and present phagocytosed antigens to T lymphocytes. In humans, cDCs are divided into CD141hi DCs, which resemble murine CD8+/CD103+ DCs, and CD1c+ DCs whose murine counterparts are defined by a CD11b+ marker expression. CD141hi DCs are functionally specialised in activating through the MHC class I receptor the CD8+ T cells, that is the T cell subset involved in destroying infected or malignant cells[33]. On the other hand, the CD1c+ DCs seems to be involved in naïve CD4+ T priming [34], that is the T cell subset involved in the regulation of immune responses by suppressing or promoting some immune responses.

In turn, pDCs have a variety of proinflammatory and tolerogenic functions. In particular, pDCs have specialised in releasing type 1 interferons in response to viruses [35], following activation through nucleic acid-sensing TLRs, such as TLR7 and TLR9. Without stimulation, pDCs seems to be tolerogenic and are implicated in inducing T-cell anergy and promoting regulatory T-cell development [36].

Under steady state situations, the main function of a DC is to phagocytose while maintaining their ability to present antigens to T cells. However, due to the lack of a coactivator expression, antigen presentation by steady-state DCs might lead to T cell unresponsiveness and might promote tolerance in the absence of co-activation [37]. This scenario completely changes under inflammatory conditions: after a transient increase in antigen-uptake, changes in endosomal trafficking and antigen processing lead to increased presentation. Along with an upregulation of co-stimulatory molecules, this results in efficient T-cell stimulation. Moreover, during inflammation, MOs might be a source of DCs with inflammation-prone nature, creating so-called inflammatory DC (infDCs).

InfDCs differentiate from MOs during inflammation[38] and are characterised by their ability to prime T cells and to migrate from tissues to lymph nodes using the chemokine CC

receptor (CCR)7-dependent [38]. The type of T cell response that they induce (which can be either a CD4+ or CD8+ response) appear to be plastic and depends on the inflammatory environment and type of infection[38–41]. Moreover, infDCs have also been shown to stimulate effector or memory T cells locally in the inflamed tissue [42]. Although the vast majority of studies have been performed in murine models, the human counterpart of infDCs has been identified in pathological inflammatory diseases, such as arthritis, and in tumour ascites[43].

1.1.2.3 Macrophages

MACs are a heterogeneous population of phagocytic mononuclear cells of the immune system with a dual role in the induction and resolution of inflammation. In tissues, MACs are organised into defined patterns with each cell occupying its own territory, a type of tissue within a tissue. Their response would acquire a lower or higher inflammatory shade depending on the MAC context and tissue.

Élie Metchnikoff discovered MACs in the 19th century from his observations of phagocytosis during tissue inflammation [44]. In the 1960s, van Furth proposed that all tissue MACs were originated from circulating adult blood MO terminal differentiation in both, steady state and inflammation[45]. Although there was some evidence that tissue MACs are independent of circulating MOs[46,47] it was not until recently that many resident tissue MACs were demonstrated to have an embryonic root [48,49]

To date, it is accepted that despite the diverse origins of tissue-specific MACs populations in adults, the majority of tissue-resident MACs have embryonic progenitors in steady-state conditions [50]. This is the case of brain microglia cells that are derived from yolk sac MAC progenitor cells, which suggest an embryonic hematopoietic wave before the development of HSCs that give rise to definitive haematopoiesis in an adult [48]. Unlike the brain, which exclusively contains yolk sac-derived microglia, other tissues such as alveolar and cardiac MACs include discrete MAC populations with mixed ontological origins [51,52]. On the other hand, in tissues such as the intestine or the skin, there is a high dependence on MOs as a source for MACs. Not surprisingly, those tissues are constantly in contact with microorganisms derived products. Some authors propose that in these tissues exist what they called a prime homeostasis [53] which means a constant presence of commensal microorganisms that may be causing low-grade chronic inflammation. In contrast to steady state, MO contribution to MAC differentiation is sharply increased under inflammatory conditions [21] .

Additionally, MACs may also give rise to another identical cell type and the proliferation of MACs is indispensable for sustaining MAC numbers under homeostatic conditions as well as

their replenishment after a severe depletion [54]. This phenomenon of MAC expansion increases under stress and shifting conditions, like in atherosclerosis [55], and also in some non-pathological conditions, such as in wound healing of skeletal muscle [48,56]

MACs have been categorised into classically activated (or M1) and alternatively activated cells (or M2), depending on the conditions of their activation state. M1 MACs are associated with pro-inflammatory situations, as they develop in response to pattern-recognition receptors from bacteria and viruses that allow them to secrete high amounts of proinflammatory cytokines, such as TNFα or other molecules like nitric oxide. Conversely, M2 MACs develop in response to type 2-associated immune mediators (such as interleukin-4 (IL-4) and IL-13), and are implicated in responses to parasitic infection, tissue remodelling, angiogenesis and tumour progression through the production of anti-inflammatory cytokines or the immunosuppressive enzyme arginase 1 [57].

Despite the well-defined dual behaviour of MACs generated *in vitro*, this nomenclature is too simplistic when applied to the range of MACs generated in vivo and MACs develop high-range transition states between M1 and M2 phenotypes when residing in a tissue [58,59]. Future approaches addressing changes at the single cell level would allow to characterise these populations in more detail.

1.1.2.4 Monocyte-derived differentiation processes.

Terminal differentiation from MOs to DCs, MACs, and other related cell types, such as osteoclasts (OCs), represent excellent models to investigate the dynamics during terminal myeloid differentiation given the difficulty of isolating some of the human myeloid precursors.

DC differentiation from peripheral human MO takes place following exposure of MO to Granulocyte-Macrophage Colony-Stimulating factor (GM-CSF) and IL-4. In contrast to mice, in humans, the presence of IL-4 during the DC production is crucial for a proper differentiation from MOs[60]. The addition of both factors to the medium is enough to activate the pathways that are able to produce a DC immature phenotype, which is usually activated by adding lipopolysaccharide (LPS) to the media, recapitulating the gram-negative infection bacteria.

In the case of MO to MAC differentiation in humans, the Macrophage Colony-Stimulating Factor 1 (M-CSF) is the classically employed cytokine. Once MACs are differentiated, their polarisation can be induced by incubating cells with molecules that are able to induce TLRs signalling, such as LPS, or by culturing cells in the presence of cytokines such as IL-4, IL-13, IL-10 or transforming growth factor-β, among others[61]. MAC differentiation from MOs in humans can also be stimulated in the presence of GM-CSF, exhibiting in this case an amplified response

similar to M1 polarizing stimuli. GM-CSF treated cells that are stimulated afterwards with LPS or/and IFNγ produce high levels of proinflammatory cytokines such as IL-23, IL-12, TNF, IL-1β and IL-6 [62].

Another MO-derived differentiation process is *in vitro* osteoclastogenesis. OCs are cells of haematopoietic origin that are uniquely specialised in bone destruction, playing in bone dynamics under physiological conditions. This differentiation process is exacerbated in the context of rheumatoid arthritis and in bone metastasis. Osteoclastogenesis pathway depends on M-CSF and receptor activator of nuclear factor κB ligand (RANKL), which can be used to *in vitro* induce OCs from peripheral blood MOs [63].

Finally, MOs can also become activated acquiring an inflammatory phenotype. In this case, several stimuli that engage TLRs or IL-1R (such as LPS or IL-1β) trigger the release of some inflammatory cytokines [64].

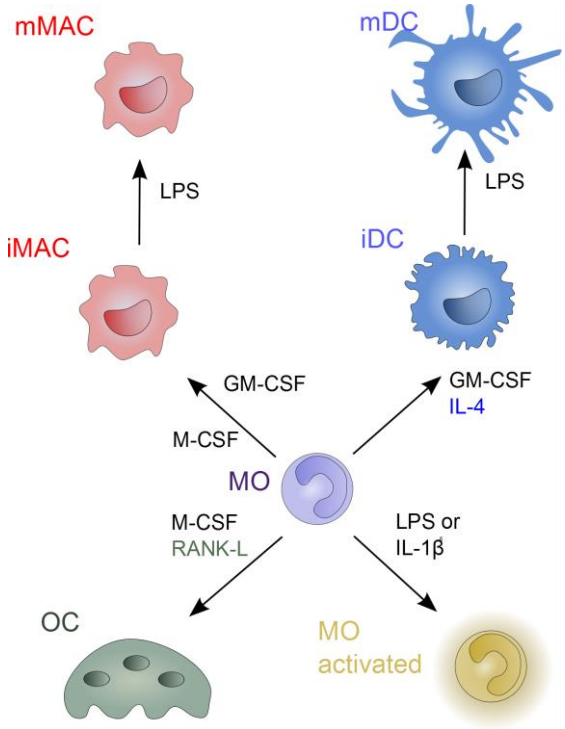

Figure 1-3 MO-related differentiation and inflammation processes *in vitro*.
Freshly isolated MOs from blood donors, can be *in vitro* differentiated to MACs and DCs by adding GM-CSF (or M-CSF) or GM-CSF + IL-4 respectively. What is notable here is how only the presence of one cytokine (IL-4) is able to produce two cellular types with specific functions. Both cellular types (MACs and DCs) are activated via TLR4, which is mediated by LPS. Another inflammatory cell type involved in bone degradation, the OCs, can also be derived from MOs *in vitro* with the addition of M-CSF and RANK-L. On the other hand, MOs activated phenotype characterised by the activity of the inflammasome and the cytokine secretion is produced by LPS or IL-1B addition to the media for 24h.

1.2 Gene regulation in myeloid differentiation and function

During hematopoietic differentiation, cells regulate their genetic information in a very specific and timely manner to guarantee a correct stepwise differentiation from progenitors in the BM to fully differentiated cells in circulation and tissues. This control of gene expression depends on the interplay between TFs and other ways of control like epigenetic regulation and post-transcriptional control mechanisms (such as non-coding RNAs).

1.2.1 Transcription Factors

TFs are nuclear proteins that generally bind to specific DNA sequences controlling the rate of transcription of DNA to mRNA. While some TFs bind to DNA promoter sequences and help to form the transcription initiation complex, other TFs bind other regulatory sequences, such as enhancers, and can modulate the transcription of the related gene. By contrast to promoter regions which are localized subsequently to transcription start site (TSS), enhancers can be situated thousands of base pairs (bp) upstream or downstream from the TSS of the gene being transcribed. TFs have been classically classified in different classes and families following their sequence similarity and the tertiary structure of their DNA-binding domains (DBD) (table 1.1) [65,66,67].

Table 1-1

Rank denomination	Definition	Example
Superclass	General topology of the DBD	Helix-turn-helix domains (Superclass 3)
Class	Structural blueprint of the DBD	Tryptophan cluster factors (Class 3.5)
Family	Sequence and functional similarities	Ets-related factors (Family 3.5.2)
Subfamily	Sequence-based subgroupings	Sp1-like factors (subfamily 3.5.2.5)
Genus	TF gene	PU.1 (Spi-1) (Genus 3.5.2.5.1)

Table 1-1 Hierarchical TF classification.
Five-level taxonomy of TF comprising the ranks superclass, class, family, subfamily and genus based on the TFClass online tool [66,67]. An example of PU.1 classification is shown.

Interestingly, it is also possible for the same DNA sequence to be bound by more than one factor, and those factors binding the same DNA sequence do not necessarily share a common DBD. For instance the TFs CTF/NFI and C/EBP (CCAAT/enhancer binding protein) both bind to the CAAT box sequence, however they achieve binding via completely different DBDs, with C/EBP having a basic DBD and CTF/NFI has a DBD distinct from that of any other factor [68].

In order for TFs to regulate transcription, they must interact with other factors or with the RNA polymerase itself, thus establishing multiprotein complexes that can influence transcription

either positively or negatively. Indeed, in some cases, TF do not bind directly to the DNA, but instead, act through the interaction with other TF [69]

Activation of gene expression by TFs can occur at different levels of transcription process to stimulate transcription. For example, activating factors can disrupt chromatin structure to allow other activating factors to bind, stimulate the rate of transcriptional initiation so that more RNA transcripts are initiated, and can also stimulate transcriptional elongation. These processes can be combined together in different ways. [70] Furthermore, although many TFs act in a positive manner, TFs can also exert inhibitory effect on transcription initiation. This effect can occur by indirect repression in which the repressor interferes with the action of an activating factor, so preventing it to stimulate transcription. Alternatively, it can occur via direct repression in which the factor reduces the activity of the basal transcriptional complex. As with transcriptional activation, transcriptional repression can also occur via the alteration of chromatin structure or at the level of transcriptional elongation[70].Moreover, two positive factors can also repress one another if they compete for the same co-factor. In some cases, one TF can be activator or inhibitor depending on the context, a mechanism that may occur through the TF interaction with different chromatin remodeling activator and/or repressor chromatin remodeling proteins [71].

TFs play a central role in a number of biological processes producing, for example, the induction of specific genes in response to particular stimuli as well as controlling the cell type specific regulated expression of genes that give rise to cellular identity during differentiation. Regulation of TF can occur either controlling the synthesis of the TF or regulating the activity of the factor only when required. Modulating the activity of TF is a rapid and flexible mean of regulate a particular factor, thus allowing a direct linkage between the inducing stimulus and the activation of the factor. One example of the activation of a TF by a biological stimulus is the activation of p65 subunit of the NF-kB complex by the LPS, produced by its dissociation from IkB and its subsequent phosphorylation.

1.2.1.1 Transcription factors in Myeloid Identity, Function and Ontogeny

The formation of myeloid cells is orchestrated by a highly regulated network of TFs, which mediate the activation and repression of different set of genes through the different steps of myelopoiesis, and the subsequent establishment of the different myeloid lineages. Among the most relevant TFs stands PU-1 [72], CCAAT/enhancer binding proteins (in particular C/EBPα, C/EBPβ and C/EBPγ) [73–75], growth-factor independent 1 (GFI1) [76], and interferon-regulatory factor 8 (IRF8) [77], and, at the stem-cell level, runx-related TF 1 (RUNX1) [78] and stem-cell leukemia factor (TAL1) [79], as well as other factors, including JUNB, Ikaros and MYC [80–82].

PU.1 is one of the TFs with more relevance during myeloid differentiation that, as shown in Table 1, is a member of the large ETS family whose expression is restricted to blood cells, and is essential for phagocyte system cells. PU.1 is activated by the major MO/MAC lineage regulator CSF-1R in MO and MACs, and the PU.1 relevance in those cells is illustrated by the fact that its deletion in mice results in a deficiency of all subtypes of MACs, as well as MO alterations [49]. PU.1 is also relevant during DCs commitment, which is reflected by the observation that transgenic mice with PU.1-deficient hematopoietic cells have fewer CD11b+ and CD8+ cDCs than those reconstituted with wild-type BM.

In both MACs and DCs, PU.1 is not the only relevant TF in cellular commitment, and other TF, such as MAFB[83] as well as other members of the ETS family (*Ets2*) are also involved in MAC differentiation. On the other hand, Ikaros and STAT families, are examples of TF responsible for DC commitment [84–8687].

The diversity of MACs and DCs is also reflected in the fact that different subsets of MAC/DCs depend on the use of different TFs. In this line, TFs such as Gata6 and Spi-c, seem key in defining several subsets of MAC with a different range of unique activities [88,89]. Moreover, MAC polarization is also determined by a different subset of TFs. For example, STAT1 is an essential mediator of M1 MAC polarization in the presence of IFNγ [57]. By contrast, STAT6 is required to drive M2 MAC activation during T_H2 cell-mediated immune responses in the presence of IL-4 and/or IL-13[57].

There is also a high spectrum of TFs that are specific of each DC subset. For example, it is possible to distinguish pDCs from cDCs in this way: the dependence on pDCs in the E2-2 TF occurs during the development of pDCs but not in cDCs [90]. Another illustration of TF specificity is Zbtb46, which is present in preDCs and differentiated cDCs but absent from pDCs or their precursors, as well as MACs and resting MOs[91].

1.2.1.1 Transcription factors in monocyte-associated models

MO-derived cells can be cultured in the presence of cocktails of cytokines that are able to activate cellular signals that trigger the activation of TFs that will drive MO cell differentiation or activation. The sole presence of GM-CSF (or M-CSF) in the media is able to induce a set of TFs that allow the differentiation of MO to MAC, and the combination of GM-CSF and IL-4 induces a different set of TF that leads to DC differentiation. In the presence of LPS, another TF subset is activated allowing DC/MAC to become active. On the other hand, MOs have specific functions on their own when they become activated by LPS or IL-1β, both signaling through common mediators that converge in the activation the same set of TFs. All those processes are clear

examples of how a stimulus is able to efficiently regulate the activation of different TF that will give rise to different pattern of gene expression, allowing cellular differentiation or activation to occur in the immune system context.

GM-CSF binds to GM-CSFR (present in myeloid cells) which activates receptor-associated Janus Kinases (JAKs) (predominantly JAK2) that will activate several TFs. In more detail, JAK2 activation results in the activation of the STAT family of TFs and the p65 subunit of the NF-kB complex, which enters into the nucleus and binds to DNA[92]. Moreover, JAK2 activation, triggers Ras-mitogen-associated protein kinase (MAPK), and phophoinositol 3-kinase (PI3K) pathways[93], which result in the activation of TF such as c-Fos and c-Jun or NF-kB. [94]

In turn, IL-4 binds to the IL-4 receptor, resulting in activation of the Jak1 and Jak3 Tyrosine (Tyr) kinases, thus causing the recruitment of signalling proteins to the receptor complex and the activation of signal transduction [95]. The axis JAK3-STAT6 is one of the most studied pathways activated by IL-4. In this case, IL-4R phosphorylation induces the recruitment of STAT6, which is in turn phosphorylated by JAK3 in their Tyr residues. This phosphorylation activates STAT6, thus allowing the binding to another STAT6 and forming a dimer that is translocated into the nucleus and binds to DNA in order to regulate gene expression [96]. Because of their exclusive activation by IL-4 (and not by GM-CSF), STAT6 is a differential factor between *in vitro* MO-derived DCs and MACs, and might be clue to define the different cellular identity between both cell types. As a consequence, the study of the regulation and activation of this TF in the context of myeloid differentiation is relevant for the modulation of both cell types during inflammation.

The STAT family of TFs are DNA binding proteins active under phosphorylation in their Tyr residues, which share certain functional domains between them [96] . The SH2 domain plays an important role in association between STATs and the activated receptors, and variability in these domains determine the selectivity of STAT recruitment to various cytokine receptors [96]. Another important region of the STATs is a conserved Tyr approximately 700 residues from the N-terminus. Once phosphorylated by activated Jaks, this Tyr allows STAT proteins to form dimers due to the interaction between the SH2 domain of each STAT and the phosphorylated Tyr on the other. N-terminus is also involved in the oligomerisation of STAT dimers to form potentially highly ordered oligomers, which are observed in some STATs such as STAT5 [97,98]. The DBD is located in the middle of the sequence that is variable between STATs and confers selectivity to their targets. Finally, the C-terminal region of STATs is the transcriptional activation domain. In the case of STAT6, the residues involved in cytokine receptor binding and dimerisation have been identified in the SH2 domain [99]. Moreover, a STAT6 mutant (STAT6VT) has been found that

is able to be activated independently of IL-4 stimulation [100]. More specifically, STAT6VT carries two amino acid changes in the SH2 domain that affect the overall structure and stability of the monomeric and dimeric proteins. When overexpressed in mammalian cells, STAT6VT enters to the nucleus, binds DNA and activates transcription in the absence of IL-4 stimulation. This mutant is relevant to study the downstream effects derived from STAT6 activation in the context of DC versus the MAC counterpart differentiation.

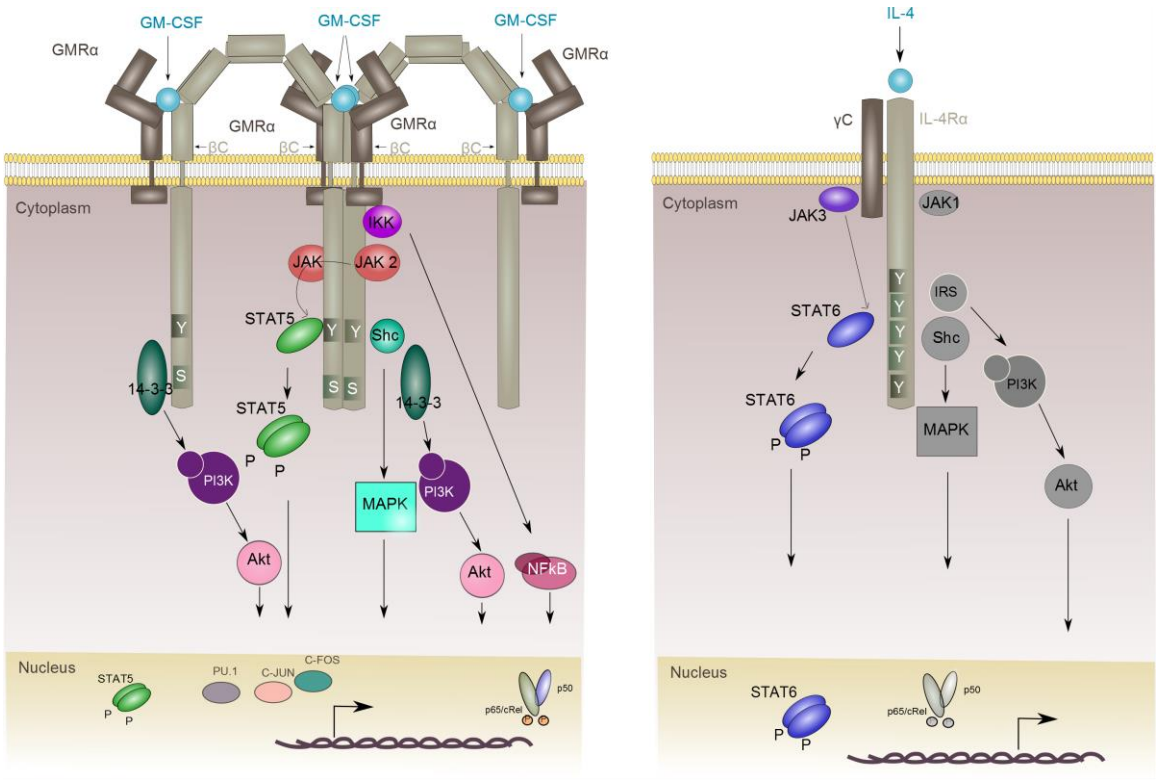

Figure 1-4 GM-CSFR and IL-4R cell signalling pathways.
GM-CSF binds to GM-CSFR, resulting in the activation of members of PI3K-Akt, MAPKs, STAT5 and NF-kB pathways, which promote cellular differentiation in the context of MOs cells through the activation of different subsets of TF. On the other hand, IL-4 binding to IL-4R, causes PI3K-Akt, MAPKs and STAT6 signalling pathways activation; together with GM-CSF pathway in the context of MOs, this drives DCs differentiation.

Several molecules, usually from microorganisms, can trigger the activation and maturation of innate immune cells, one of which is LPS, a glycolipid complex that is a major component of Gram-negative membranes and that binds TLR4 receptor [101]. In more detail, in the presence of LPS, the dimerisation of the two TLR4/MD-2 complexes in the extracellular space is produced, likely facilitating the dimerisation of the TLR4 intracellular TIR domain that subsequently initiated TLR signalling [102]. This signalling results in a rapid activation of the NF-

κB and MAPK-dependents pathways that lead to the activation of some TF like C-JUN, C-FOS or p65 [103] and the subsequent production of pro-inflammatory cytokines such as tumour necrosis factor (TNF)[104,105]. TLR4 is also internalised into endosomes which through their signal stimulates sustained NF-κB activity and also triggers TF, such as IRF7 or IRF3, to promote type 1 IFN expression[106,107].

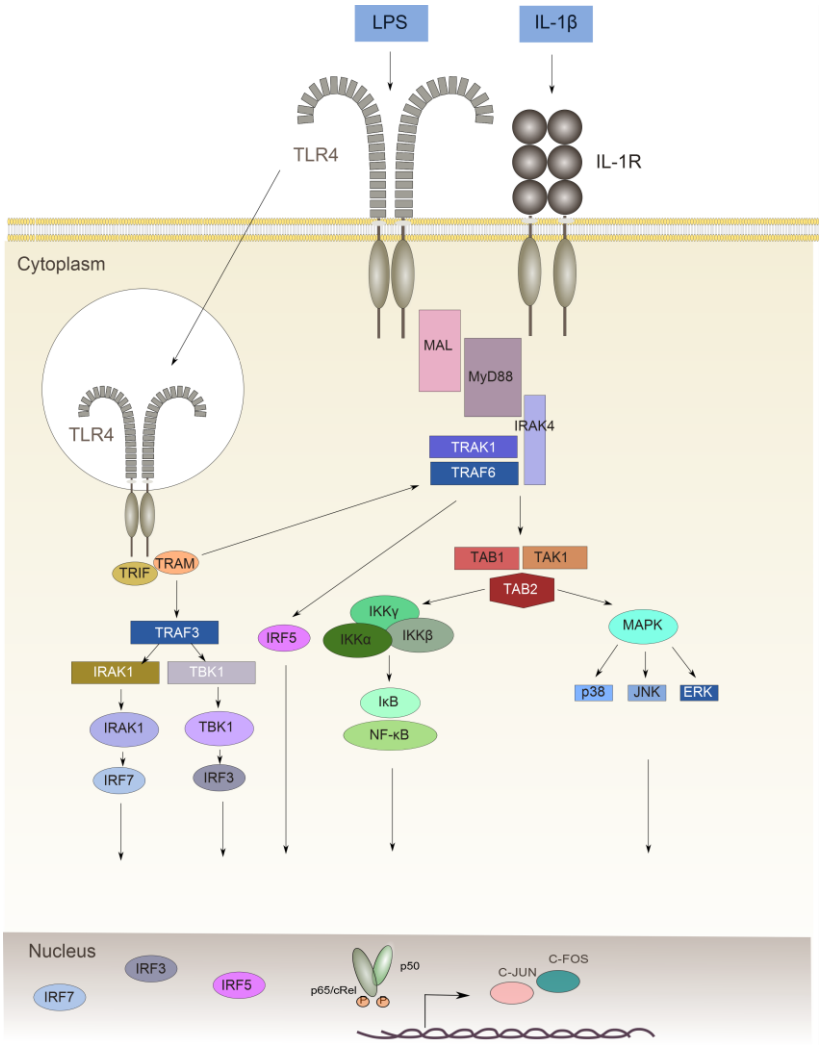

Figure 1-5 The TLR4 and IL-1R cell signalling pathways
Upon ligand-induced TLR4 and IL-1R dimerisation, the MyD88- dependent signalling pathway is activated. Activated IL-1R or TLR4 associates with a cytoplasmic adaptor molecule, MyD88, which mediates the association with IRAK proteins. Subsequently, multiple transcription factors, including MAPK, IRFs and NF-κB are activated. In turn, TLR4 can be internalised into endosomes and signal by the MyD88-independent pathway, which induces MyD88 adaptor protein and the activation of IRF7 and IRF3 transcription factors.

IL-1β also activates MOs, and this inflammatory cytokine activates almost all pathways activated during LPS cell signalling. IL-1β acts through IL-1R1, expressed in a high variety of cells, which results in the activation of signalling via NF-κB, as well as to p38, c-Jun N-terminal kinases (JNKs), extracellular signal-regulated kinases (ERKs) and mitogen-activated protein kinases

(MAPKs) routes [108]. Those pathways result in an increase in the mRNA expression of hundreds of genes such as IL6. In fact, IL-1β starts a positive-feedback loop, inducing its own expression [109] However, it is transcribed as a pro-protein that needs to be processed by the inflammasome in order to become biologically active.

Although we have discussed here how different stimuli control a subset of TF that control gene expression, cellular responses are not linear and are often branched. For example, in cell signalling is a common fact that different concentrations of one stimulus induce alternative pathways, and this is the case for GM-CSF, [110]. Moreover, the TFs response to two different stimuli do not involve the addition of all TFs activated, since different pathways and TFs can interfere which each other. It is also a fact that different specific TFs present in a cellular type that are not activated by the stimulus, could drive gene expression responses [111]. Different molecular mechanisms might explain this fact, for example genome regions that were not accessible before the stimulus become accessible after the stimulus, or also, because the TF is recruited by other TF activated by the stimulus. On the other hand, it is difficult to determine which genes are under control of one TF, which would be ideal to predict cellular responses. Although there are some bioinformatics tools that allow us to predict the probability of binding of a specific DBD to the DNA (such as the TRANSFAC^R database), other components such as the accessibility to the DNA in this region, or the concentration of TF could also influence the TF binding to the DNA.

1.2.2 Epigenetic Control in myeloid differentiation

Epigenetic control refers to those mechanisms of chemical signalling that take place in the chromatin that modify or perpetuate the transcriptional potential of a cell without the involvement of changes in the DNA nucleotide sequence, and includes histone modifications and DNA methylation.

1.2.2.1 DNA Methylation

DNA methylation is a covalent modification of DNA that allows DNA to create variability without altering the content of the base sequence. DNA methylation consists in the addition of a methyl group to the 5’ position of the pyrimidine ring of cytosines (C) that are adjacent to guanines in the DNA (known as CpG dinucleotides). This modification of the DNA can modulate the binding of certain TFs to their associated sites or influence the binding of other nuclear factors that display higher or lower affinity for methylated CpGs, eventually influencing TF accessibility or altering chromatin structure [112,113]

DNA methylation has a diversity of functional consequences for the cell, including the control of gene expression and, their exact role depends on the genomic location where the modification takes place. If CpGs are located near the TSS or the first exon of a gene [in clusters called CpG Islands (CGIs)], the correlation with gene expression is generally negative[114]. By contrast, a positive association between gene methylation and gene expression is detected when CpGs are found in the gene body context, where DNA methylation might be involved in other types of regulation, such as alternative splicing [115] .

DNA methylation is also found in intragenic regions; in this context, however, consequences for gene expression are more complex to define. Along these lines, DNA methylation is found at the borders of CGIs (up to 2kb), in regions characterised as "shores", which are also hotspots for hypomethylation and hypermethylation in malignant cells [116]. When the regions are located 2-4 kb from the CGIs, they are called "shelves", and when they are outside the CGI context, they are called "open sea".

DNA methyltransferases (DNMTs), the enzymes involved in catalysing the addition of the methyl group to the cytosine, are DNMT1, DNMT3a and DNMT3b. DNMT1 is responsible for the maintenance of the methylation patterns throughout DNA replication cycles, while DNMT3a and DNMT3b, are in charge of *de novo* DNA methylation[117] .

The mechanisms involved in the removal of DNA methylation involve the coordinated participation of several enzymes that are able to remove the methyl group of cytosine, known as active DNA demethylation. On the other hand, passive DNA demethylation takes place when the loss of methylcytosine occurs during successive rounds of replication in the absence of efficient maintenance by the DNA methylation machinery.

TET proteins are the main enzymes involved in the active demethylation (AD), a process that consists of the progressive oxidation of 5 methylcytosine (5mC) followed by the action of the DNA repair machineries. The process starts with the oxidation of 5mC by TET enzymes to generate 5-hydroxymethylcytosine (5hmC), which is further oxidised by TET proteins to produce 5-formylcytosine (5fC) and 5-carboxylcytosine (5caC) [118]. This base can be further processed through either passive dilution (AD-PD) or active restoration (AD-AR). PD is generated due to the poor capacity of intermediaries to be recognised by DNMTs, which determines the incapability to be maintained during the process of replication[119,120]. By contrast, during AR the different intermediaries are recognised by different enzymes that an end the removal process. For example, is has been proposed that 5hmC can be deaminated by AID and APOBEC to become 5-hydroxymethyluracil (5hmU) [121] . This 5hmU (as well as 5fC and 5caC) can be excised from DNA

by glycosylases, with TDG being the one of most closely studied among them[122]. Additionally, two more mechanisms for removing the methyl group from the cytosine have been recently described: the dehydroxymethylation of 5hmC by DNMTs generating cytosines [123,124], and the descarboxylation of 5caC to C [125].

The intermediates of methylation have consequences on gene expression, although they have not been entirely explained yet. In this line, 5hmC is the most common methyl intermediate present in the genome and its occurrence in some cases may relieve the silencing effect of 5mC by preventing the binding of methyl-CpG binding proteins [126]

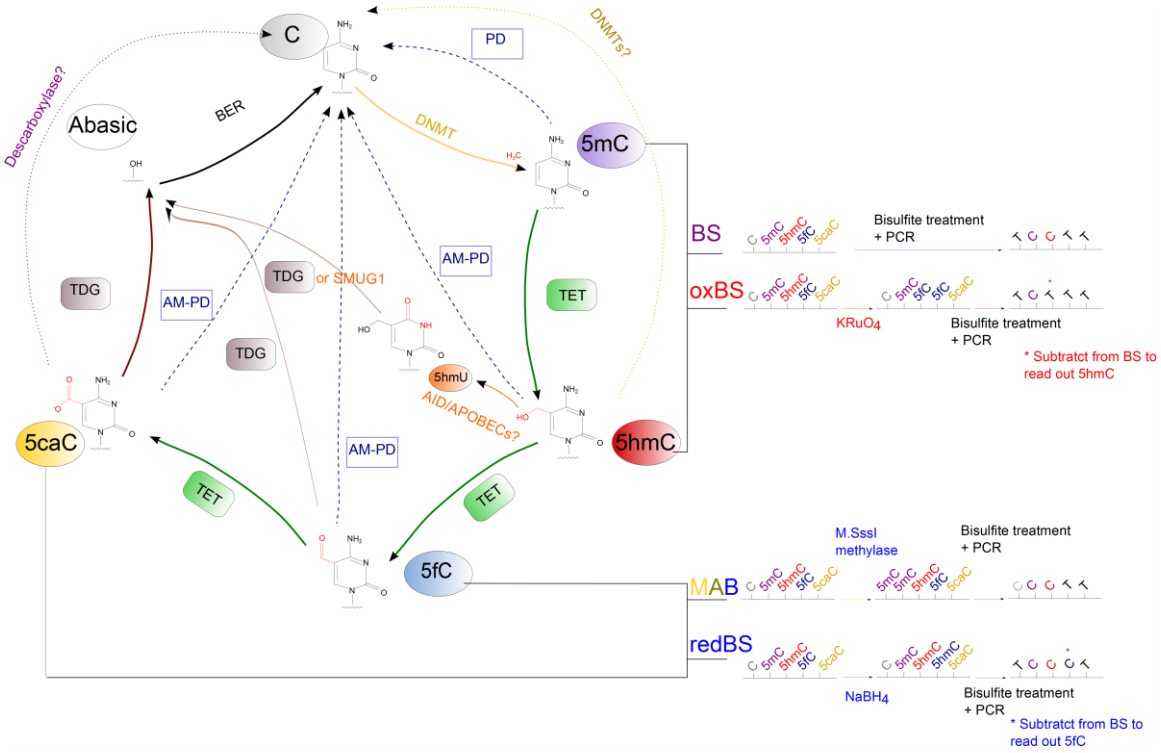

Figure 1-6 Schematic of major DNA methylation and demethylation pathways.
DNA methyltransferases (DNMTs) methylate cytosine by transferring the methyl group from S-adenosylmethionine (SAM) to cytosine. TET enzymes are able to oxidize 5mC to 5hmC, 5fC, 5caC. (together: oxi-mC). Through oxi-mC production, TET proteins mediate multiple pathways of DNA demethylation, including TDG-mediated BER and replication-dependent passive demethylation. Recently investigations show that activation-induced deaminase (AID)/APOBEC can mediate the deamination of 5hmC to 5hmU followed by TDG-mediated BER. The most relevant methods used to detect methyl intermediaries are shown on the right. These include BS and oxBS, when in conjunction with one another, they are used to detect 5mC and 5hmC, MAB and redBS, which are able to detect 5fC and 5caC.

Although the most common techniques to detect the presence of the methyl intermediaries in the genome are those based on bisulphite (BS) modification, there are alternative methods that rely on restriction endonucleases or antibodies that are able to

discriminate specific oxidation states of modified cytosines. BS is based on the fact that deamination of cytosines originates uracil, but does not alter 5mC [127]. Following DNA sequencing, the cytosines will be deaminated and converted to uracil, except those coming from methylated cytosines. A limitation of BS treatment is that that both 5mC and 5hmC are unable to be deaminate in the presence of BS, so it is impossible to know which modification was in the original sequence[128]. Given the different consequences of the intermediaries on gene expression, more accurate techniques based on BS treatment have been recently developed, like the detection of 5hmC by oxBS, based on a previous oxidation of the 5hmC by potassium perruthenate ($KRuO_4$). $KRuO_4$ converts 5hmC into 5fm, which is an intermediary susceptible to being modified by BS treatment [129]. As a result, an accurate measurement of 5mC is completed. In addition, 5hmC levels are therefore calculated by subtracting the exact content to 5mC to the total content of 5mC+ 5hmC (conventional BS). Other examples of new techniques include the detection of 5fC and 5caC by red-BS and MAB [130131] . Novel techniques of single molecule sequencing based on the different physical properties of each modified base are starting to be used, like Nanopore sequencing [132].

1.2.2.1.1 DNA methylation in Myeloid Identity, Function and Ontogeny

A proper control of DNA methylation is needed to regulate HSC self-renewal during hematopoiesis. In this context, DNMT1 is crucial for protecting HSCs from the premature activation of predominant differentiation programs[133]. The other DNA methyltransferases (DNMT3a and DNMT3b) also play a key role in this early stage; by suppressing the expression of TF related to self-renewal and multipotency, they allow differentiation to proceed [134]. On the other hand, enzymes involved in removal of the methyl group from Cs in the DNA are also vital for HSC self-renewal, as it is observed by the enhanced repopulation capacity linked to lower levels of 5hmC in HSCs in TET2-deficient mice [135].

During haematopoiesis, two different tendencies exist in regards to DNA methylation with an increase of DNA methylation upon lymphoid commitment, and the opposite effect when myeloid differentiation progresses [136]. Accordingly, in mice with reduced expression of DNMT1, HSC are unable to differentiate to lymphoid cells due to the inability to silence some myeloid defining TF and genes [133]. DNA methylation signatures of terminally differentiated human blood cells show a marked hypomethylation pattern in myeloid cells compared to lymphoid, highlighting that this DNA methylation trend in both lineages is maintained across the differentiation process [136,137].

Despite global loss of methylation is observed during myeloid differentiation, variation in DNA methylation in both directions is observed during granulopoiesis. More specifically, during the transition of CMPs to GMPs, there is an increase in DNA methylation, which is associated with the necessary silencing of pluripotency-related genes [138]. This increase is followed by a slight reduction in methylation between GMP and premyelocyte stages of development [139]

When using models of *ex vivo* differentiation, a significant reduction of DNA content is also observed. For example, MO differentiation to MAC and DC is associated with a loss of DNA methylation mediated by active mechanisms [140]. Active mechanisms of demethylation also have been observed when B cells are transdifferentiated *in vitro* into MAC by overexpressing C/EBPα [141]. In this specific case, TET2 (which is activated by C/EBPα) is able to promote hydroxymethylation and facilitate the depression of myeloid target genes during this process [142]. Curiously, no change in methylation is observed during this process [143], suggesting a positive relationship between hydroxymethylation and gene expression.

Little is known about the mechanisms that mediate the recruitment of TET2 to the DNA, but in a model of MO-derived differentiation, PU.1 binds to TET2 and induce the specific hypomethylation during the process [144]. In the same study, the crucial TF PU.1 is also responsible for inducing hypermethylation through the binding to DNMT3b.

1.2.2.2 Histone Modifications

Genomic DNA in eukaryotic cells is packed onto nucleosomes, which comprise the basic building blocks of chromatin. The nucleosome is made by core histones, namely two H2A-H2B dimers and a $H3_2$-$H4_2$ tetramer ultimately forming an octamer where 147 bp of DNA are wrapped. Another histone, the H1, is in charge of binding the nucleosomes between them.

Nucleosomes may change position, which alter the accessibility of the underlying DNA, or they can be post-translationally modified by proteins known as chromatin remodelers. Post-translational modifications occur in the histone protein tail, resulting in changes in nucleosome compaction and gene expression. The most extensively studied histone modification occurred at H3 lysine, although other histone proteins and residues can also be modified [145]. Methylation and acetylation are the most commonly known modifications in the amino-terminal region of a histone; other modifications that are less studied include phosphorylation, methylation, ubiquitylation or sumoylation[146]. Histone modifications are designated according to their location in histone tail and the type modification: for example, H3K27me3 indicated that the H3 tail is trimethylated on the lysine located in position 27.

Histone acetylation of a lysine residue occurred when an acetyl group is transferred to the ε-amino group of lysine side chains on the histone protein. As a result, the positive charge on lysine is reduced, thus decreasing the affinity of the histone tail that protrudes from the nucleosome core of DNA, acquiring a more relaxed structure and enabling the recruitment of the transcriptional machinery [146]. While histone acetyltransferases (HATs) are the enzymes that are able to catalyse this reaction, histone deacetylase (HDACs) enzymes have the opposite effect.

On the other hand, histone methylation does not change the charged state. By contrast, the various methyl marks act as binding sites for other proteins that compact nucleosomes together or bring additional regulatory proteins to chromatin sites marked by methylation [147].In this case, the enzymes that are able to add the methyl group are called histone methyltransferases (HMTs) and those that remove it are histone demethylases (HDMs). Histone lysine methylation can be associated with either transcriptional activation or repression.

The genome is organized in regions that are functionally different. Euchromatin, or active chromatin is characterized by a more lrelaxed structure, it is more accessible to TFs and is associated with histone modifications characteristic of transcriptionally active genes [148].In contrast, heterochromatin, often contains stably repressed, inaccessible genomic elements [149] . Both chromatin types are associated with distinct types of histone modifications. For example, in the promoter region, H3K4me3 is a hallmark of transcriptionally active genes, whereas H3K9me3 and H3K27me3 are associated with silenced genes[150].

Histone modifications are also of high relevance when they are located in the enhancer regions. Enhancer regions are distal regulatory elements that may function in combination with promoters or other enhancers to influence the transcription of one or more genes through the binding of TF. The main histone modifications associated with enhancer regions are H3K4me1 and H3K27ac [151].

1.2.2.2.1 Histone Modifications in Myeloid Identity, Function and Ontogeny

In addition to DNA methylation, histone modification factors also have a key role during myeloid differentiation. A good illustration of this is the role of HDAC1 and HDAC2 in BM progenitors. It has been observed that the ablation of *HDAC1* and *HDAC2* in murine BM progenitor cells impedes the development of erythrocytes and megakaryocytes[152]. Moreover, committed CMPs differentiate into megakaryocyte-erythroid lineages when *HDAC1* expression is sustained by the GATA-binding protein 1 (GATA1); conversely, when *HDAC1* expression is downregulated by C/EBP TF, committed CMPs give rise to myeloid cells, in particular granulocytes [153]

The importance of HDAC for MAC development has also been described in the context of B cell transdifferentiation overexpressing C/EBPα. In this case, HDAC7 have a role in repressing MAC-specific genes and is strongly downregulated during the process, allowing genes that are necessary for adopting MAC commitment to be expressed[154].

Moreover, histones modifications provide clues for determining MAC polarisation. Another deacetylase member, HDAC3, has been proved to be required for inflammatory M1 activation of certain LPS –induced inflammatory genes, such as IL6, when using mouse BM - derived MAC [155]. In addition, the histone demethylase Jumonji domain-containing 3 (JMJD3) activated in M2 is in charge of the removal of repressive marks found in M2 specific genes, such as Irf4[156,157].

Upon LPS mediated activation of M1, histone acetyltransferase p300 binds to enhancers of genes that are activated [158] and some modification changes are stimulated by LPS, with *de novo* enhancers due to H3k4 methylation.

The innate defensive responses mediated by myeloid cells are also influenced by changes in histone modifications. Some years ago, innate immunity was seen as a crude and unspecific part of the immune system; however, most recent studies have reshaped the view of innate immunity being non-specific. Moreover, the absence of the innate immune system's ability to adapt in response to past alterations has also been questioned; subsequently, the term "trained immunity" has been coined to explain the acquisition of memory by the innate immune system. Trained immunity is a form of immunological memory defined as a heightened response to a secondary infection that can be exerted both toward the same microorganism and a different one – also known as cross-protection [159]. In line with this, when adding β-glucans to the media, MOs that have been previously exposed to the stimulus present an enhanced inflammatory response. This concept differs from adaptive immune memory in the highest degree of specificity and amplification required on the adaptive immune memory.

Notably, chromatin structure and epigenetic modifications are crucial for such processes to occur and to be sustained. Although little is known about the mechanisms in trained immunity, a type of enhancer that undergoes H3K4 methylation and H3K27 acetylation in the presence of the stimulus has been described in innate immunity. Once the stimulus is removed, H3K27 acetylation disappear but H3K4me1 persists at the latent enhancers, and upon re-stimulation, those genes associated with the enhancer regions respond more efficiently to the new stimulus [160]. In the case of β-glucan training, the presence of H3K4 methylation in promoters[161] and H3K27 acetylation in promoters and enhancers [162]has been identified. More

interestingly, it has been concluded that these changes in histone modifications define a metabolic signature that underlies the metabolic switch required for MO activation and training[163]

Epigenetics also have a crucial role in the cell fate determination of the different subsets of MACs located in different tissues. In the same vein, it has been seen how different MACs located in several tissues across the body present variations in their histone modification patterns of their enhancer regions [164]. Taking this into consideration, when fully differentiated MACs were transferred to an alternate tissue, the new environment was sufficient to reshape their expression. The chromatin landscape is therefore specialised within the tissue; however, it still retains the capacity to be reversed and reprogrammed.

1.2.3 Non-coding RNAs

Non-coding RNAs are functional RNA molecules that regulate gene expression without translating into a protein. The most studied non-coding RNAs are the small RNAs, which are RNAs from 20 to 30 nucleotides that operate by supressing unwanted genetic material and transcripts [165]. In animals, small RNAs are classified into three classes: microRNA (miRNA), siRNA and PIWI-interacting RNA. miRNAs constitute the dominating class of small RNAs and it has been determined that more than 60% of human protein-coding genes contain at least one conserved miRNA-binding site [166]. These miRNAs have a role in fine-tuning the development and function of innate and adaptive systems, namely in the immune system[167].

1.2.3.1 miRNAs

miRNAs bind to the 3' untranslated region (UTR) of mRNAs and either inhibit translation or accelerate mRNA degradation [168]. During the binding, the domain at the 5' end of miRNAs is crucial for target recognition and has been termed as the "miRNA seed". Other regions of the miRNAs are also important for stabilising the binding.

The synthesis of the miRNAs starts when miRNAs are transcribed into a primary transcript (primiRNA) and subsequently undergoes several steps of maturation [169]. Pri-miRNA is long (typically over 1kb) and contains local stem-loop structures in which mature miRNA sequences are embedded. Then, the nuclear RNase III Drosha, in conjunction with the essential cofactor DGCR8, initiates the maturation process by cropping the stem-loop to release a small hairpin-shaped RNA of approximately 65 nucleotide length (premiRNA) [170]. Following exportation into cytoplasm by the protein exportin 5 (EXP5) [171] pre-miRNA is cleaved by Dicer near the terminal loop, liberating a small RNA duplex [172]. These 19- to 24-bp deliberated miRNAs are incorporated into the RNA-induced silencing complex (RISC) containing the Argonaute (AGO)

protein [173]. Finally, AGO proteins induce translational repression and decay of target mRNAs through interaction with the translational machinery and mRNA decay factors[166]. Each miRNA has the ability to inhibit many mRNAs: in fact, a single miRNA can affect over 100 genes and one mRNA can be targeted by more than one miRNA [165]

While some miRNAs reside in intronic or exonic gene region, other ones have an intergenic localization. The exact promoter region of all miRNAs has not yet been identified for all miRNAs, but several bioinformatics prediction tools are able to predict them using information from RNA-sequencing data and chromatin immunoprecipitation (ChIP)-seq from the main histone modifications[174]. Interestingly, it is common for several miRNAs located closely in the genome (miRNA cluster) to remain co-transcribed. This does not mean that they would be always expressed at the same levels, as other post-transcriptional changes might be regulating individual miRNAs that form the cluster.

As is the case with gene expression, miRNA expression is also regulated by a network of factors that include TF, epigenetic control and non-coding RNAs [71,165]. For example, the BLIMP1 TF is able to activate the level of let-7c miRNA expression during DC activation[175]

1.2.3.1.1 miRNAs in Myeloid Identity, Function and Ontogeny

Several reports highlight the importance of miRNAs during myelopoiesis[176]. For example, miR-223 and miR424 are activated by master regulator TF C/EBPα and PU.1; additionally, they are able to inhibit NF1-A, a negative inhibitor of granulocyte and MO differentiation. Another example in monocytopoiesis is the downregulation of the cluster miR-17-5p-92 that targets AML1, which is a protein that can induce the M-CSF expression clue for MO development [177]

miRNAs are also involved in the control of ligand stimulation of the immune system, such as TLR4 activation by LPS. More specifically, LPS stimulation turns on the expression of miR-146a, which decreases the expression of TRAF6 and IRAK1 - two positive regulators of TLR4 signalling pathways[178,179]

In addition to regulating stimulus responses and cellular differentiation, miRNAs can also affect the function of innate immune cells. For instance, miRNAs can both potentiate and reduce the capacity of DCs to present antigens. In line with this, epidermal Langerhans cells (LC) from miR-150-deficient mice have reduced soluble antigen cross-presentation abilities, possibly by affecting antigen processing [180]. On the other hand, miR-223 increases the capacity of LC to cross-present antigens (the mechanism is still unknown, however) [181].

1.3 Autoinflammatory syndromes

Inflammation is a protective immune response carried out by the evolutionary conserved innate immune system in response to harmful stimuli. The inflammation process needs to be regulated by multiple checkpoints in the host as insufficient inflammation can lead to persistent infection of pathogens, whereas excessive inflammation can cause inflammatory syndromes.

1.3.1 The Inflammasome

A crucial component of the host defence in charge of guarding the host from the assault of microbial pathogens and endogenous danger signals is the inflammasome. The inflammasome is a multimeric protein complex that assemble in the cytosol after sensing pathogens or damage-associated molecular patterns (PAMPs or DAMPs, respectively), such as microbial pathogens or endogenous ATP danger signals [182]. Once assembled, caspase-1 (CASP-1) is recruited and activated by the inflammasome, thus being able to cleave and secrete the precursor cytokines of IL-1β and IL-18, and induce an inflammatory form of cell death known as pyroptosis[183]. Both cytokines are key for the inflammation response due to their function in orchestrating the innate and adaptive immune response, such as their function in mediating the interaction between NK cells and DC [184], or their capacity to induce T cell polarisation [185].

More specifically, inflammasomes consist of a sensor molecule, the adaptor molecule ASC (apoptosis-associated speck-like protein containing a caspase activation and recruitment domain (CARD), also called PYCARD) and the effector molecule CASP-1. Inflammasome sensor molecules in charge of detecting danger signals are either members of the NOD-like receptor (NLR) or the absent melanoma 2 (AIM2)-like receptor (ALR) families [182] . The adaptor molecule ASC contains CARD domains needed for a proper interaction and activation of CASP-1 that once activated, is able to mediate the inflammasome functions [186]. The adaptor molecule ASC is not always essential for recruiting CASP-1, as some members of the NLR family (such as the NLRP1 inflammasome) contain the CARD domain [187] .

The NLRP3 inflammasome remains the best-studied inflammasome and reacts to a wide variety of stimulus. NLRP3 inflammasome activation requires two signals: a priming step (through a TLR that leads to inflammasome components transcription and preparation, for example) and a second signal that leads to inflammasome and CASP-1 activation. Priming involves the increase of NLRP3 expression through NF-κB signalling [188] , as well as their deubiquitination[189] . Once primed, NLRP3 can respond to its stimuli and assemble the NLRP3 inflammasome. Additionally, ASC must be linearly ubiquitinated for NLRP3 inflammasome assembly [190]. The second stimuli needed for inflammasome activation include ATP, pore-forming

toxins, crystalline substance such as MSU, nucleic acids, or some pathogens [182]. With these stimuli, activated NLRP3 nucleated ASC into prion-like filaments through PYD-PYD interactions [191,192]. Pro-CASP-1 then interacts with ASC trough CARD-CARD interactions and forms its own prion-like filaments that branch off of the ASC filaments. The close proximity of pro-CASP-1 proteins then induces autoproteolytic maturation of pro-CASP-1 into active CASP-1. Finally, active CASP-1 is able to induce the cleavage and secretion of IL-1β and IL-18, as well as promote pyroptosis. Also notable is that in contrast to MO derived MAC, stimulation with TLR ligands in human MO is enough to induce the release of IL-1β in the absence of exogenous stimulation with ATP, maybe through the release of endogenenous ATP after TLR stimulation [193,194] .

Interestingly, a central role has been identified for CASP-8 in inflammasome activation and pro-IL-1β processing, although the exact mechanism of action needs to be explained more [182]. Another protein from the NLR family with a role in the inflammasome activation is the NLRC5 [195], which is a protein with a high range of functions in the innate and the adaptive immunity, such as antigen presentation [196]. NLRC5 can associate with NLRP3 when the inflammasome is formed, thus increasing the range of pathogens that activate NLRC5.

Another inflammasome studied in depth is the AIM2 inflammasome. In this case, AIM2 protein is able to bind directly to cytosolic dsDNA, which may be encountered in the cytosol during pathogenic infection [197]. DNA binding displaces the PYD domain, freeing the PYD domain to recruit ASC to the complex, and starting the recruitment and activation of CASP-1.

Other inflammasomes studied and relevant during inflammation are NLRP4, NLRP6, NLRP7, NLRP12 and IFI16 [198]. Moreover, apart from the canonical inflammasomes, noncanonical inflammasomes that are formed by CASP-11 have been described in mice, which has been demonstrated to be important for processing pro-IL1β and pro-IL18 [199]. In humans, CASP-4 and CASP-5 have been found to have a similar function [200] .

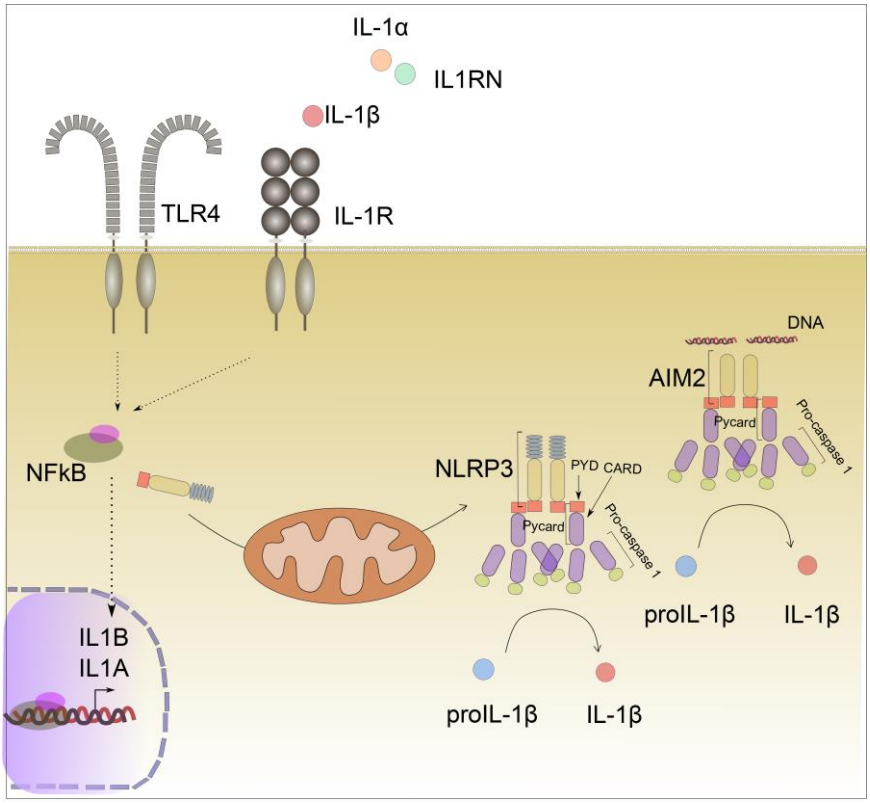

Figure 1-7 Inflammasome activation by TLR4 and IL-1R pathways.
TLR4 and IL-1R activated NF-κB–pathway, which induces elevated expression of some inflammasome related proteins, including IL-1β. Inflammasome components need to be posttranscriptional modified before their binding, which occurs through the PYD-PYD and CARD-CARD interactions, mediated by the adaptor protein PYCARD (composed of a PYD and a CARD domain). The cleavage of IL-1β and IL-18 is mediated by CASP-1, which is autoproteolytic activated when pro-caspase-1 is bound by PYCARD to the inflammasome. Processed IL-1β, as well as IL-1α, are able to bind to IL-1R that, in turn, primes for the inflammasome activity by promoting the transcription activation of some of their components. In contrast, IL1RN is an antagonist of IL-1β that are able to bind to IL-1R without activating the pathways associated to this receptor.

Although IL-1α and IL-1β are proinflammatory cytokines that activate cells by binding and signalling to IL-1R, IL-1α secretion mechanism is completely different from the IL-1β mechanism. By contrast to IL-1β, IL-1α is active without cleavage, though a processed active form could be processed via the actions of calpain [201,202]. The release of IL-1α can be dependent and independent from the inflammasome [203]. For an inflammasome-independent IL-1α release, it has been described that calcium influx induced by the opening of cation channels are sufficient enough for their secretion. On the other hand, it has been shown that some stimulators of the NLRP3 inflammasome, such as ATP or nigericin, are able to increase the secretion of the IL-1α in a NLRP3 inflammasome-dependent manner. Several proteins involved in the inflammasome complex also have a role in IL-1α release, although the release is dependent on CASP-1, is independent of their catalytic activity, and is dependent on their protease activity.

A third member of that family, the IL-1 receptor antagonist (IL-1Ra, whose gene is also called *IL-1RN*), regulates IL-1 signalling at the receptor level by competing with IL-1α and IL-1β for IL-1RI binding, thus preventing the formation of a receptor signalling complex and terminating IL-1α and IL-1β-mediated signalling.

1.3.2 Inflammasome associated diseases

Autoinflammatory diseases are innate immune disorders triggered by exogenous or endogenous components, and are characterised by system inflammation that are usually associated with an IL-1β/IL-18 signature, resulting in the constant activation of the inflammasome. It is important to distinguish autoinflammatory from autoimmune diseases, where both innate and adaptive responses are altered[204] .

The classically monogenic autoinflammatory syndromes include those diseases with a mutation in one of the components of the inflammasome. Among them, familial Mediterranean fever (FMF) and the cryopirin-associated periodic syndromes (CAPS) have been the most studied, but other syndromes including TRAPS, MKD and DIRA, also reflects the importance of well-regulated inflammasome machinery [205] .

Other diseases not classically considered as autoinflammatory (but which are increasingly considered as having an inflammatory component) include some neurological disorders and metabolic diseases. In these cases, misfolded proteins aggregates and aberrant accumulation of metabolites trigger the activation of the inflammasomes [182] .

1.3.2.1 Familial Mediterranean fever

FMF is the most prevalent autoinflammatory syndrome worldwide with more than 100.000 affected individuals [206] and is associated with mutations in the *MEFV*, a gene coding for the protein pyrin, which is involved in the regulation of inflammation and apoptosis. Pyrin interacts with ASC, and this interaction not only mediates CASP-1 activation that leads to the release of mature IL-1β but also is involved in the regulation of leukocyte apoptosis and the modulation of nuclear factor (NF)-κB activation [205]. Although considered to be an autosomal recessive disorder, patients with classical clinical picture and mutations in only one allele have been commented on. [207]

Individuals with FMF suffer from repeated, self-limiting acute attacks lasting 12-72 hours, characterised by fever, peritoneal abdominal pain and/or pleuritic chest pain, arthritis splenomegaly, and skin rashes (one of which includes erypsipelas-like erythema of the lower limb)[205]. Other forms of serosal inflammation include nonuremic pericarditis, pericardial

tamponade, or acute inflammation of the scrotum [198]. Arthritis is most often monoarticular, affecting the knee, ankle or hip. Long-term complications of FMF include renal disease, which can manifest itself as glomerulonephritis or secondary to systemic amyloidosis, with deposits forming in the glomeruli, tubules, and interstitium of kidneys.

Their treatment is usually based on colchicine, whose mechanism of action is still unclear. It has been observed that colchicine reduces the formation of ASC specks and downregulates MEFV expression in THP-1 cells and affect reorganisation of the actin cytoskeleton[208,209]. This action in the reorganisation of the actin cytoskeleton may be a key mechanism behind the efficacy of colchicine in limiting inflammation in FMF, since it is known that pyrin binds to the polymerised actin in the cytoskeleton [210,211]. Also of importance is that some recent case reports have detailed improvement of FMF using IL-1 blockade with ankinra and canakinumab [206] .

1.3.2.2 Cryopirin-associated periodic syndromes

CAPS comprise a group of autoinflammatory syndromes that are caused by the gain-of-function mutations in *NLRP3* [212]. This term encompasses different clinical entities including chronic infantile neurological cutaneous and articular/neonatal onset multisystem inflammatory syndrome (CINCA/NOMID), Muckle-Wells syndrome (MWS), and familial cold-induced autoinflammatory syndrome (FCAS). They differed in intensity with CINCA/NOMID at the severe end, FCAS at the milder end, and MWS with moderate severity [205]. Individuals with intermediate clinical pictures (CAPS overlap) have been reported [213,214] .

All three subphenotypes, collectively referred to as CAPS, are characterised by systemic inflammation with fever and blood neutrophilia and localised neutrophilic inflammation in multiple tissues, including skin, joints, muscles, and conjunctiva, and in cerebrospinal fluid [198] . Furthermore, each of the subphenotypes displays characteristic clinical features, including cold-induced symptoms in FCAS, hearing loss and systemic amyloidosis in Muckle–Wells syndrome, and more severe central nervous system and bone involvement in NOMID[215]. While patients with the CINCA or severe CAPS phenotype exhibit a continuous inflammatory state, patients with milder MWS and FCAS usually have an episodic course. Due to their inflammatory state, CAPS patients display elevated inflammatory markers (which include C-reactive protein or serum amyloid A), and elevated cytokines (such as IL-6) [198]. However, direct inflammasome-associated cytokines, such as IL-1β and IL-18, are frequently undetectable or inconsistently elevated when compared with human controls using highly sensitive assays, presumably due to serum protein or cell membrane binding [216]. CAPS can also be caused by somatic mosaicism in NLRP3 [217].

In the past years, successful treatments for CAPS based on the targeting of the inflammasome products IL-1β and IL-18 have been developed. Those include the recombinant IL-1RA anakinra, the neutralizing IL-1β antibody canakinumab, and the soluble decoy IL-1 receptor rilonacept, IL-18–binding protein, soluble IL-18 receptors, and anti–IL-18 receptor monoclonal antibodies[206,218]

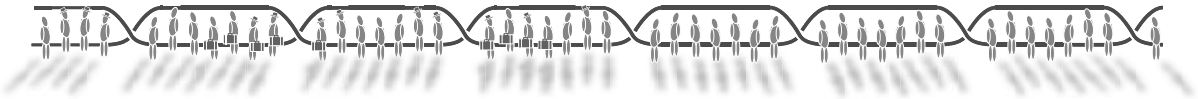

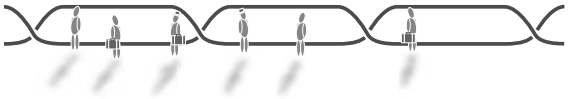

OBJECTIVES

2 OBJECTIVES

Myeloid differentiation requires a highly hierarchical and structured signalling network to guarantee a timely regulation of gene expression. Transcription factors and epigenetic machinery are main players for dictating the proper regulation across the different stages of myeloid ontogeny. These elements are linked to upstream signalling pathways and extracellular signals. The profiles of different epigenetic marks for each differentiation step have started to be generated, however little is known about the interplay between these epigenomes, their targeted deposition and erasure, and their connections with upstream signalling pathways in this context. *In vitro* MO-related differentiation processes provide excellent models to address questions on epigenetic aspects and those related to the effect of cytokines and inflammatory factors. In this thesis, we aimed at investigating the molecular sequence of events that link stimulation by cytokines and its downstream mediators that have consequently experienced changes in DNA methylation, histone modifications, and miRNA expression in the context of *in vitro* MO-derived models.

This main objective of the thesis was achieved by the establishment of the following specific objectives:

1. To dissect the mechanisms underneath the targeting of specific DNA demethylation associated with *in vitro* MO differentiation to DCs and MACs, in relation to the upstream mechanisms.

A detailed study of DNA methylation profiles in both differentiation processes will allow us to characterise specific changes for each differentiation. As IL-4 is the differential cytokine in both differentiation processes, tracking their downstream signalling will inform on how such extracelular factor is able to orchestrate in a DC specific manner TFs and their interplay with the enzymatic machinery responsible for changes in DNA methylation and gene expression.

2. To explore the potential role of DNA methylation changes in inflammasome-related genes expressed in MO-to-MAC differentiation and MO activation, comparing samples from patients of representative autoinflammatory syndromes (CAPS and FMF) versus healthy individuals.

CAPS and FMF are autoinflammatory syndromes characterised by inflammasome activation under steady-state conditions. Despite the fact that several mutations in genes related to inflammasome have been characterized for CAPS and FMF, an important number of these disorders cannot be explained by genetic defects alone. Little is known about the possible epigenetic alterations involved in autoinflammatory syndromes, although these alterations might play a crucial role in the establishment of the disease. Investigating the implications of epigenetic mechanisms of CAPS and FMF may be crucial for the discovery of new treatments and prognosis for these patients

3. To analyse the role of gains of DNA methylation in the acquisition of the DC phenotype.

Although MO to MAC/DC differentiation is mainly associated with DNA demethylation, moderate but significant gains of DNA methylation take place in a few genes important for the function of MO derived cells. Studying the dynamics of DNA methylation in assocciation with active and repressive histone modifications can help understanding the hierarchy and role of these changes in gene expression and phenotype acquisition.

4. To compare the role and participation of miRNA-mediated control in three related MO-derived differentiation processes: MO-to-OC, MO-to-DC, MO-to-MACs.

Non-coding RNAs play a key role in the regulation of gene expression and phenotype acquisition, in which miRNAs are the most widely studied. As a consequence, studying the role of miRNA in differentiation processes and the mechanisms that mediate their control might be crucial for determining the different cell identities.

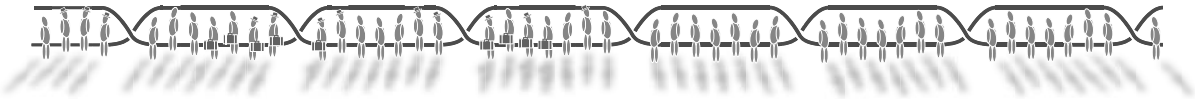

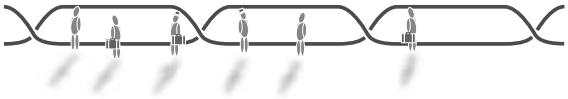

RESULTS

3 RESULTS

I certify that the PhD student ROSER VENTO TORMO will defend her Doctoral Thesis by article publication compendium, two of which have already been published. Her contribution to each article is specified below:

ARTICLE 1:

Vento-Tormo R, Company C, Rodríguez-Ubreva J, de_la_Rica L, Urquiza JM, Javierre BM, Radhakrishnan S, Luque A., Esteller, Aran JM, Alvarez-Errico D & Ballestar E.

TITLE: IL-4 orchestrates STAT6 -mediated DNA demethylation leading to dendritic cell differentiation

JOURNAL: *In Press* in ***Genome Biology*** (Impact Factor: 10.8)

In this article, Roser Vento-Tormo was the main person responsible, along with Damiana Alvarez-Errico and myself, for conceiving the majority of the experiments and performing them. She was in charge of establishing the MO derived MAC and DC model in the laboratory, as well as all the experiments involved in cell identity of MACs and DCs (markers by qPCRs and flow-cytometry). She also generated all MO derived cell differentiations and performed all pyrosequencing analysis, qPCRs, drug treatments, specific targeting by siRNAs and lentiviral infections of primary cell lines (figure 1G,2G-H,3 and 4B-G and supplementary 1,2,3,4,5 and 6). Moreover, she also was involved in the Bioinformatic data analysis decisions, of the analysis done by José M. Urquiza and Carlos Company (Figure 1A-F, 2A-F) During STAT6 ChIP experiments, she collaborated with Javier Rodríguez-Ubreva (Figure 4A). Finally Roser, along with Damiana and I, interpreted all of the results. She addressed all assembly figures and was involved in the writing and revision of the article.

ARTICLE 2:

Vento-Tormo R, Alvarez-Errico D, García-Gomez A & Ballestar E.

[With the participation of the Autoinflammatory Diseases Clinical Unit and Vasculitis Research Unit Internal Medicine and Department of Immunology (Hospital Clínic-IDIBAPS) and the Autoimmune and Systemic diseases Services (Hospital Vall d'Hebron)]

TITLE: A DNA demethylation Signature in Inflammasome Genes Features Autoinflammatory Syndromes

In this article, Roser Vento-Tormo was the main person responsible, along with Damiana Alvarez-Errico and myself, for conceiving the majority of the experiments and performing them. She and Damiana generated all MO derived MACs differentiations, MO inflammatory stimulations and samples processing, and performed all pyrosequencing analysis, qPCRs, functional assays, specific targeting by –siRNAs and flow cytometry analysis (Figure 1,2,3 and 4). Finally Roser, along with Damiana and I, interpreted all of the results. She addressed all figures assembly and was involved in the writing and revision of the article.

ARTICLE 3:

Vento-Tormo R, Alvarez-Errico D, Rodríguez-Ubreva J, Ballestar E.

TITLE: Gains of DNA methylation in myeloid terminal differentiation are dispensable for gene silencing but influence the differentiated phenotype.

JOURNAL: ***FEBS Journal*** 2015 May;282(9):1815-25 (Impact Factor: 4.001)

In this article, Roser Vento-Tormo was the main person responsible, along with Damiana Alvarez-Errico and myself, for conceiving the majority of the experiments and performing them. She generated all MO derived cell differentiations and performed all pyrosequencing analysis, qPCRs, proliferation assays, ChIPs experiments, drugs treatments and flow cytometry analysis (Figure 1-3 and Supplementary Figure 1-3). Finally Roser, along with Damiana and I, interpreted all of the results. She addressed all assembly figures with Javier Rodriguez Ubreva and was involved in the writing and revision of the article.

ARTICLE 4:

De_la_Rica L, García-Gómez A, Comet NR, Rodríguez-Ubreva J, Ciudad L, **Vento-Tormo R**, Company C, Álvarez-Errico D, García M, Gómez-Vaquero C & Ballestar E.

TITLE: NF-κB-direct activation of microRNAs with repressive effects on MO-specific genes is critical for osteoclast differentiation.

JOURNAL: ***Genome Biology***. 2015 Jan 5;16:2. (Impact Factor: 10.8)

In this article, Roser Vento-Tormo was involved in the conception and performance of some of the main experiments. She and Lorenzo de la Rica were in charge of generating the miRNAs expression profile of MO derived cells. As the miRNA profile was very similar for all three MO differentiations, the study was only carried out on the MOs to OC model, as it is a process whose dynamics could be better studied because of the 21 days of differentiation. Specifically, Roser Vento-Tormo performed MO to MACs and DCs miRNA analysis (Figure 4) and Lorenzo de la Rica focused on miRNA assays in the osteoclastogenesis model. Lorenzo de la Rica included miRNAs deregulation during osteoclastogenesis in his thesis but he did not comment on miRNAs in other MO differentiation models. Roser was also responsible for optimizing the techniques for transfecting and detecting miRNAs in primary cells (Figure 1-3), as well as the optimization miRNA regulation by the NF-kB pathway, including NF-kB inhibition using drugs and –siRNA specific targets (figure 5-6). Finally, Roser participated in the revision of the article.

In witness whereof, I hereby sign the present doctoral thesis,

27th September 2015, L'Hospitalet de Llobregat (Barcelona)

Esteban Ballestar, Ph.D.
Chromatin and Disease Group, Leader |Cancer Epigenetics and Biology Programme (PEBC)
Bellvitge Biomedical Research Institute (IDIBELL)
Avda. Gran Via 199-203 08908 L'Hospitalet de Llobregat, Barcelona, Spain
Tel: +34 93207133 Fax:+34 932607219 e-mail: eballestar@idibell.org

3.1 ARTICLE 1

Journal:

In Press in **Genome Biology.**

Title:

IL-4 orchestrates STAT6 -mediated DNA demethylation leading to dendritic cell differentiation

Authors:

Roser Vento-Tormo[1], Carlos Company[1,2*],Javier Rodríguez-Ubreva[1*], Lorenzo de la Rica[1,3], José M. Urquiza[1], Biola M. Javierre[1,4], Radhakrishnan Sabarinathan[5], Ana Luque[6], Manel Esteller[7], Josep M. Aran[6], Damiana Álvarez-Errico[1], and Esteban Ballestar[1]

Affiliations:

[1] Chromatin and Disease Group, Cancer Epigenetics and Biology Programme (PEBC), Bellvitge Biomedical Research Institute (IDIBELL), 08908 L'Hospitalet de Llobregat, Barcelona, Spain [2] Present address: Bioinformatics Core, Centre for Genomic Regulation (CRG), 08003 Barcelona, Spain [3] Present address: Barts and The London School of Medicine and Dentistry, Centre for Neuroscience & Trauma, Blizard Institute, 4 Newark Street, London E1 2AT, UK [4] Present address: Nuclear Dynamics Programme, The Babraham Institute, Cambridge CB22 3AT, UK [5] Department of Experimental and Health Sciences, Barcelona Biomedical Research Park, Universitat Pompeu Fabra (UPF), 08003 Barcelona, Spain [6] Human Molecular Genetics Group, Bellvitge Biomedical Research Institute (IDIBELL), 08908 L'Hospitalet de Llobregat, Barcelona, Spain [7] Cancer Epigenetics Group, Cancer Epigenetics and Biology Programme (PEBC), Bellvitge Biomedical Research Institute (IDIBELL), 08908 L'Hospitalet de Llobregat, Barcelona, Spain *Equal contributors

Abstract

Background: The role of cytokines in establishing specific transcriptional programs in innate immune cells has long been recognized. However, little is known about how these extracellular factors instruct innate immune cell epigenomes to engage specific differentiation states. Human monocytes differentiate under inflammatory conditions into effector cells with non-redundant functions, such as dendritic cells and macrophages. In this context, interleukin 4, IL-4, and granulocyte-macrophage colony-stimulating factor, GM-CSF, drive dendritic cell differentiation, whereas GM-CSF alone leads to macrophage differentiation.

Results: Here, we investigate the role of IL-4 in directing functionally relevant dendritic-cell-specific DNA methylation changes. The comparison of DNA methylome dynamics during differentiation from human monocytes to dendritic cells and macrophages identifies gene sets undergoing dendritic cell or macrophage-specific demethylation. Demethylation is TET2-dependent and is essential for acquiring proper dendritic cell and macrophage identity. Most importantly, activation of the JAK3-STAT6 pathway, downstream of IL-4, is required for the acquisition of the dendritic-cell-specific demethylation and expression signature, following STAT6 binding. A constitutively activated form of STAT6 is able to bypass IL-4 upstream signalling and instruct dendritic-cell-specific functional DNA methylation changes.

Conclusions: Our study is the first description of a cytokine-mediated sequence of events leading to direct gene-specific demethylation in innate immune cell differentiation.

Keywords: DNA demethylation, IL-4, STAT6, dendritic cell, TET2, differentiation

Introduction

DNA methylation plays a fundamental role in differentiation by driving and stabilising gene activity states during cell-fate decisions. DNA methylation maps at different steps of haematopoietic differentiation have yielded essential information about the different regulatory roles of DNA methylation in the various genomic regions (promoters, enhancers, etc) that contribute to cell identity [1, 2] and support the notion that DNA methylation changes are tightly coupled to transcription factors (TFs) [3, 4]. However, we know little about the mechanisms directing the targeted deposition or erasure of DNA methylation, and the upstream mechanisms associated with them. Terminal differentiation from monocytes (MOs) to dendritic cells (DCs), macrophages (MACs), and other related cell types, like osteoclasts (OCs), represent ideal biological processes to investigate the mechanisms by which extracellular stimulation is translated in nuclear epigenetic control. Mononuclear phagocytes are crucial components of a wide range of important biological functions, such as the maintenance of homeostasis of several tissues, coordination of the innate immune response, and participation in adaptive immunity to proper activation, regulation and resolution [5]. These cells express high levels of the methylcytosine dioxygenase TET2 [6, 7], a key enzyme that successively oxidizes 5-methylcytosines, generating intermediate forms in the pathway towards demethylation [8], a process that takes place in these differentiation processes [6, 9]. In addition, the sets of TFs and upstream signalling pathways in DC and MAC differentiation have been well studied. This is useful for investigating the interplay between DNA methylation changes and TFs. By examining the differentiation of these closely related cell types, we can dissect the specific role and relationship between TFs and upstream signalling pathways and downstream interacting DNA methylation-related enzymes.

MOs, in response to inflammatory signals, such as those associated with bacterial infection [10], extravasate and are directed to inflamed peripheral tissues, where they terminally differentiate into MACs and/or DCs. This process occurs locally and is driven and determined by microenvironmental stimuli [11]. Although closely related, MO-derived DCs and MACs exert a variety of non-redundant functions as a result of activation of specific cell-restricted transcriptional programs. MO conversion into inflammatory DCs or MACs, can be recapitulated *in vitro*, by exposing cells to IL-4/GM-CSF or GM-CSF only, respectively [12]. Human inflammatory DCs have recently been identified as the *in vivo* counterpart of *in vitro* IL-4/GM-CSF MO-derived DCs [13]. The GM-CSF receptor (GM-CSFR) activates JAK2 and downstream mediators in an inflammatory setting since GM-CSF constitutes a *bona fide* danger signal advising that levels have exceeded steady state levels in conditions of inflammation or infection

[14]. The IL-4 receptor (IL-4R) signals the activation of the JAK3-STAT6 pathway through its common γ chain [15], which leads to the development of immature DCs. Full functionality is achieved in DCs and MACs upon maturation by engaging surface receptors, including several pattern recognition receptors such as Toll-like receptors (TLRs). Acting through outside-to-inside mechanisms, TLR-mediated signals shape a specific response aimed at triggering appropriate effector mechanisms to eliminate pathogens [16]. Bacteria-derived lipopolysaccharide (LPS) is a well known maturation molecule that acts through TLR4 in MO-derived DCs and MACs *in vitro* and *in vivo*. Despite the recognition of the role of these and other factors in determining differentiation of these cell types, our knowledge of their contribution to the acquisition of functionally relevant epigenetic changes remains limited.

In the present work, we compared the specific DNA methylation changes associated with the differentiation from MOs to DCs and from MOs to MACs, as well as those occurring during the LPS-mediated maturation of these two cell types. These two differentiation processes differ only by the exposure to IL-4 to the former and so enabled the contribution to DNA methylation changes downstream of this external signal to be determined. Most changes occurred in the direction of DNA demethylation, during the differentiation step, whereas very few occurred during the LPS-mediated activation step. In contrast, thousands of genes became upregulated or downregulated in both the differentiation and maturation stages. Some of the DNA methylation and expression changes were common to DC and MAC differentiation, whereas others were specific to each differentiation process. In both cases, downregulation of TET2 impaired the acquisition of DNA demethylation and DC/MAC specific surface markers, highlighting the functionality of DNA methylation changes. For a subset of genes, DNA demethylation during the differentiation step preceded any change in gene expression, which only occurred at the activation step, suggesting that DNA methylation changes prepare an epigenetic context suitable for the quick response necessary during activation. Most importantly, manipulation of the JAK3-STAT6 pathway downstream of IL-4 in DC differentiation altered the demethylation, expression and STAT6 binding in genes that are specifically demethylated in DCs. On the other hand, inhibition of this pathway allows demethylation of genes that are exclusively demethylated in MACs. Consistently, overexpression of a constitutively active form of STAT6 in MOs in the absence of IL-4 prevents specific demethylation of MAC genes at the time that promotes demethylation of DC specific genes. This reveals the involvement of the IL-4-JAK3-STAT6 pathway in determining demethylation of DC-specific genes and preventing it in MAC specific genes. The results of our study enable us to identify for the first time the elements downstream of an external signal, in this case IL-4 in myeloid immune

cells, which are translated into cell-type-specific functional DNA methylation changes that are essential for conferring identity and function.

Results

Differentiation from MOs to DCs and from MOs to MACs results in cell type specific demethylation of thousands of genes

To dissect the downstream contribution of IL-4 in the acquisition of cell-type-specific DNA methylation changes in MO-to-DC differentiation we generated three sets of matching samples corresponding to MOs from human peripheral blood, immature DCs and MACs (iDCs and iMACs), following incubation of MOs with GM-CSF/IL-4 and GM-CSF only, respectively, and mature DCs and MACs (mDCs and mMACs), exposing iDCs and iMACs to LPS (Figure 1A). The comparison of MO-to-DC and MO-to-MAC differentiation allows isolating the specific effect of IL-4, which is the differential factor in these two processes. We monitored these processes testing different markers by quantitative RT-PCR (Additional File 1A) and by FACS (Additional File 1B). For instance, we determined by quantitative RT-PCR upregulation of DC markers (CD209), mature DC markers (CD83) and the level of expression of CD14 receptor is high in MOs, intermediate in MACs and low/negative in DCs. FACS analyses revealed that MOs are efficiently differentiated to iDCs (87-93%, according to CD209 and CD206) and iMACs (88%, according to CD206), and observed a shift in the CD83 and CD86 markers that support efficient maturation of these cells, generating 79% mDCs and 81% mMACs (Additional File 1B).

We then performed DNA methylation profiling using bead arrays that interrogated the DNA methylation status of >450,000 CpG sites across the entire genome, covering 99% of RefSeq genes. Statistical analysis of the combined data from the three biological replicates of MO-to-DC and MO-to-MAC revealed large changes in DNA methylation during the differentiation step (1,780 and 2,644 CpG sites, respectively). In contrast, only a few genes displayed differential DNA methylation during the maturation step (75 and 27 CpG sites, for DC and MAC maturation, respectively) (Figure 1B and Additional File 2). In all cases, demethylation prevailed over gains in DNA methylation, consistent with the results reported by others [6, 17, 18]. Specifically, demethylated CpG sites represented 92.9% of total differentially methylated CpGs in MO-to-iDC (1,654 CpGs) and 97.8% of differentially methylated CpG in MO-to-iMAC (2,586 CpGs). This contrasts with the findings in MO-to-osteoclast (OC) differentiation in which *de novo* deposition of the DNA methylation occurs to a similar extent as demethylation [9]. Changes corresponding to the average of three sample sets were almost identical to the pattern obtained for each individual sample, highlighting the specificity of the differences observed (Figure 1C and

Additional File 3A). The results for DC differentiation were similar to those by Zhang and colleagues [17] (78% of the demethylated genes in such study were present in our own data, Additional File 3B).

Although most CpGs displaying a loss of methylation were common to the two differentiation processes (Figure 1D), a significant fraction of demethylated CpGs were specific to each process: 14.2% in MO-to-iDC differentiation (235 genes) and 45.1% in MO-to-iMAC differentiation (1,167 genes). This implies that DNA demethylation may be important in determining the differences between the lineages. Given that IL-4 is the only cytokine to differ between these two processes, our findings not only suggest that events downstream of IL-4 may be responsible for the set of genes specifically demethylated in DCs, but also may directly block demethylation of those that are specific to MACs.

The analysis of the distribution of CpGs with a significant decrease in DNA methylation (Figure 1E), revealed that most of them map to gene bodies (789 CpGs in MO-to-iDCs and 1,242 in MO-to-iMACs). Over 22% were located at intergenic regions in both differentiation processes. Only about 15% of the changes occurred near the TSS (Figure 1E). This reinforces the notion that a high proportion of the changes occur in regulatory regions outside promoters, such as enhancers located in the body of genes. Using the Illumina annotation tool we determined that indeed 41% and 43% of all demethylated CpG sites in DC and MAC differentiation respectively are located in enhancers. The proportion of enhancers was particularly high in gene bodies and intergenic regions, as expected (Figure 1E).

Gene ontology analysis of hypomethylated CpG revealed significant enrichment (FDR<0.05) of a variety of functional categories important in iDC and iMAC differentiation and function, including inflammatory and innate immune response (Figure 1F). These data suggest that DNA demethylation is targeted to genomic regions that are activated during DC and MAC differentiation.

As expected, we identified changes in several genes involved in DC and MAC function among the group of demethylated genes in both iDCs and iMACs (Additional File 4). For example, *CSF1R*, which codes for the receptor of the cytokine CSF1 involved in macrophage differentiation, and *CCL22*, a cytokine that is released by DCs and MACs, are dramatically demethylated (Additional File 4). Immature MACs displayed specific demethylation on *CCL20*, an inflammation chemokine, and *IL1B*, a cytokine involved in immune and inflammatory response. On the other hand, we observed very specific demethylation in DC differentiation at

a CpG site in the gene bodies of *DUOX1*, an oxidase involved in the antimicrobial-mediated response, and the signalling receptor *SLAMF1* (Additional File 4).

We then confirmed the robustness of the DNA methylation data in MO-to-iDC and MO-to-iMAC differentiation by bisulphite genomic pyrosequencing of CpG sites. The selection included genes that were demethylated in both differentiation processes (*CSF1R, CCL22*, *DUSP5*), and some that were only demethylated in MAC (*IL1B*, *ARSB, CCL20*) or DC differentiation only (*SLAMF1*, *DUOX1, PFAS*). In all cases, bisulphite pyrosequencing confirmed the results of the beadchip array (Figure 1G and Additional File 3C) and the demethylation at the aforementioned genes. It is well established that terminal differentiation of MOs into DCs/MACs occurs in the absence of cell division, indicating the occurrence of active DNA demethylation mechanisms. To further confirm this, we measured the extent of DNA replication in our DC and MAC differentiation experiments by treating cells with BrdU pulses. Consistent with previous observations [18], we found no significant differences between the negative control and the BrdU pulses, implying that DNA methylation changes observed during this period are independent of DNA replication (Additional File 1C). The participation of active DNA demethylation events in this process is reinforced by the previous findings of our and other groups [6, 9]. In fact, we observed changes in 5hmC, which is an intermediate oxidized base, resulting from TET2 activity and leading to active demethylation (Additional File 3D).

To test the implication and functionality of the methylcytosine dioxygenase TET2 in demethylation during DC and MAC differentiation, we downregulated TET2 levels using siRNA transfection against various TET2 sites and compared it to transfection with a control siRNA before DC/MAC differentiation was induced. TET2 downregulation partially impaired demethylation of both common and DC/MAC specific genes. The impairment was partial due to a technical aspect related to the inability to achieve the maximum downregulation of TET2 before the differentiation processes had already started. In addition to the reduced demethylation, TET2 dowregulation also resulted in a decrease of surface CD209 and CD83 markers; together with an increase in CD14 (which is higher in MOs than in DCs and MACs) (Additional File 5) demonstrating the functionality of DNA demethylation during these two processes.

<u>Expression changes and their relationship with DNA demethylation in MAC and DC differentiation and maturation</u>

To further investigate the functionality of DNA methylation changes, we then generated expression profiles for the same cell types (MOs and derived iDCs, iMACs, mDCs and mMACs).

We noted large changes in expression in both processes. Specifically, we observed upregulation of 2,920 and 3,095 genes and downregulation of 1,513 and 1,476 genes during the differentiation of MOs to iDCs and to iMACs, respectively (>2-fold change or <0.5-fold change; p-value<0.01; FDR<0.05) (Figure 2A). We also identified large changes in the maturation process, whereby 927 and 1,461 genes were upregulated, and 1,961 and 2,829 were downregulated in the maturation from iDCs and iMACs to mDCs and mMACS, respectively, after LPS-mediated activation (Figure 2A). Unlike changes in DNA methylation, which occur primarily in the direction of demethylation and concentrate in the differentiation of MOs to iDCs and iMACs, expression changes occurred in the direction of upregulation and downregulation, and large changes were observed during differentiation and maturation. A high proportion of expression changes were common to the processes of differentiation into DCs and MACs (Figure 2B). Specifically, 73.12% and 68.98% of the upregulated genes and 72.24% and 74.05% of the downregulated genes were common to MO-to-iDC and MO-to-iMAC differentiation, respectively, whereas 54.37% and 34.49% of the upregulated genes and 61.09% and 42.88% of the downregulated genes were common to the two maturation processes.

To investigate the relationship between DNA methylation and expression changes, we compared the two data sets, focusing on genes that underwent significant demethylation. We found that DNA demethylation events were associated with both gene upregulation and downregulation (Figure 2C), although most genes that become demethylated were overexpressed (70.4% for MO-to-iDC and 67.1 % for MO-to-iMAC). We also examined whether the location of a given CpG site was related to the effects on expression. CpGs located in the TSS200 and the first exon had the strongest association between demethylation and overexpression (Figure 2D) for both MO-to-iDC and MO-to-iMAC. Analysing the list of genes that are both demethylated and overexpressed during the differentiation step revealed the enrichment of categories of genes that are functionally relevant to DC and MAC biology (Additional File 6). For instance, we observed that genes in the inflammasome pathway that leads to IL1-mediated inflammation (including *PYCARD*, *IL1B* and *IL1A*, which act together during the MAC innate response [19]) are demethylated and overexpressed during MAC differentiation. The inflammasome sensor protein gene *AIM2* [20], was also demethylated during MAC differentiation and overexpressed in the MAC maturation step, strongly suggesting the need for additive signals to trigger this supramolecular inflammatory system.

As mentioned above, most DNA methylation changes occur at the differentiation level, both for DC and MAC differentiation, whereas large expression changes occur at the activation step, suggesting that a proportion of genes may undergo DNA methylation changes before their

expression levels change. Indeed, we identified a set of genes for DC and MAC differentiation/maturation that became demethylated during differentiation but were only overexpressed at the maturation level (Figure 2E), as if demethylation were priming these genes for upregulation once they need to be expressed, i.e., when DCs or MAC encounter a compound such as LPS. Some of these genes were common to DC and MACs, but others were specific to each cell type (Figure 2F). Among these genes we identified some like *IL1B* or *CCL20* that undergo DNA demethylation during MAC differentiation, but only achieve overexpression in MACs following LPS treatment (Figure 2G) (Additional File 6). In such cases, time-course analysis of histone modifications like H3K27me3 and H3K9me3 revealed that changes in these marks also precede LPS-mediated stimulation (Figure 2H and Additional File 7), suggesting that other regulatory elements are the direct responsible for activation of these genes, once the chromatin context allow them to take place. Interestingly, the increase of these two heterochromatic marks took place in DCs, and not in MACs, where expression does not increase upon LPS-mediated stimulation.

Other genes had different relationships with DNA methylation changes, suggesting a variety of functional consequences associated with DNA demethylation observed at the differentiation step (Additional File 7).

Inhibition of the JAK3-STAT6 pathway impairs DNA methylation and expression changes of DC-specific genes and is a positive switch for changes at MAC-specific genes

IL-4 signalling is crucial and indispensable to the development of human monocyte-derived DCs. One of the most important outcomes of our DNA methylation analysis was the identification of a subset of genes that are specifically demethylated in DC differentiation in response to IL-4. To address the role of IL-4 in driving these DC-specific DNA methylation changes, we studied the contribution of signalling mediators downstream of IL-4R. Membrane-bound type I IL-4R activates the tyrosine kinase JAK3, which phosphorylates STAT6 at Tyr641, leading to its translocation to the nucleus and binding to target genes [21-23] (Figure 3A). To examine the role of the IL-4-JAK3-STAT6 pathway in the acquisition of DC-specific DNA methylation and expression changes, we first tested the impact of JAK3 inhibition on the regulation of the aforementioned genes. To this end, we first used a JAK3-selective inhibitor, namely PF-956980 [24]. We differentiated MOs to DCs and MACs with two different concentration of PF-956980 to select the conditions under which it is active. STAT6 phosphorylation, which renders STAT6 in its active form, is only present under the conditions for DC differentiation and not for MAC differentiation (when IL-4 is absent). As expected, STAT6 phosphorylation disappeared following

JAK3 inhibition with 400 nM and 1000 nM PF-956980 (Figure 3B). In the case of MACs, we did not observe STAT6 phosphorylation, given the lack of stimulation of JAK3 and therefore the addition of PF-956980 did not make any difference (Figure 3B). Treatment with PF-956980 affected the presence of surface markers CD209 and CD83 during GM-CSF/IL-4 mediated differentiation to DCs (Figure 3C and Additional File 8), resulting in the generation of profiles closer to those displayed by MAC, demonstrating the functional effects of these inhibitors in inhibiting DC differentiation.

The effect of PF-956980 was very specific to the impairment of demethylation of DC-specific genes in DC differentiation (Figure 3D), and had little effect on the demethylation of MAC-specific genes in MAC differentiation or in genes that are commonly demethylated in both DC and MAC differentiation (Figure 3D and Additional File 8B). Interestingly, in the presence of JAK3 inhibitors and under the conditions required for DC differentiation, DNA methylation levels of genes that were specifically demethylated in MO-to-iMAC differentiation resembled those observed in the absence of IL-4, indicating that inhibition of the pathway downstream of IL-4 removed the constraints on this set of genes towards their DNA demethylation under the standard conditions for DC differentiation (Figure 3D).

In general, the effects at the expression level were as expected, and impaired DNA demethylation was associated with diminished overexpression of DC-specific genes during differentiation. Most notably, we observed impaired overexpression of genes that only underwent expression changes in the maturation step, once DNA demethylation had been inhibited through the action of JAK3 inhibitors. (Additional File 8C).

To explore the extent of the role of the IL-4-JAK3-STAT6 pathway in the acquisition of DC-specific methylation signature, we performed a new methylation profiling to test the effects of inhibiting JAK3. The comparison of MOs with MOs differentiated to iDCs and iMACs both in the presence of absence of the JAK3 inhibitor PF-956980, revealed that the DNA methylation patterns of iDCs incubated with PF-956980 cluster together with iMACs (Additional File 8D). In other words, treatment with PF-956980 erases the DC-specific signature, and renders a DNA demethylation pattern indistinguishable of that of iMACs (Figure 3E). The specific analysis of some of the previously studied genes confirmed this effect (Additional File 8E).

To unequivocally test the potential causal relationship between JAK3 and STAT6 in the demethylation of DC-specific genes, we investigated the consequences of ablating JAK3 and STAT6 expression in MOs. We downregulated JAK3 and STAT6 levels in MOs using transient transfection experiments with siRNA cocktails that target different sites for each of these two

proteins in comparison with a control siRNA. 24 h after transfection, we induced DC differentiation with GM-CSF/IL-4. Under these conditions, we used western blot to check the effects on JAK3 and STAT6 levels 4 days after GM-CSF/IL-4 stimulation of MOs. This method enabled us to confirm that the levels of STAT6 and JAK3 downregulation were close to 50% and 20% (Figure 3F), respectively. As a result, we observed a noticeable shift of surface DC markers CD209 and CD83 (Additional File 9A).

We then checked the effects of JAK3 and STAT6 depletion on the demethylation of DC-specific, MAC-specific and DC/MAC common genes. Similar to the results obtained from the pharmacological inhibition of JAK3, siRNA-mediated depletion of JAK3 and STAT6 was very specific for the impairment of demethylation of DC-specific genes in DC differentiation (Figure 3G) and had little effect on the demethylation of MAC-specific genes in MAC differentiation (Additional File 9B) or in genes that are commonly demethylated in both DC and MAC differentiation. These results not only confirmed the participation of JAK3, downstream to IL-4, in the demethylation of DC-specific genes, but also the participation of STAT6, the target of JAK3.

Constitutively activated STAT6 induces demethylation of DC-specific genes during GM-CSF-only differentiation

To further investigate the potential direct involvement of STAT6 in the demethylation of DC-specific genes, we performed ChIP assays with STAT6. We found that STAT6 did interact specifically with DC-specific genes like *DUOX1* and *SLAMF1* in DC differentiation (Figure 4A), whilst there was no binding of these genes during MAC differentiation. Interestingly, pharmacological inhibition of JAK3 led to impaired binding of STAT6 in DC-specific genes (Figure 4A) reinforcing the notion of the dependence on IL-4 and JAK3 for this interaction. We then investigated whether STAT6 interacts with TET2, either directly or through other intermediates such as PU.1. However, we were unable to identify any direct interaction between STAT6 and TET2 (not shown). Although these experiments are technically challenging and it cannot be fully discarded such interaction. An alternative mechanism may be provided if STAT6 recruits PU.1, which has been proven to recruit TET2 [9] in a related monocyte differentiation process. In fact, synergism between STAT6 and PU.1 has been previously shown [25]. To test a potential participation of PU.1 in demethylating these genes, we also performed siRNA experiments against PU.1. We determined that PU.1 downregulation also impairs demethylation of some of these genes, although in a less specific manner than STAT6. In addition, we also observed an effect on surface markers of both DCs and MACs (Additional File 10).

To conclusively establish the role of IL-4/JAK3-dependent demethylation of DC-specific genes via STAT6, we performed gain-of-function experiments in MOs stimulated exclusively with GM-CSF and transfected with a constitutively activated form of STAT6. STAT6VT carries two amino acid changes in the SH2 domain that affect the overall structure and stability of the monomeric and dimeric protein [26] (Figure 4B). When overexpressed in mammalian cells, STAT6VT undergoes tyrosine phosphorylation, is translocated to the nucleus (Figure 4C), where it binds DNA, and activates transcription in an IL-4-independent manner. We infected MOs with a GFP-expressing lentiviral MIG vector (pCDH-MIG) containing STAT6VT and, in parallel, an empty GFP-expressing MIG vector as a negative control. Following infection, we stimulated cells with GM-CSF in the absence of IL-4, i..e. under our conditions for MAC differentiation. Despite low efficiency of infection of MOs with the GFP-expressing empty vector was higher than the levels achieved with STAT6VT GFP vector, probably due to the lower titre of lentiviruses containing a larger construct (Figure 4D), we were able to isolate GFP+ cells in both conditions, following 9 days after GM-CSF stimulation. Not surprisingly, the ectopic expression of STAT6VT resulted in increased levels of the DC specific marker DC-sign, following GM-CSF stimulation and in the absence of IL-4 (Figure 4E). We then performed bisulphite pyrosequencing of DC- and MAC-specific genes and found that STAT6VT overexpression was able to induce demethylation of DC-specific genes, such as *DUOX1* and *SLAMF1*, by-passing IL-4R upstream signalling (Figure 4F). In addition, MAC specific genes *CCL20* and *ARSB*, which are normally demethylated in the presence of GM-CSF, did not become demethylated under the presence of STAT6VT (Figure 4F) strongly indicating that STAT6 prevents their demethylation under the conditions of DC differentiation. In contrast, genes that are demethylated under our standard DC and MAC differentiation conditions (like *CCL22* and *CSF1R*) were not affected by the overexpression of STAT6VT. In summary, STAT6 is not only responsible for demethylating DC-specific genes but also to prevent demethylation of MAC-specific genes.

Altogether, our results demonstrate a direct relationship between the extracellular stimulation through IL-4 leading to MO-to-DC differentiation and the acquisition of DC-specific DNA methylation and expression patterns, together with the inhibition of MAC-specific genes. Moreover, we prove the role of the IL-4-JAK3-STAT6 pathway in instructing the cell epigenome to engage a specific differentiation state towards DCs, at the expense of MAC differentiation.

Discussion

Our results identify for the first time the sequence of downstream events to a cytokine in instructing specific TET2-mediated active DNA demethylation associated with the differentiation

of effector cells of the innate immune response. Specifically, we have established that IL-4 targets a demethylation signature of a specific subset of genes in DC differentiation (and also prevents demethylation of inappropriate MAC-specific genes) in a STAT6-dependent manner, providing a direct causal relationship between external stimulation by this cytokine and targeted epigenetic changes that are necessary for the acquisition of identity. These changes, as well as the majority of DNA methylation changes in DC and MAC differentiation, occur during the differentiation step from MOs, before LPS-induced maturation. The direction of DNA methylation changes in DC and MAC, as well as their occurrence during the differentiation step, contrast with the expression changes that occur in both steps and both directions (upregulation and downregulation). We have identified a set of genes in which DNA demethylation precedes the upregulation, indicating that DNA demethylation prepares those genes for subsequent overexpression during the maturation step.

In accordance with the findings of others [6], differentiation from MOs to DCs and from MOs to MACs is associated with a predominant occurrence of DNA demethylation. Conversely, very few DNA demethylation changes occur during the activation of these two cell types, when exposed to LPS, which activates these cells to respond through TLR4 and CD14. The predominance of demethylation changes differs from the direction of changes in a related model, specifically the M-CSF/RANKL-mediated differentiation of MOs to OCs, in which gains of both DNA methylation and demethylation occur to a similar extent [9]. As in the cases of MO-to-DC and MO-to-MAC differentiation, demethylation in OC differentiation takes place through active mechanisms [6, 9] and occurs to a similar extent. In contrast, unlike in DC and MAC differentiation, where gain of DNA methylation is restricted to a few genes, thousands of CpG sites become hypermethylated in OC differentiation. It is likely that the widespread occurrence of deposition of DNA methylation in OC differentiation is due to the fact that OC differentiation takes place over a few weeks. It is also remarkable that the vast majority of DNA demethylation events in DC and MAC differentiation/maturation occur in the differentiation step and that only a few changes take place during the maturation of these cells following exposure to LPS. If DNA methylation changes have an effect on the stability of cell identity, it might simply reflect that this control is more important in the initial differentiating step, from MOs to iDCs/iMACs, as it also prepares those cells and their chromatin for a potentially rapid response to fulfil their function in immunity in case of an insult.

The gene expression data show that large changes in upregulation and downregulation occur in the differentiation and maturation steps, reflecting the activation of specific response transcriptional programs. In a general way, demethylation is associated with transcriptional

activation, whereas gain of methylation is often associated with gene silencing. Although the current view is now more complex and involves different types of relationship between DNA methylation and expression status, our data on MO-to-DC and MO-to-MAC differentiation also show a prevalence of an association between demethylation and gene activation that is particularly evident in demethylated CpGs near the TSS and the first exon of genes. Identifying genes displaying both demethylation and overexpression during differentiation revealed an enrichment of genes relevant to DC/MAC function. However, it is of particular note that there is a set of genes that undergo large changes in gene expression (particularly genes that become overexpressed) only during the maturation step, although their demethylation occurred previously, during differentiation. It is as if their demethylation were a prerequisite for their subsequent overexpression, and a second signal were needed ultimately to trigger the activation once the unmethylated/competent status has been achieved. This separation between demethylation and overexpression in the differentiation and maturation steps may constitute a mechanism that facilitates a rapid response following activating stimuli, such as an encounter with a bacterial antigen, whereas keeping the existence of a threshold that prevents improper triggering. In this respect, demethylation preceding stimuli-mediated activation may act both as a gate-keeper and a facilitator of stimulus-dependent gene expression. A preparation of the genome in non-cycling cells has recently been described in naïve B cells, whereby ssDNA-seq experiments show that most of the genome is poised for antigen-driven activation [27].

The comparison of two *in vitro* differentiation models that only differ in the participation of cytokine IL-4 allowed us to dissect its direct implications in the acquisition of DNA methylation changes underlying fine-tuning of cell fate acquisition. Differentiation to DCs and MACs involves demethylation of a large common set of genes, while other CpGs become demethylated in a DC- and MAC-specific manner. The acquisition of a fate of DC or MAC in our model differed only with respect to the exposure to IL-4, so we reasoned that the difference is largely determined by events downstream of IL-4R. It is conceivable that IL-4-dependent cell specification of DC identity relies not only on determining which genes are specifically demethylated in DCs, but also on preventing demethylation of those that are specifically demethylated in MAC differentiation. It was reported some time ago that IL-4 inhibits the production of TNF-a, IL-1, and prostaglandin E2 (PGE2) in human monocytes [28] in a STAT6-dependent and a STAT6-independent manner [29]. Our results could provide molecular evidence of such inhibition, given that IL1a, IL1b and TNF all become demethylated in our system.

Human monocytes bind IL-4 to membrane-bound dimeric IL-4R, which consists of the IL-4Ralpha chain that recognises IL-4 with high affinity [30], and a second chain that forms either

Type I (with γc chain) or Type II receptors (with IL13Ra1). Upon dimerization, signal transduction leads to the activation of several routes, with STAT6 activation and translocation to the nucleus following JAK3-mediated phosphorylation as a hallmark [31]. Our study has shown that the IL-4-JAK3-STAT6 pathway plays a major role in the specific methylation changes that drive DC differentiation (Figure 4G). We have demonstrated that JAK3 and STAT6 downregulation impairs DC-specific demethylation and that the ectopic expression of a constitutively activated/nuclear form of STAT6 leads to specific demethylation of DC genes under the conditions of MAC differentiation (in the absence of IL-4). These results suggest a direct role of IL-4-JAK3-STAT6 in promoting specific demethylation and subsequent activation of a subset of DC genes, as well as impairing the demethylation of MAC-specific genes. The inhibitory effect of STAT6 has been described in Th2 differentiation of human T cells in which STAT6 regulates the expression of around 80% IL-4-responsive genes [32]. Our results are in line with a recently proposed model of assymetric participation of different STATs in response to combinations of cytokines, which strongly suggests that in response to two cytokine signals, one STAT may provide a wider transcriptional program that is restricted to gain specificity by the superimposed action of another STAT [33]. In the present work, we extend this notion to epigenetic regulation in particular DNA-methylation.

Given the participation of TET2 in the active demethylation of DC and MAC differentiation, as shown in this study, it seemed likely that STAT6 would recruit this enzyme. However, immunoprecipitation experiments were unable to demonstrate such interaction. Since PU.1 has been shown to associate and recruit TET2 to genes that become demethylated [9] and that PU.1 also interacts with STAT6 [25], a possible scenario could involve STAT6 recruitment of PU.1-TET2 to genes that become specifically demethylated in DCs (Figure 4G). It is likely that other TFs also participate in this process. In fact, there are various connections and mechanisms that associate DNA methylation changes and TF binding [34]. Our analysis of the enrichment of TF-binding motifs near demethylated CpGs supports this notion and some of them, like the GATA1 binding motif, are specifically enriched in genes demethylated in DCs, whereas C/EBPα/β, MITF, NANOG and CREB are enriched at the demethylated sites in iMAC differentiation. However, the participation of these factors in DNA methylation could also be indirect. It will also be interesting to establish whether STAT6, or any other additional TF, is able to directly recruit TET proteins to the sites undergoing DNA demethylation.

The finding that a cytokine like IL-4 drives the DNA demethylation of specific sets of genes that are crucial for DC versus MAC identity and function opens up a number of possibilities

from the fundamental and translational points of view, as new targets for pharmacological intervention of innate immune cell responses.

Conclusions

In the present study we have compared the DNA methylation changes during human MO-to-DC and MO-to-MAC differentiation, in which IL-4 represents the sole differential factor determining DC versus MAC fate. Our data reveal the existence of both common and cell-type specific DNA demethylation of many genes, and that such DNA demethylation depends on TET2 and is essential for the acquisition of proper DC and MAC identity. We demonstrate that upon IL-4R engagement by its ligand, the activation of the JAK3-STAT6 pathway leads to the acquisition of DC-specific demethylation and expression profiles, by activating DC-specific genes and repressing MAC-specific genes. Furthermore, we show that IL-4R signalling can be by-passed with the introduction a constitutively activated STAT6 form that instructs DC-specific methylation changes in the absence of IL-4. In summary, our results constitute the first report of cytokine-mediated downstream sequence of events leading to direct gene-specific demethylation in innate immune cell differentiation.

Data Access

Methylation array and expression array data for this publication have been deposited in the NCBI Gene Expression Omnibus and are accessible through GEO Series accession number: GSE71837 (methylation data for DC and MAC differentiation, corresponding to Figure 1C), GSE75937 (methylation data for DC and MAC differentiation in the presence of JAK3 inhibitors, corresponding to Figure 3E), GSE75938 (expression data, corresponding to Figure 2A). Material and Methods

<u>Differentiation of DCs and MACs from peripheral blood mononuclear cells</u>

Human samples (blood) used in this study came from anonymous blood donors and were obtained as buffy coats from the Catalan Blood and Tissue Bank (Banc de Sang i Teixits) in Barcelona. The anonymous blood donors received oral and written information about the possibility that their blood would be used for research purposes, and any questions that arose were then answered. Before obtaining the first blood sample all donors signed a consent form at the Banc de Teixits. The Banc de Sang follows the principles set out in the WMA Declaration of Helsinki. The protocol used to isolate and differentiate cells from these anonymous donors was approved by the Ethics Committee of the University Hospital of Bellvitge (CEIC) on 28 May 2011 (and renovated on 4 December 2014). The blood was carefully layered on a Ficoll–Paque

gradient (Amersham, Buckinghamshire, UK) and centrifuged at 2000 rpm for 30 min without braking. Peripheral blood mononuclear cells (PBMCs), from the interface between the plasma and the Ficoll–Paque gradient, were then collected and washed twice with ice-cold PBS, followed by centrifugation at 2000 rpm for 5 min. Pure MOs were isolated from PBMCs using positive selection with MACS magnetic CD14 antibody (Miltenyi Biotec, Bergisch Gladbach, Germany). Cells were then resuspended in RPMI Medium 1640 (1X) + GlutaMAXTM-1 (Gibco, Life Technologies^{TM}) containing 10% foetal bovine serum, 100 units/ml penicillin, 100 µg/ml streptomycin and antimycotic. For DC differentiation, medium was supplemented with 500U human IL-4 and 800U GM-CSF (Gentaur Molecular Products). For MAC differentiation, medium was supplemented with 800U GM-CSF (Gentaur Molecular Products).

Depending on the amount needed, cells were seeded at a density of 3•105 cells/well in 96-well plates, 5•106 cells/well in 6-well plates, or 40•106 cells in 10-mm plates and cultured for 4 days (unless otherwise noted); medium and cytokines were changed every two days. On day 4, cell maturation was induced by culturing cells with 5 µG/ml LPS (Sigma-Aldrich) for 24 h.

The presence of DCs and MACs was checked at the protein level by flow cytometry (Gallios Flow Cytometer, Beckman Coulter) and analysed with FlowJo software (Tree Star, Inc.) testing upregulation of specific DC markers CD209 conjugated to V450 (BD Horizon), and maturation DC marker CD83 conjugated to APC (Miltenyi). Expression of CD14 (Milteny), which is high for MOs, medium for MACs and low for DCs was also confirmed. MACs and DCs were also analysed at the mRNA level with respect to the upregulation of key DC and macrophages markers: *CD206*, *CD209*, *CD86*, *CD83*, *MSR1*, *CXCL13* and MO marker *CD14*.

DNA methylation profiling using universal bead arrays

Infinium HumanMethylation450 BeadChips (Illumina, Inc.) were used to analyse DNA methylation. This array allows >485,000 methylation sites per sample to be interrogated at single-nucleotide resolution. This encompasses 99% of RefSeq genes, with an average of 17 CpG sites per gene region distributed across the promoter, 5'UTR, the first exon, the gene body and 3'UTR. It covers 96% of CpG islands, with additional coverage in CpG island shores and the regions flanking them. DNA samples were bisulphite-converted using the EZ DNA methylation kit (Zymo Research, Orange, CA). After bisulphite treatment, the remaining assay steps were performed following the specifications and using the reagents supplied and recommended by the manufacturer. The array was hybridised using a temperature gradient program, and arrays were imaged using a BeadArray Reader (Illumina Inc.). The image processing and intensity data extraction software and procedures were as previously described. Each methylation data point

is obtained from a combination of the Cy3 and Cy5 fluorescent intensities from the M (methylated) and U (unmethylated) alleles. Background intensity computed from a set of negative controls was subtracted from each data point. For representation and further analysis we used beta and M values [35]. The beta value is the ratio of the methylated probe intensity to the overall intensity (the sum of the methylated and unmethylated probe intensities). The M value is calculated as the $\log_2$ ratio of the intensities of the methylated versus unmethylated probe. Beta values range from 0 to 1 and make intuitive sense. They were used to derive heatmaps and for comparisons with DNA methylation percentages from bisulphite pyrosequencing experiments. However, for statistical purposes, the use of M values is more appropriate.

Detection of differentially methylated CpGs

The approach to selecting differentially methylated CpGs was implemented in the statistical language R. To process Illumina Infinium HumanMethylation450 methylation data we used the methods available in the limma, genefilter and lumi packages, which are accessible from the Bioconductor repository. Before statistical analysis, a pre-processing stage was applied, the main steps being: 1) colour balance adjustment, i.e., normalisation between two colour channels; 2) quantile normalisation based on colour balance-adjusted data, and 3) variance filtering by IQR (interquartile range) using 0.50 as the threshold value. Results were analysed using an eBayes moderated t-statistical test carried out with the limma package [5]. Specifically, a paired limma was performed as implemented in the IMA package [6]. Several criteria have been proposed to represent significant differences in methylated CpGs. In this study, we considered a probe to be differentially methylated if it had shown a >2-fold (hypermethylation) or <0.5-fold (hypomethylation) difference, and if the statistical test was significant ($p<0.01$ and FDR<0.05), using M values for the statistical analysis and cut-off. For candidate gene selection we added the requisite that the difference of beta values was at least 20%.

Bisulphite sequencing and pyrosequencing

Bisulphite pyrosequencing was used to validate CpG methylation changes resulting from the analysis with the Infinium HumanMethylation450 BeadChips. Bisulphite modification of genomic DNA isolated from MOs, DCs, and MACs was performed by standard methods. Oxidative bisulphite modifications was performed as described recently by Booth and colleagues [36]. The time course was measured in biological triplicates. Briefly, 2 µl of the converted DNA (corresponding to approximately 20-30 ng) were used as a template in each subsequent PCR. Primers for PCR amplification and sequencing were designed with the PyroMark® Assay Design

2.0 software (Qiagen). PCRs were performed with the HotStart Taq DNA polymerase PCR kit (Qiagen), and the success of amplification was assessed by agarose gel electrophoresis. PCR products were pyrosequenced with the PyromarkTM Q24 system (Qiagen). All primer sequences are listed in Additional File 11.

Gene ontology analysis

Gene ontology (GO) was analysed with the FatiGO tool, which uses Fisher's exact test to detect significant over-representation of GO terms in one of the sets (list of selected genes) with respect to the other (the rest of the genome). Multiple test correction to take into account multiple hypothesis testing (one hypothesis for each GO term) was applied, reducing the possibility of false-positive results. GO terms with adjusted values of $p<0.05$ were considered significant.

Analysis of transcription factor binding

We used meme tool and TRANSFAC database to identify STAT6 binding motifs in the 1000bp region upstream/downstream the centre of hypomethylated CpG sites. ChIP primers were designed flanking those regions.

Expression array

Expression studies were performed using the Affymetrix platform according to manufacturer's instructions. 1 μg total RNA was extracted with Trizol from monocytes, DCs and macrophages and hybridised to an Affymetrix Human Prime View Array (Affymetrix Inc., Santa Clara, CA, USA). Probe intensities normalization and downstream analysis were obtained using statistical analysis language R in combination with Bioconductor repository functions (http://bioconductor.org). Normalized data obtained with "affy" package algorithm *vsnrma* [37] was followed by probe id filtering, under strong statistical confidence thresholds (P-value < 0.01 ; Adj.Pvalue (BH) < 0.05; FC < 2 & FC > 2 for downregulated and upregulated respectively). Finally, comparison of expression and DNA methylation data were performed applying custom R scripting.

Graphs and heatmaps

All graphs were created using Prism5 Graphpad. Heatmaps of the expression or methylation data were generated using the Genesis program (Graz University of Technology).

BrdU proliferation assays

BrdU was used at a final concentration of 300 □M, as previously described. On the days specified, BrdU pulsing solution was added to each well for 2 days. For flow cytometry assays CD14+ cells

were seeded in 6-well plates and cultured in differentiation media. BrdU was added to the medium at different times and after 2 days cells were fixed (4% paraformaldehyde, 30 minutes, RT), permeabilised (PBS-BSA-Triton X-100 0.8%, 10 min, RT) and treated with HCl 2N for 30 min. After DNA opening, HCl was neutralised by two 5-min washes with NaBo (0.1M, pH 8.5) and two 5-min washes with PBT. Cells were incubated with anti-BrdU antibody (18 h at 4ºC, 1:1000 dilution) and an anti-mouse Alexa-488 conjugated antibody was added to detect the BrdU-positive nuclei.

Transfection of primary human MOs

We used ON-TARGETplus siRNAs against STAT6, JAK3 and TET2 to perform knockdown experiments in peripheral blood MOs. We also used ON-TARGETplus Non-targeting Control Pool as a negative control. For PU.1 silencing experiments, two different Silencer® select pre-designed siRNAs against human PU.1 (one targeting exon 2 and another targeting the 3′ UTR) and a Silencer® select negative control were used. We transfected MOs with siRNAs using Lipofectamine 3000 Reagent (Thermo Fisher Scientific Co., Carlsbad, CA, USA) and added cytokines 24 h later. We refreshed transfection 3 days after starting the culture. We examined the levels of the target proteins by western blot 2 and 4 days after siRNA transfection. Three biological replicates of the experiments were performed.

Chromatin immunoprecipitation (ChIP) assays

For ChIP assays, CD14+ cells (MOs) treated with IL-4/GM-CSF for 0 and 2 days were crosslinked with 1% formaldehyde and subjected to immunoprecipitation after sonication. ChIP experiments were performed using a low cell ChIP kit (Diagenode SA, Seraing, Belgium). They were analysed by real-time quantitative PCR. Data are represented as the ratio of the bound fraction to the input for each specific factor. We used an antibody against STAT6 (Santa Cruz, sc-981x), and histone marks H3K9me3 (Abcam, ab8898) and H3K27me3 (Millipore 07-449). Human IgG was used as a negative control. Primer sequences were designed to contain predicted or known TF binding (from TRANSFAC or ChIPseq data) as close as possible to the CpG undergoing methylation changes. Primer sequences are shown in Additional File 11. Three biological replicates of the experiments were performed.

Inhibition of the Janus kinase 3

The Janus kinase 3 (JAK3) was pharmacologically inhibited using the specific inhibitor PF-956980 [24] (Sigma) following the manufacturer's instructions. MOs were pre-treated for 1 h with PF-

956980 on day 0 of differentiation. Following preincubation, MO differentiation was induced with IL-4/GM-CSF or GM-CSF alone in the presence of PF-956980.

STAT6 constructs, generation of lentiviral supernatants and cellular transduction

We amplified the STAT6 coding DNA sequence (CDS) using PCR with AccuPrime Pfx high-fidelity DNA Polymerase (Invitrogene) following the manufacturer's instructions. A reverse primer containing an HA tag was introduced in the sequence N-terminal end. The double mutant STAT VT was prepared by point mutagenesis using PCR to introduce two alanine residues at amino acid positions 547/548. Sequences were subcloned in pCDH-MIG vector and verified by sequencing.

Two culture supernatants were generated by transient transfection of 293FT cells and were collected 48 and 72h post-transfection. The first supernatant contained the pMSCV-GFP (Mock) or the pMSCV-GFP-STAT6VT, and the second supernatant contained the SIVmac-derived helper particles that pack the Vpx protein able to degrade SAMHD1[38]. Viral supernatants were concentrated x10 by ultracentrifugation at 20000rpm at 4 °C for 2h using Sorvall centrifuge (Thermo Scientific) and fresh monocytes were infected with both viral supernatant. Infected monocytes were cultured with GM-CSF for 9 days at 37°C. Media was refreshed every 2 days. GFP positive cells were sorted in a MoFlo Astrios (Beckman Coulter), lysed in Proteinase K buffer and incubated ON at 65ºC. Genomic DNA was isolated by standard phenol-chloroform extraction for bilsulphite pyrosequencing.

5hmC detection

5hmC was analysed using oxBS technique

Competing interests

The authors declare that they have no competing interests

Authors' contributions

RVT, DAE and EB conceived the experiments; RVT, JRU, LR, BJ, DAE performed the experiments; CC, JU and SR did the biocomputational analysis; RVT, LR, JU, AL, ME, JA, DAE and EB analysed the data; DAE and EB wrote the paper.

Acknowledgements

We would like to thank Dr Núria López-Bigas for advice on analysis of transcription factor binding motifs. We also thank Dr Thomas Graf for critical reading of the manuscript. This work was

supported by grant SAF2014-55942-R from the Spanish Ministry of Science and Innovation and the EU FP7 306000 STATegra project. RVT is supported by a PFIS predoctoral fellowship.

References

1. Ji H, Ehrlich LI, Seita J, Murakami P, Doi A, Lindau P, Lee H, Aryee MJ, Irizarry RA, Kim K *et al*: Comprehensive methylome map of lineage commitment from haematopoietic progenitors. *Nature* 2010, 467(7313):338-342.

2. Deaton AM, Webb S, Kerr AR, Illingworth RS, Guy J, Andrews R, Bird A: Cell type-specific DNA methylation at intragenic CpG islands in the immune system. *Genome Res* 2011, 21(7):1074-1086.

3. Tsankov AM, Gu H, Akopian V, Ziller MJ, Donaghey J, Amit I, Gnirke A, Meissner A: Transcription factor binding dynamics during human ES cell differentiation. *Nature* 2015, 518(7539):344-349.

4. Hogart A, Lichtenberg J, Ajay SS, Anderson S, Margulies EH, Bodine DM: Genome-wide DNA methylation profiles in hematopoietic stem and progenitor cells reveal overrepresentation of ETS transcription factor binding sites. *Genome Res* 2012, 22(8):1407-1418.

5. Geissmann F, Manz MG, Jung S, Sieweke MH, Merad M, Ley K: Development of monocytes, macrophages, and dendritic cells. *Science* 2010, 327(5966):656-661.

6. Klug M, Schmidhofer S, Gebhard C, Andreesen R, Rehli M: 5-Hydroxymethylcytosine is an essential intermediate of active DNA demethylation processes in primary human monocytes. *Genome Biol* 2013, 14(5):R46.

7. Kallin EM, Rodriguez-Ubreva J, Christensen J, Cimmino L, Aifantis I, Helin K, Ballestar E, Graf T: Tet2 facilitates the derepression of myeloid target genes during CEBPalpha-induced transdifferentiation of pre-B cells. *Mol Cell* 2012, 48(2):266-276.

8. Ito S, D'Alessio AC, Taranova OV, Hong K, Sowers LC, Zhang Y: Role of Tet proteins in 5mC to 5hmC conversion, ES-cell self-renewal and inner cell mass specification. *Nature* 2010, 466(7310):1129-1133.

9. de la Rica L, Rodriguez-Ubreva J, Garcia M, Islam AB, Urquiza JM, Hernando H, Christensen J, Helin K, Gomez-Vaquero C, Ballestar E: PU.1 target genes undergo Tet2-coupled demethylation and DNMT3b-mediated methylation in monocyte-to-osteoclast differentiation. *Genome Biol* 2013, 14(9):R99.

10. Serbina NV, Pamer EG: Monocyte emigration from bone marrow during bacterial infection requires signals mediated by chemokine receptor CCR2. *Nat Immunol* 2006, 7(3):311-317.

11. Shi C, Pamer EG: Monocyte recruitment during infection and inflammation. *Nat Rev Immunol* 2011, 11(11):762-774.

12. Sallusto F, Lanzavecchia A: Efficient presentation of soluble antigen by cultured human dendritic cells is maintained by granulocyte/macrophage colony-stimulating factor plus interleukin 4 and downregulated by tumor necrosis factor alpha. *J Exp Med* 1994, 179(4):1109-1118.

13. Segura E, Touzot M, Bohineust A, Cappuccio A, Chiocchia G, Hosmalin A, Dalod M, Soumelis V, Amigorena S: Human inflammatory dendritic cells induce Th17 cell differentiation. *Immunity* 2013, 38(2):336-348.

14. Hamilton JA: Colony-stimulating factors in inflammation and autoimmunity. *Nat Rev Immunol* 2008, 8(7):533-544.

15. Pesu M, Takaluoma K, Aittomaki S, Lagerstedt A, Saksela K, Kovanen PE, Silvennoinen O: Interleukin-4-induced transcriptional activation by stat6 involves multiple serine/threonine kinase pathways and serine phosphorylation of stat6. *Blood* 2000, 95(2):494-502.

16. Coll RC, O'Neill LA: New insights into the regulation of signalling by toll-like receptors and nod-like receptors. *J Innate Immun* 2010, 2(5):406-421.

17. Zhang X, Ulm A, Somineni HK, Oh S, Weirauch MT, Zhang HX, Chen X, Lehn MA, Janssen EM, Ji H: DNA methylation dynamics during ex vivo differentiation and maturation of human dendritic cells. *Epigenetics Chromatin* 2014, 7:21.

18. Klug M, Heinz S, Gebhard C, Schwarzfischer L, Krause SW, Andreesen R, Rehli M: Active DNA demethylation in human postmitotic cells correlates with activating histone modifications, but not transcription levels. *Genome Biol* 2010, 11(6):R63.

19. Dinarello CA: Immunological and inflammatory functions of the interleukin-1 family. *Annu Rev Immunol* 2009, 27:519-550.

20. Fernandes-Alnemri T, Yu JW, Datta P, Wu J, Alnemri ES: AIM2 activates the inflammasome and cell death in response to cytoplasmic DNA. *Nature* 2009, 458(7237):509-513.

21. Kaplan MH, Schindler U, Smiley ST, Grusby MJ: Stat6 is required for mediating responses to IL-4 and for development of Th2 cells. *Immunity* 1996, 4(3):313-319.

22. Shimoda K, van Deursen J, Sangster MY, Sarawar SR, Carson RT, Tripp RA, Chu C, Quelle FW, Nosaka T, Vignali DA *et al*: Lack of IL-4-induced Th2 response and IgE class switching in mice with disrupted Stat6 gene. *Nature* 1996, 380(6575):630-633.

23. Takeda K, Tanaka T, Shi W, Matsumoto M, Minami M, Kashiwamura S, Nakanishi K, Yoshida N, Kishimoto T, Akira S: Essential role of Stat6 in IL-4 signalling. *Nature* 1996, 380(6575):627-630.

24. Changelian PS, Moshinsky D, Kuhn CF, Flanagan ME, Munchhof MJ, Harris TM, Whipple DA, Doty JL, Sun J, Kent CR *et al*: The specificity of JAK3 kinase inhibitors. *Blood* 2008, 111(4):2155-2157.

25. Stutz AM, Woisetschlager M: Functional synergism of STAT6 with either NF-kappa B or PU.1 to mediate IL-4-induced activation of IgE germline gene transcription. *J Immunol* 1999, 163(8):4383-4391.

26. Daniel C, Salvekar A, Schindler U: A gain-of-function mutation in STAT6. *J Biol Chem* 2000, 275(19):14255-14259.

27. Kouzine F, Wojtowicz D, Yamane A, Resch W, Kieffer-Kwon KR, Bandle R, Nelson S, Nakahashi H, Awasthi P, Feigenbaum L *et al*: Global regulation of promoter melting in naive lymphocytes. *Cell* 2013, 153(5):988-999.

28. Hart PH, Vitti GF, Burgess DR, Whitty GA, Piccoli DS, Hamilton JA: Potential antiinflammatory effects of interleukin 4: suppression of human monocyte tumor necrosis factor alpha, interleukin 1, and prostaglandin E2. *Proc Natl Acad Sci U S A* 1989, 86(10):3803-3807.

29. Levings MK, Schrader JW: IL-4 inhibits the production of TNF-alpha and IL-12 by STAT6-dependent and -independent mechanisms. *J Immunol* 1999, 162(9):5224-5229.

30. Kelly-Welch AE, Hanson EM, Boothby MR, Keegan AD: Interleukin-4 and interleukin-13 signaling connections maps. *Science* 2003, 300(5625):1527-1528.

31. Martinez FO, Helming L, Gordon S: Alternative activation of macrophages: an immunologic functional perspective. *Annu Rev Immunol* 2009, 27:451-483.

32. Elo LL, Jarvenpaa H, Tuomela S, Raghav S, Ahlfors H, Laurila K, Gupta B, Lund RJ, Tahvanainen J, Hawkins RD *et al*: Genome-wide profiling of interleukin-4 and STAT6 transcription factor regulation of human Th2 cell programming. *Immunity* 2010, 32(6):852-862.

33. Hirahara K, Onodera A, Villarino AV, Bonelli M, Sciume G, Laurence A, Sun HW, Brooks SR, Vahedi G, Shih HY *et al*: Asymmetric Action of STAT Transcription Factors Drives Transcriptional Outputs and Cytokine Specificity. *Immunity* 2015, 42(5):877-889.

34. Blattler A, Farnham PJ: Cross-talk between site-specific transcription factors and DNA methylation states. *J Biol Chem* 2013, 288(48):34287-34294.

35. Du P, Zhang X, Huang CC, Jafari N, Kibbe WA, Hou L, Lin SM: Comparison of Beta-value and M-value methods for quantifying methylation levels by microarray analysis. *BMC Bioinformatics* 2010, 11:587.

36. Booth MJ, Ost TW, Beraldi D, Bell NM, Branco MR, Reik W, Balasubramanian S: Oxidative bisulfite sequencing of 5-methylcytosine and 5-hydroxymethylcytosine. *Nat Protoc* 2013, 8(10):1841-1851.

37. Huber W, von Heydebreck A, Sultmann H, Poustka A, Vingron M: Variance stabilization applied to microarray data calibration and to the quantification of differential expression. *Bioinformatics* 2002, 18 Suppl 1:S96-104.

38. Berger G, Durand S, Goujon C, Nguyen XN, Cordeil S, Darlix JL, Cimarelli A: A simple, versatile and efficient method to genetically modify human monocyte-derived dendritic cells with HIV-1-derived lentiviral vectors. *Nat Protoc* 2011, 6(6):806-816.

Figure legends

Figure 1. High-throughput DNA methylation comparison between monocytes (MOs) and derived dendritic cells (DCs) and macrophages (MACs). (A) Scheme depicting the differentiation system. Peripheral blood MOs were either exposed to GM-CSF + IL-4 or GM-CSF only to generate immature DCs and MACs (iDCs and iMACs), respectively. Maturation of these two cells types to mDCs and mMACs was achieved following incubation with LPS. (B) Summary of the DNA methylation changes obtained when comparing MOs differentiating to iDCs and iMACs, and the maturation towards mDCs and mMACs. Number of CpG sites and genes displaying signicant gain (hyper) or loss (hypo) of DNA methylation changes are shown (C) Heatmap of three paired samples (D1, D2 and D3) of MOs and their derived iMACs, iDCs, mMACs and mDCs. The heatmap includes all CpG-containing probes displaying significant methylation changes (>2-fold or <0.5-fold change; $p<0.01$ and FDR<0.05) (Data in Additional File 2). A scale is shown at the bottom, wherein beta values (i.e., the ratio of the methylated probe intensity to the overall intensity) range from -3 (lower DNA methylation levels, blue) to +3 (higher methylation levels, red). (D) Venn diagram showing the degree of overlap of demethylated CpGs/genes between MO-to-iDC

and MO-to-iMAC differentiation. (E) Distribution of demethylated CpGs among genomic regions (intergenic, promoter (1500 and 200 upstream of the TSS, 5'UTR, first exon, gene body, and 3'UTR) for MO-to-iDC and MO-to-iMAC differentiation. The darker insets within each bar indicates the number of sites annotated as enhancers. (F) Gene ontology enrichment analysis of demethylated CpGs in differentiation to iMACs and iDCs showing the most important categories. (G) Technical validation of the array data by bisulphite pyrosequencing of modified DNA. Three groups of genes are represented: demethylated genes specific to iDC differentiation, demethylated genes specific to iMAC differentiation and genes that are commonly demethylated in iDC and iMAC differentiation.

Figure 2. Comparison between methylation and expression data for MAC and DC differentiation and maturation (A) Heatmap of significant changes between MOs-to-iDC and MO-to-iMAC differentiation (left) and two additional heatmaps showing significant changes between iDC-to-mDC, and iMAC-to-mMAC maturation. The heatmaps include all the genes displaying significant expression changes (>2-fold or <0.5-fold change; $p<0.01$ and FDR<0.05). A scale is shown at the bottom, wherein expression values range from -3 (lower expression levels, blue) to +3 (higher expression levels, red). (B) Venn diagrams showing the degree of overlap of genes upregulated and downregulated between MO-to-iDC and MO-to-iMAC differentiation and iDC-to-mDC and iMAC-to-mMAC activation. (C) Scatterplots showing the relationship between the $\log_2$-transformed FC in expression and the $\log_2$-transformed FC in DNA methylation. (D) Correlation between DNA methylation and expression data (the mean value for all CpG sites within a given sequence region is shown) for all the significantly demethylated genes organised by genomic location (intergenic, promoter (1500 and 200 upstream of the TSS, 5'UTR, first exon, gene body, and 3'UTR). (E) Box-plots representing the DNA methylation and expression values of all genes that are demethylated during DC and MAC differentiation and whose upregulation is stronger in the maturation step than in the previous differentiation step. (F) Diagram showing the proportion of genes among the DC-specific, MAC-specific and those that are demethylated in both processes with no significant changes in expression during the differentiation step and upregulated during the LPS-dependent activation step. (G) Time-course analysis of DNA methylation and expression in two selected genes (*IL1B* and *CCL20*) during DC and MAC differentiation/maturation, among those displaying no changes in the differentiation step and a sharp increase in the maturation step. (H) Chromatin immunoprecipitation (ChIP) assays in *IL1B* and *CCL20* with anti-histone H3K27me3 and anti-histone H3K9me3 in MOs, and in a time course manner in differentiation to iDCs and iMACs, as well as mDCs and mMACs (120 h + LPS). The Y-axis shows the relative enrichment in arbitrary units.

Figure 3. The IL-4-JAK3-STAT3 pathway has a direct role in targeting DNA demethylation in specific DC genes. (A) Diagram depicting the pathway donstream to IL-4, cinluding the IL-4 receptor (IL-4-R), JAK3 and STAT6. IL-4, is able to activate and translocate STAT6 transcription factor to the nucleus, through STAT6 phosphorylation by JAK3 kinase. (B) Western blot assay confirming the presence of JAK3 and STAT6 in all cell types studied and the exclusive existence of the phosphorylated form of STAT6 in DC. Inhibitor PF-956980 at a concentration of 400 and 1000 nM throughout the entire differentiation process is able to prevent STAT6 phosphorylation. (C) Effects of PF-956980 on CD209 and CD14 in both GM-CSF/IL-4- and GM-CSF-stimulated cells at 96 h, as measured by FACS (D) Effects of JAK3 inhibition by PF-956980 on DNA methylation over time of DC (GM-CSF/IL-4) differentiation focusing on two DC-specific genes (left), MAC-specific genes (center) and two genes demethylated in both DC and MAC differentiation (right) (E) Heatmap showing the effect in DNA methylation of JAK3 inhibition by PF-956980. This treatment is able to erase the DC-specific methylation signature in MOs treated with GM-CSF/IL-4. (F) Western blot assays showing levels of STAT6, phospho-STAT6 and JAK3, 96 h after treatment with GM-CSF/IL-4 and transfection with siRNA for STAT6. B-actin has been used as loading control (G) Effects of siRNA against STAT6 (left panel) and JAK3 (right panel) on DNA methylation changes over time focusing on two DC-specific genes (top), MAC-specific genes (middle) and two genes demethylated in both DC and MAC differentiation (bottom).

Figure 4. Directly involvement of STAT6 in targeting DNA demethylation in specific DC genes. (A) ChIP assays confirming STAT6 binding to two genes (*DUOX1*, *SLAMF1*) that become specifically demethylated in DC differentiation. The panel also shows the loss of STAT6 to DC-specific genes following treatment with JAK3 inhibitor PF-956980. Lack of binding of STAT6 under the conditions of MAC differentiation (also in the presence of PF-956980) is also shown. (B) Diagram showing STAT6 gene domains and the double mutant that mimics phosphorylated STAT6 (STAT6 VT) and leads to a gain of function. (C) Western blot of 293T cells transfected with wild type STAT6 (STAT6 wt) and the activating double mutant STAT6 VT showing the presence of the protein in the cytosolic or nuclear fraction. (D) FACS analysis showing the GFP labelling of cells infected with a GFP-expressing lentiviral MIG vector (pCDH-MIG) containing STAT6VT (right panel) and empty GFP-expressing MIG vector as a negative control (left panel). (E) CD209 mean fluorescence measured by flow cytometry in monocytes infected with STAT6 VT and the MOCK control vector after 9 days of culture with GM-CSF. Analysis was done setting a gate to select cells with high GFP expression. (F) Effects on the DNA methylation levels of two DC-specific genes in MOs treated with GM-CSF for 48 with followed by infection with mock or STAT STAT6V. Both the GFP+ and GFP- negative fractions are shown. Examples of two DC-specific genes (right),

MAC-specific genes (middle) and two genes demethylated in both DC and MAC differentiation (left) are shown (G) Model depicting the participation of the IL-4-JAK3-STAT6 pathway in targeting demethylation of DC-specific genes

Figure 1

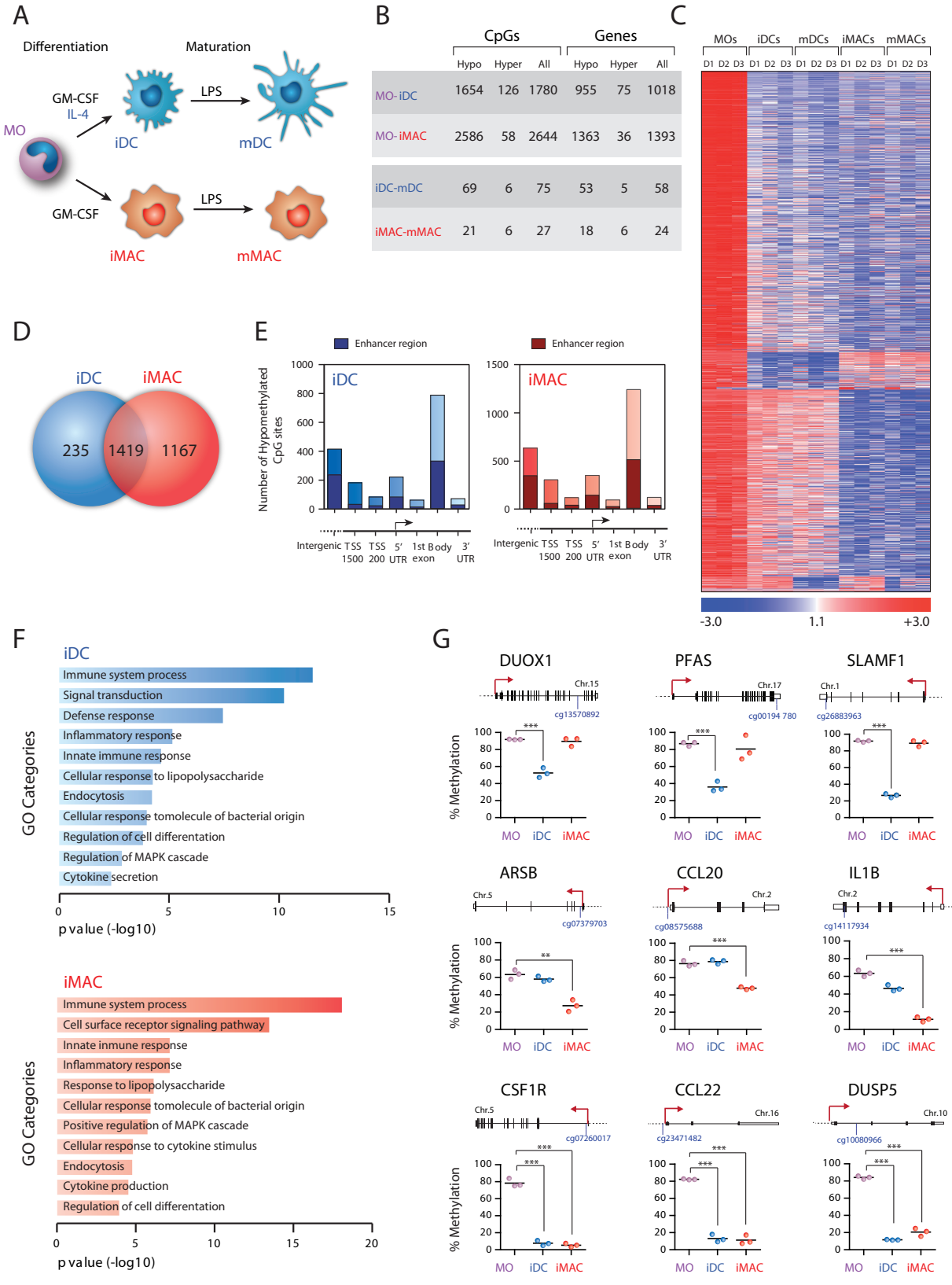
A
Differentiation
Maturation
GM-CSF
IL-4
LPS
MO
iDC
mDC
GM-CSF
LPS
iMAC
mMAC
B
CpGs
Genes
Hypo Hyper All Hypo Hyper All
MO- iDC 1654 126 1780 955 75 1018
MO- iMAC 2586 58 2644 1363 36 1393
iDC-mDC 69 6 75 53 5 58
iMAC-mMAC 21 6 27 18 6 24
C
MOs iDCs mDCs iMACs mMACs
D1 D2 D3 D1 D2 D3 D1 D2 D3 D1 D2 D3 D1 D2 D3
-3.0 1.1 +3.0
D
iDC iMAC
235 1419 1167
E
Enhancer region
Enhancer region
Number of Hypomethylated CpG sites
iDC
iMAC
Intergenic TSS 1500 TSS 200 5' UTR 1st Exon Body 3' UTR
F
iDC
Immune system process
Signal transduction
Defense response
Inflammatory response
Innate immune response
Cellular response to lipopolysaccharide
Endocytosis
Cellular response tomolecule of bacterial origin
Regulation of cell differentation
Regulation of MAPK cascade
Cytokine secretion
GO Categories
p value (-log10)
iMAC
Immune system process
Cell surface receptor signaling pathway
Innate immune response
Inflammatory response
Response to lipopolysaccharide
Cellular response tomolecule of bacterial origin
Positive regulation of MAPK cascade
Cellular response to cytokine stimulus
Endocytosis
Cytokine production
Regulation of cell differentation
GO Categories
p value (-log10)
G
DUOX1
PFAS
SLAMF1
ARSB
CCL20
IL1B
CSF1R
CCL22
DUSP5
% Methylation
MO iDC iMAC

Figure 2

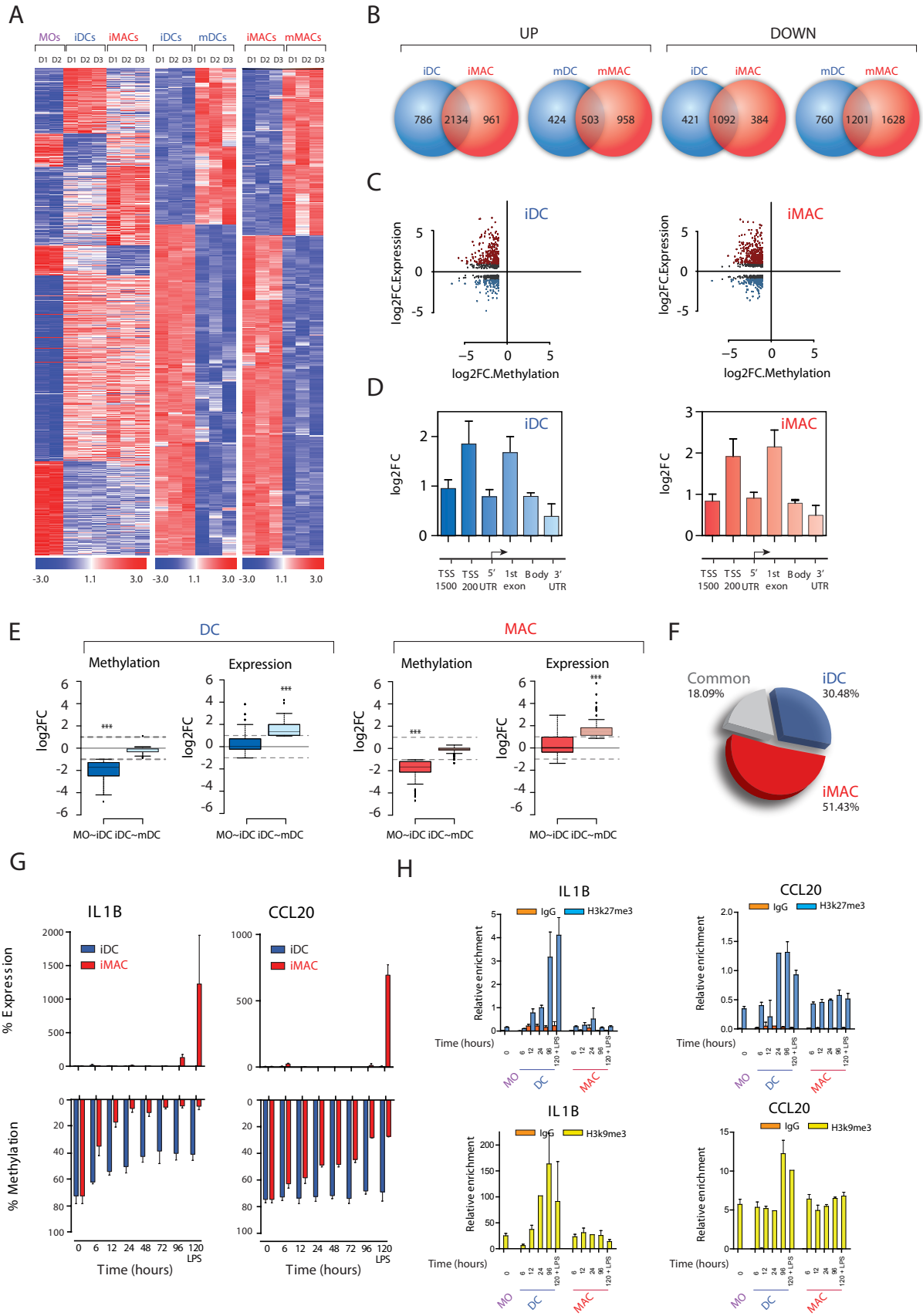
A
MOs iDCs iMACs iDCs mDCs iMACs mMACs
D1 D2 D1 D2 D3 D1 D2 D3 D1 D2 D3 D1 D2 D3 D1 D2 D3
-3.0 1.1 3.0 -3.0 1.1 3.0 -3.0 1.1 3.0
B
UP
DOWN
iDC iMAC mDC mMAC iDC iMAC mDC mMAC
786 2134 961 424 503 958 421 1092 384 760 1201 1628
C
iDC
iMAC
log2FC.Expression
log2FC.Methylation
D
iDC
iMAC
log2FC
TSS 1500 TSS 200 5' UTR 1st exon Body 3' UTR
E
DC
MAC
Methylation
Expression
log2FC
MO~iDC iDC~mDC
F
Common 18.09%
iDC 30.48%
iMAC 51.43%
G
IL1B
CCL20
iDC
iMAC
% Expression
% Methylation
Time (hours)
LPS
H
IL1B
CCL20
IgG H3k27me3
IgG H3k9me3
Relative enrichment
Time (hours)
MO DC MAC

Figure 3

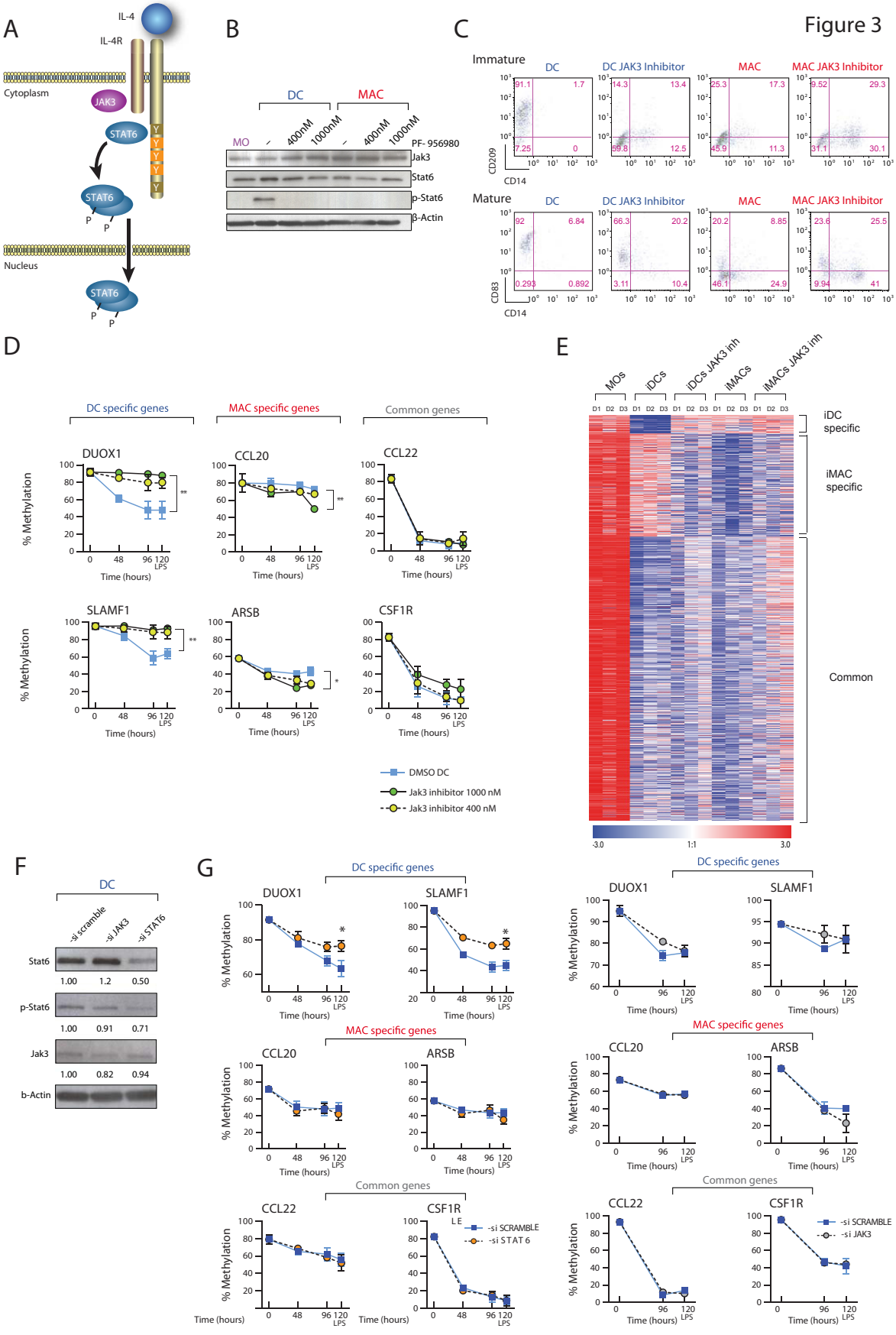
A
IL-4
IL-4R
Cytoplasm
JAK3
STAT6
STAT6
P
P
Nucleus
STAT6
P
P
B
DC
MAC
MO
400nM
1000nM
400nM
1000nM
PF- 956980
Jak3
Stat6
p-Stat6
β-Actin
C
Immature
DC
DC JAK3 Inhibitor
MAC
MAC JAK3 Inhibitor
CD209
CD14
Mature
CD83
CD14
D
DC specific genes
MAC specific genes
Common genes
DUOX1
CCL20
CCL22
SLAMF1
ARSB
CSF1R
% Methylation
Time (hours)
LPS
DMSO DC
Jak3 inhibitor 1000 nM
Jak3 inhibitor 400 nM
E
MOs
iDCs
iDCs JAK3 inh
iMACs
iMACs JAK3 inh
iDC specific
iMAC specific
Common
F
DC
-si scramble
-si JAK3
-si STAT6
Stat6
p-Stat6
Jak3
b-Actin
1.00 1.2 0.50
1.00 0.91 0.71
1.00 0.82 0.94
G
DC specific genes
MAC specific genes
Common genes
DUOX1
SLAMF1
CCL20
ARSB
CCL22
CSF1R
-si SCRAMBLE
-si STAT 6
-si JAK3

Figure 4

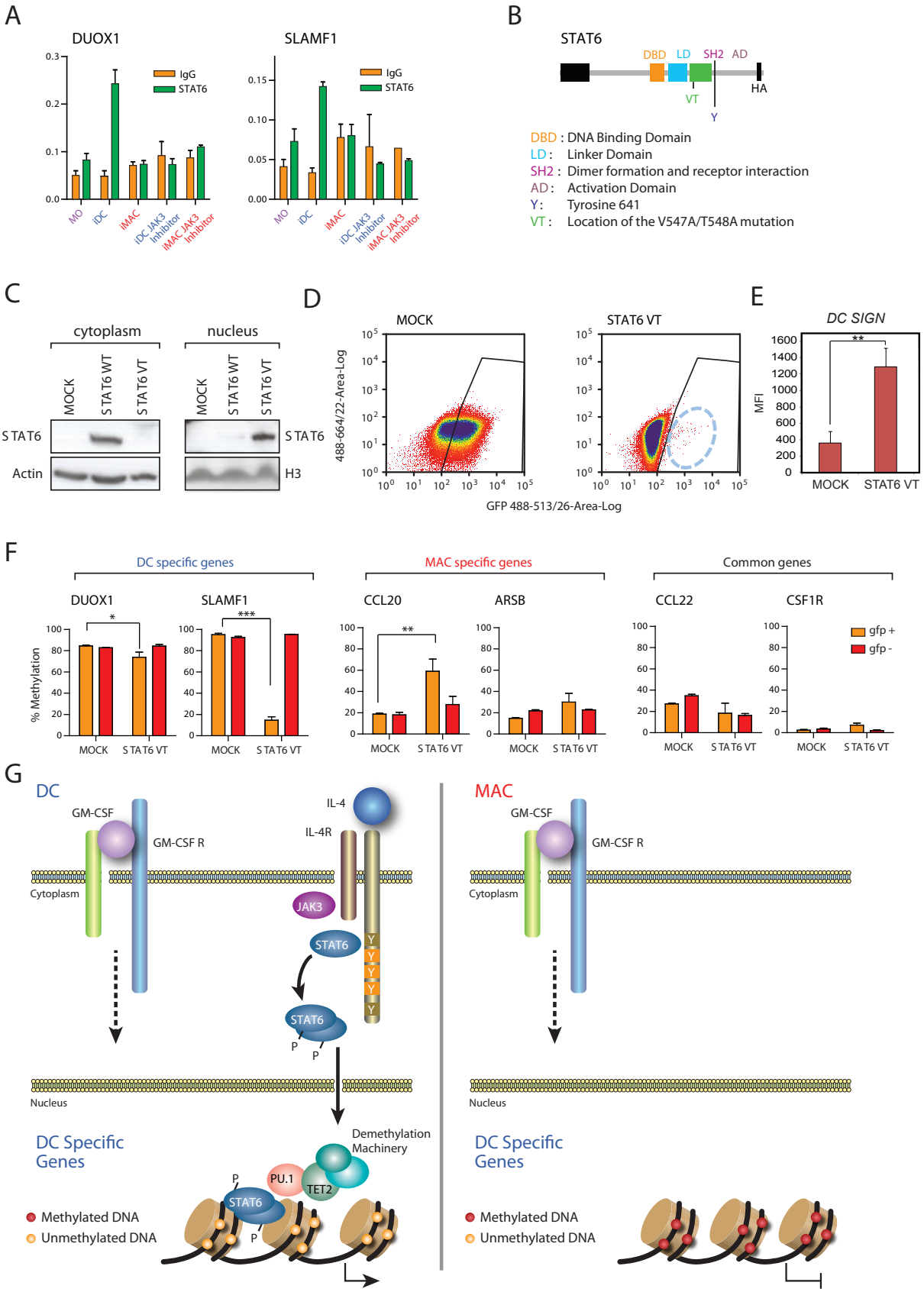
A
DUOX1
SLAMF1
IgG
STAT6
MO
iDC
iMAC
iDC JAK3 Inhibitor
iMAC JAK3 Inhibitor
B
STAT6
DBD
LD
SH2
AD
HA
VT
Y
DBD : DNA Binding Domain
LD : Linker Domain
SH2 : Dimer formation and receptor interaction
AD : Activation Domain
Y : Tyrosine 641
VT : Location of the V547A/T548A mutation
C
cytoplasm
nucleus
MOCK
STAT6 WT
STAT6 VT
STAT6
Actin
H3
D
MOCK
STAT6 VT
488-664/22-Area-Log
GFP 488-513/26-Area-Log
E
DC SIGN
MFI
MOCK
STAT6 VT
F
DC specific genes
MAC specific genes
Common genes
DUOX1
SLAMF1
CCL20
ARSB
CCL22
CSF1R
% Methylation
gfp +
gfp -
G
DC
MAC
GM-CSF
GM-CSF R
IL-4
IL-4R
JAK3
STAT6
Cytoplasm
Nucleus
DC Specific Genes
Demethylation Machinery
PU.1
TET2
Methylated DNA
Unmethylated DNA

Additional File 1

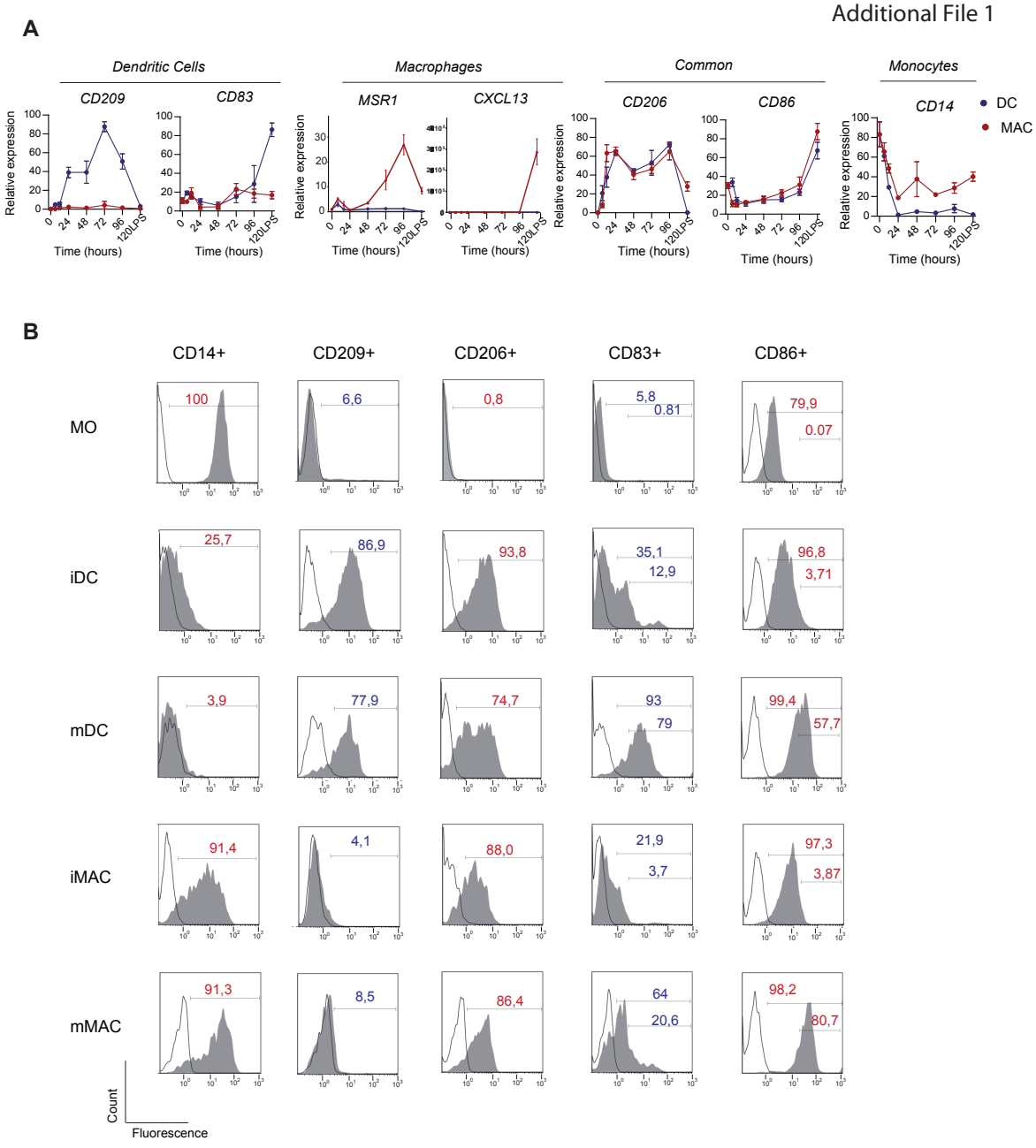

Additional File 3

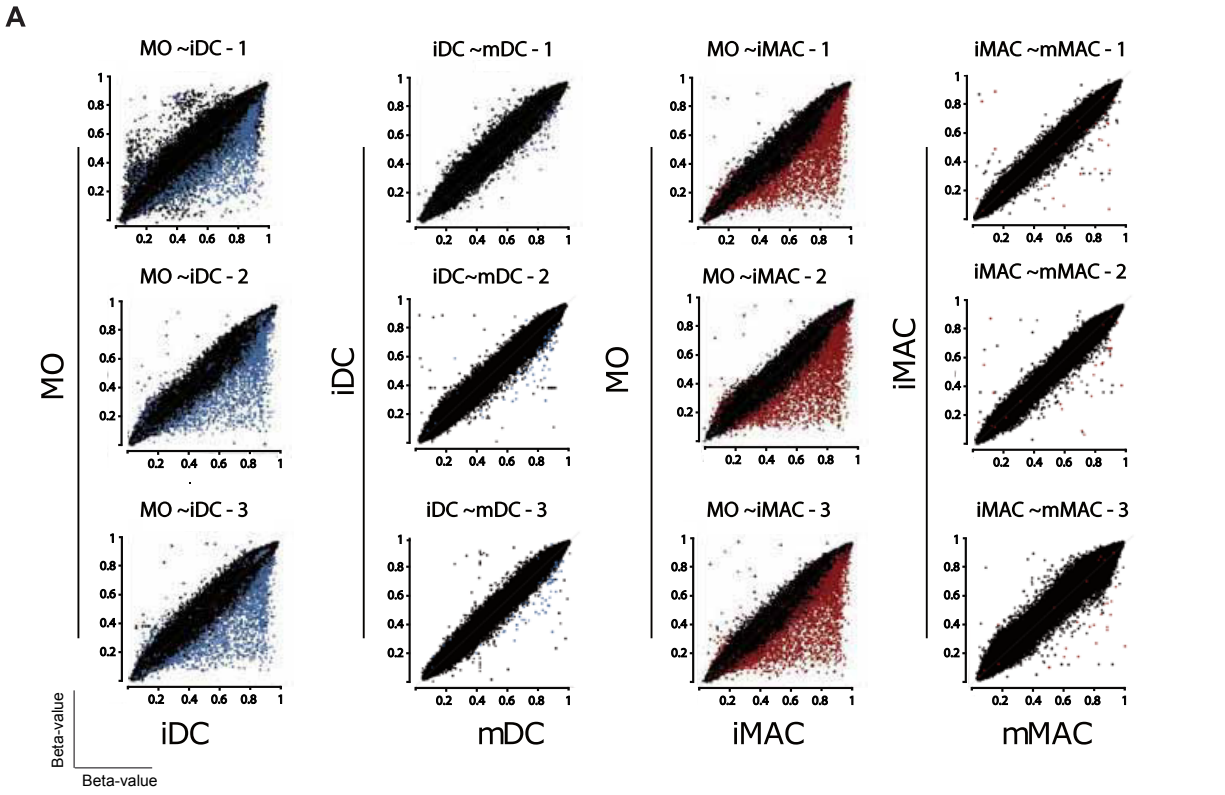

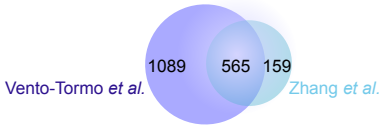

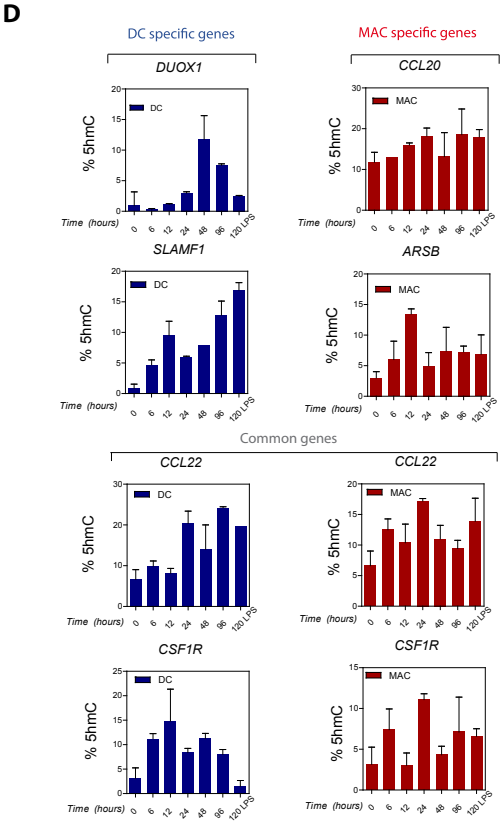

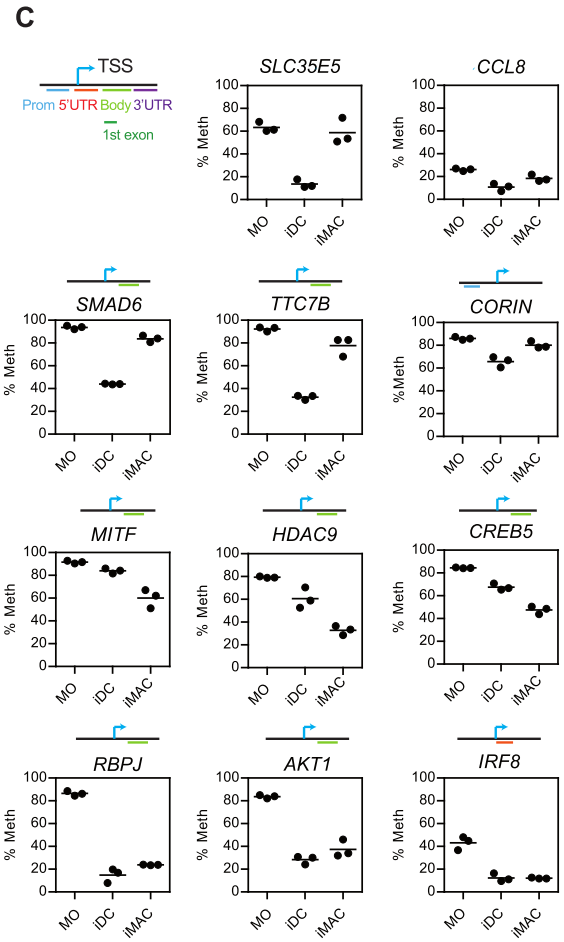

Additional File 4

Gene	CpG number	Localization	LogFC [DC,MAC]	Diff. beta [DC,MAC]	Relevance of gene products in inflammatory context
DUOX1	cg13570892	Body	[-2.62;-]	[-0.28;-]	Protein from NADPH family, involved in lactoperoxidase-mediated defense
SLAMF1	cg26883963	3'UTR	[-4.03;-]	[-0.58;-]	Receptor involved in T and B cell activation, and promotes DC maturation
PFAS	cg00194780	3'UTR	[-2.25;-]	[-0.33;-]	Enzyme involved in purine biosynthesis
SMAD6	cg01339004	Body	[-2.42;-]	[-0.29;-]	Mediator of TGF beta antinflammatory activity
CORIN	cg02955940	TSS1500	[-1.98,-]	[-0.25;-]	Serine protease class of the trypsin superfamily.
CCL8	cg01636591	1stExon;5 'UTR	[-1.33,-]	[-0.20;-]	Chemotactic factor, pro-1nflammatory
TAL1	cg00408773	Body	[-1.02,-]	[-0.15;-]	Transcription factor involved in hematopoyesis.
RUNX1	cg02869559 cg12477880	Body 1stExon; Body	[-1.00;-] [-1.02;-]	[-0.15;-] [-0.15;-]	Transcription factor involved in hematopoyesis.
ARSB	cg07379703	TSS1500	[-;-2.13]	[-0.35;-]	Hydrolisis of sulfate groups of N-Acetyl-D-galactosamine, chondriotin sulfate, and dermatan sulfate
CCL20	cg08575688	TSS200	[-;-1.09]	[-0.17;-]	Chemotactic factor
IL1B	cg14117934	3'UTR	[-;-2.54]	[-0.39;-]	Proinflammatory cytokine and pyrogen
MITF	cg04811592	Body	[-;-2.78]	[-0.31;-]	Transcription factor involved in myeloid differentiation
NLRC5	cg08159663	TSS1500	[-;-1.27]	[-0.21;-]	Inflammasome sensing protein
HDAC9	cg04892643	Body	[-;-2.38]	[-0.35;-]	Histone deacetylase
CASP1	cg17008031	TSS1500	[-;-1.44]	[-0.19;-]	Gene involved in activate the inactive precursor of interleukin-1.
CSF1R	cg07260017 cg12974258	5'UTR TSS200	[-3.81;-3.85] [-1.29;-2.18]	[-0.57;-0.58] [-0.19;-0,19]	M-CSF receptor
CCL22	cg23471482 cg04250732	TSS1500 TSS1500	[-3.22;-3.29] [-1.31;-1.51]	[-0.50;-0.50] [-0.20;-0.20]	Chemotactic factor
DUSP5	cg10080966	Body	[-3.75;-2.82]	[-0.56;-0.57]	Phosphatase that negatively regulates members of the mitogen-activated protein (MAP) kinase superfamily (MAPK/ERK,SAPK/JNK,p38)
IRF8	cg07955474	5'UTR	[-2.09;-2.41]	[-0.33;-0.33]	Transcription factor that regulates myeloid differentiation
RBPJ	cg04722169	Body	[-3.03;-2.29]	[-0.38;-0.38]	Transcriptional regulator from the Notch pathway
AKT1	cg26099837 cg15912732 cg12789068 cg04971812	Body Body Body 3'UTR	[-5.82;-5.72] [-5.33;-4.70] [-1.88;-2.03] [-1.16;-1.42]	[-0.73;-0.73] [-0.71;-0.71] [-0.24;-0.24] [-0.09;-0.09]	Serine/threonine kinase that regulate many processes including metabolism, proliferation, cell survival, growth and angiogenesis
CREB5	cg09930712	Body	[-1.17;-2.65]	[-0.10;-0.10]	Member of the CRE (cAMP response element)-binding protein family.
IL1RN	cg11783497	TSS200	[-2.63;-3.18]	[-0.38;-0.38]	Member of the interleukin 1 cytokine family. Inhibits the activities of interleukin 1, alpha and beta.

Additional File 5

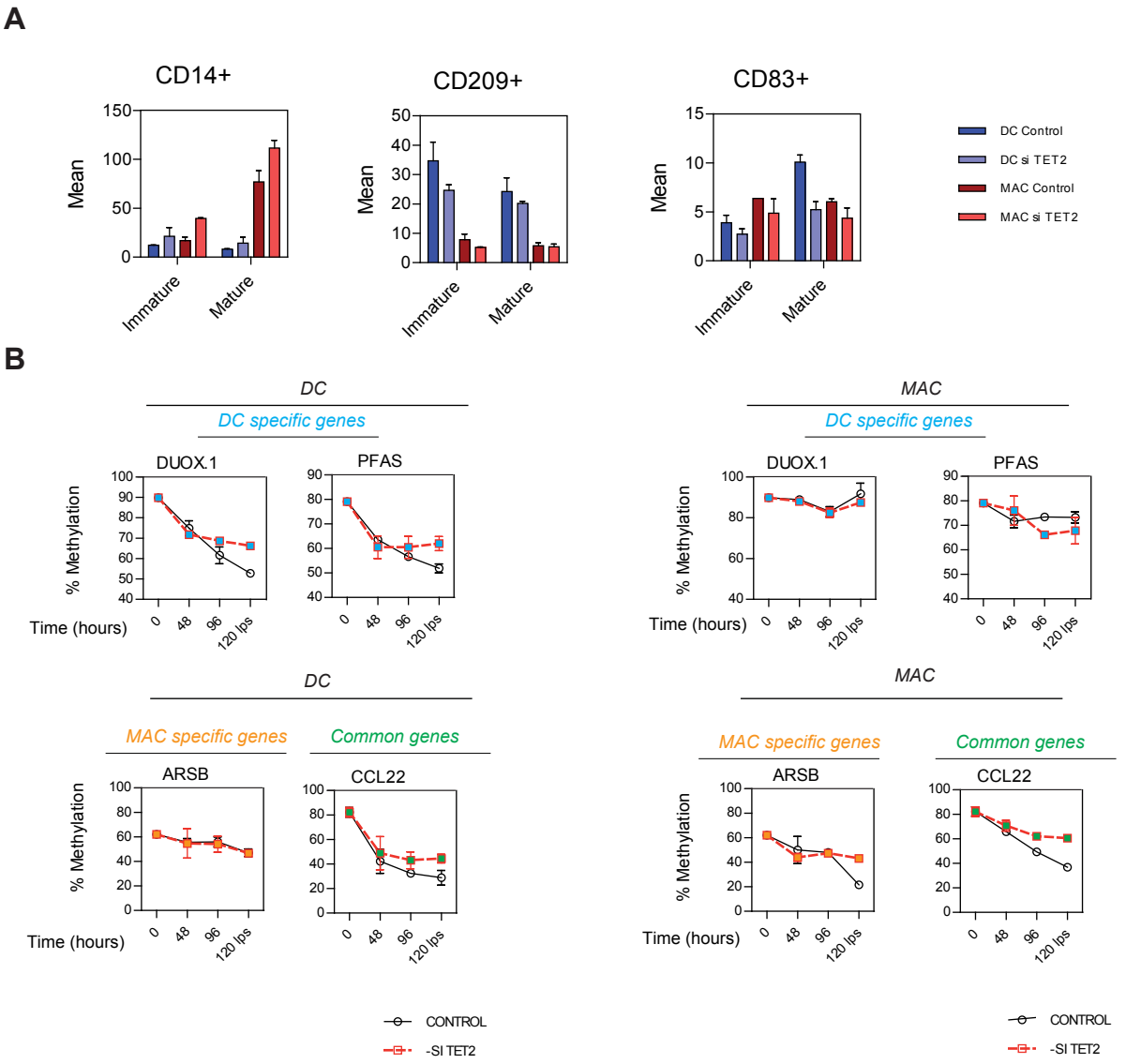

Additional File 7

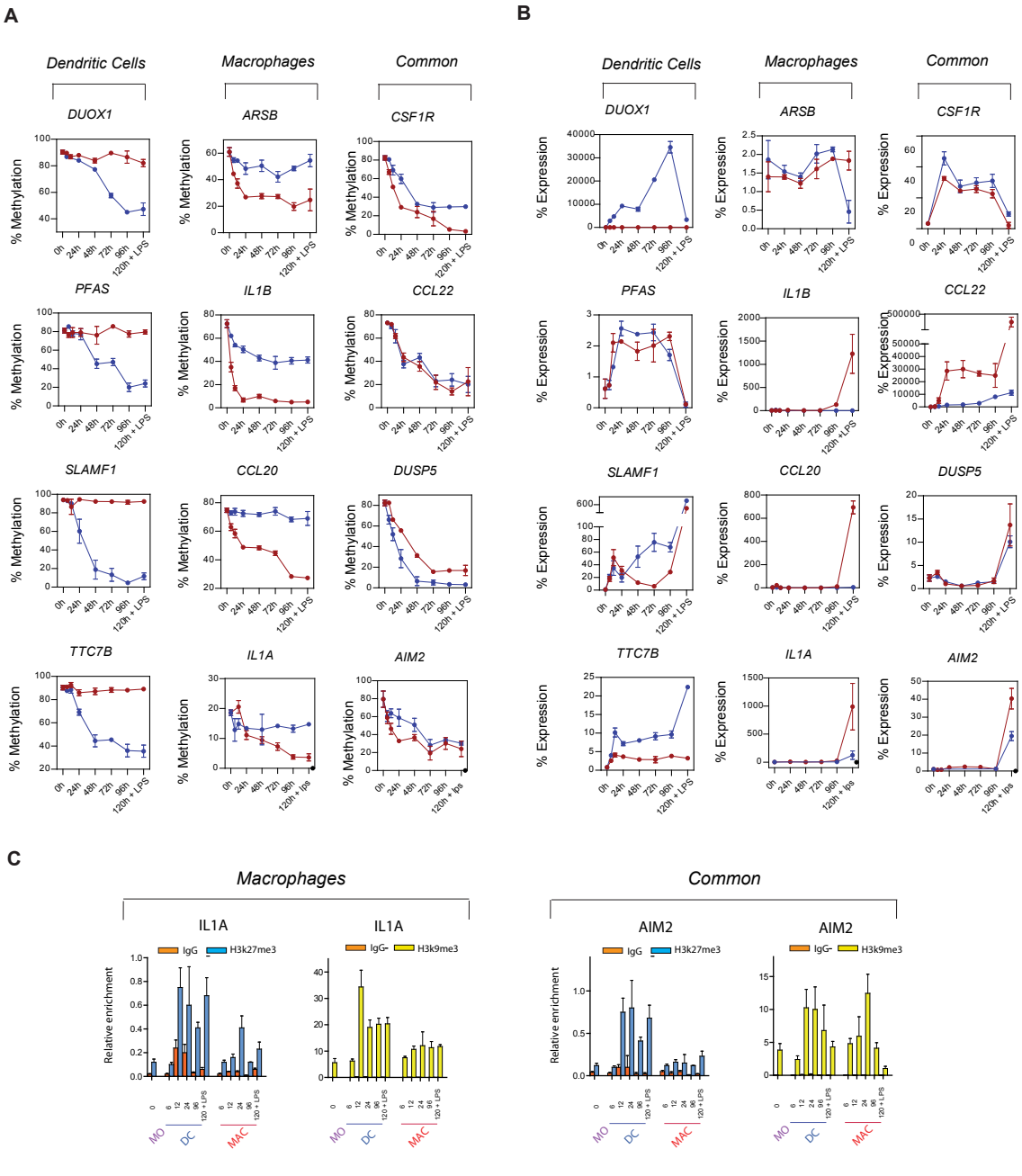

Additional File 8

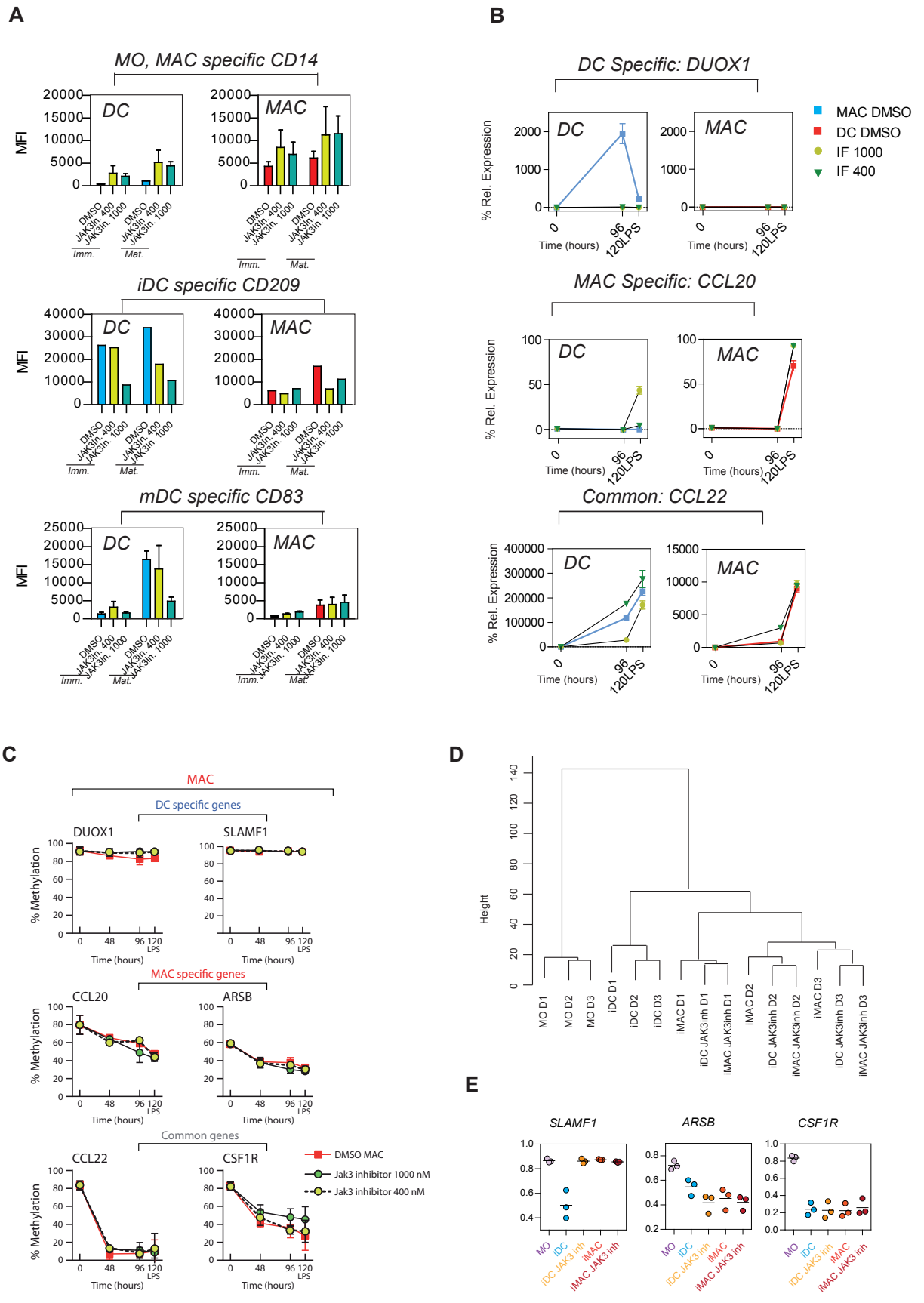

Additional File 9

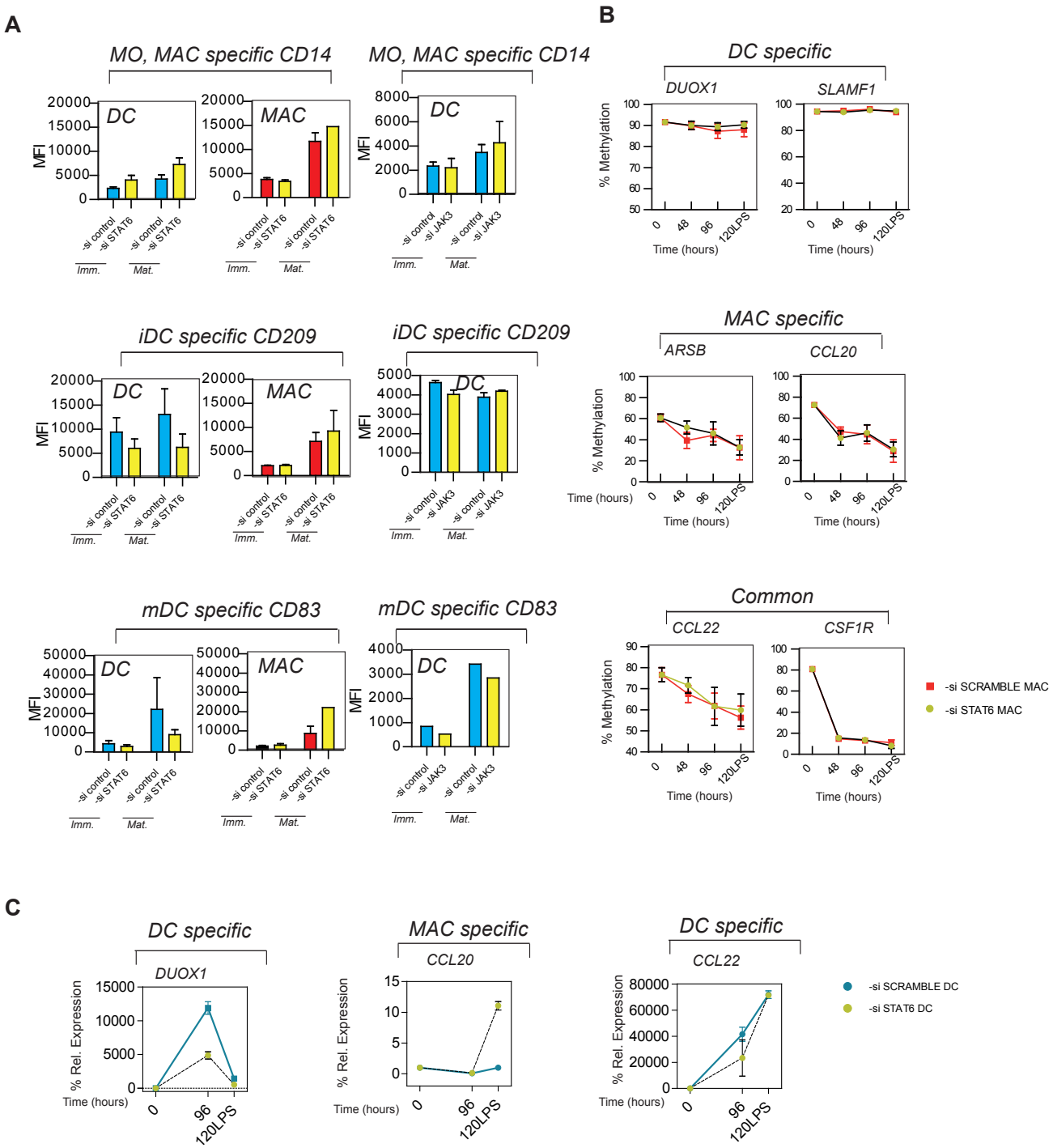

Additional File 10

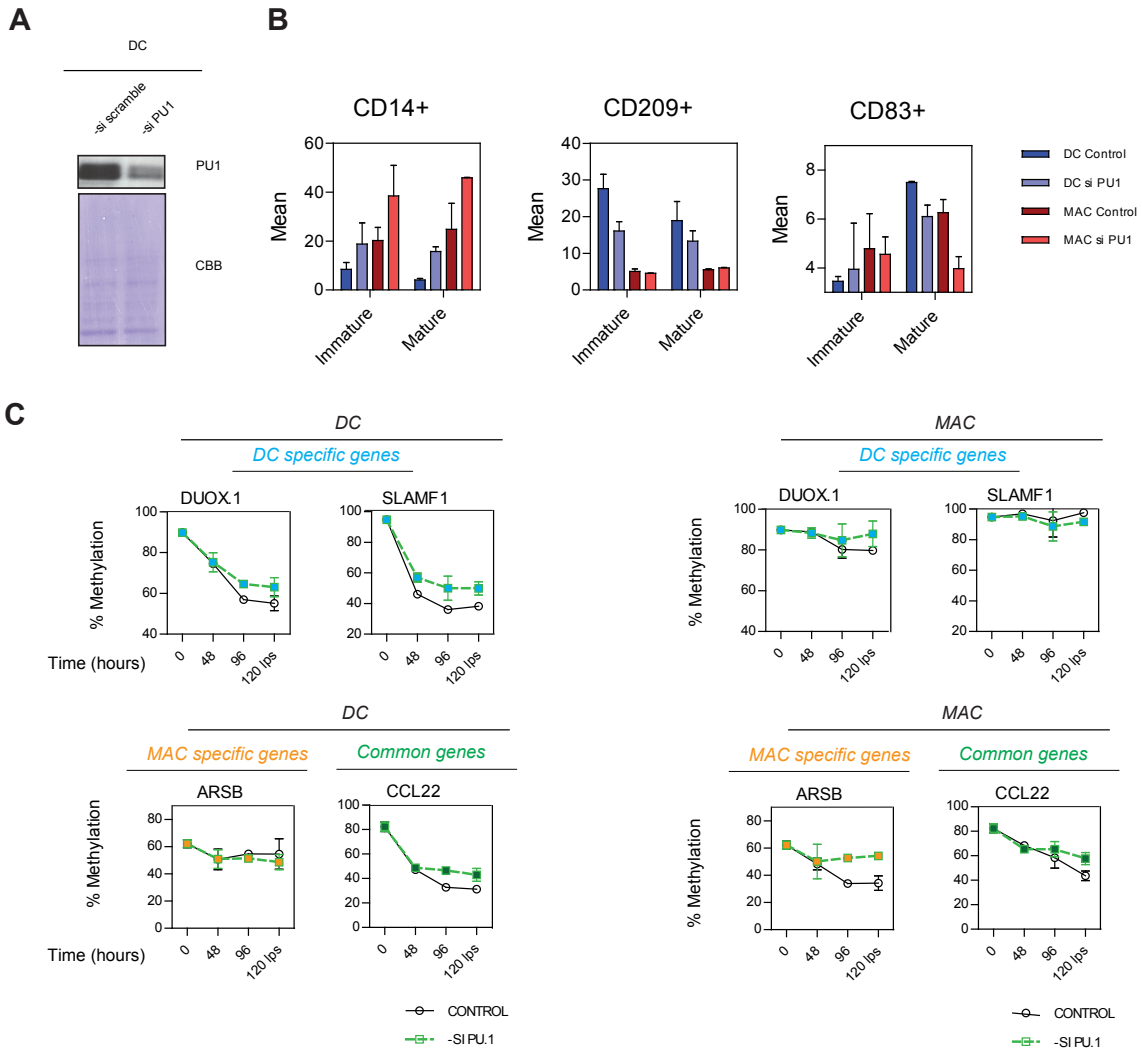

3.2 ARTICLE 2

Title:

A DNA demethylation Signature in Inflammasome Genes Features Autoinflammatory Syndromes

Authors:

Roser Vento-Tormo[1,], Damiana Álvarez-Errico[1,], Antonio García-Gómez[1] and Esteban Ballestar[1]

With the participation of the Autoinflammatory Diseases Clinical Unit and Vasculitis Research Unit Internal Medicine and Department of Immunology (Hospital Clínic-IDIBAPS) and the Autoimmune and Systemic diseases Services (Hospital Vall d'Hebron)

Affiliations:

[1] Chromatin and Disease Group, Cancer Epigenetics and Biology Programme (PEBC), Bellvitge Biomedical Research Institute (IDIBELL), 08908 L'Hospitalet de Llobregat, Barcelona, Spain

Abstract

Monocyte (MO) to macrophage (MAC) differentiation requires the activation of critical genes governing inflammatory and innate immunity functions. A central element of MAC function is the inflammasome, a cytosolic multiprotein complex that assembles in response to infection- or stress-associated stimuli and activates both caspase-1-mediated inflammatory cytokine secretion and pyroptosis, an inflammatory form of cell death. The relevance of the inflammasome is highlighted by its relationship with monogenic autoinflammatory syndromes, which are consequence of gene mutations leading to increased inflammasome activity. Although familial cases are common, penetrance among patients sharing gene mutations can be different, suggesting the participation of mechanisms beyond the gene sequence defect. In this study, we initially observed that inflammasome-related genes are rapidly demethylated during human MO-to-MAC differentiation. Demethylation is associated with increased gene expression and both mechanisms are impaired when methylcytosine dioxygenase TET2 is downregulated. We also determined that DNA demethylation of inflammasome-related genes also occurs when MOs are directly exposed to inflammatory conditions. We also demonstrate a direct role of NF-kB in the regulation of demethylation of these genes. We explored the existence of DNA methylation alterations in patients with Cryopyrin-Associated Periodic Syndromes (CAPS) and Familial Mediterranean fever (FMF), two archetypical monogenic autoinflammatory syndromes. Under the above conditions, MOs from patients undergo more efficient DNA demethylation than those from healthy individuals, revealing that patients are poised for an epigenetically-regulated faster inflammatory response. Our results demonstrate the implication of DNA methylation-associated mechanisms in these disorders and open up prospects for novel therapeutic targets.

Introduction

Innate immune myeloid cells such as monocytes (MOs) and macrophages (MACs) are crucial effectors and regulators of inflammation and adaptive immunity, and are also involved in the maintenance of tissue homeostasis [1]. In response to inflammatory signals (i.e. bacterial infection [2]), circulating MOs extravasate and reach the inflamed tissues, where they terminally differentiate into MACs and/or dendritic cells (DCs). MO-to-MAC differentiation can be recapitulated *in vitro* by exposing them to GM-CSF or M-CSF, with *in vitro* differentiated GM-CSF-MACs producing larger amounts of pro-inflammatory cytokines than M-CSF-MACs. Moreover, MOs can themselves respond to inflammatory cytokines, such as interleukin (IL)-1β, which promotes their activation.

Inflammation is critical to protect the host against pathogen infection but must be tightly regulated. Insufficient inflammation can lead to persistent infection of pathogens whereas excessive inflammation can cause inflammatory diseases. A crucial component of the MO/MAC defence against microbial pathogens and endogenous danger signals is the inflammasome. The inflammasomes are multimeric complexes, that assemble in the cytosol after sensing pathogens- or danger-associated molecular patterns (microbial pathogens, endogenous ATP, uric acid) [3]. Once assembled, caspase-1 (CASP-1) is recruited and activated by the inflammasome, thus being able to produce the active forms of IL-1β and IL-18, and induce an inflammatory form of cell death known as pyroptosis [4]. Both cytokines are key for the inflammation response, due to their function in orchestrating the innate and adaptive immune response, such as their function in mediating the interaction between NK cells and DCs [5], or their capacity to induce T cell polarisation [6].

Inflammasomes consist of a sensor molecule, an adaptor molecule, and the effector molecule CASP-1. The sensor molecules are either members of the NOD-like receptor (NLR) or the absent in melanoma 2 (AIM2)-like receptor (ALR) families [3]. The adaptor molecule apoptosis-associated speck-like protein containing a caspase activation and recruitment domain (ASC), contains specific domains needed for a proper interaction between sensor molecules and CASP-1. Once activated by the inflammasome, CASP-1 is able to cleave different inflammatory proteins (IL-1 β, IL-18, IL-33) into their bioactive forms [7]. Interestingly, the adaptor molecule ASC is not always essential for recruiting CASP-1, as some sensor molecules of the NLR family (i.e. NLRP1) contain the CARD domain [8].

Related with these molecules, Interleukin-1 receptor antagonist (encoded by *IL1RN*) is a potent anti-inflammatory molecule that modulates the biological activity of IL-1 by competing

with IL-1α and IL-1β for IL-1RI binding, thus preventing the formation of a receptor signalling complex and terminating IL-1α and IL-1β-mediated signalling.

The NLRP3 inflammasome is the most extensively studied inflammasome, and is formed after oligomerization of NLRP3, ASC and pro-CASP-1. Other inflammasomes studied and relevant during inflammation are NLRP4, NLRP6, NLRP7, NLRP12, IFI16 and AIM2 [9]. The relevance of the NLRP3 inflammasome is evidenced by the fact that *gain-of-function* mutations in the *NLRP3* gene [also known as *Cold Induced Autoinflammatory Syndrome 1* (*CIAS1*) gene] cause a monogenic autoinflammatory disease named Cryopyrin-Associated Periodic Syndromes (CAPS) which include three different phenotypes named familial cold autoinflammatory syndrome, the Muckle-Wells syndrome and neonatal-onset multisystem inflammatory disease. Autoinflammatory syndromes are a distinct group of diseases characterized by periodic or chronic episodes of systemic inflammatory attacks in the absence of infection or autoimmune disease. Currently, there are over 20 genes that have been associated with different monogenic autoinflammatory syndromes [10]. Other examples besides *NLRP3* include the *MEFV* gene, which encodes the pyrin protein that is mutated in Familial Mediterrean fever (FMF), and the *PSTPIP1* gene, which is mutated in the pyogenic sterile arthritis, pyoderma gangrenosum and acne (PAPA) syndrome.

Despite the well established genetic nature of these syndromes, it had been reported genetically-confirmed healthy individuals in these syndromes, which suggest that the penetrance of the diseases may vary probably as consequence of factors beyond the specific genetic defect. In this sense, it is likely that epigenetic alterations may also participate in the pathogenesis of these syndromes.

Epigenetic modifications, including methylation at cytosines followed by guanines (CpGs) and histone post-translational modifications, are associated with the gene expression status. Changes in these two types of epigenetic modifications take place during cell differentiation. Specifically, genes relevant to MAC function become demethylated (and overexpressed) during MO-to-MAC differentiation [11]. We can hypothesize whether altered epigenetic changes could drive differentiation, or alternatively, whether the aforementioned mutations in autoinflammatory syndromes-associated genes have downstream consequences that eventually drive altered patterns of methylation. By inspecting data from our previous study (Vento-Tormo et al. 2015, *In Press*; GEO Series accession number GSE71837), we observed that several of the inflammasome-related genes become demethylated during MO-to-MAC differentiation, suggesting a role for DNA methylation in the regulation of the transcriptional

status of these genes. In this sense, we hypothesized that these genes are differentially methylated in MOs or MACs from patients with autoinflammatory syndromes with respect to those from healthy individuals. To explore this hypothesis, we performed bisulfite pyrosequencing of these inflammasome-associated genes and confirmed a time dependent demethylation during MO-to-MAC differentiation, correlating with upregulation, either during the differentiation step, or following stimulation with lipopolysaccharide (LPS). Downregulation of the methylcytosine dioxygenase TET2, an enzyme involved in the multistep mechanism leading to active demethylation, resulted in impaired demethylation of these genes, as well as decreased upregulation, demonstrating the relevance of the methylation status of these genes in their transcriptional status. We found that inflammasome-related genes are also demethylated in MOs under inflammatory conditions, such as IL-1 β exposure. Both differentiation and inflammation-related demethylation of inflammasome genes directly depends on stimulation of the NF-kB pathway, as demonstrated by its pharmacological inhibition and the direct interaction of the NF-kB p65 subunit with inflammasome genes that become demethylated. Finally, we have demonstrated that inflammasome genes display more efficient demethylation in activated MOs from patients with CAPS and FMF. Lower DNA methylation levels in these patients correlate with higher gene expression, supporting the functional relevance of DNA demethylation in the abnormal expression levels of these gene products in autoinflammatory syndromes.

Results

A DNA demethylation signature of inflammasome-associated genes during monocyte-to-macrophage differentiation

The comparison of DNA methylation changes during GM-CSF-mediated differentiation from primary human MOs to MACs (followed by LPS-mediated activation) had revealed loss of methylation in thousands of CpG sites, many of which occur in genes relevant to MAC identity and function and are accompanied by subsequent gene expression upregulation (from Vento-Tormo et al. 2015, *In Press*). Interestingly, among those genes displaying significant demethylation, we identified several related with the inflammasome or its targets (Figure 1A). Specifically, genes like those encoding interleukins IL-1α and IL-1 β; the IL-1 α receptor antagonist encoding gene *IL1RN*; the enzyme responsible for cleaving IL-1 β, *CASP-1*; genes encoding inflammasome sensor proteins like AIM2 [12] and NLRC5 [13]; or the adaptor PYCARD [7], displayed loss of methylation in CpG sites in different genomic locations (Figure 1B). Bisulfite pyrosequencing of these CpG sites during MO-to-MAC differentiation confirmed these changes

over time (Figure 1C). In some cases, like *IL1B*, changes were very fast and a demethylation change of over 80% occurred within 24 h after exposure to GM-CSF (Figure 1C). Other genes (*IL1RN*, *NLRC5* and *AIM2*) displayed more gradual methylation changes. Interestingly, in other situations it has been reported that *IL1B* and its antagonist *IL1RN* tend to undergo parallel changes in expression. In these analyses, we included control genes that do not become demethylated during MO-to-MAC differentiation (only after the combined exposure of GM-CSF and IL-4), like *DUOX1*.

In parallel, we also performed quantitative RT-PCR (qRT-PCR) to investigate expression changes of these inflammasome-associated genes over time. These analyses showed that several of these genes, like *IL1A* and *IL1B*, undergo an increase in their mRNA levels, but only after LPS-mediated activation (Figure 1C). In summary, our results showed that inflammasome-associated genes were either concomitantly activated as demethylation progressed, or that demethylation seemed to constitute a necessary and previous step to ensure upregulation of gene expression during the LPS-mediated activation step.

To explore the dependence of DNA demethylation on the gain of expression of these genes, we downregulated the methylcytosine dioxygenase TET2, which has been shown to participate in active demethylation in MOs [14]. To this end, we performed siRNA experiments to test the effects of depleting this enzyme on the demethylation and the upregulation of inflammasome genes. In addition, we also tested the effects on control genes like *DUOX1*. We observed partial impairment of demethylation following TET2 depletion (Figure 1D). The impairment was partial due to a technical aspect related to the inability to achieve the maximum downregulation of TET2 before the differentiation processes had already started. We also observed that these genes accumulate 5-hydroxymethylcytosine (5hmC), the result of the activity of TET2, and that the levels of 5hmC are decreased following TET2 downregulation (Figure 1D). In summary, we can conclude that inflammasome-associated genes depend on TET2-mediated demethylation to become activated.

<u>Direct stimulation of the inflammasome in MOs results in active demethylation of IL-1B, IL1RN and CASP-1</u>

In recent years, it has become clear that MOs carry out specific effector functions during inflammation [15]. MOs can therefore be directly stimulated under inflammatory conditions such as the direct encounter with bacterial antigens, like LPS, or even interleukin IL-1 β.

Our previous results had demonstrated the dependence of expression of inflammasome genes on TET2-mediated DNA demethylation in GM-CSF-mediated MO-to-MAC differentiation.

We now wondered whether these genes also become demethylated in MOs exposed to inflammatory conditions, such as those resulting from toll-like receptors (TLRs) stimulation. To this end we compared the DNA methylation changes in MOs under exposure to IL-1 β and LPS (Figure 2A).

To explore the ability of inflammasome-associated genes to become demethylated we used different conditions to stimulate the inflammasome. We exposed MOs to IL-1 β (20 ng/ml) and LPS (1000 ng/ml) over a period of 24 h. In the case of LPS, we used it alone or in combination with monosodium urate (MSU) crystals (at 200 ng/ml), an NLRP3 inflammasome inducer [16], or in the presence of ATP (at 1 mM) [17]. These conditions were compared to the exposure of MOs to GM-CSF (leading to MAC differentiation).

To test whether these conditions induce apoptosis or necrosis we performed flow cytometry analysis using Annexin V and 7-aminoactinomycin D (7-AAD) staining, and with exposure to camptothecin as a positive control of apoptosis (Figure 2B). We observed that GM-CSF and IL-1 β did not stimulate apoptosis.

Following exposure of MOs to these different stimuli, we performed bisulfite pyrosequencing and quantitative RT-PCR of inflammasome-associated genes. To test the specificity of the observed changes we also analyzed genes that undergo demethylation during MO-to-MAC differentiation but are not necessarily linked to inflammation (i.e. *MITF*). We observed that both LPS and IL-1 β stimulation only resulted in demethylation of inflammasome-associated genes like *IL1B* in a 24 h period (Figure 2C). Our results were also consistent with the property of MSU crystals to enhance LPS-induced release of IL-1 β by MOs through a CASP-1-mediated process [18]. Under our conditions, demethylation associated with IL-1 β or LPS stimulation only affected inflammasome genes (Figure 2C). Changes in DNA methylation of inflammasome genes were associated with a peak of increased mRNA levels around 3-6 h following stimulation (Figure 2D), whereas control genes (*DUOX1* or *MITF*) displayed a different expression dynamics over time.

<u>NF-kB mediates demethylation of inflammasome-associated genes</u>

It is known that TLR-initiated signals generate a strong NF-kB mediated response in MOs and MACs (Figure 3A). Analysis of the sequences in a 5000 bp window around the TSS in genes demethylated in inflammasome-associated genes showed enrichment of NF-kB p65 subunit binding sites (Figure 3B). To investigate the involvement of NF-kB in the DNA demethylation process affecting inflammasome genes, we first explored the influence of NF-kB inhibitors on DNA demethylation. To this end, we treated MOs with the NF-κB inhibitor Bay 11-7082 and

investigated its effects on the DNA methylation changes of inflammasome-associated genes following in different conditions (GM-CSF, IL-1 β and LPS in the absence or presence of MSU and ATP). Bay 11-7082 selectively and irreversibly inhibits the TNF-α-inducible phosphorylation of IκBα, resulting in the reduced expression of NF-κB and of adhesion molecules. Bay 11-7082 eventually reduces the levels of phosphorylated Ser536 of p65, which corresponds to its active form. We tested similar concentrations to the ones previously tested [19], and selected 10 μM for Bay 11-7082. We then performed bisulfite pyrosequencing to measure the effects of this NF-kB inhibitor on the DNA methylation levels of inflammasome-associated genes. Bay 11-7082 dramatically impaired DNA demethylation in all cases (Figure 3C). Control genes not related with inflammation like *MITF* did not display this impairment in demethylation or occurred at a smaller degree (Figure 3D). These effects were also observed at the expression level (Figure 3D).

To test the potential direct effect of NF-kB on these methylation changes, we then performed ChIP assays to assess the binding of NF-κB subunit p65 to inflammasome genes. We confirmed the specific binding of NF-kB p65 to these genes (Figure 3E), particularly evident following stimulation with IL-1 β and LPS, reinforcing the notion that NF-kB participates in the regulation of these genes.

Patients with monogenic autoinflammatory diseases are more prone to demethylation of inflammasome genes

The ability of inflammasome-associated genes to become demethylated and activated provides a potential mechanism that could be dysregulated under certain conditions. As previously introduced, monogenic autoinflammatory syndromes depend on activating genetic mutations like those in the *NLRP3* or *MEFV* genes, associated with CAPS and FMF, respectively. These two genes encode the cryopyrin and pyrin proteins, respectively, which are prototypical inflammasome-related proteins. Given the enhanced pro-inflammatory response of MOs and MACs in patients affected from these syndromes, we wondered whether inflammasome-related genes would also display aberrant methylation levels.

We therefore compared the ability to demethylate inflammasome-related genes in MOs following stimulation by GM-CSF, leading to differentiation to MACs, or under the aforementioned inflammatory conditions in the presence of IL-1 β, in a small cohort of patients with CAPS (n=8), patients with FMF (n=5) and healthy controls (n=13). Patients with CAPS and FMF displayed *bona fide* mutations (Supplementary Table 1).

We observed that unstimulated MOs from patients and healthy controls displayed virtually identical levels of DNA methylation for genes like *IL1B*, *ILR1N* and *NLRC5*. However, we

observed that MOs treated with IL-1β undergo significantly more efficient demethylation in patients with CAPS when compared to healthy controls. This tendency was also observed for MOs stimulated with GM-CSF for 24 h. (Figure 4A and 4B). Despite the small range of the differences observed, these results suggest that inflammasome-related genes have a tendency to become demethylated in patients with monogenic autoinflammatory diseases.

In summary, our results indicate that IL-1 β and LPS-stimulated MOs from patients with CAPS patients display lower methylation and higher gene expression levels than their healthy counterparts. The difference between our observations for CAPS and FMF patients may add an additional potential biomarker that suggest a difference in the epigenetic pathway related to the exacerbated upregulation of inflammasome related genes in these two diseases.

Discussion

Our results identify for the first time the existence of a TET2-dependent DNA demethylation signature for inflammasome-related genes both in MO-to-MAC differentiation and in MOs under inflammatory conditions. The ability of inflammasome-related genes to become demethylated is also dependent on NF-kB. Moreover, we report that the DNA methylation-dependent regulation of inflammasome product genes, notably *IL1B,* is altered in autoinflammatory diseases like CAPS and FMF, providing a complementary mechanism, in addition to the well described genetic defects, for the exacerbated inflammatory function in these diseases, and a potential source for therapeutic targeted treatments.

Our study reports the relationships between DNA demethylation and upregulation of inflammasome-related genes both in MO-to-MAC differentiation and also upon direct TLR-mediated stimulation of MOs. Moreover, we have demonstrated in the case of GM-CSF-mediated MO-to-MAC differentiation that, for several of these genes, DNA demethylation occurs during the differentiation step, prior to their increase in expression which occurs only once MACs are activated with LPS. This suggests that DNA demethylation is a first and required step to guarantee a proper and fast response of the inflammasome against an external aggressor. DNA demethylation is also TET2 dependent, as demonstrated by the partial impairment of these effects following TET2 downregulation. In fact, TET2 downregulation prevents DNA demethylation, upregulation and proper inflammasome-mediated response, thus supporting the relevance of active DNA demethylation during the process. Once again, these results are in agreement with the general observation of DNA demethylation during *in vivo* myeloid differentiation, studied previously by our group and others (Vento-Tormo et al, *In Press*; [11, 20]).

For the majority of inflammasome-related genes, DNA demethylation is rapidly induced within the first 24 h following MO stimulation with GM-CSF, LPS or IL-1 β. On a practical note, this rapid demethylation dynamics limits the possibility of performing optimal inhibition experiments to downregulate efficiently TET2.

Our data shows that several of the genes in the inflammasome cascade are regulated by DNA methylation changes. For example, we found DNA demethylation of genes encoding for sensor molecules *NLRC5* and *AIM2*. NLRC5, a member of the NLRs family, is activated by a variety of signals including LPS, and AIM2 assembles upon sensing foreign cytoplasmic double-stranded DNA. When these proteins detect danger signals, they are able to oligomerize and form the inflammasome structure. PYCARD and CASP-1, respectively adaptor and effector molecules of the inflammasome, are also demethylated. PYCARD is an adaptor protein that is able to recruit CASP-1, which is involved in the production of active forms of inflammatory cytokines like IL-1α or IL-1β, which are also regulated by demethylation during both MO-to-MAC differentiation and MO direct activation. Other proteins associated with the inflammasome activity, for which their encoding genes become demethylated in these processes, include IL1RN and PSTPIP2. *IL1RN* is an antagonist of the *IL1B* gene and is overexpressed during inflammation, perhaps as a compensatory mechanism for IL-1β signaling. On the other hand, PSTPIP2 is a negative regulator of caspase-1-autonomous IL-1β production.

Our results also prove the implication of NF-kB in relation with DNA demethylation and upregulation of inflammasome-related genes during MO activation. NF-kB may participate directly or indirectly in the recruitment of TET2 resulting in subsequent DNA demethylation. However, in a previous study from our group focusing on another MO-derived differentiation model, we were unable to identify an interaction between the p65 subunit of NF-kB and TET2, but interaction with other sub-units cannot be ruled out [21]. Additional experiments to explore the potential interaction between other NF-kB subunits and TET2 would be needed. Due to the relevance of DNA methylation mechanisms in the disease, one could speculate whether NF-kB pathway modulators could be employed in patients with autoinflammatory diseases in order to improve their therapies.

Finally, we have also demonstrated that this DNA demethylation signature occurs in two representative IL-1β -driven monogenic autoinflammatory diseases such as CAPS and FMF, which are associated with increased activity of inflammasome and increased production of biologically active IL-1β. Despite the well recognized associations of these diseases with mutations in inflammasome-related genes (*NLRP3* and *MEFV*), there are both patients with the

archetypical clinical features (periodic fever, sterile inflammation) carrying low-penetrance variants or even healthy individuals carrying *bona fide* mutations. It is likely that alternative mechanisms, including DNA methylation alterations, related to the aberrant activation of the inflammasome could also participate in the pathogenesis of these disorders. In this sense, our findings support the notion that DNA demethylation is associated with the acquisition of the CAPS and FMF phenotype, and could set a lower threshold for IL-1 β production, establishing a positive loop leading to more IL-1 β production and further inflammasome activation. It is remarkable that non stimulated MOs or differentiated MACs do not display differences in these genes respect to the DNA methylation status of the inflammasome-related genes among patients and healthy controls, and only IL-1β stimulation is capable of discriminating or evidencing a difference between them. Such result would suggest that the presence of IL-1β, which recapitulates the natural environment of MOs in these diseases, poises DNA methylation changes in patients, causing a major induction of gene expression in contrast to controls. In other words, the presence of IL-1β induces DNA demethylation of inflammasome-related genes that are at the same time stimulating the production of IL-1β. In patients, MOs present a higher rate of IL-1β production than in healthy individuals, and therefore stimulating DNA demethylation at a faster rate.

In our experiments, we had a few examples of patients harboring different mutations who exhibited a similar methylation profile in IL-1 β -stimulated MOs in genes like *IL1B, ILR1N* and *NLRC5*. These findings suggest that DNA methylation alterations could potentially be used as a biomarker for these diseases, reaching to those symptomatic patients that do not meet the genetic diagnostic criteria. In this sense, the generation of high-throughput profiles of DNA methylation for these patients could provide further insight into pathogenic mechanisms as well as broaden diagnostic capacity.

For the selected inflammasome-related genes we did not observe any pre-existing DNA methylation defect in MOs. Perhaps inflammasome activation could cause pyroptosis (a type of cell death), and therefore these cells would be discarded (and not isolated with our separation procedure). For that reason, it is possible that these discarded cells correspond to those that are exposed longer to IL-1β stimulus and consequently, with higher rates of DNA hypomethylation. In any case, further high-throughput DNA methylation analysis would allow identifying potential pre-existing epigenetic lesions in MOs that occur before any type of induction.

In summary, our study suggests the existence of a DNA methylation-mediated control of inflammasome-related genes in MOs that is likely to contribute to set a quick response in an

inflammatory environment. These changes are exacerbated in the context of IL-1 β mediated monogenic autoinflammatory diseases. Whether these alterations are causal or consequence of an upstream dysregulated signal (perhaps additional mutations) remains to be determined. However, our results provide additional targets for potential therapeutic intervention and highlight the need of exploring these mechanisms further to test the possibility of using these epigenetic events as biomarkers in the context of autoinflammation.

Material and Methods

Isolation of peripheral blood MOs and differentiation and activation experiments

Human samples (blood) corresponding to healthy controls (or for MO differentiation or activation) purposes used in this study came from anonymous blood donors and were obtained as buffy coats from the Catalan Blood and Tissue Bank (Banc de Sang i Teixits) in Barcelona. The anonymous blood donors received oral and written information about the possibility that their blood would be used for research purposes, and any questions that arose were then answered. Before obtaining the first blood sample all donors signed a consent form at the Banc de Teixits. The Banc de Sang follows the principles set out in the WMA Declaration of Helsinki. Regarding the blood samples corresponding to CAPS and FMF patients, they came from Hospital Clínic and Hospital Vall d'Hebron, both in Barcelona. Clinicians had approval from their corresponding Ethics committees and patients signed an informed consent. The blood was carefully layered on a Ficoll–Paque gradient (Amersham, Buckinghamshire, UK) and centrifuged at 2000 rpm for 30 min without braking. Peripheral blood mononuclear cells (PBMCs), from the interface between the plasma and the Ficoll–Paque gradient, were then collected and washed twice with ice-cold PBS, followed by centrifugation at 2000 rpm for 5 min. Pure MOs were isolated from PBMCs using positive selection with MACS magnetic CD14 antibody (Miltenyi Biotec, Bergisch Gladbach, Germany). Cells were then resuspended in RPMI Medium 1640 (1X) + GlutaMAXTM-1 (Gibco, Life Technologies^{TM}) containing 10% foetal bovine serum, 100 units/ml penicillin, 100 µg/ml streptomycin and antimycotic. For MAC differentiation, medium was supplemented with 800U GM-CSF (Gentaur Molecular Products). MOs were also activated either with LPS (1 µg/ml, Sigma-Aldrich) or with IL-1 β (10ng/ml, Peprotech) and samples were harvested at different time points between 0 and 24 h.

Bisulphite sequencing and pyrosequencing

Bisulphite pyrosequencing was used to validate CpG methylation changes resulting from the analysis with the Infinium HumanMethylation450 BeadChips. Bisulphite modification of

genomic DNA isolated from MOs, DCs, and MACs was performed by standard methods. Oxidative bisulphite modifications was performed as described recently by Booth and colleagues [22]. The time course was measured in biological triplicates. Briefly, 2 µl of the converted DNA (corresponding to approximately 20-30 ng) were used as a template in each subsequent PCR. Primers for PCR amplification and sequencing were designed with the PyroMark® Assay Design 2.0 software (Qiagen). PCRs were performed with the HotStart Taq DNA polymerase PCR kit (Qiagen), and the success of amplification was assessed by agarose gel electrophoresis. PCR products were pyrosequenced with the PyromarkTM Q24 system (Qiagen). All primer sequences are listed in Supplementary Table 2.

Quantitative RT-PCR

For quantitative RT-PCR of cellular genes, cDNA was produced with the SuperScript II Reverse Transcriptase (Invitrogen Co). Quantitative Real-Time PCR (Q-RT-PCR) was done on a LightCycler 480 II System using LightCycler 480 SYBR Green Mix (Roche). Reactions were carried out in triplicate and qRT-PCR data were analyzed using the standard curve method. We used the housekeeping gene RPL38 and HPRT1 as a control. All primer sequences are listed in Supplementary Table 2.

Transfection of primary human MOs

We used ON-TARGETplus siRNAs against TET2 to perform knockdown experiments in peripheral blood MOs. We also used ON-TARGETplus Non-targeting Control Pool as a negative control. We transfected MOs with siRNAs using Lipofectamine 3000 Reagent (Thermo Fisher Scientific Co., Carlsbad, CA, USA) and added cytokines 24 h later. We examined the levels of the target proteins by western blot 4 days after siRNA transfection. Three biological replicates of the experiments were performed.

Graphs and heatmaps

All graphs were created using Prism5 Graphpad. Heatmaps of the expression or methylation data were generated using the Genesis program (Graz University of Technology).

Putative binding of NF-kB motifs

Possible occurrence of NF-kB subunit binding motifs in the region comprising 2500 bp upstream and 2500 bp downstream with respect to transcription start site was inspected using TRANSFAC and ConSite matrices. The matches of the sequences against the set of TRANSFAC matrices were

performed using R environment, specifically the functions countsPWM and matchPWM contained in the Bioconductor package Biostrings.

Chromatin immunoprecipitation (ChIP) assays

To test the binding of p65 NF-kB to inflammasome gene portions with putative binding sites, we performed ChIP assays as previously described. We used a rabbit polyclonal against the C-t of NF-kB p65 (sc-372, Santa Cruz Biotechnology. Immunoprecipitated material was used for analyses of specific sequences by quantitative RT-PCR (see primers sequences in Supplementary Table 2).

References

1. Geissmann F, Manz MG, Jung S, Sieweke MH, Merad M, Ley K. Development of monocytes, macrophages, and dendritic cells. Science 2010; 327:656-61.

2. Serbina NV, Pamer EG. Monocyte emigration from bone marrow during bacterial infection requires signals mediated by chemokine receptor CCR2. Nat Immunol 2006; 7:311-7.

3. Guo H, Callaway JB, Ting JP. Inflammasomes: mechanism of action, role in disease, and therapeutics. Nat Med 2015; 21:677-87.

4. Vanaja SK, Rathinam VA, Fitzgerald KA. Mechanisms of inflammasome activation: recent advances and novel insights. Trends Cell Biol 2015; 25:308-15.

5. Mailliard RB, Alber SM, Shen H, Watkins SC, Kirkwood JM, Herberman RB, et al. IL-18-induced CD83+CCR7+ NK helper cells. J Exp Med 2005; 202:941-53.

6. O'Shea JJ, Paul WE. Mechanisms underlying lineage commitment and plasticity of helper CD4+ T cells. Science 2010; 327:1098-102.

7. Srinivasula SM, Poyet JL, Razmara M, Datta P, Zhang Z, Alnemri ES. The PYRIN-CARD protein ASC is an activating adaptor for caspase-1. J Biol Chem 2002; 277:21119-22.

8. Faustin B, Lartigue L, Bruey JM, Luciano F, Sergienko E, Bailly-Maitre B, et al. Reconstituted NALP1 inflammasome reveals two-step mechanism of caspase-1 activation. Mol Cell 2007; 25:713-24.

9. Broderick L, De Nardo D, Franklin BS, Hoffman HM, Latz E. The inflammasomes and autoinflammatory syndromes. Annu Rev Pathol 2015; 10:395-424.

10. Martinon F, Aksentijevich I. New players driving inflammation in monogenic autoinflammatory diseases. Nat Rev Rheumatol 2015; 11:11-20.

11. Klug M, Heinz S, Gebhard C, Schwarzfischer L, Krause SW, Andreesen R, et al. Active DNA demethylation in human postmitotic cells correlates with activating histone modifications, but not transcription levels. Genome Biol 2010; 11:R63.

12. Hornung V, Ablasser A, Charrel-Dennis M, Bauernfeind F, Horvath G, Caffrey DR, et al. AIM2 recognizes cytosolic dsDNA and forms a caspase-1-activating inflammasome with ASC. Nature 2009; 458:514-8.

13. Davis BK, Roberts RA, Huang MT, Willingham SB, Conti BJ, Brickey WJ, et al. Cutting edge: NLRC5-dependent activation of the inflammasome. J Immunol 2011; 186:1333-7.

14. Klug M, Schmidhofer S, Gebhard C, Andreesen R, Rehli M. 5-Hydroxymethylcytosine is an essential intermediate of active DNA demethylation processes in primary human monocytes. Genome Biol 2013; 14:R46.

15. Auffray C, Sieweke MH, Geissmann F. Blood monocytes: development, heterogeneity, and relationship with dendritic cells. Annu Rev Immunol 2009; 27:669-92.

16. Martinon F, Petrilli V, Mayor A, Tardivel A, Tschopp J. Gout-associated uric acid crystals activate the NALP3 inflammasome. Nature 2006; 440:237-41.

17. Gattorno M, Tassi S, Carta S, Delfino L, Ferlito F, Pelagatti MA, et al. Pattern of interleukin-1beta secretion in response to lipopolysaccharide and ATP before and after interleukin-1 blockade in patients with CIAS1 mutations. Arthritis Rheum 2007; 56:3138-48.

18. Giamarellos-Bourboulis EJ, Mouktaroudi M, Bodar E, van der Ven J, Kullberg BJ, Netea MG, et al. Crystals of monosodium urate monohydrate enhance lipopolysaccharide-induced release of interleukin 1 beta by mononuclear cells through a caspase 1-mediated process. Ann Rheum Dis 2009; 68:273-8.

19. de la Rica L, Garcia-Gomez A, Comet NR, Rodriguez-Ubreva J, Ciudad L, Vento-Tormo R, et al. NF-kappaB-direct activation of microRNAs with repressive effects on monocyte-specific genes is critical for osteoclast differentiation. Genome Biol 2015; 16:2.

20. Alvarez-Errico D, Vento-Tormo R, Sieweke M, Ballestar E. Epigenetic control of myeloid cell differentiation, identity and function. Nat Rev Immunol 2015; 15:7-17.

21. de la Rica L, Rodriguez-Ubreva J, Garcia M, Islam AB, Urquiza JM, Hernando H, et al. PU.1 target genes undergo Tet2-coupled demethylation and DNMT3b-mediated methylation in monocyte-to-osteoclast differentiation. Genome Biol 2013; 14:R99.

22. Booth MJ, Ost TW, Beraldi D, Bell NM, Branco MR, Reik W, et al. Oxidative bisulfite sequencing of 5-methylcytosine and 5-hydroxymethylcytosine. Nat Protoc 2013; 8:1841-51.

Figure legends

Figure 1. Inflammasome genes are prone to DNA methylation during MO to MAC differentiation. (A) Diagram depicting the activation of the inflammasome upon LPS or IL1A/IL1B binding to their receptor (TLR4 or IL-1R respectively), κ pathway activation and induction of inflammasome components. Stress or cell damage signals trigger inflammasome assembly and activate pro-caspase 1. In turn, activated Caspase 1 cleaves pro-IL1βinto bioactive IL1β that is released. Mature IL1βbinds IL1R, establishing a positive loop of inflammasome activation. (B) Heatmaps showing methylation and expression changes in genes related to inflammasome, between MOs, iMACs and mMACs. A scale is shown at the bottom, where normalized beta-values (for DNA methylation), and expression values (for gene expression, in arbitrary units) range from -3 (lower levels, blue) to +3 (higher levels, red) (C) Dynamics of loss of DNA methylation measured by bisulphite pyrosequencing of modified DNA and gain of gene expression (qRT-PCR) during MO to MAC differentiation in the presence of GM-CSF. Data were relative to HPRT1 and RPL38, used as controls. (D) Effects of siRNA silencing of TET2 on DNA methyl intermediates over time are

shown. We analyze both 5-methylcytosine (5mC) and 5-hydroxymethylcytosine by combining DNA bisulphite (BS) and oxidative bisulphite (oxBS) techniques (BS = 5mC + 5hmC, oxBS= 5mC).

Figure 2. Loss of DNA methylation in inflammasome genes occurs both in MO-to-MAC differentiation and MO activation. (A) A scheme depicting the different treatments applied to MOs. (B) Viability and apoptosis in MO cultured using different inflammasome stimuli (from left to right and top to bottom: LPS, LPS+ATP, LPS+MSU, IL1B, GM-CSF and camptothecin) were analysed with assays using Annexin V and 7-aminoactinomycin D (7-AAD). (C) DNA methylation quantified by bisulphite pyrosequencing of modified DNA, in MOs cultured in different stimuli over time (LPS, LPS+ATP, LPS+MSU in blue, IL-1β in red, and GM-CSF in green). Besides inflammasome-associated genes, we included two control genes, *DUOX1* and *MITF* (D) Changes of gene expression by qRT-PCR in MOs cultured in the same conditions described above.

Figure 3. Analysis of NF-kB pathway contribution to demethylation of inflammasome genes. (A) Scheme showing NF-kB pathway activated by TLR4 and IL1R. The inhibition point of BAY11-7082 is depicted in red. (B) NF-kB subunit p65 binding sites in inflammasome genes that undergo demethylation were predicted using match analysis based on TRANSFAC matrix and ConSite predicting tool and are represented. P65 Binding sites were calculated from +/-2500 bp around TSS. The regions selected for designing primers for ChIP assays are underlined (C) Time course analysis of DNA methylation of inflammasome genes upon indicated inflammasome stumuli in the presence or absence of the NF-kB inhibitor BAY 11-7082 was performed by bisulphite modified DNA pyrosequencing. The graphs in the left side show the results obtained for 5 different genes in a time course manner. Each point is the average of independent biological duplicates. The name of each of the genes analyzed is indicated on the left, and the treatments (LPS, IL-1 β and GM-CSF) on top of each graph. In the right panel, heatmaps for each of the treatment (LPS, IL-1 β and GM-CSF) summarize the level of methylation for a panel of 8 genes. (D) Effects on gains of gene expression for the same inflammaose-associated genes in the absence or presence of the NF-kB inhibitor BAY 11-7082, as analyzed by qRT-PCR in MOs cultured in the same conditions described above (E) ChIP assays for a selection of inflammasome genes showing the binding of the NF-kB p65 12 and 24 h following stimulation of MOs with IL-1B, LPS, GM-CSF.

Figure 4. Comparison of the demethylation of inflammasome genes in CAPS and FMF MOs versus those from healthy individuals. (A) Methylation levels of MOs stimulated with IL-1 β for 24 h, as estimated by bisulphate pyrosequencing. (B) Methylation levels of MOs stimulated with GM-CSF for 24 h, as estimated by bisulphate pyrosequencing

Figure 1

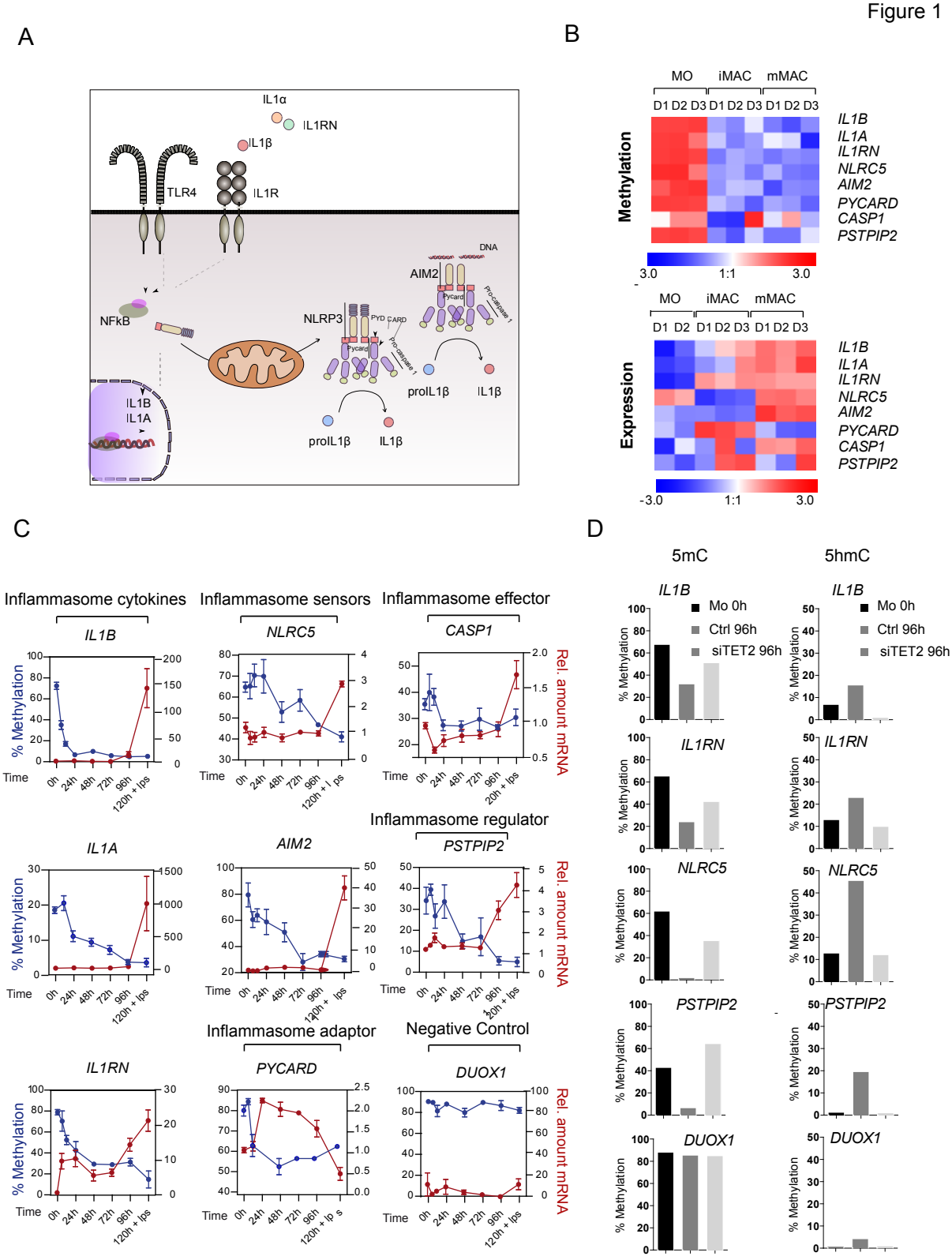
A
IL1α
IL1RN
IL1β
TLR4
IL1R
DNA
AIM2
Pycard
Pro-caspase 1
NFkB
NLRP3
PYD CARD
Pycard
Pro-caspase 1
proIL1β
IL1β
IL1B
IL1A
proIL1β
IL1β
B
MO
iMAC
mMAC
D1 D2 D3 D1 D2 D3 D1 D2 D3
Methylation
IL1B
IL1A
IL1RN
NLRC5
AIM2
PYCARD
CASP1
PSTPIP2
3.0
1:1
3.0
MO
iMAC
mMAC
D1 D2 D1 D2 D3 D1 D2 D3
Expression
IL1B
IL1A
IL1RN
NLRC5
AIM2
PYCARD
CASP1
PSTPIP2
-3.0
1:1
3.0
C
Inflammasome cytokines
Inflammasome sensors
Inflammasome effector
IL1B
NLRC5
CASP1
% Methylation
Rel. amount mRNA
Time
0h 24h 48h 72h 96h 120h + lps
Inflammasome regulator
IL1A
AIM2
PSTPIP2
Inflammasome adaptor
Negative Control
IL1RN
PYCARD
DUOX1
D
5mC
5hmC
IL1B
IL1RN
NLRC5
PSTPIP2
DUOX1
Mo 0h
Ctrl 96h
siTET2 96h
% Methylation

Figure 2

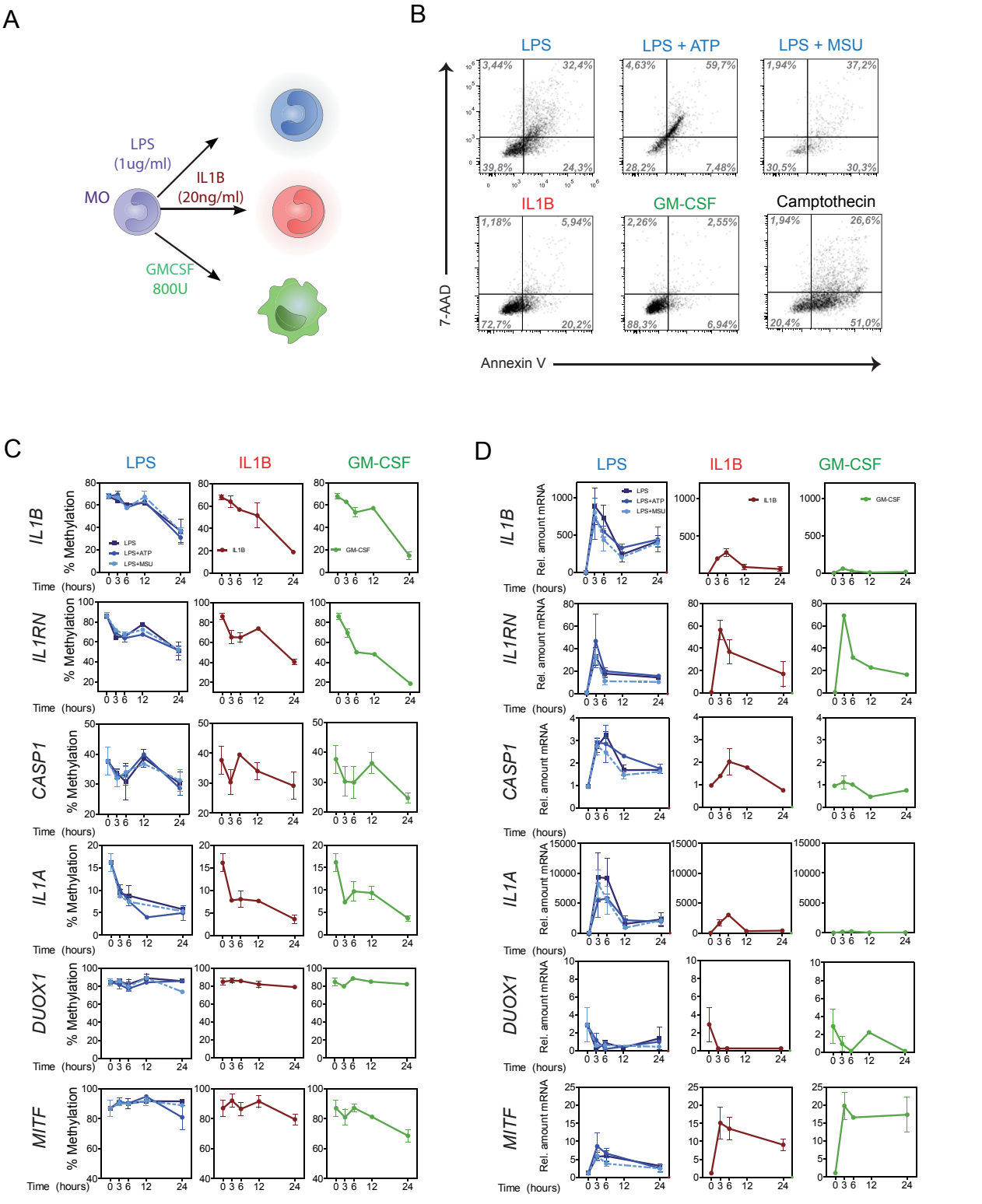
A
LPS
(1ug/ml)
MO
IL1B
(20ng/ml)
GMCSF
800U
B
LPS
LPS + ATP
LPS + MSU
IL1B
GM-CSF
Camptothecin
7-AAD
Annexin V
C
LPS
IL1B
GM-CSF
IL1B
IL1RN
CASP1
IL1A
DUOX1
MITF
% Methylation
Time (hours)
D
Rel. amount mRNA
Time (hours)

Figure 3

A

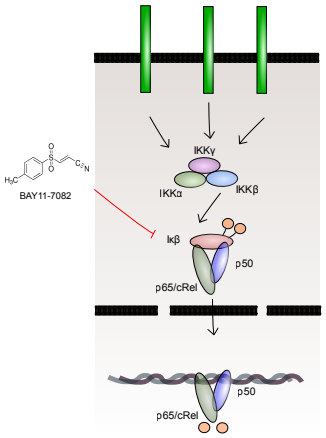

B

	CONSITE (80%)
IL1B	702(-); 703(-); 1878(-); 2205(+); 2206(-); 3004(-); 3004(+); 4710(-); 4710(+)
IL1A	616(+); 617(-); 2248(+); 2336(+); 2653(+);3311(-);3722(+); 3759(-); 4047(-); 4047(+)
IL1RN	469(-); 469(+); 470(-); 959(+); 960(-); 985(-); 1056(-); 1069(-); 1069(+); 1114(+); 1998(+); 2067(+); 2068(-); 2636(-); 4084(+); 4085(+)
NLRC5	210(-); 210(+); 211(-); 997(-); 1174(-); 2251(+); 2472(-); 2473(-); 2720(-); 3692(+); 3735(+); 4480(-); 4642(-)
AIM2	1220(-); 1556(-); 1740(-); 1740(+); 1741(-); 1940(+); 1941(-); 1941(+); 2029(-); 2029(+); 2030(-); 2051(-)
PYCARD	82(-); 590(-); 1051(+); 1994(-); 1994(+); 1995(-); 2696(+); 3354(+); 3355(-); 3355(+); 3385(-); 3516(+); 3648(-); 3715(-)
CASP1	253(+); 751(-); 1075(+); 1076(-); 1076(+); 1077(-); 1626(+); 1716(-); 2360(-); 2453(-); 3055(+); 3056(-); 3056(+); 3079(+); 4063(-); 4173(-); 4173(+); 4543(-); 4543(+)
PSTPIP2	2470(+); 2704(+); 2705(-); 2705(+); 3170(+); 3186(+); 3303(+); 3304(-); 3304(+); 3814(+)

C

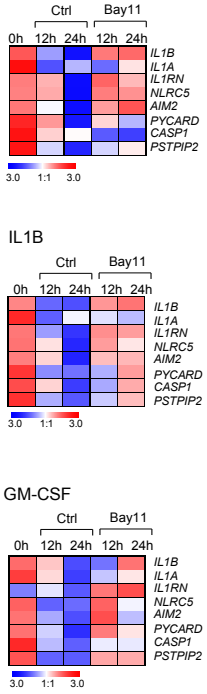

D

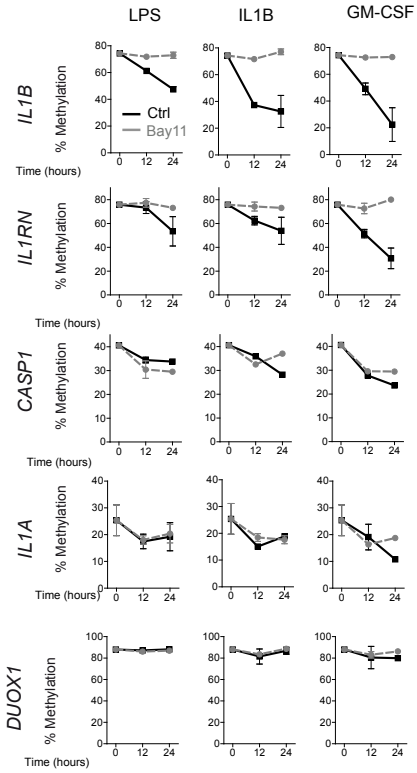

E

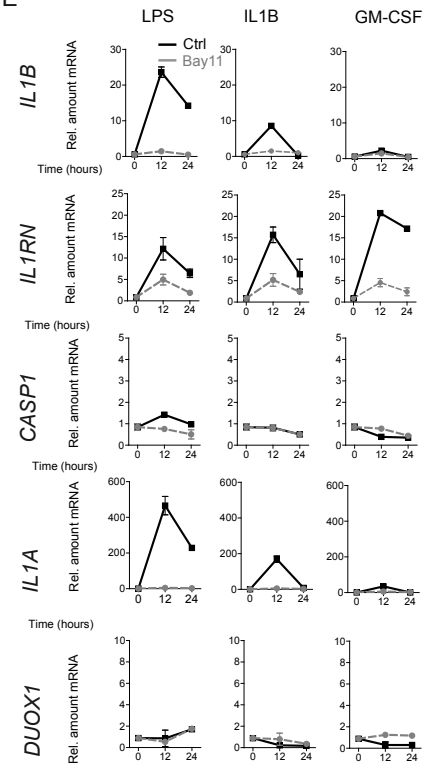

E

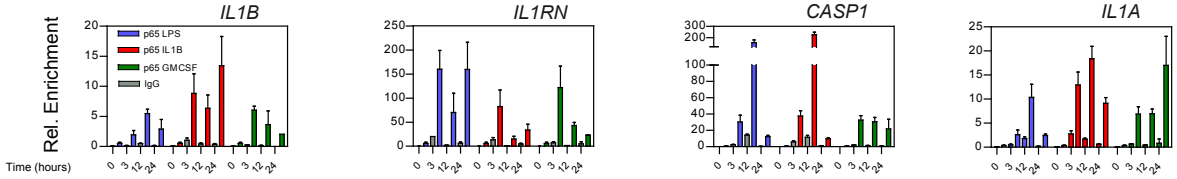

Figure 4

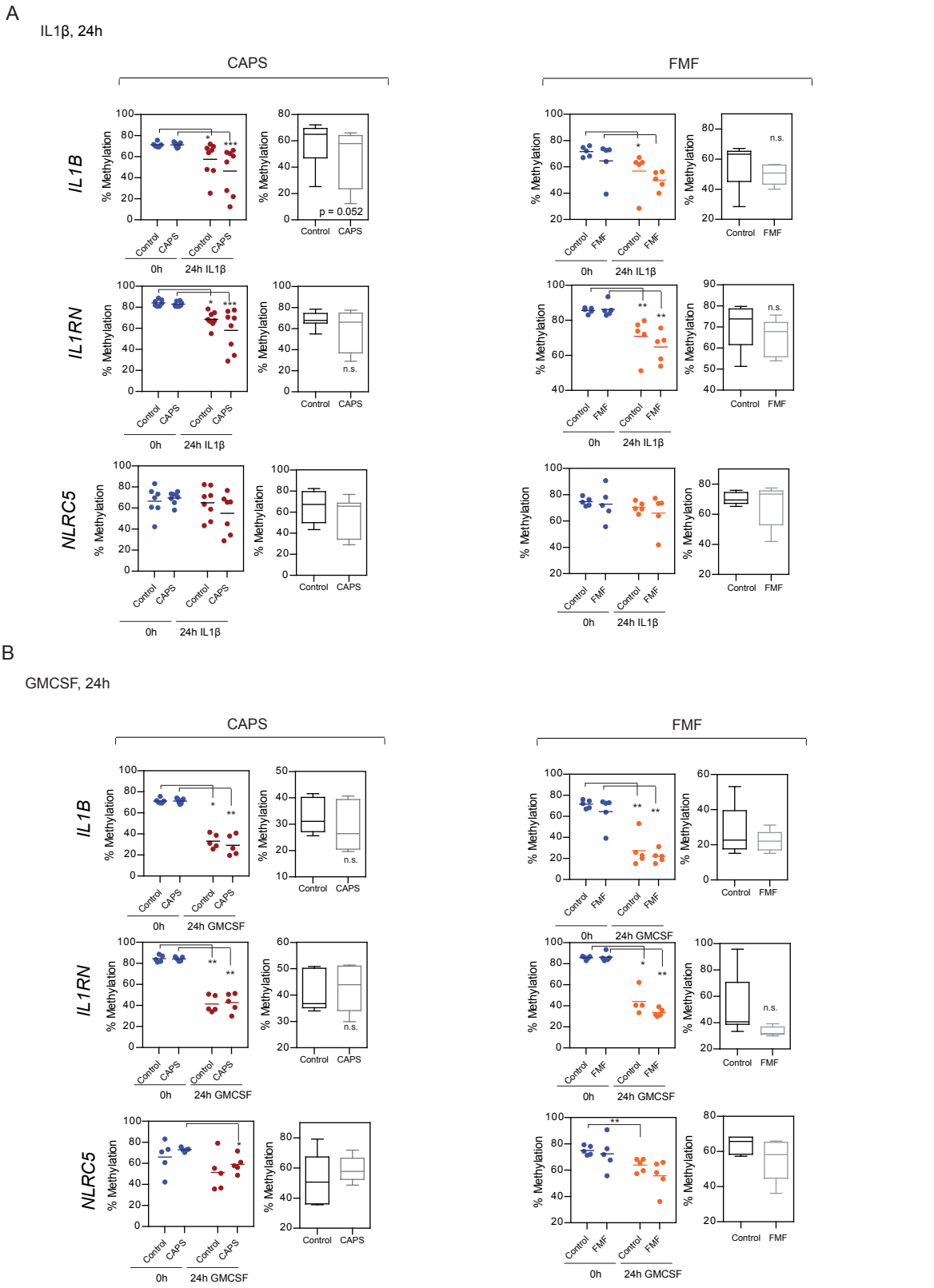
A
IL1β, 24h
CAPS
FMF
IL1B
IL1RN
NLRC5
% Methylation
Control
CAPS
FMF
0h
24h IL1β
p = 0.052
n.s.
B
GMCSF, 24h
24h GMCSF

Supplementary Table 1

Disease phenotipe	Genetic variant in	Sex	Age at Disease onset	Age at the time of the Study	Treatment
CAPS	NLRP3 (exon)				
	A439V (3) / WT	F	4	41	Canakinumab
	A439V (3) / WT	F	8	43	Canakinumab
	A439V (3) / WT	F	14	56	Symptomatic
	A439T (3) / WT	M	15	75	Anakinra
	A439T (3) / WT	F	20	49	Anakinra
	A439T (3) / WT	F	15	17	Anakinra
	A439T (3) / WT	M	42	62	Anakinra
	A439T (3) / WT	M	3	40	Anakinra
FMF	MEFV (exon)				
	M694I (10) / WT	M	8	28	Colchicine
	P369S-R408Q* (3) / WT	M	36	40	Colchicine
	A744S (10) / WT	M	30	39	Canakinumab
	M694V (10) / V726A (10)	M	3	38	Anakinra
	M694V (10) / WT	M	36	49	Canakinumab

Abbreviations: WT= wild type allele; F= female; M= male.
* heterozygous complex allele.

3.3 ARTICLE 3

Journal:

FEBS J. (2015, 282(9):1815-25. doi: 10.1111/febs.13045)

Title:

Gains of DNA methylation in myeloid terminal differentiation are dispensable for gene silencing but influence the differentiated phenotype

Authors:

Roser Vento-Tormo, Damiana Álvarez-Errico, Javier Rodríguez-Ubreva and Esteban Ballestar

Affiliations:

Chromatin and Disease Group, Cancer Epigenetics and Biology Programme (PEBC), Bellvitge Biomedical Research Institute (IDIBELL), 08908 L'Hospitalet de Llobregat, Barcelona, Spain

Abstract

DNA methylation-mediated regulation drives and stabilizes transcription states throughout development. In myeloid differentiation, DNA methylation changes occur predominantly in the direction towards hypomethylation. Also, *in vitro* differentiation of monocytes to dendritic cells and macrophages is characterized by DNA demethylation. In this study, we identified the existence of methylation changes in the direction of hypermethylation among genes that become repressed during monocyte-to-dendritic cell differentiation. We identified the acquisition of DNA methylation in genes such as *CSF3R, FYN*, and *CX3CR1,* but not in others, such as *CD14.* Analysis of the dynamics of methylation and expression changes of these genes revealed that loss of expression was rapid and was associated with the loss of H3K4me3 and H3K36me3, whereas gains of DNA methylation were progressive and partially concomitant with increases in H3K9me3 and H3K27me3. Inhibition of DNA methyltransferases, with the DNA replication-independent drug nanaomycin A, revealed that there were no effects on expression and H3K4me3 changes, despite the partial impairment of DNA methylation and H3K27me3 acquisition. However, cells treated with the DNA methyltransferase inhibitor showed lower levels of dendritic cell surface markers, suggesting a potential effect on the stability of the differentiated phenotype. Our data give rise to a novel perspective on the functional relevance and mechanisms of the acquisition of DNA methylation in myeloid cell differentiation.

Introduction

DNA methylation is a major epigenetic mechanism involved in determining and stabilising cell-fate decisions. Differentiation changes during haematopoiesis are directional; cells become less methylated as differentiation progresses in the myeloid branch [1–4], and this is accompanied by the upregulation of lineage-specific genes. Comparison of progenitors and cells at the various stages of differentiation in the lymphoid and myeloid branches has confirmed this hypomethylation trend in the latter, in contrast to the changes observed in lymphoid differentiation. Demethylation also characterizes myeloid cell terminal differentiation processes that lead to functional mature cell types. The findings obtained with in vitro models that recapitulate terminal differentiation in the myeloid lineage are consistent with the findings obtained from comparing cells isolated at different stages of differentiation. For instance, monocyte (MO)-to-dendritic cell (DC) and MO-to-macrophage (MAC) differentiation are also accompanied by DNA demethylation [5,6], although other MO-related differentiation models, such as MOto-osteoclast differentiation, show acquisition of DNA methylation to a similar extent as demethylation events [7]. However, this latter differentiation process might be an exception, given that it is accompanied by massive cellular fusion and generation of polykaryons, in which the genetic material is redundant and high levels of repression are required. The restricted occurrence of hypermethylation events in myeloid differentiation processes raises questions about the functional relevance and mechanisms involved in silencing inappropriate genes during lineage commitment. In fact, examining the dynamics of DNA methylation changes in both directions reveals that the timing is different for DNA demethylation and gene activation than for acquisition of DNA methylation and gene silencing [7].

The establishment of de novo DNA methylation has been well studied in oocytes and during development [8,9], and also in the context of cancer, where many CpG islands become hypermethylated [10]. Findings in recent years have revealed that DNA hypermethylation in cancer is mainly driven by instructive mechanisms [11]. On the other hand, hypermethylation in cancer cells constitutes a mechanism leading to the inappropriate silencing of genes, particularly when it involves cell cycle or tumour suppressor genes. This has given rise to an interest in the generation of drugs that can reverse aberrant hypermethylation.

As this process is rather limited in the context of differentiation, e.g. in myeloid cells, where DNA demethylation seems to predominate, little is known about the roles and mechanisms associated with genes that become hypermethylated. We do not know whether hypermethylation occurs mainly in a passive manner. Also, we do not fully understand why

certain genes that are repressed become hypermethylated, whereas others do not. It is likely that acquisition of DNA methylation during differentiation occurs through instructive mechanisms as well.

Here, we investigated the dynamics of the setting of DNA methylation during MO-to-DC and MO-to-MAC differentiation, and its potential functional relevance to these differentiation processes. To this end, we chose several genes that are repressed when MOs differentiate to DCs and MACs. We identified changes towards hypermethylation in a few CpG sites near the transcription start sites (TSSs) of genes such as the granulocyte-specific gene CSF3R and the kinase gene FYN. In contrast, CD14, which is also repressed during these two differentiation processes, showed no changes in DNA methylation. These changes occurred after a decrease in histone H3K4me3 and H3K36me3, but were coincident with the increase in repressive markers such as H3K9me3 and H3K27me3. Inhibition of DNA methyltransferases (DNMTs) with nanaomycin A, a replication-independent specific inhibitor of DNMT3b, did not alter the repression of these genes, even though the acquisition of hypermethylation was partially abolished. Flow cytometry analyses indicated that such decreases in the acquisition of DNA methylation affected the expression levels of DC-characteristic surface markers, suggesting a potential role in establishing the phenotype of these cells. Our results indicate that acquisition of DNA methylation has little effect on the direct expression changes of hypermethylated genes, although a general role in stabilising the differentiated phenotype cannot be discounted.

Results

Acquisition of DNA methylation in genes that are repressed during the MO-derived differentiation processes

DNA methylation changes in MO-to-MAC and MO to-DC differentiation mainly occur in the direction of demethylation [5,6]. This is consistent with the results obtained from comparing the DNA methylation profiles of isolated cells at different stages of myeloid differentiation, in which demethylation occurs as differentiation progresses. The above-referenced analyses on MO-to-MAC and MO-to-DC differentiation were performed with a low-resolution method [5] or an array-based method [6], which, although having a coverage of 99% of RefSeq genes, allows the analysis of ~ 480 000 of the 28 million CpG sites (~ 1.5%) of the human methylome. This means that, despite the overall prevalence of DNA demethylation events, the acquisition of DNA methylation at individual CpG sites in these differentiation processes might have been underestimated. To investigate the potential acquisition of DNA methylation at CpGs in genes that are repressed during these processes, we focused on a selection of genes. To this end, we

first derived MACs and DCs from MOs by stimulating peripheral blood monocytes with granulocyte-MAC colony-stimulating factor (GM-CSF) and GM-CSF + interleukin (IL)-4, respectively. We also stimulated immature MACs (iMACs) and immature DCs (iDCs) with lipopolysaccharide (LPS) to generate their mature counterparts (Fig. 1A). These cells showed the expected changes in surface markers such as CD14, the level of which decreased during differentiation towards DCs, whereas the decrease in CD14 level in MACs was less marked (Fig. 1B). On the other hand, the level of CD209 increased in DCs, but not in MACs, as expected. Finally, the level of the mature DC surface marker CD83 increased only DCs after exposure to LPS, but not in MACs (Fig. 1B), as revealed by fluorescenceactivated cell sorting (FACS) analysis. We also used quantitative RT-PCR to determine the mRNA levels of these and specific markers of DCs and MACs (Fig. 1C). These included not only CD209 and CD83, but also CD206 (common to DCs and MACs), CD86 (characteristic of mature DCs and MACs), LAIR1 (specific to MACs), and CXCL13 (specific to mature MACs) (Fig. 1C). We then tested the occurrence of cell division during these two differentiation processes. We measured the levels of cell proliferation by incubating cells with bromodeoxyuridine (BrdU). Fewer than 10% were found to be BrdU-positive between 1 and 5 days, confirming the low replication rate of these cells (Fig. 1D). This supports the notion that any DNA methylation changes observed in this period are independent of DNA replication.

We next investigated changes in the DNA methylation status of selected CpG sites around the TSSs of selected genes during MO-to-DC and MO-toMAC differentiation. To this end, we chose genes that are known to become totally or partially silenced during these differentiation processes. Genes in this selection included the granulocyte-specific gene CSF3R, which codes for a cytokine that controls the production, differentiation and function of granulocytes, and CX3CR1, another MO-specific gene. We also included CD14, which codes for the membrane receptor, and is downregulated in DCs and, to a lesser extent, in MACs. Previous DNA methylation studies had reported no changes for this gene. Other genes included NLRP3, which codes for a member of the Nod-like receptor family that is involved in recognising the molecular patterns expressed by invading pathogens, and FYN, a gene encoding a member of the src-family Tyr kinases. Finally, we looked at PRKCE, on the basis of our own expression array data (unpublished results by Vento-Tormo and colleagues). A schematic representation of these genes and the locations of primers for the expression and DNA methylation analysis is shown in Fig. 1E. We performed real-time quantitative PCR and compared the expression levels of all the aforementioned genes between peripheral blood MOs and derived iDCs and iMACs (Fig. 1F). In all of these comparisons, we found lower levels of expression in the differentiated cells than in the originating MOs.

To test the potential increase in the DNA methylation levels in these genes between MOs and DCs, we first performed bisulfite pyrosequencing of CpG sites located near the TSSs for all of the genes. Our analysis revealed significantly higher methylation levels in DCs for CSF3R, FYN, NLRP3 and PRKCE, although no differences were observed for CD14 (Fig. 1G). Changes were relatively small, and genes such as CSF3R experienced an increase in methylation from 20% in MOs to 40% in DCs. However, these changes were reproducible in different experiments. The expression data for these genes in MOs and DCs confirmed an inverse relationship in all cases.

We found changes in almost all cases in the transition from MOs to iDCs and iMACs, with no further increase in the transition to their mature counterparts following exposure to LPS. In all cases, except for FYN, DNA methylation was acquired during differentiation to both DCs and MACs. For this reason, we focused on the MO-to-iDC conversion in the subsequent experiments.

Silencing and loss of activating histone modifications precede hypermethylation during MO-to-DC differentiation

We observed acquisition of DNA methylation in various genes that become repressed during differentiation from MOs. Experiments in a related model of MO-toosteoclast differentiation had revealed that genes that become hypermethylated are silenced before acquiring DNA methylation [7], indicating that expression changes are driven by other mechanisms. In this context, DNA methylation changes in such genes would be more likely to play a stabilising role than be a driving mechanism. This contrasts with the concomitant demethylation associated with activation that was observed in the same differentiation model [7]. We explored the dynamics of expression and DNA methylation changes through differentiation to DCs by focusing on three of the above genes: CSF3R and FYN, in which DNA methylation increases, and CD14, in which it does not. CSF3R and FYN were chosen because they were among those showing the greatest changes, and also because of their physiological relevance in the context of DC-to-MAC differentiation. We found that CSF3R and FYN showed a sharp decrease in expression during the first 6 h following the addition of GM-CSF and IL-4 (Fig. 2B), whereas DNA methylation increased more gradually and was delayed with respect to silencing (Fig. 2C).

Our results suggest that expression changes, which occur earlier than DNA methylation changes, are associated with other regulatory mechanisms, perhaps those related to transcription factor binding, and possibly with specific histone modifications. Changes in DNA methylation could also be associated with the subsequent acquisition of other histone modifications. This prompted us to perform chromatin immunoprecipitation (ChIP) experiments with four histone modifications, including H3K4me3 and H3K36me3, which are characteristic of

active transcription at the TSS and downstream of the TSS, respectively, and H3K9me3 and H3K27me3, which are generally associated with repression. We observed that H3K4me3 and H3K36me3 decreased early on, whereas changes in H3K9me3 and H3K27me3 coincided in time with the increase in DNA methylation (Fig. 2D). Remarkably, the transient re-expression of FYN at intermediate time points during DC differentiation was also reflected by the histone modifications, with an increase in H3K4me3 and a decrease in H3K27me3 (see the central panel in Fig. 2). In general, histone modification changes occurred in the proximity of the TSS and were less apparent when the region from –500 to +500 bp relative to the TSS was analysed (not shown). Interestingly, we observed that changes in these histone modifications occurred in the three studied genes, CSF3R, FYN, and CD14, regardless of the acquisition of DNA methylation, indicating that DNA methylation may not be functionally relevant in the silencing of these genes.

Functional relevance of DNA methylation changes during MO-to-DC differentiation

To test the functional relevance of DNA methylation in MO-to-DC differentiation, we investigated the potential effects of inhibiting DNMTs throughout the process. We used two DNMT inhibitors, 5-aza20-deoxycytidine (5azadC) and nanaomycin A. 5azadC induces DNA demethylation in a replication-coupled manner, and therefore should have a limited effect in this model, given that ~ 10% of the cells divide during differentiation. Nanaomycin A directly inhibits DNMT3b activity [12,13]. We used two different concentrations for both inhibitors: 50 and 500 nM for 5azadC, and 100 nM and 500 nM for nanaomycin A. In the case of 5azadC, we used these concentrations to minimize unwanted secondary effects, including cell death of primary MOs, which we had tested in pilot studies. These concentrations are slightly lower than the standard ones used for cancer cell lines. We then investigated the ability of these drugs to inhibit the acquisition of DNA methylation by the aforementioned genes, and the ability of these genes to become silenced during differentiation. In addition, we investigated whether these compounds caused changes in surface markers that can be tested by FACS, but found no effects on cell viability over the entire differentiation time frame at the concentrations used.

Analysis of the DNA methylation changes during differentiation with pyrosequencing revealed that both 5azadC and nanaomycin A affected the ability of genes such as CSF3R and FYN to become hypermethylated (Fig. 3A). The results were more evident for CSF3R, where the acquisition of methylation was reduced by half, than for FYN, which also has a more complex pattern of expression and histone modifications over time. We observed that 5azadC had a moderate effect on the acquisition of DNA methylation, which is likely to be related to the low division rate of these cells, as cell division is essential for the effect of this drug.

We then tested the effects of these drugs on the expression levels of CSF3R and FYN. We found that neither 5azadC nor nanaomycin A influenced the loss of expression or the dynamics of this, reinforcing the notion that expression changes of these genes occur before the acquisition of DNA methylation, and that inhibition of DNMTs does not affect their ability to be silenced (Fig. 3B). We also compared the expression levels of DNMT3b in cells treated with nanaomycin A and untreated cells by using real-time quantitative PCR, and found no differences (not shown). This is consistent with the findings of others that specific inhibition by nanaomycin A does not involve changes in the levels of DNMT3b [12].

We also investigated the levels of H3K4me3, H3K36me3, H3K9me3 and H3K27me3 in the genes in MOs and iDCs and mDCs in the absence or presence of these DNMT inhibitors. Whereas we did not find differences in the pattern of H3K4me3 for CSF3R, and only moderate differences for FYN, with respect to control cells, we observed that the acquisition of H3K27me3 was significantly impaired (Fig. 3C); this may be associated with the existing links between this histone modification and DNA methylation [14], which is affected by treatment with these DNMT inhibitors. For H3K36me3 and H3K9me3, as for H3K4me3, we did not see any differences in cells treated with demethylating agents (not shown).

We then investigated whether the two compounds influenced the ability of cells to differentiate by studying the surface markers CD209, which is characteristic of DCs, and CD83, which is characteristic of mature DCs. We observed that, although the numbers of viable cells were similar in 5azadC-treated and nanaomycin A-treated cells, the levels of CD209 were significantly lower in those treated with nanaomycin A (Fig. 3D), indicating that inhibition of DNMT3B affects the stability of the differentiated phenotype of these cells. In parallel, we used real-time quantitative PCR to analyse these two markers and CD206, as an additional iDC marker. We found that both CD209 and CD206 levels were decreased in both 5azadC-treated and nanaomycin A-treated cells, although, again, nanaomycin A had a greater effect than 5azadC (Fig. 3E).

Discussion

Our results provide evidence for the de novo acquisition of DNA methylation in certain genes that become repressed during MO-to-MAC and MO-to-DC differentiation. These changes occur progressively, and are delayed with respect to the loss of expression of such genes. The changes in expression appear to be more closely correlated with the loss of active histone modifications such as H3K4me3 and H3K36me3, and are perhaps associated with the direct control of specific transcriptional repressors. On the other hand, gains of DNA methylation are associated with the

acquisition of repressive markers such as H3K27me3 and H3K9me3. We assessed the functional relevance of these DNA methylation changes in the genes considered here by using two DNMT inhibitors. The results suggest that partial impairment of DNA methylation acquisition does not alter the ability of these genes to become repressed. However, we did note an effect of DNMT inhibition on the phenotype of the DCs, which suggests that it has a role in stabilizing the differentiated phenotype.

There is compelling evidence that differentiation in the myeloid lineage is associated with changes in DNA methylation biased towards demethylation [2,3]. This is compatible with the observation that postmitotic terminal differentiation from MOs to DCs and MACs is accompanied by demethylation [5,6]. These analyses were performed by combining methyl-CpG immunoprecipitation with hybridization on promoter microarrays or by using 450K arrays. These are robust methods, but are insufficient for full coverage of individual CpG sites. Despite the predominance of changes in the direction of demethylation, it seems to us that acquisition of DNA methylation at specific CpG sites could have been underestimated. Our analysis has shown that certain CpG sites near the TSSs of genes that become repressed undergo acquisition of DNA methylation. In principle, this is consistent with a repressive role.

Comparison of the dynamics of expression and DNA methylation changes in another MO-related differentiation model [7] revealed that demethylation and increased mRNA levels occur concomitantly, suggesting a causal relationship between the loss of DNA methylation and gene activation. However, analysis of this relationship in genes that become repressed and have their DNA methylation levels increased led to different conclusions [7]. In fact, gene silencing occurs before the acquisition of DNA methylation. This also occurs in MO-to-DC differentiation, where repression of certain genes also precedes their hypermethylation. These findings imply that the roles of demethylation and acquisition of DNA methylation are somewhat different, at least in these myeloid-related differentiation processes, and are just not antagonistic mechanisms. Cells in the myeloid lineage, in particular MOs, express high levels of Tet2 [15,16], a member of the TET family of methylcytosine dioxygenases, which generates intermediates in the route towards DNA demethylation. In fact, myeloid cells constitute an excellent system in which active DNA demethylation appears to play a key role in activating specific genes. In contrast, the delay in the changes to the acquisition of DNA methylation for those genes that become repressed suggests a different role. In fact, DNA methylation in these genes might be passively acquired, and might only play a role in stabilizing gene repression, rather than being a primary driver of expression changes.

The final experiment in our study, which tested the functional effects of two DNMT inhibitors, addressed the functional relevance of the acquisition of DNA methylation by these genes. Our results provide evidence that DNA methylation changes in genes such as CSF3R and FYN are not necessary for their repression. CSF3R is the receptor for granulocyte colonystimulating factor, which is essential for granulocyte development [17], and so its silencing is required for MAC versus granulocyte commitment. FYN is a Tyr kinase from the Src family that promotes proliferation and is upregulated in chronic myeloid leukaemia [18]. Its silencing may reflect the need for cell cycle arrest in MO-to-DC differentiation. Therefore, we cannot rule out the possibility that DNA methylation stabilizes this expression status once it has been achieved, at least over the long term. On the other hand, we found that the expression of DC-specific surface markers is reduced following treatment with these DNMT inhibitors. Specifically, we observed that DC-SIGN (CD209) expression declined following treatment with nanaomycin A. DC-SIGN is a well-recognized DC marker that mediates several DC functions, including antigen uptake, intercellular adhesion, and signalling [19]. Given the decrease in expression observed for this molecule upon de novo methylation inhibition, our data indicate that DNA methylation may play a role in the stabilization of the differentiated phenotype of DCs.

Our results introduce a novel concept concerning the role of DNA methylation changes. Our current view of the role of DNA methylation takes into account that the location of a CpG site determines the functionality of its methylation (differing according to its location in a CpG island, shore, open sea, or enhancer, or in the context of a transcription factorbinding site), but our experiments also indicate that the directionality of the change, i.e. the gain or loss of DNA methylation at specific genes, can have different roles. Whereas loss of DNA methylation is associated with the concomitant activation of certain genes, acquisition of DNA methylation by other genes is not necessarily associated with their immediate silencing, and it seems rather to have a longer-term effect related to the stabilization of the phenotype.

Experimental procedures

Differentiation of DCs from peripheral blood mononuclear cells (PBMCs)

For this study, we obtained human blood samples (buffy coats) from anonymous donors through the Catalan Blood and Tissue Bank (Barcelona). The donors were informed about the potential use of their blood for research, and had any questions arising during the interview answered. The donors signed a consent form at the Catalan Blood and Tissue Bank before samples were obtained. This Blood Bank follows the WMA Declaration of Helsinki principles. Blood samples were carefully deposited on Ficoll-Paque gradients (Amersham, Buckinghamshire, UK), and then

centrifuged at 800 g (30 min) with minimum deceleration. Following centrifugation, we collected PBMCs, and washed them twice with ice-cold NaCl/Pi at 600 g for 5 min. We then used positive selection with MACS magnetic CD14 antibody (Miltenyi Biotec, Bergisch Gladbach, Germany) to isolate pure CD14+ cells from PBMCs. We then resuspended CD14+ cells in RPMI Medium 1640 (1X) + GlutaMAXTM-1 (Gibco, Life Technologies, Carlsbad, CA, USA) supplemented with 10% fetal bovine serum,100 unitsmL1 penicillin, and 100 lgmL1 streptomycin. For DC differentiation, the medium was supplemented with 500 U of human IL-4 and 800 U of GM-CSF (Gentaur Molecular Products, Kampenhout, Belgium). For MAC differentiation, the medium was supplemented with 800 U of GM-CSF (Gentaur Molecular Products).

We seeded the cells at different densities, depending on the cell numbers required for specific techniques. These numbers were 3 9 105 cells per well (96-well plates), 5 9 106 cells per well (six-well plates), and 40 9 106 cells (10-mm plates). We cultured these cells for 4 days, and changed the media and cytokines every 2 days. To induce maturation on day 4, we supplemented cells with 5 lgmL1 LPS (Sigma-Aldrich, St Louis, MO, USA) for 24 h.

Bisulfite sequencing and pyrosequencing

We carried out bisulfite modification of genomic DNA isolated from MOs, and derived DCs and MACs with the protocol described by Herman et al. [20]. We then used 2 lL of the modified DNA (20–30 ng) as a template for the subsequent analysis. We designed primers for amplification and sequencing with PYROMARK ASSAY DESIGN 2.0 software (Qiagen, Venlo, Limburg, The Netherlands). We performed PCR amplifications with the HotStart Taq DNA polymerase PCR kit (Qiagen), and then tested the quality of the amplified products by agarose gel electrophoresis. We pyrosequenced the PCR products with the Pyromark Q24 system (Qiagen). The list of all primer sequences is included in Table S1.

ChIP assays

We crosslinked CD14+ cells at 0, 3, 6, 24 and 96 h after treatment with GM-CSF + IL-4 with 1% formaldehyde, and performed ChIP assays after sonication. We used the standard protocol for ChIP experiments, and the results were analysed with real-time quantitative PCR. For each specific antibody/sample, we represented data as the ratio of the bound fraction versus the input. We used the following antibodies: anti-H3K4me3 IgG rabbit monoclonal (ref. 17614; Millipore, Billerica, MA, USA), anti-H3K36me3 serum (ref. ab9050; Abcam, Cambridge, UK), anti-H3K9me3 serum (ref. ab8898; Abcam), and anti-H3K27me3 serum (ref. 07-449; Millipore). We used IgG as a negative control. We designed primer sequences to overlap with regions showing

hypermethylation at given CpG sites, generally close to the TSS. Primer sequences are shown in Table S1. Three biological replicates of these experiments were carried out.

BrdU proliferation assays

We used BrdU at a final concentration of 300 lM, and BrdU pulses were applied to each well for 2 days. For flow cytometry assays, we seeded CD14+ cells on six-well plates, and cultured them in differentiation medium. In this case, we added BrdU to the medium at different times. We then fixed cells after 2 days with 4% paraformaldehyde (30 min, room temperature), permeabilized them with NaCl/Pi/BSA/Triton X100 0.8% (10 min, room temperature), and treated them with 2 M HCl for 30 min. We then neutralized the HCl with two 5min washes with NaBo (0.1 M, pH 8.5) and two 5-min washes with NaCl/Pi. Cells were incubated with anti-BrdU mouse IgG1 (18 h at 4 °C, 1 : 1000 dilution), and anti-mouse Alexa488-conjugated serum was added to detect the BrdU-positive nuclei.

FACS staining

For FACS analysis, we directly stained CD14+ MOs and DCs with phycoerythrin-conjugated mAbs against CD14 (Miltenyi), Horizon V450-conjugated mAbs against CD209 (BD), and allophycocyanin-conjugated mAbs against CD83 (Miltenyi). We incubated 0.3 9 106 cells with the indicated antibodies for 30 min at 4 °C, and washed them once with ice-cold NaCl/PiBSA 0.1%. We analysed cells with a Gallios Flow Cytometer (Beckman Coulter, Brea, CA,

USA) and FLOWJO software (Tree Star, Ashland, OR, USA).

Abbreviations

5azadC, 5-aza-20-deoxycytidine; BrdU, bromodeoxyuridine; ChIP, chromatin immunoprecipitation; DC, dendritic cell; DNMT, DNA methyltransferase; FACS, fluorescence-activated cell sorting; GM-CSF, granulocyte–macrophage colony-stimulating factor; iDC, immature dendritic cell; IL, interleukin; iMAC, immature macrophage; LPS, lipopolysaccharide; MAC, macrophage; MO, monocytes; PBMC, peripheral blood mononuclear cell; TSS, transcription start site.

Author contributions

E. Ballestar and R. Vento-Tormo designed the research, R. Vento-Tormo and J. Rodrıguez-Ubreva performed the experiments, E. Ballestar, R. VentoTormo, J. Rodrıguez-Ubreva and D. Alvarez-Errico analysed the data and E. Ballestar wrote the paper.

Acknowledgements

This study was funded by grant SAF2011-29635 (Spanish Ministry of Science and Innovation), grant CIVP16A1834 (Fundacion Ram on Areces), and grant 2009SGR184 (AGAUR, Catalan Government). R. Vento-Tormo is supported by a PFIS predoctoral fellowship.

References

1 Broske AM, Vockentanz L, Kharazi S, Huska MR, Mancini E, Scheller M, Kuhl C, Enns A, Prinz M, Jaenisch R et al. (2009) DNA methylation protects hematopoietic stem cell multipotency from myeloerythroid restriction. Nat Genet 41, 1207–1215.

2 Ji H, Ehrlich LI, Seita J, Murakami P, Doi A, Lindau P, Lee H, Aryee MJ, Irizarry RA, Kim K et al. (2010) Comprehensive methylome map of lineage commitment from haematopoietic progenitors. Nature 467, 338–342.

3 Hodges E, Molaro A, Dos Santos CO, Thekkat P, Song Q, Uren PJ, Park J, Butler J, Rafii S, McCombie WR et al. (2011) Directional DNA methylation changes and complex intermediate states accompany lineage specificity in the adult hematopoietic compartment. Mol Cell 44, 17–28.

4 Ronnerblad M, Andersson R, Olofsson T, Douagi I,Karimi M, Lehmann S, Hoof I, de Hoon M, Itoh M, Nagao-Sato S et al. (2014) Analysis of the DNA methylome and transcriptome in granulopoiesis reveal timed changes and dynamic enhancer methylation. Blood 123, 79–89.

5 Klug M, Heinz S, Gebhard C, Schwarzfischer L,Krause SW, Andreesen R & Rehli M (2010) Active DNA demethylation in human postmitotic cells correlates with activating histone modifications, but not transcription levels. Genome Biol 11, R63.

6 Zhang X, Ulm A, Somineni HK, Oh S, Weirauch MT,Zhang HX, Chen X, Lehn MA, Janssen EM & Ji H (2014) DNA methylation dynamics during ex vivo differentiation and maturation of human dendritic cells.Epigenetics Chromatin 7, 21.

7 de la Rica L, Rodriguez-Ubreva J, Garcia M, Islam AB, Urquiza JM, Hernando H, Christensen J, Helin K, Gomez-Vaquero C & Ballestar E (2013) PU.1 target genes undergo Tet2-coupled demethylation and DNMT3b-mediated methylation in monocyte-toosteoclast differentiation. Genome Biol 14, R99.

8 Okano M, Bell DW, Haber DA & Li E (1999) DNA methyltransferases Dnmt3a and DNMT3b are essential for de novo methylation and mammalian development. Cell 99, 247–257.

9 Sasaki H & Matsui Y (2008) Epigenetic events in mammalian germ-cell development: reprogramming and beyond. Nat Rev Genet 9, 129–140.

10 Esteller M (2007) Cancer epigenomics: DNA methylomes and histone-modification maps. Nat Rev Genet 8, 286–298.

11 Ohm JE & Baylin SB (2007) Stem cell chromatin patterns: an instructive mechanism for DNA hypermethylation? Cell Cycle 6, 1040–1043.

12 Kuck D, Caulfield T, Lyko F & Medina-Franco JL (2010) Nanaomycin A selectively inhibits DNMT3B and reactivates silenced tumor suppressor genes in human cancer cells. Mol Cancer Ther 9, 3015–3023.

13 Caulfield T & Medina-Franco JL (2011) Molecular dynamics simulations of human DNA methyltransferase 3B with selective inhibitor nanaomycin A. J Struct Biol 176, 185–191.

14 Schlesinger Y, Straussman R, Keshet I, Farkash S, Hecht M, Zimmerman J, Eden E, Yakhini Z, BenShushan E, Reubinoff BE et al. (2007) Polycombmediated methylation on Lys27 of histone H3 premarks genes for de novo methylation in cancer. Nat Genet 39, 232–236.

15 Klug M, Schmidhofer S, Gebhard C, Andreesen R & Rehli M (2013) 5-Hydroxymethylcytosine is an essential intermediate of active DNA demethylation processes in primary human monocytes. Genome Biol 14, R46. 16 Kallin EM, Rodriguez-Ubreva J, Christensen J,

Cimmino L, Aifantis I, Helin K, Ballestar E & Graf T (2012) Tet2 facilitates the derepression of myeloid target genes during CEBPalpha-induced transdifferentiation of pre-B cells. Mol Cell 48, 266–276.

17 Demetri GD & Griffin JD (1991) Granulocyte colonystimulating factor and its receptor. Blood 78, 2791–2808.

18 Ban K, Gao Y, Amin HM, Howard A, Miller C, Lin Q, Leng X, Munsell M, Bar-Eli M, Arlinghaus RB et al. (2008) BCR-ABL1 mediates up-regulation of Fyn in chronic myelogenous leukemia. Blood 111, 2904–2908.

19 Garcia-Vallejo JJ & van Kooyk Y (2013) The physiological role of DC-SIGN: a tale of mice and men. Trends Immunol 34, 482–486.

20 Herman JG, Graff JR, Myohanen S, Nelkin BD & Baylin SB (1996) Methylation-specific PCR: a novel PCR assay for methylation status of CpG islands. Proc Natl Acad Sci USA 93, 9821–9826.

Figure legends

Figure 1. Identification of DNA methylation changes in candidate genes during MO-to-DC and MO-to-MAC differentiation. (A) Depiction of the differentiation system. MOs from peripheral blood were exposed to either G-MSF or GM-CSF + IL-4 to generate iMACs or iDCs, respectively. Maturation of these two cell types to give mature MACs (mMACs) and mature DCs (mDCs) was achieved following incubation with LPS. (B) Flow cytometry analysis of cell types to test changes in surface markers, including CD14, CD209 (specific to DCs), and CD83 (specific to mDCs). MFI, median fluorescence intensity. (C) Real-time quantitative PCR analysis of selected gene markers and their levels in MOs, iDCs, mDCs, iMACs and mMACs. (D) BrdU assay showing the percentages of replicating cells at different times during MO-to-DC and MO-to-MAC differentiation. From day 1 to day 3, only ~ 10% of cells divided. Ctrl, control. (E) Schematic representation of the six genes analysed in this study. The analysed CpG sites (vertical black line), the TSS (arrow) and the location of primers for ChIP (blue), expression (red, real-time quantitative PCR) and methylation (green, bisulfite pyrosequencing) analysis are indicated. Exons are marked as boxes, but look like lines (given the length of the genes) in all cases except for CD14, which is shorter. (F) Real-time quantitative PCR analysis of selected genes that become repressed during differentiation. (G) Bisulfite pyrosequencing data showing the DNA methylation changes.

Figure 2. Dynamics of DNA methylation, expression and histone modification changes for CSF3R, FYN and CD14 during MO-to-DC differentiation. (A) Depiction of the structure of CSF3R, FYN and CD14 including the TSS (arrow), the exons (black boxes). (B) Real-time quantitative PCR analysis of the genes during MO-to-DC differentiation. Values are relative to RPL38 levels. (C) Bisulfite pyrosequencing data over time showing the acquisition of DNA methylation changes during differentiation. (D) Changes in H3K36me3, H3K4me3, H3K9me3 and H3K27me3. Relative

enrichment is the fraction of the input immunoprecipitated for each antibody. Data for each antibody are accompanied by IgG as a negative control.

Figure 3. Effects of the DNMT inhibitors 5azadC and nanaomycin A on DNA methylation, expression and histone modification changes during MO-to-DC differentiation. (A) Effects of two concentrations of 5azadC (50 and 500 nM) and nanaomycin A (100 and 500 nM) on the acquisition of DNA methylation changes in CSF3R and FYN over time with respect to untreated control cells. (B) Effects of 5azadC and nanaomycin A (conditions as above) on the expression changes for the same genes as above. (C) Effects of 5azadC and nanaomycin A (conditions as above) on the changes in H3K4me3 (red bars) and H3K27me3 (blue bars). (D) Effects of 5azadC and nanaomycin A on the levels of the surface markers CD209 (specific to DCs) and CD83 [specific to mature DCs (mDCs)]. The viabilities of cells in the presence of these concentrations of drugs are also shown. (E) Real-time quantitative PCR analysis of the selected DC surface markers CD209, CD206 and CD83 during DC differentiation. The effects of two concentrations of DNMT inhibitors, i.e. nanaomycin A (100 and 500 nM) and 5azadC (50 and 500 nM), are compared with those on control cells, in the absence of these inhibitors. Ctrl, control.

Figure 1

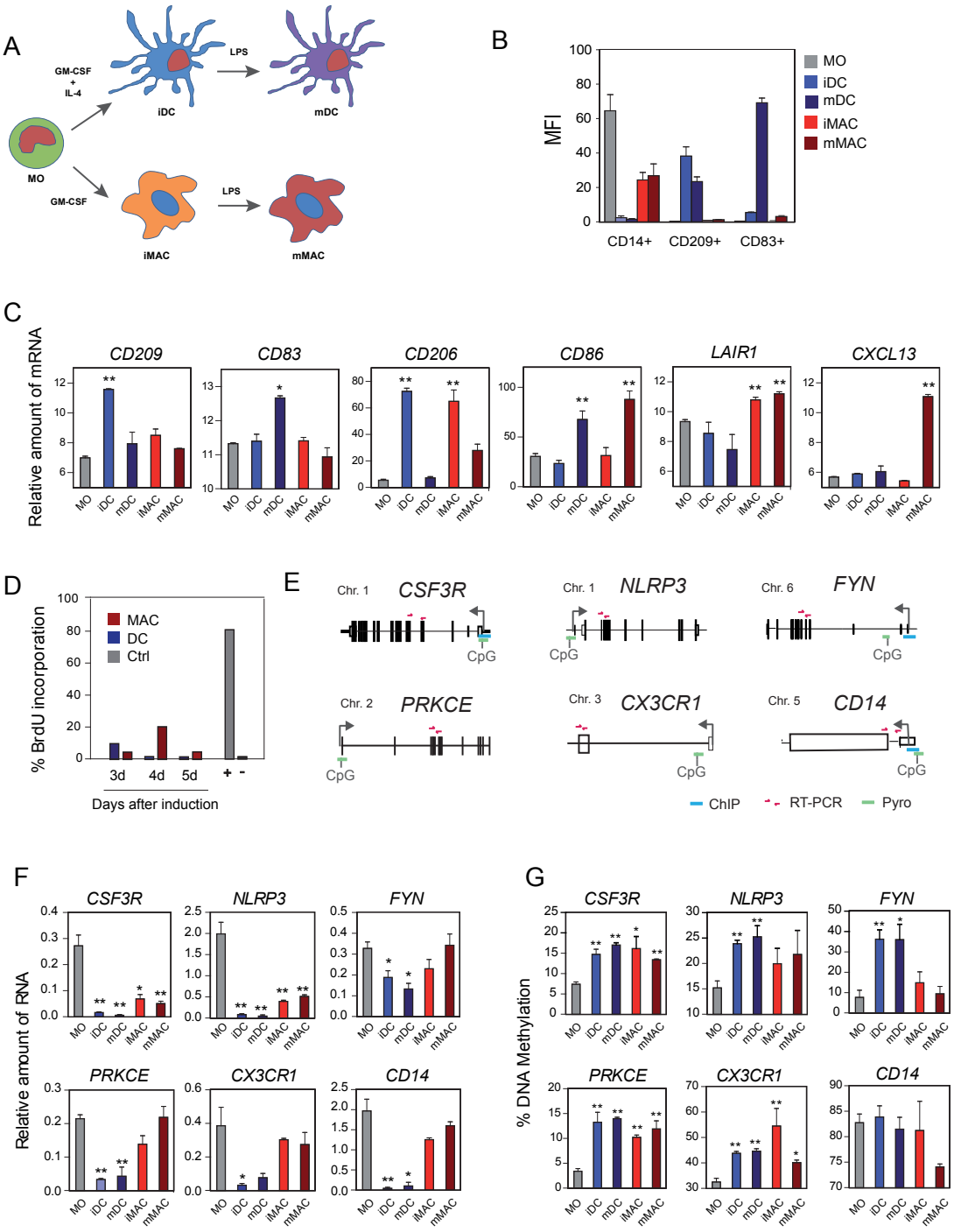
A
GM-CSF + IL-4
LPS
iDC
mDC
MO
GM-CSF
LPS
iMAC
mMAC
B
MFI
MO
iDC
mDC
iMAC
mMAC
CD14+
CD209+
CD83+
C
Relative amount of mRNA
CD209
CD83
CD206
CD86
LAIR1
CXCL13
MO
iDC
mDC
iMAC
mMAC
D
% BrdU incorporation
MAC
DC
Ctrl
3d
4d
5d
+ -
Days after induction
E
Chr. 1
CSF3R
CpG
Chr. 1
NLRP3
CpG
Chr. 6
FYN
CpG
Chr. 2
PRKCE
CpG
Chr. 3
CX3CR1
CpG
Chr. 5
CD14
CpG
ChIP
RT-PCR
Pyro
F
Relative amount of RNA
CSF3R
NLRP3
FYN
PRKCE
CX3CR1
CD14
MO
iDC
mDC
iMAC
mMAC
G
% DNA Methylation
CSF3R
NLRP3
FYN
PRKCE
CX3CR1
CD14
MO
iDC
mDC
iMAC
mMAC

Figure 2

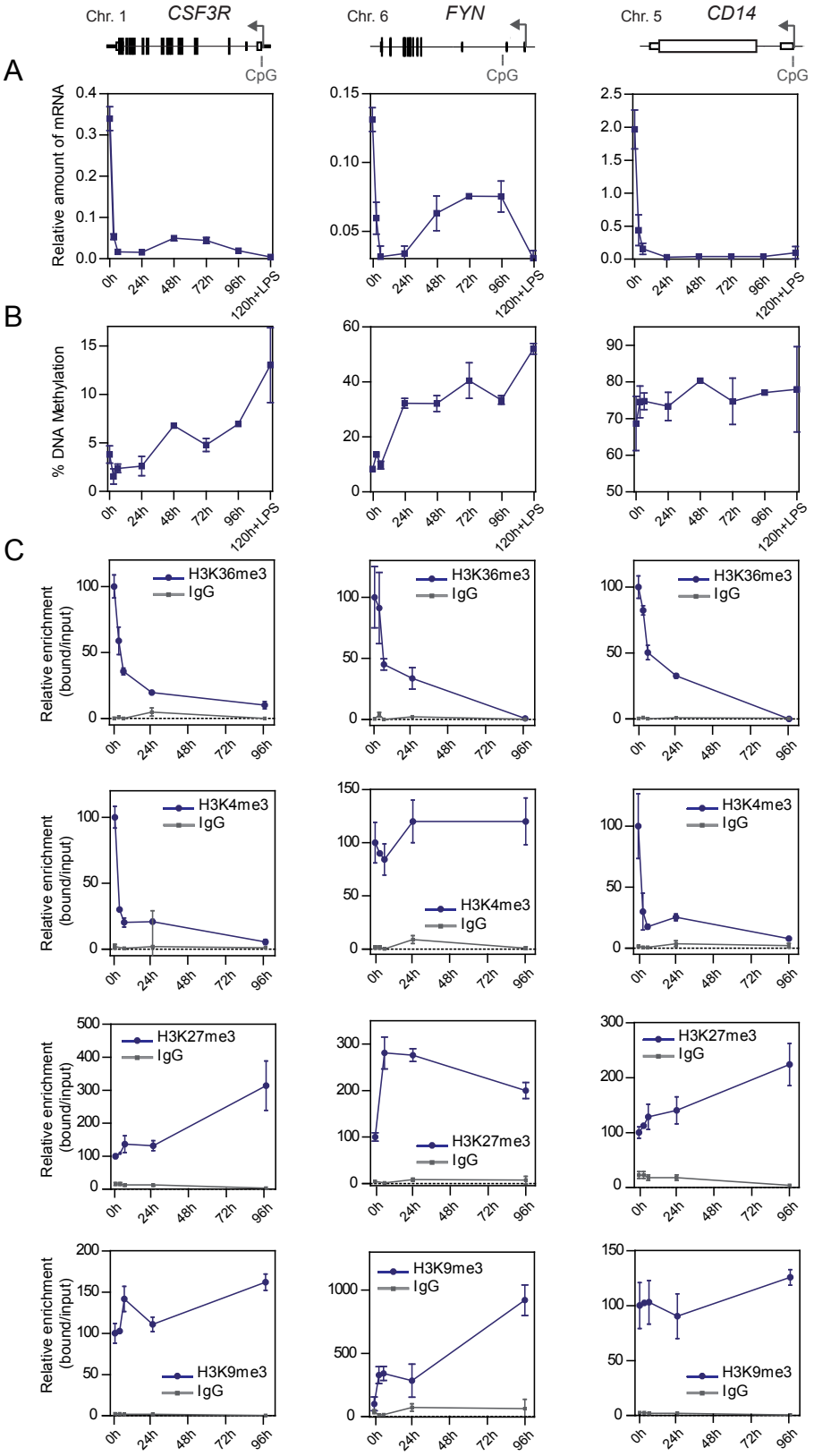
A
B
C
Chr. 1
CSF3R
Chr. 6
FYN
Chr. 5
CD14
CpG
Relative amount of mRNA
% DNA Methylation
Relative enrichment (bound/input)
H3K36me3
H3K4me3
H3K27me3
H3K9me3
IgG
0h
24h
48h
72h
96h
120h+LPS

Figure 3

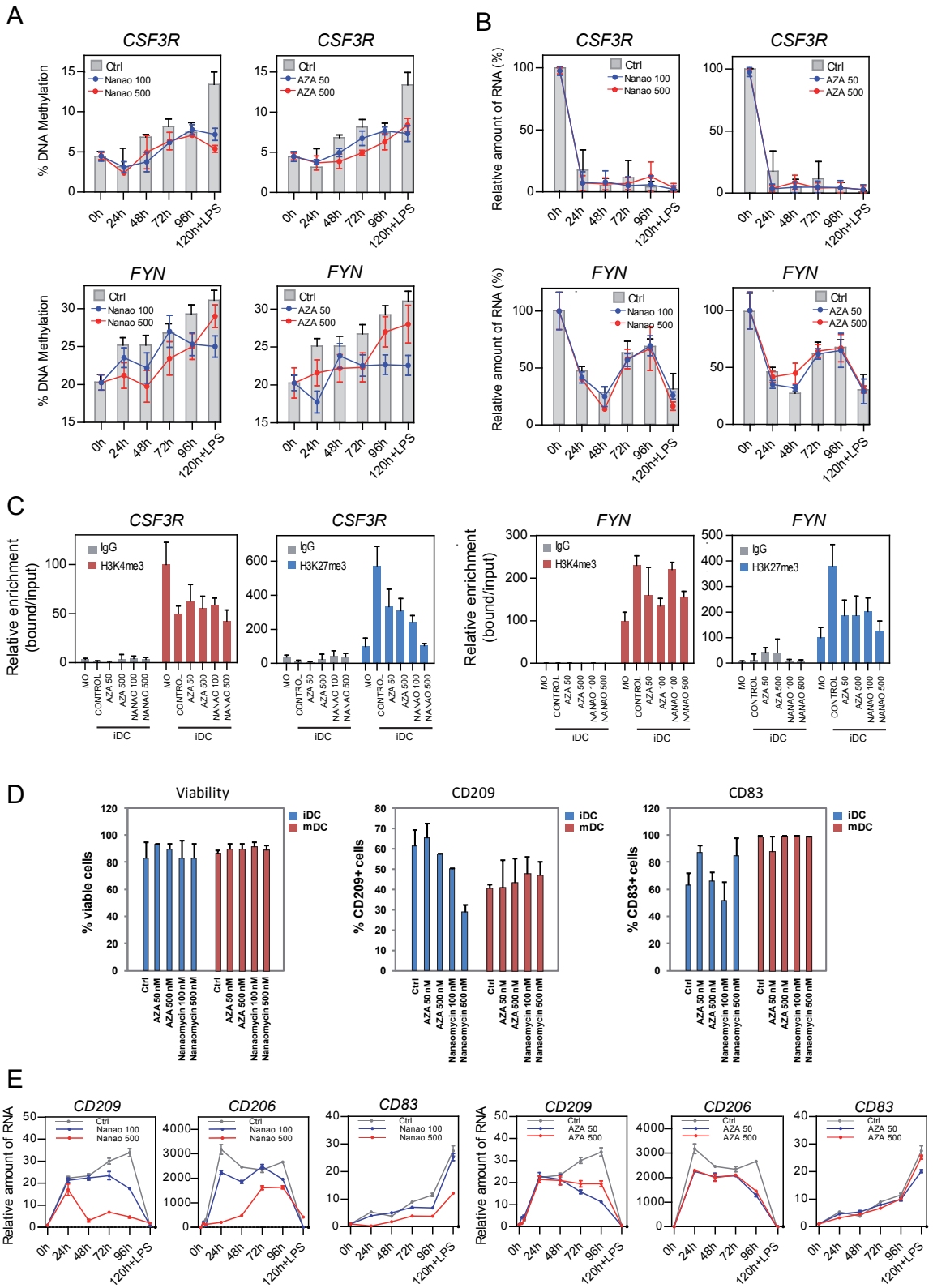
A
CSF3R
CSF3R
FYN
FYN
% DNA Methylation
Ctrl
Nanao 100
Nanao 500
AZA 50
AZA 500
0h
24h
48h
72h
96h
120h+LPS
B
Relative amount of RNA (%)
C
Relative enrichment (bound/input)
IgG
H3K4me3
H3K27me3
MO
CONTROL
AZA 50
AZA 500
NANAO 100
NANAO 500
iDC
D
Viability
CD209
CD83
% viable cells
% CD209+ cells
% CD83+ cells
iDC
mDC
Ctrl
AZA 50 nM
AZA 500 nM
Nanaomycin 100 nM
Nanaomycin 500 nM
E
CD209
CD206
CD83
Relative amount of RNA

3.4 ARTICLE 4

Journal:

Genome Biol. (2015, 16:2. doi: 10.1186/s13059-014-0561-5)

Title:

NF-κB-direct activation of microRNAs with repressive effects on monocyte-specific genes is critical for osteoclast differentiation.

Authors:

Lorenzo de la Rica1,2†, Antonio García-Gómez1†, Natalia R Comet1, Javier Rodríguez-Ubreva1, Laura Ciudad1, Roser Vento-Tormo1, Carlos Company1, Damiana Álvarez-Errico1, Mireia García3, Carmen Gómez-Vaquero3 and Esteban Ballestar1* (†Equal contributors)

Affiliations:

1Chromatin and Disease Group, Cancer Epigenetics and Biology Programme (PEBC), Bellvitge Biomedical Research Institute (IDIBELL), 08908 L'Hospitalet de Llobregat, Barcelona, Spain. 2Present address: Barts and The London School of Medicine and Dentistry, Centre for Neuroscience & Trauma, Blizard Institute, Queen Mary University of London, 4 Newark Street, London E1 2AT, UK. 3 Rheumatology Service, Bellvitge University Hospital (HUB), 08908 L'Hospitalet de Llobregat, Barcelona, Spain.

Abstract

Background: Monocyte-to-osteoclast conversion is a unique terminal differentiation process that is exacerbated in rheumatoid arthritis and bone metastasis. The mechanisms implicated in upregulating osteoclast-specific genes involve transcription factors, epigenetic regulators and microRNAs (miRNAs). It is less well known how downregulation of osteoclast-inappropriate genes is achieved.

Results: In this study, analysis of miRNA expression changes in osteoclast differentiation from human primary monocytes revealed the rapid upregulation of two miRNA clusters, miR-212/132 and miR 99b/let-7e/125a. We demonstrate that they negatively target monocyte-specific and immunomodulatory genes like TNFAIP3, IGF1R and IL15. Depletion of these miRNAs inhibits osteoclast differentiation and upregulates their targets. These miRNAs are also upregulated in other inflammatory monocytic differentiation processes. Most importantly, we demonstrate for the first time the direct involvement of Nuclear Factor kappa B (NF-κB) in the regulation of these miRNAs, as well as with their targets, whereby NF-κB p65 binds the promoters of these two miRNA clusters and NF-κB inhibition or depletion results in impaired upregulation of their expression.

Conclusions: Our results reveal the direct involvement of NF-κB in shutting down certain monocyte-specific genes, including some anti-inflammatory activities, through a miRNA-dependent mechanism for proper osteoclast differentiation.

Background

The successful generation of differentiated cell types from their progenitors depends on the highly coordinated regulation of gene expression by transcription factors, epigenetic enzymes, and small non-coding RNAs, of which microRNAs (miRNAs) are the best studied. These regulate gene expression through sequence complementarity with their target mRNAs by mediating their decay or interfering with their translation [1]. miRNAs are known to have a major role in cell differentiation. However, their specific contribution in terminal differentiation processes remains poorly understood.

One such process is monocyte (MO)-to-osteoclast (OC) differentiation. OCs are giant, multinucleated cells that degrade bone [2] and differentiate from monocytic progenitors under inflammatory conditions. Their deregulation is associated with several diseases, either through deficient function that results in osteopetrosis [3] or aberrant hyperactivation that gives rise to generalized bone loss in osteoporosis [4] and rheumatoid arthritis [5]. Moreover, OCs cause bone complications in multiple myeloma [6] and in cancer metastasis, including prostate and breast cancers [7]. OCs differentiate from MO/macrophage progenitors [8] after macrophage colony-stimulating factor (M-CSF) [9] and receptor activator of nuclear factor kappa-B ligand (RANKL) [10] stimulation. In vitro generation of OCs from peripheral blood MOs allows differentiation to be studied in this model, since isolation of primary bone OCs can otherwise be challenging [11]. During osteoclastogenesis, progenitor cells fuse, reorganize their cytoskeleton [12] and activate the gene expression profile necessary for bone destruction. Several signalling pathways activate nuclear factor-kappa B (NF-κB), mitogen-activated protein kinase (MAPK)and c-Jun [13], which coordinately turn on NFATc1 [14], the osteoclastogenesis master transcription factor. NFATc1 acts in conjunction with PU.1 and MITF [15], activating OC-specific genes such as those encoding tartrate-resistant acid phosphatase (TRAP or ACP5) [16], cathepsin K (CTSK) [17], dendritic cell-specific transmembrane protein (DC-STAMP or TM7SF4) [18], matrix metallopeptidase 9 (MMP9) [19] and carbonic anhydrase 2 (CA2). Most importantly, other genes like CX3CR1, a MO-specific gene, and TNFAIP3, a deubiquitinating protease that mediates TRAF6 degradation and impairs NF-κB activation [20], need to be silenced during OC differentiation. It is not well understood how the silencing program is established during MO-to-OC differentiation. The importance of miRNAs in OC differentiation has been established through the observation that knock-out models for the miRNA processing machinery impair OC formation and reduced expression of TRAP and NFATc1 [21]. In addition, silencing of miRNAs, such as miR-29b [22] and miR-124 [23], is essential for the upregulation of pro-osteoclastic genes.

In this study, we investigated the role of miRNAs in establishing and maintaining a repressive program during OC differentiation. To this end, we performed high- throughput miRNA expression profiling of human peripheral blood MOs before and 2 and 20 days after stimulation with RANKL and M-CSF. We identified different dynamics in miRNA expression changes. Two miRNA clusters, miR-212/132 and miR-99b/let-7e/ 125a, are highly upregulated during the early stages of osteoclastogenesis. Functional analysis of these miRNAs revealed that their depletion impairs proper OC differentiation. Interestingly, these miRNAs target MO-specific and anti-inflammatory genes that are downregulated during differentiation, such as TNFAIP3, IGF1R, THBS1, ITGA4, IL15 and PTGS2. We investigated the potential involvement of the NF-κB transcription factor in the upregulation of these miRNAs. We demonstrated the direct association of p65 NF-κB with the transcription start site (TSS) of these miRNA clusters. Most importantly, we found that the pharmacological inhibition of the p65 subunit of NF-κB or its depletion results in impaired overexpression of these miRNAs and affects the downregulation of their targets. Our results demonstrate the direct relation- ship between p65 NF-κB and miRNA-mediated repression of several MO-specific and anti-inflammatory genes that is key for proper osteoclastogenesis and reveal novel potential pathways for therapeutic intervention in the treatment of bone complications in diseases such as rheumatoid arthritis and bone metastases.

Results

The miRNA expression profile changes drastically during osteoclastogenesis

To determine the dynamics of miRNA expression during human osteoclastogenesis, we first generated three sets of matching samples corresponding to peripheral blood MOs (CD14+ cells), MOs 48 hours after RANKL/M-CSF treatment, and mature OCs obtained from the same sets of MOs, 21 days after RANKL/M-CSF stimulation. The quality of the OCs was confirmed microscopically by the presence of three or more nuclei in TRAP-positive cells and the formation of the actin ring (Figure 1A). At the molecular level, we confirmed the upregulation of osteoclastic markers (CA2, CTSK, MMP9, ACP5/TRACP and TM7SF4/DCSTAMP) and the silencing of the MO- specific gene CX3CR1 (Figure 1B). We then performed miRNA expression profiling during the differentiation of MOs to OCs using the three sets of samples. Statistical analysis of the combined expression data from three bio- logical replicates showed 115 miRNAs that were differentially expressed at one or more of the times analysed (Figure 1C; Additional file 1). miRNAs displayed different expression profiles over time that enabled them to be classified into eight groups (Figure 1C) according to the combination of upregulation or downregulation at the

initial or late stages of OC differentiation. Of particular interest were the miRNAs whose expression increased rapidly in the initial stages (groups I, V and VI; Figure 1C), regardless of their subsequent changes over time. miRNAs that become upregulated immediately after M-CSF and RANKL stimulation are potentially more important for the differentiation process than for the function of fully differentiated OCs. miRNAs within two clusters ranked top in terms of the coefficient of change and relative expression levels, specifically miR-99b/let-7e/125a (group I, average fold change = 49.4 between MOs and 48 h post-M-CSF/ RANKL stimulation) and miR-212/132 (group VI, average fold change = 50.57 between MOs and 48 h post-M-CSF/ RANKL stimulation) (Figure 1D). Several other activated miRNAs identified in our analysis have already been de- scribed in human and mouse experiments concerning OC differentiation (Figure 1C) like miR-124, a negative regulator of NFATc1 expression [23], and miR-155, also upregulated in bone marrow macrophage-derived OCs [24,25].

We confirmed the overexpression of all the miRNAs within the miR-99b/let-7e/125a and miR-212/132 clusters using quantitative RT-PCR (qRT-PCR) (Figure 1E). This analysis also confirmed that individual miRNAs from each of the two clusters do not reach the same expression levels. For example, miR-99b and miR-125a levels are in- creased by 300-fold and 100-fold respectively, whereas miR-let-7e induction is only increased by 10- to 12-fold. This strongly suggests that miRNAs in these clusters are regulated not only transcriptionally but also post- transcriptionally during MO-to-OC differentiation, as it has previously been observed for other miRNAs in other differentiation programs [26]. To refine the expression dynamics of these miRNAs during the differentiation process further, we generated a time course of osteoclastogenesis from three different healthy donors, and checked the miRNA levels at several times during the entire differentiation process. The two clusters showed different dynamics when we analysed their expression levels over time. Specifically, after RANKL/M-CSF stimulation, the miR-99b/let-7e/125a cluster miRNAs underwent rapid overexpression during the first four days and the levels remained stably high until day 21 (Figure 1F, top). In contrast, miR-212/132 cluster miRNAs peaked at day 3, displaying an increase of around 50-fold (miR132) to 170- fold (miR-212), followed by an approximately 5-fold drop (Figure 1F, bottom). This suggests that the functions of miR-132 and miR-212 are involved in the early events of osteoclastogenesis, since their expression levels are tightly regulated and constrained to the first four days of differentiation.

Inhibition of miRNAs within the miR-99b/let-7e/125a and miR-212/132 clusters impairs osteoclastogenesis

To investigate the role of the individual miRNAs within the two aforementioned clusters in OC differentiation, we performed loss of function experiments. We transfected primary MOs with specific inhibitors or antagomirs for each of the individual miRNAs contained in the miR-99b/let-7e/125a and miR-212/132 clusters. In these experiments, transfections with miRNA inhibitors were performed simultaneously with RANKL/M-CSF stimulation. We collected samples at 4 days. Then we tested the expression of OC markers to assess the impact of depleting these miRNAs on the differentiation process. Simultaneously, we checked the efficiency of transfection by flow cytometry of cells transfected with a control antagomir fluorescein-conjugate, recording efficiencies of 93% and 97.6% depending on the reagent used for transfection (Figure 2A). qRT-PCR analysis revealed that individual inhibition of each of the miRNAs within the two clusters results in a delay and decrease in the levels of OC markers like ACP5, CA2, CTSK and MMP9 (Figure 2B) at 4 days after RANKL/M-CSF stimulation. An opposite effect was observed for the MO-specific gene CX3CR1 with miR-99b and miR-125a (Figure 2B). We also performed double-transfection experiments with two combinations of miRNA inhibitors, containing two miRNAs within each cluster. In these experiments with two miRNA inhibitors we observed higher inhibition of OC markers than in single transfections (Figure 2C), further demonstrating the functional role of these miRNAs in the proper differentiation of OCs.

We then investigated the effects of depleting these miRNAs on the acquisition of two essential OC mem- brane proteins, CCR1 [27] and TM7SF4/DCSTAMP [28] (Figure 2D). Flow cytometry analysis of these two surface markers revealed that the depletion of any of the individual miRNAs within the two clusters decreases their levels 4 days after RANKL/M-CSF stimulation.

Finally, we tested whether depletion of these miRNAs impacts the ability of MOs to fuse and form OCs following RANKL/M-CSF stimulation. To this end, we performed TRAP staining 4 days after RANKL/M-CSF treatment on cells transfected with power inhibitors for each of the miRNAs, when the first multinucleated OCs start to be apparent. We observed a delay in OC formation in all cases, proving the relevance of these miRNAs for the differentiation and fusion in TRAP+ OCs (Figure 2E). These effects were less obvious at longer differentiation times; however, this is not surprising given the medium/long-term instability of antagomirs transfected into cells. In summary, all these results indicate that the high levels of the miRNAs from these two clusters are necessary for proper differentiation of OCs.

<u>Upregulated miRNAs target monocyte-specific and immunomodulatory genes that need to be silenced during osteoclastogenesis</u>

Our results demonstrated that the miRNAs within the most strongly activated miRNA clusters have a functional effect on OC differentiation when inhibited in MOs, as reflected by the decrease and delay in the up- regulation of OC markers, including OC-specific surface proteins, as well as in the ability to form multinuclear cells. To identify the targets of these miRNAs, we retrieved a list of putative targets using miRWalk [29], which contains prediction databases like TargetScan [30], miRDB [31] and others, as well as information about validated targets. We then linked the list of potential targets with previously reported high-throughput data on expression changes during OC differentiation [32], assuming an inverse relationship between the levels of a given miRNA and the expression levels of its tar- gets. For this analysis, we imposed the criteria that the targets should be predicted by at least four databases (Figure 3A) and that downregulation was defined as a minimum 0.5-fold change. Applying these conditions we identified a number of putative downregulated targets for each overexpressed miRNA (Additional file 2). We then used the Database for Annotation, Visualization and Integrated Discovery (DAVID) to identify functional categories. This tool revealed a highly significant enrichment of categories related to the immune system (Figure 3B), including immune system development (P-value 1.69 E-11) and cytokine production (P-value 3.04 E-11). We identified a number of critical factors from among these (Figure 3C). For instance, miR-99b was found to target the 3′ UTRs of IGF1R, miR-125a targeted ETV6, TNFAIP3 and CX3CR1, and let7e targeted TNFAIP3 and ITGA4. In the case of the miRNAs in the miR-212/132 cluster, miR-212 was found to target CX3CR1 and HBEGF, and miR-132 targeted IRF1 and NR4A2. Some of these genes are also silenced by other mechanisms during OC differentiation. Two ex- amples are the MO-specific gene CX3CR1 and the anti-inflammatory gene TNFAIP3, which are rapidly silenced after M-CSF/RANKL stimulation, and their promoters are hypermethylated [33].

To validate the putative targets, we performed luciferase reporter assays using a vector containing the renilla luciferase coding region plus the wild type or a mutant form (Mut) of the putative 3′ UTR target sites of each potentially targeted gene. We carried out these assays in HeLa cells, in which we had previously estimated the expression of high levels of miRNAs of the miR-99b/let- 7e/125a and miR-212/132 clusters. These assays confirmed that miR-99b targets IGF1R, miR-125a targets TNFAIP3, and let-7e targets ITGA4 and THBS1. On the other hand, miR-132 targets PTGS2, and miR-212 also targets PTGS2 and IL15 (Figure 3D).

To obtain further evidence of the in vivo effect of the miRNAs on their putative targets, we performed qRT-PCR and western blotting in MOs transfected with each of the miRNA inhibitors. In the case of the miR-99b/let- 7e/125a cluster, inhibition of miR-99, miR-125a and let- 7e resulted in the specific upregulation of IGF1R, TNFAIP3 and IGF1R, and of ITGA4 and

THBS1, respectively. With respect to the miR-212/132 cluster, inhibition of miR-132 and miR-212 gave rise to the upregulation of PTGS2 and the inhibition of miR-212 resulted in the upregulation of IL15 (Figure 3E). We also observed crossover effects between some miRNAs and targets. For instance, inhibition of miR-99b and miR- 125a also affected PTGS2, which was not validated in luciferase assays but also contains putative recognition sites at its 3′ UTR for miR-99b and miR-125. We observed increased mRNA and protein levels for some of these targets in double transfection experiments with antagomirs (Figure 3F). Together with the luciferase assays, all these results confirmed the essential role of the miRNAs in the downregulation of these genes during OC differentiation.

Changes in the miRNA cluster expression levels in related inflammatory-driven monocyte differentiation processes

We also investigated whether the observed miRNA expression changes occurring in OC differentiation constitute a more general regulatory mechanism also operating in another two related differentiation processes involving MOs, specifically MO-to-dendritic cell differentiation and MO-to- macrophage differentiation. These two processes are triggered following stimulation with granulocyte-macrophage CSF/IL-4 or granulocyte-macrophage CSF alone (Figure 4A). Analysis of the expression changes of all miRNAs within the miR-99b/let-7e/125a and miR-212/132 clusters showed these are common to all three processes (Figure 4B). Specifically, we observed that all these miRNAs increased more markedly in macrophages than in dendritic cells, suggesting a bias towards the ability to generate a strong NF-κB-mediated response, such as TLR4-initiated signals occurring in inflammatory macrophages. Given the negative relation- ship between these miRNAs and the regulation of their tar- gets, it is feasible that they have a key role in the extinction of mRNAs that are characteristic of a less inflammatory prone state. This prompted us to investigate the relationship between the increase in these miRNAs and the expression levels of their validated targets in MO-to-dendritic cell and MO-to-macrophage differentiation. We also noted a decrease in the mRNA levels of TNFAIP3, ITGA4, THBS, IL5, and PTGS2 during the three differentiation pro-cesses (Figure 4C). The only exception was IGF1R, which appeared to increase over time in OC and dendritic cell differentiation, consistent with the findings of others [34]. This could perhaps be due to the predominant effect of other regulatory mechanisms, probably at the transcription level (Figure 4C). In this case, the upregulation of miR-99b, which targets IGF1R, could be related more to fine-tuning regulation in order to achieve the proper levels of this protein instead of blocking the expression of it.

A direct role for NF-κB in the upregulation of miRNAs?

Our results supported the notion that miRNAs play a role in the efficiency of OC differentiation and enabled us to identify two upregulated miRNA clusters whose participation in downregulating genes is key to this process. As explained above, MO-to-OC differentiation is induced by RANKL, which ultimately stimulates NF- κB, a transcription factor once it has been translocated into the nucleus. NF-κB acts in concert with PU.1, Jun and the OC-specific transcription factor NFATc1. NF- κB helps regulate many OC-specific genes. The transcription factor NF-κB is also likely to participate in shutting down MO-specific genes through the activation of miRNAs. To explore the potential involvement of NF-κB in the changes in miRNAs during MO-to-OC differentiation, we first investigated the enrichment of the consensus binding site for the p65 NF-κB subunit in a window of 500 bp upstream and downstream of the TSS of the miRNAs (determined from the miRStart database) [35]. This analysis showed that the p65 NF-κB consensus binding site is present in the majority of miRNA TSSs, including the miRNAs within the miR- 99b/let-7e/125a and miR-212/132 clusters (Figure 5A). We then investigated the presence of p65 NF-κB around the TSSs of these two miRNA clusters by performing chromatin immunoprecipitation (ChIP) assays with anti-p65 antibodies in MOs before and 48 h and 96 h after induction with RANKL/M-CSF. We also used primers near the TSS of CCL5 as a positive control. We noted specific enrichment of p65 at 48 h and 96 h after RANKL/M-CSF stimulation in the two upregulated miRNA clusters (Figure 5B), demonstrating a direct association of NF-κB p65 with the encoding sequence of the upregulated miRNAs. We also found that p65 bound near the TSSs of other miRNAs, such as miR-34a (Figure 5B), suggesting that this may be a general mechanism of miRNA upregulation in OC differentiation.

To investigate the involvement of the NF-κB pathway in the activation of these miRNAs in greater depth, we treated MOs with two NF-κB inhibitors, Bay 11-7082 and sodium aurothiomalate (SATM), and investigated the effects on the expression of the aforementioned miRNAs following induction by RANKL/M-CSF. SATM inhibits the activity of IκB kinase by modifying cysteine residues within its catalytic domain. Bay 11-7082 selectively and irreversibly inhibits the tumour necrosis factor-α- inducible phosphorylation of IκBα, resulting in reduced expression of NF-κB and adhesion molecules. Both inhibitors eventually reduce the levels of phosphorylated Ser536 of p65, which correspond to its active form. To test the toxicity of these two inhibitors, we first performed MTT assays over a wide range of concentrations with primary MOs (not shown), and selected 10 μM for Bay 11-7082 and 100 μM for SATM. Consistent with a relevant role of the NF-κB pathway in the activation of these miRNAs, we observed that phosphorylation of p65 increases following RANKL/M-CSF stimulation of MOs (Figure 5C). Under

our conditions we observed potent inhibition of p65, as reflected by the reduced levels of phospho-Ser536 p65, especially at 2 days, whereas at 4 days the inhibitory effects of Bay 11-7082 were significantly reduced, perhaps due to its instability in the culture medium (Figure 5C). We then investigated the effects of these two inhibitors on miRNA expression. Both inhibitors decreased expression of upregulated miRNAs (Figure 5D), reinforcing the notion of the direct role of NF-κB in mediating their upregulation. Consistent with the results obtained with the western blotting (Figure 5C), the reduction in miRNA upregulation was more obvious only at 2 days, whereas at 4 days the miRNAs of cells treated with Bay 11-7082 had reached the levels of cells treated with the vehicle. As mentioned above, this is perhaps due to the stability of the inhibitors in the culture medium, which are added only at the beginning. It could also be due to the contribution of additional regulatory mechanisms that could be compensating for the inhibition of the NF-κB pathway. We also checked the effects on both classical OC markers and miRNA-validated targets. The two inhibitors reduced the levels of OC markers, as determined by qRT-PCR after 4 days (Figure 5E). Conversely, both SATM and Bay 11-7082 had an overall positive effect on miRNA targets, providing evidence that NF-κB helps repress these targets through miRNAs (Figure 5F). We observed different effects in terms of which of the two drugs was more effective or whether the effect was more evident at 2 or 4 days, but we cannot discard the occurrence of pleiotropic effects, or interference with other regulatory mechanisms.

Therefore, as an unequivocal test of a potential causal relationship between NF-κB and miRNA expression changes in MO-to-OC differentiation, we investigated the consequences of ablating p65 expression in MOs. To this end, we downregulated p65 levels in MOs using transient transfection experiments with a small interfering RNA (siRNA) that targets exon 11 of p65 (Figure 6A). In parallel, we used a control siRNA. Following transfection we stimulated differentiation with RANKL/M-CSF. Under these conditions, we used qRT-PCR and western blotting to check the effects on p65 levels 1, 2 and 4 days after RANKL/M-CSF stimulation of MOs. By this means, we were able to confirm that the level of p65 downregulation was close to 50% (Figure 6A). siRNA-mediated downregulation of p65 resulted in decreased binding of the miRNAs to TSSs (Figure 6B). We also examined the expression levels of these miRNAs following p65 depletion and found that the RANKL/M-CSF-stimulated upregulation of the miRNAs within the miR-99b/let-7e/125a cluster was partially impaired following p65 depletion (Figure 6C). We also analysed two miRNAs that are not direct p65 tar- gets and observed no effect on their levels following p65 depletion (not shown).

We investigated the effects of depleting p65 on the expression of OC markers (ACP5, CTSK and TM7SF4) as well as on miRNA targets. Whereas depletion of p65 led to a decrease in

the upregulation of OC markers (Figure 6D), it resulted in an increase in miRNA targets (Figure 6E), thereby confirming the direct role of p65 in regulating this process.

Taken together, our findings are the first demonstration that NF-κB is directly associated with and activates miRNAs that are essential for the regulation of critical targets whose downregulation is essential for proper OC differentiation.

Discussion

Our results provide novel insights into the role and mechanisms of the fine-tuned control of expression and its relation with inflammatory pathways in MO-to-OC differentiation. Firstly, we identified a set of miRNAs that are required for OC differentiation. Most importantly, these miRNAs target and repress OC-inappropriate genes, including several MO- specific and immunomodulatory genes. Secondly, our results reinforce the key role of the NF-κB transcription factor as a direct regulator of miRNA upregulation, specifically focusing on the miR-99b/let-7e/125a and miR-212/132 clusters.

Screening miRNA expression changes at two points during differentiation revealed different groups of miRNAs based on their expression profiles over time. Overall, our data show prevalent upregulation of miRNAs in OC differentiation. Twenty-three miRNAs displayed fast upregulation followed by sustained expression levels, 20 miRNAs had a rapid increase followed by downregulation over a longer period following induction until day 21, and 26 miRNAs were upregulated only at later stages. In contrast, there were significantly fewer miRNAs whose expression levels decreased over time. The predominance of upregulated miRNAs may suggest that their primary role is to repress or ensure the maintenance of low levels of OC-inappropriate genes that could also be repressed through other mechanisms. Previous data from our group have already shown this type of behaviour in B cell-to-macrophage transdifferentiation [36]. Our analysis of the functional effects of the depletion of the miRNAs within the miR-99b/let-7e/125a and miR- 212/132 clusters, as well the analysis of their targets, shows that these molecules have a direct role in repressing MO-specific and immunomodulatory genes like TNFAIP3, IGF1R and IL15. In addition, loss of function experiments using specific inhibitors for the above miRNAs influences the efficiency of osteoclastogenesis, as determined by analysing expression changes of standard markers of OC differentiation at the RNA and protein levels, the effects on validated targets of these miRNAs and the ability of cells to fuse to yield multinucleated OCs.

Our results suggest that fine-tuning modulation through miRNA-mediated repression drives the monocytic steady state program into an NF-κB-driven proinflammatory differentiation program. This idea is reinforced by the observation that the upregulation of these

miRNAs also occurs in related inflammatory-related monocytic differentiation processes, including MO-to-dendritic cell differentiation and MO-to-macrophage differentiation. MOs are heterogeneous circulating progenitors that can either patrol the resting endothelium or migrate into tissues in response to inflammatory signals. Regulation of switching between these different states requires the ability to respond rapidly to changes that may include silencing of undesired response pathways, and the commitment to ensure proper outcomes. miRNAs may contribute to this process as a flexible regulatory mechanism, as it has been described for miR146a and Relb pathway Ly6Chigh inflammatory MO responses [37]. Our analysis on the functional effects of depletion of the miRNAs within the miR-99b/let-7e/125a cluster reveals a possible common pathway of commitment into cells with strong NF-κB- dependent responses, suggesting the targeting of the anti-inflammatory molecule TNFAIP3 (A20) by these microRNAs, which are upregulated in the conversion into OCs, dendritic cells and macrophages. In addition, depletion of the miR-212/132 cluster, as well as the analysis of their targets, shows that these elements have a direct role in repressing genes like IRF1 or IL15, which could also shape inflammation.

Ly6Chigh MO conversion to Ly6Clo anti-inflammatory macrophages with a restorative phenotype in murine hepatic fibrosis requires the upregulation of genes encoding molecules of the anti-inflammatory macrophage program, like CX3CR1, or with anti-fibrotic effects, like CD74 [38]. Interestingly, both genes are targeted by the miR-212/132 cluster in our MO-based differentiation models that con- verge on the set-up of inflammatory or NF-κB programs in different cell types. In addition, an immunosuppressive role has also been assigned to the IGF1R-IGF1 axis, and cord blood mononuclear cells as well as peripheral blood mononuclear cells (PBMCs) treated with IGF1 show a de- crease NF-κB binding activity [39]. Our results show that IGF1R is targeted by miR99b and miR125a also suggesting a coordinated shutdown of signal transduction that block NF-κB pathways.

The second major conclusion of our study is the role of NF-κB in directly upregulating the miR-212/132 and miR- 99b/let-7e/125a clusters, and perhaps other miRNAs. Multiple genes implicated in inflammation, including pro- inflammatory cytokines and their receptors, are under the transcriptional control of the transcription factor NF-κB [40]. A few reports have recently proved that NF-κB has a direct role in regulating miRNA expression [41,42]. To the best of our knowledge, however, this is the first report demonstrating a direct role for NF-κB in miRNA control in OC differentiation. NF-κB is a major target of RANKL, which is used together with M-CSF to stimulate differentiation of MOs into OCs. However, only a few direct NF-κB targets have so far been described. For instance, it has been shown that NF-κB cooperates with

NFATc2 to induce expression of NFATc1, with NF-kB p50 and p65 being recruited to the NFATc1 promoter within 1 hour of treatment of OCPs with RANKL, resulting in transient auto-amplification of NFATc1 expression, which is crucial for OC formation [14]. To date, the participation of NF-κB in this context had been restricted to an activator of genes that are necessary for OC differentiation. Our findings re- veal a novel role for NF-κB in activating miRNAs that re- press the expression of OC-inappropriate genes that are not required for differentiation. This perhaps includes not only MO-to-OC differentiation, but also other related MO-related differentiation processes where NF-κB plays a key role. Several papers have come out showing regulatory programs of Ly6Chigh inflammatory MOs/macrophages versus Ly6Clo resting cells [37,38,43]. Nonetheless, unraveling the mechanisms that delineate NF-κB versus other programs in human MOs has been more difficult and this issue is directly addressed by the present work.

The results of our study constitute the first clear evidence that NF-κB directly regulates miRNAs, showing together with our findings on the miRNA targets and the impact on OC differentiation that this is a novel mechanism of gene repression of OC-inappropriate genes in this differentiation process. In addition, our conclusions open up possibilities for exploiting novel pathways for therapeutic intervention.

Conclusions

Our study on miRNA expression changes during MO-to- OC differentiation reveals the occurrence of rapid upregulation of two miRNA clusters. We have demonstrated that miRNAs within these two clusters are necessary for MOs to differentiate into OCs. These miRNAs are key to repressing OC-inappropriate genes, including certain anti- inflammatory genes, and are needed for proper OC differ- entiation. We demonstrate that these changes and their functional effects also occur in other MO differentiation processes, indicating that these miRNAs are needed for the downregulation of OC-inappropriate genes in MOs. Most importantly, we demonstrate for the first time that NF-κB directly regulates these miRNAs and is thus directly implicated in the inhibition of the less differentiated monocytic expression program.

Materials and methods

Differentiation of osteoclasts from peripheral blood mononuclear cells

Human blood samples came from anonymous blood donors through the Catalan Blood and Tissue Bank in Barcelona as thrombocyte concentrates (buffy coats). The anonymous blood donors received oral and written information about the possibility that their blood would be

used for research purposes, and any questions that arose were then answered. Before giving their first blood sample the donors signed a consent form at the Banc de Teixits, which adheres to the principles set out in the WMA Declaration of Helsinki. The blood was carefully layered on a Ficoll-Paque gradient (Amersham, Buckinghamshire, UK) and centrifuged at 2,000 rpm for 30 minutes without braking. After centrifugation, PBMCs at the interface between the plasma and the Ficoll-Paque gradient were collected and washed twice with ice-cold phosphate-buffered saline, followed by centrifugation at 2,000 rpm for 5 minutes. Pure CD14+ cells were isolated from PBMCs using positive selection with MACS magnetic CD14 antibody (Miltenyi Biotec, Bergisch Gladbach, Germany). Cells were then resuspended in α-minimal essential medium (α-MEM Gluta-MAX Supplement, no nucleosides; Invitrogen, Carlsbad, CA, USA) containing 10% fetal bovine serum, 100 units/ml penicillin, 100 µg/ml streptomycin and antimycotic, supple-mented with 25 ng/ml human M-CSF and 50 ng/ml soluble hRANKL (PeproTech EC, London, UK). Depending on the amount needed, cells were seeded at a density of 3 × 105 cells/well in 96-well plates, 5 × 106 cells/well in 6-well plates or 40 × 106 cells in 10-mm plates and cultured for 21 days (unless otherwise noted); media and cytokines were chan- ged twice a week. The presence of OCs was checked by TRAP staining using the Leukocyte Acid Phosphatase Assay Kit (Sigma-Aldrich, St. Louis, Missouri, USA) ac- cording to the manufacturer s instructions. Phalloidin/DAPI staining enabled us to confirm that the populations were highly enriched in multinuclear cells, some of which con- tained more than 40 nuclei. We used several methods to determine that on day 21 almost 85% of the nuclei detected were osteoclastic nuclei (in polykaryons; nuclei, rather than cells, were quantified). OCs (TRAP-positive cells with three or more nuclei) were also analysed at the mRNA level: upregulation of key OC markers (CA2, CTSK, MMP9, ACP5/TRAP and TM7SF4/DCSTAMP) and down- regulation of the MO marker CX3CR1 were confirmed.

Visualization of osteoclasts with phalloidin and DAPI staining

Pure isolated CD14+ cells were seeded and cultured in glass Lab-Tek Chamber Slides (Thermo Fisher Scientific, Waltham, MA, USA) for 21 days in the presence of hu- man M-CSF and human RANKL. OCs were then washed twice with phosphate-buffered saline and fixed (3.7% paraformaldehyde, 15 minutes). Cells were perme- abilized with 0.1% (V/V) Triton X-100 for 5 minutes and stained for F-actin with 5 U/ml Alexa Fluor® 647- Phalloidin (Invitrogen). Cells were then mounted in Mowiol-DAPI mounting medium. Cultures were visualized by confocal laser scanning microscopy (Leica TCP SP2 AOBS confocal microscope).

Flow cytometry

Cells were stained with fluorochrome-conjugated antibodies against CCR1 (R&D Systems, reference FAB145A-100) and TM7SF4 (R&D Systems, reference FAB7824-A) (Both anti- bodies are from R&D Systems, Minneapolis, MN, USA) 0 and 4 days after RANKL/M-CSF stimulation. CCR1 and TM7SF4 expression were monitored on a Gallios Flow Cytometer (Beckman Coulter, Pasadena, California, USA) and analysed by FlowJo software (Tree Star, Inc., Ashland, Oregon, USA). All experiments were performed in triplicate and bar graphs correspond to independent biological samples.

MicroRNA expression screening and target prediction

Total RNA was extracted with TriPure (Roche,Basel, Switzerland) following the manufacturers instructions. Ready-to-use miRNA PCR Human Panel I V2.R from Exiqon (reference 203608) was used according to the instruction manual (Exiqon, Vedbeak, Denmark). Total RNA (30 ng) was used for each RT-PCR reaction. Paired samples of MOs at 0 (MO), 2 (OC 48 h) and 21 (OC) days after M- CSF and RANKL stimulation were obtained from three fe- male healthy donors (aged 25 to 28 years), and were analysed with a Roche LightCycler® 480 real-time PCR system. Results were converted to relative values using the interplate calibrators included in the panels (log2 ratios). Average expression values of MO, OC 48 h and OC were normalized with respect to the reference gene miR-103. A t-test was then performed and differentially expressed miRNAs (fold change >2 or <0.5), with a significant P-value ($P < 0.05$) in at least one of the comparisons, were selected and represented on a heatmap. The raw expression data are listed in full in Additional file 1. The array expression data were validated in the samples used (validation set), and in a larger cohort of samples obtained from independent donors (replication set) using Exiqon microRNA LNA™ PCR primer sets (hsa-miR-99b-5p, reference 204367; hsa-miR-125a-5p, reference 204339; hsa-miR-132-3p, reference 204129; hsa- miR-212-3p, reference 204170; hsa-miR-103a-3p, reference 204063).

To predict the potential targets of the deregulated miRNAs, we used the algorithms from several databases: TargetScan, PicTar, PITA, miRBase, microRNA.org, miRDB/ MirTarget2, TarBase, miRecords and StarBase/CLIPseq. Only targets predicted by at least four of these databases were retained for further analysis.

Bioinformatics analysis of expression data

To compare the expression data with the methylation data, we used CD14+ and OC expression data from the ArrayExpress database [44] (accession EMEXP-2019) from a previous publication

[32]. Affymetrix GeneChip Human Genome U133 Plus 2.0 expression data were processed using the limma and affy packages from Bio- conductor. The pre-processing stage was divided into three main steps: background correction, normalization and reporter summarization. We chose the expresso function of the affy package for preprocessing. Thus, the robust multi-array average (RMA) method was used for background correction. Quantile normalization was then done. We also introduced a specific step for PM (perfect matchprobes) adjustment, using the PM-only model-based expression index (option pmonly). Finally, for the summarization step, the median polish method was used. Next, variance filtering by IQR (inter- quartile range) was carried out, taking 0.50 as the threshold value. After preprocessing, data were analysed using the empirical Bayes moderated t-test available in the limma statistics package. Expression data were validated by qRT-PCR.

Transfection of primary human monocytes with miRNA inhibitors and p65 NF-κB siRNA

To perform the miRNA inhibitor experiments, we used unlabeled miRCURY LNA™ microRNA Power inhibitors to inhibit miR-99b (reference 4101513), miR-let-7e (reference 4103550), miR-125a (reference 4103094), miR-132 (reference 4103093), miR-212 (reference 4104787) or a control (Negative Control A, reference 199006) Exiqon, Vedbaek, Denmark. Power inhibitors (5 or 10 nM) were transfected into CD14+ MOs using HappyFect Transfec- tion Reagent (Tecan, Weymouth, UK) or Lipofectamine®3000 (Life Technologies). Cells were simultaneously incubated in the presence of RANKL/M-CSF in the conditions previously described. The efficiency of transfection was quantified by flow cytometry using the 5′ -fluorescein-labeled Negative Control A. For samples collected at 4 days or after, we added a fresh aliquot of miRNA inhibitors after 48 h. To silence p65, we used Silencer® Select Pre- Designed siRNA (Life Technologies) against human RELA (p65), targeting exon 11 (reference s11916) in parallel with a Silencer® Select negative control in purified CD14+ MOs in the presence of M-CSF, followed by stimulation with RANKL (and M-CSF) 24 h after siRNA transfection. We used Lipofectamine RNAiMAX Transfection Reagent (Invitrogen) for efficient siRNA transfection. mRNA and protein levels were examined by qRT-PCR and western blotting 1, 2, and 4 days after siRNA transfection. These experiments were performed with at least three biological replicates.

Luciferase assays

The putative miRNA binding sites in the 3′ UTRs of IGF1R, TNFAIP3, ITGA4, THBS1, IL15, and PTGS2 were amplified by PCR from genomic DNA derived from CD14+ cells. The PCR products were cloned into pGEM®-T Easy Vector (Promega, Madison, Wisconsin, USA) and four to seven point mutations were introduced into each target site by site-directed mutagenesis. Each of the

fragments containing the 3′ UTR of putative miRNA binding sites was cloned into psiCHECK-2 vector (Promega). 293 T cells were cultured for 24 h and then co-transfected using lipofectamine RNAimax with 10 ng of psiCHECK-2 vector containing wild-type or mutant 3′ UTR plus 50 nM of miRNA power inhibitors per well. The luciferase analysis was performed 48 h later using the Dual- Luciferase Reporter Assay (Promega). Primers to clone the 3′ UTR of putative miRNA binding sites are listed in Additional file 3.

Chromatin immunoprecipitation assays

For ChIP assays, CD14+ cells 0, 2 and 4 days after treatment with M-CSF and RANKL were crosslinked with 1% formaldehyde and subjected to immunoprecipitation after sonication. ChIP experiments were performed as de- scribed elsewhere [33]. Analysis involved real-time qPCR. Data are represented as the ratio of bound fraction to in- put for each specific factor. We used a mouse monoclonal antibody against the carboxyl terminus of human NF-κB p65 (sc-372, Santa Cruz Biotechnology, Dallas, Texas,

USA). Primer sequences are shown in Additional file 3. Experiments included three biological replicates.

Quantitative RT-PCR and western blotting

RNA was isolated by TRIzol extraction (Invitrogen) and reverse-transcribed using SuperScriptTM II Reverse Transcriptase (Invitrogen). Primers for conventional and qRT- PCR were designed using Primer3 v.0.4.0 (Table S1 in Additional file 1). qRT-PCR was performed in triplicate using LightCycler 480 SYBR Green Mix (Roche). PCR reactions were run and analysed using the LightCycler 480 II System (Roche). Expression values were normalized against the expression of the endogenous gene controls RPL38, HPRT1 and GAPDH. Primers are listed in Additional file 3.

For western blots, protein lysates were generated and western blotting performed using standard procedures using antibodies against phospho-Ser536 p65 (Cell Sig- naling, 3033 Danvers, Massachusetts, USA), p65 (Santa Cruz Biotechnologies, sc-372), IGF1R (Abcam, ab32823, Cambridge, UK), PTGS2 (Abcam, ab15191), TNFAIP3 (Abcam, ab92324), IL15 (Abcam, ab7213), ITGA4 (Abcam, ab81280), THBS1 (Thermo Scientific, MA5-13398), α- tubulin (Sigma, 1142) and total histone 3 (Abcam, ab1791).

Graphs and heatmaps

All graphs were created using Prism5 Graphpad (Graph- Pad Software, San Diego, California, USA). Heatmaps were generated from expression or methylation data using the Genesis program (Graz University of Technology).

Data access

Raw data for microRNA expression profiling as obtained following qRT-PCR amplification of Ready-to-use micro- RNA PCR Human Panel I V2.R from Exiqon (reference 203608) is available in Additional file 1. It is also available in NCBI s Gene Expression Omnibus through GEO Series accession number GSE63773.

Abbreviations

bp: base pair; ChIP: chromatin immunoprecipitation; IL: interleukin; M-CSF: macrophage colony-stimulating factor; miRNA: microRNA; MO: monocyte; NF-κB: nuclear factor-kappa B; OC: osteoclast;

PBMC: peripheral blood mononuclear cell; qRT-PCR: quantitative RT-PCR;

RANKL: receptor activator of nuclear factor kappa-B ligand; SATM: sodium aurothiomalate; siRNA: small interfering RNA; TSS: transcription start site; UTR: untranslated region.

Competing interests

The authors declare that they have no competing interests.

Authors' contributions

LR and EB conceived experiments; LR, AGG, NC, JRU, LC and RVT performed experiments; CC performed biocomputing analysis; LR, AGG, JRU, DAE, MG, CGV and EB analysed the data; EB wrote the paper. All authors read and approved the final manuscript

References

1. Ambros V: microRNAs: tiny regulators with great potential. Cell 2001,107:823–826.

2. Blair HC, Teitelbaum SL, Ghiselli R, Gluck S: Osteoclastic bone resorption by a polarized vacuolar proton pump. Science 1989, 245:855–857.

3. Tolar J, Teitelbaum SL, Orchard PJ: Osteopetrosis. N Engl J Med 2004,351:2839–2849.

4. Rachner TD, Khosla S, Hofbauer LC: Osteoporosis: now and the future. Lancet 2011, 377:1276–1287.

5. Scott DL, Wolfe F, Huizinga TW: Rheumatoid arthritis. Lancet 2010, 376:1094–1108.

6. Mundy GR, Raisz LG, Cooper RA, Schechter GP, Salmon SE: Evidence for the secretion of an osteoclast stimulating factor in myeloma. N Engl J Med 1974, 291:1041–1046.

7. Yoneda T: Cellular and molecular mechanisms of breast and prostate cancer metastasis to bone. Eur J Cancer 1998, 34:240–245.

8. Yasuda H, Shima N, Nakagawa N, Yamaguchi K, Kinosaki M, Mochizuki S, Tomoyasu A, Yano K, Goto M, Murakami A, Tsuda E, Morinaga T, Higashio K, Udagawa N, Takahashi N, Suda T: Osteoclast differentiation factor is a ligand for osteoprotegerin/osteoclastogenesis-inhibitory factor and is identical to TRANCE/RANKL. Proc Natl Acad Sci U S A 1998, 95:3597–3602.

9. Wiktor-Jedrzejczak W, Bartocci A, Ferrante AW Jr, Ahmed-Ansari A, Sell KW, Pollard JW, Stanley ER: Total absence of colony-stimulating factor 1 in the macrophage-deficient osteopetrotic (op/op) mouse. Proc Natl Acad Sci USA 1990, 87:4828–4832.

10. Lacey DL, Timms E, Tan HL, Kelley MJ, Dunstan CR, Burgess T, Elliott R, Colombero A, Elliott G, Scully S, Hsu H, Sullivan J, Hawkins N, Davy E, Capparelli C, Eli A, Qian YX, Kaufman S, Sarosi I, Shalhoub V, Senaldi G, Guo J, Delaney J, Boyle WJ: Osteoprotegerin ligand is a cytokine that regulates osteoclast differentiation and activation. Cell 1998, 93:165–176.

11. Nicholson GC, Malakellis M, Collier FM, Cameron PU, Holloway WR, Gough TJ, Gregorio-King C, Kirkland MA, Myers DE: Induction of osteoclasts from CD14-positive human peripheral blood mononuclear cells by receptor activator of nuclear factor kappaB ligand (RANKL). Clin Sci (Lond) 2000, 99:133–140.

12. Saltel F, Chabadel A, Bonnelye E, Jurdic P: Actin cytoskeletal organisation in osteoclasts: a model to decipher transmigration and matrix degradation. Eur J Cell Biol 2008, 87:459–468.

13. Ikeda F, Nishimura R, Matsubara T, Tanaka S, Inoue J, Reddy SV, Hata K, Yamashita K, Hiraga T, Watanabe T, Kukita T, Yoshioka K, Rao A, Yoneda T: Critical roles of c-Jun signaling in regulation of NFAT family and RANKL- regulated osteoclast differentiation. J Clin Invest 2004, 114:475–484.

14. Takayanagi H, Kim S, Koga T, Nishina H, Isshiki M, Yoshida H, Saiura A, Isobe M, Yokochi T, Inoue J, Wagner EF, Mak TW, Kodama T, Taniguchi T: Induction and activation of the transcription factor NFATc1 (NFAT2) integrate RANKL signaling in terminal differentiation of osteoclasts. Dev Cell 2002, 3:889–901.

15. Sharma SM, Bronisz A, Hu R, Patel K, Mansky KC, Sif S, Ostrowski MC: MITF and PU.1 recruit p38 MAPK and NFATc1 to target genes during osteoclast differentiation. J Biol Chem 2007, 282:15921–15929.

16. Yu M, Moreno JL, Stains JP, Keegan AD: Complex regulation of tartrate- resistant acid phosphatase (TRAP) expression by interleukin 4 (IL-4): IL-4 indirectly suppresses receptor activator of NF-kappaB ligand (RANKL)- mediated TRAP expression but modestly induces its expression directly. J Biol Chem 2009, 284:32968–32979.

17. Matsumoto M, Kogawa M, Wada S, Takayanagi H, Tsujimoto M, Katayama S, Hisatake K, Nogi Y: Essential role of p38 mitogen-activated protein kinase in cathepsin K gene expression during osteoclastogenesis through association of NFATc1 and PU.1. J Biol Chem 2004, 279:45969–45979.

18. Kim K, Lee SH, Ha Kim J, Choi Y, Kim N: NFATc1 induces osteoclast fusion via up-regulation of Atp6v0d2 and the dendritic cell-specific transmem- brane protein (DC-STAMP). Mol Endocrinol 2008, 22:176–185.

19. Sundaram K, Nishimura R, Senn J, Youssef RF, London SD, Reddy SV: RANK ligand signaling modulates the matrix metalloproteinase-9 gene expression during osteoclast differentiation. Exp Cell Res 2007, 313:168–178.

20. Mabilleau G, Chappard D, Sabokbar A: Role of the A20-TRAF6 axis in lipopolysaccharide-mediated osteoclastogenesis. J Biol Chem 2011, 286:3242–3249.

21. Mizoguchi F, Izu Y, Hayata T, Hemmi H, Nakashima K, Nakamura T, Kato S, Miyasaka N, Ezura Y, Noda M: Osteoclast-specific Dicer gene deficiency suppresses osteoclastic bone resorption. J Cell Biochem 2010, 109:866–875.

22. Rossi M, Pitari MR, Amodio N, Di Martino MT, Conforti F, Leone E, Botta C, Paolino FM, Del Giudice T, Iuliano E, Caraglia M, Ferrarini M, Giordano A, Tagliaferri P, Tassone P: miR-29b negatively regulates human osteoclastic cell differentiation and function: Implications for the treatment of multiple myeloma-related bone disease. J Cell Physiol 2013, 228:1506–1515.

23. Lee Y, Kim HJ, Park CK, Kim YG, Lee HJ, Kim JY, Kim HH: MicroRNA-124 regulates osteoclast differentiation. Bone 2013, 56:383–389.

24. Bluml S, Bonelli M, Niederreiter B, Puchner A, Mayr G, Hayer S, Koenders MI, van den Berg WB, Smolen J, Redlich K: Essential role of microRNA-155 in the pathogenesis of autoimmune arthritis in mice. Arthritis Rheum 2011, 63:1281–1288.

25. Zhang J, Zhao H, Chen J, Xia B, Jin Y, Wei W, Shen J, Huang Y: Interferon- beta-induced miR-155 inhibits osteoclast differentiation by targeting SOCS1 and MITF. FEBS Lett 2012, 586:3255–3262.

26. Nowak JS, Choudhury NR, de Lima AF, Rappsilber J, Michlewski G: Lin28a regulates neuronal differentiation and controls miR-9 production.Nat Commun 2014, 5:3687.

27. Hoshino A, Iimura T, Ueha S, Hanada S, Maruoka Y, Mayahara M, Suzuki K, Imai T, Ito M, Manome Y, Yasuhara M, Kirino T, Yamaguchi A, Matsushima K, Yamamoto K: Deficiency of chemokine receptor CCR1 causes osteopenia due to impaired functions of osteoclasts and osteoblasts. J Biol Chem 2010, 285:28826–28837.

28. Kukita T, Wada N, Kukita A, Kakimoto T, Sandra F, Toh K, Nagata K, Iijima T, Horiuchi M, Matsusaki H, Hieshima K, Yoshie O, Nomiyama H: RANKL- induced DC-STAMP is essential for osteoclastogenesis. J Exp Med 2004, 200:941–946.

29. Dweep H, Sticht C, Pandey P, Gretz N: miRWalk–database: prediction of possible miRNA binding sites by 'walking' the genes of three genomes. J Biomed Inform 2011, 44:839–847.

30. Lewis BP, Burge CB, Bartel DP: Conserved seed pairing, often flanked by adenosines, indicates that thousands of human genes are microRNA targets. Cell 2005, 120:15–20.

31. Wang X: miRDB: a microRNA target prediction and functional annotation database with a wiki interface. RNA 2008, 14:1012–1017.

32. Gallois A, Lachuer J, Yvert G, Wierinckx A, Brunet F, Rabourdin-Combe C, Delprat C, Jurdic P, Mazzorana M: Genome-wide expression analyses establish dendritic cells as a new osteoclast precursor able to generate bone-resorbing cells more efficiently than monocytes. J Bone Miner Res 2009, 25:661–672.

33. de la Rica L, Rodriguez-Ubreva J, Garcia M, Islam AB, Urquiza JM, Hernando H, Christensen J, Helin K, Gomez-Vaquero C, Ballestar E: PU.1 target genes undergo Tet2-coupled demethylation

and DNMT3b-mediated methyla- tion in monocyte-to-osteoclast differentiation. Genome Biol 2013, 14:R99.

34. Moreaux J, Hose D, Kassambara A, Reme T, Moine P, Requirand G, Goldschmidt H, Klein B: Osteoclast-gene expression profiling reveals osteoclast-derived CCR2 chemokines promoting myeloma cell migration. Blood 2011, 117:1280–1290.

35. Chien CH, Sun YM, Chang WC, Chiang-Hsieh PY, Lee TY, Tsai WC, Horng JT, Tsou AP, Huang HD: Identifying transcriptional start sites of human microRNAs based on high-throughput sequencing data. Nucleic Acids Res 2011, 39:9345–9356.

36. Rodriguez-Ubreva J, Ciudad L, van Oevelen C, Parra M, Graf T, Ballestar E: C/ EBPa-mediated activation of miR-34a and miR-223 inhibits Lef1 expression to achieve efficient reprogramming into macrophages. Mol Cell Biol 2014, 34:1145–1157.

37. Etzrodt M, Cortez-Retamozo V, Newton A, Zhao J, Ng A, Wildgruber M, Romero P, Wurdinger T, Xavier R, Geissmann F, Meylan E, Nahrendorf M, Swirski FK, Baltimore D, Weissleder R, Pittet MJ: Regulation of monocyte functional heterogeneity by miR-146a and Relb. Cell Rep 2012, 1:317–324.

38. Ramachandran P, Pellicoro A, Vernon MA, Boulter L, Aucott RL, Ali A, Hartland SN, Snowdon VK, Cappon A, Gordon-Walker TT, Williams MJ, Dunbar DR, Manning JR, van Rooijen N, Fallowfield JA, Forbes SJ, Iredale JP: Differential Ly-6C expression identifies the recruited macrophage phenotype, which orchestrates the regression of murine liver fibrosis. Proc Natl Acad Sci U S A 2012, 109:E3186–E3195.

39. Puzik A, Rupp J, Troger B, Gopel W, Herting E, Hartel C: Insulin-like growth factor-I regulates the neonatal immune response in infection and maturation by suppression of IFN-gamma. Cytokine 2012, 60:369–376.

40. Baeuerle PA, Baltimore D: NF-kappa B: ten years after. Cell 1996, 87:13–20.

41. Taganov KD, Boldin MP, Chang KJ, Baltimore D: NF-kappaB-dependent induction of microRNA miR-146, an inhibitor targeted to signaling proteins of innate immune responses. Proc Natl Acad Sci U S A 2006, 103:12481–12486.

42. Vento-Tormo R, Rodriguez-Ubreva J, Lisio LD, Islam AB, Urquiza JM, Hernando H, Lopez-Bigas N, Shannon-Lowe C, Martinez N, Montes-Moreno S, Piris MA, Ballestar E: NF-kappaB directly mediates epigenetic deregulation of common microRNAs in Epstein-Barr virus-mediated transformation of B-cells and in lymphomas. Nucleic Acids Res 2014, 42:11025–11039.

43. Hanna RN, Shaked I, Hubbeling HG, Punt JA, Wu R, Herrley E, Zaugg C,Pei H, Geissmann F, Ley K, Hedrick CC: NR4A1 (Nur77) deletion polarizes macrophages toward an inflammatory phenotype and increases atherosclerosis. Circ Res 2012, 110:416–427.

44. Rustici G, Kolesnikov N, Brandizi M, Burdett T, Dylag M, Emam I, Farne A, Hastings E, Ison J, Keays M, Kurbatova N, Malone J, Mani R, Mupo A, Pedro Pereira R, Pilicheva E, Rung J, Sharma A, Tang YA, Ternent T, Tikhonov A, Welter D, Williams E, Brazma A, Parkinson H, Sarkans U: ArrayExpress update–trends in database growth and links to data analysis tools. Nucleic Acids Res 2013, doi:10.1093/nar/gks1174. Pubmed ID 23193272.

Figure legends

Figure 1 MicroRNA expression profiling during monocyte-to-osteoclast differentiation. (A) Validation of the presence of OCs by TRAP and phalloidin staining, showing the presence of TRAP activity/multiple nuclei and the actin ring, respectively. (B) Molecular characterization of OC differentiation. Several OC markers are upregulated (CA2, CTSK, MMP9, ACP5/TRAP, and TM7SF4/DCSTAMP), and the MO marker CX3CR1 is silenced. Data for MOs, MOs 48 h after M-CSF and RANKL treatment and OCs at 21 days are presented. RPL38 gene expression levels were used for normalization. Error bars correspond to the standard deviation of three individual measurements. (C) Heatmap showing expression array data from the miRNA expression screening. miRNAs were subdivided into eight groups (I to VIII) according to their expression profile (diagram); the number of miRNAs in each group is indicated inside the expression dynamics diagram. Scale shown at the bottom, whereby normalized expression units ranges from -1 (blue) to +1 (red). (D)Representation of the genomic distribution of miR-99b/125a/let7e and miR-132/212 clusters, including the TSS (indicated with an arrow). (E) Validation of array data by quantitative PCR in independent biological replicates. Analysis in MOs, MOs incubated 48 h with RANKL/M-CSF and fully differentiated OCs. Data normalized with respect to miR-103. (F) Expression dynamics of the indicated miRNAs during OC differentiation, also normalized with respect to miR-103.

Figure 2 Influence of miRNAs in modulating monocyte-to-osteoclast differentiation. (A) Quantification by flow cytometry of the transfection efficiency using a fluorescent control power inhibitor or antagomir. (B) Functional effect of miRNA inhibition using power inhibitors (or antagomirs) for the individual miRNAs in the miR-99b/125a/let7e and miR-132/212 clusters on CA2, CTSK, MMP9, ACP5 and CX3CR1 expression levels 4 days after M-CSF/RANL stimulation. Quantification was done using qRT-PCR with specific primers for each gene and using the RPL38 gene for normalization. (C) Functional effect of miRNA inhibition using double transfections with power inhibitors for two miRNAs within the miR-99b/125a/let7e and miR-132/ 212 clusters. Quantification was carried out using qRT-PCR with specific primers for each gene and using the RPL38 gene for normalization. (D) Effect of miRNA inhibition on the levels of surface markers CCR1 and TM7SF4. A bar diagram summarizing the results of the individual inhibition of each

miRNA of the two clusters is presented. Also, a plot of the fluorescence-activated cell sorting (FACS) analysis is presented. (E) Effect of miRNA inhibition on the ability of cells to differentiate in OCs. Cells were arrested at 4 days after inducing differentiation. OCs were stained with TRAP. Cells with three or more nuclei were counted as OCs. In the images, multinuclear OCs are indicated with a red arrow. On the right, a bar diagram showing the percentage of OCs under

each condition (center) and a bar diagram showing the number of cells with two, three or four or more nuclei under each condition (right). Error bars correspond to the standard deviation of three independent measurements; *corresponds to P-value <0.05; **means P-value <0.01.

Figure 3 Analysis of miRNA targets. (A) Venn diagram summarizing the rationale for selecting putative miRNA targets by combining the lists generated with prediction algorithms with those generated from expression datasets (1,858 genes with a fold change <0.5). (B) Gene Ontology (GO) enrichment analysis of putative miRNA targets from the previous analysis. (C) Summary of putative targets and their corresponding miRNA matches among the miR-99b/125a/let7e and miR-132/212 clusters. (D) Luciferase assays of HeLa cells cotransfected with different luciferase reporter psiCheck2 constructs containing the 3′ UTR of putative targeted transcription factors (wild type (WT) or mutant (Mut) forms). (E) Effects on validated targets of the single transfection with miRNA power inhibitors in MOs 4 days after being stimulated with RANKL/M-CSF, as assessed by qRT-PCR and western blotting. Expression data are relative to the levels obtained for the samples transfected with control power inhibitor or antagomir (a-miR) and are normalized to the RPL38 gene. Protein data have been normalized against α-tubulin, using the sample transfected with the control power inhibitor as a reference. At the bottom, quantification of the levels of protein relative to the control for each antagomir. (F) Effects on validated targets of the double transfection with miRNA power inhibitors in MOs 4 days after being stimulated with RANKL/M-CSF, as assessed by qRT-PCR and western blotting. Data analyzed as above. Error bars correspond to standard deviation of three independent experiments; *corresponds to P-value <0.05; **means P-value <0.01; ***means P-value < 0.001.

Figure 4 Comparison of changes in the expression levels of the miRNAs within the miR-99b/125a/let7e and miR-132/212 clusters during osteoclast differentiation, and changes during monocyte-to-macrophage and monocyte-to-dendritic cell differentiation. (A) Diagram depicting the three differentiation models used in this experiment. GM-CSF, granulocyte-macrophage colony-stimulating factor. (B) Relative expression levels of the miRNAs in matching samples of MOs (grey), immature dendritic cells (iDC, red), macrophages (green,) and monocytes stimulated with RANKL/M-CSF after 1, 2 and 4 days (immature OCs (iOC) (blue)). qRT-PCR data were normalized with respect to miR-103. (C) Relative expression levels of miRNA targets in the same set of samples. qRT-PCR data were normalized with respect to the RPL38 gene. Error bars correspond to standard deviation of three independent measurements.

Figure 5 NF-κB dependence of miRNA expression changes. (A) Analysis of the presence of NF-κB subunit binding motifs (from TRANSFAC database) in a 1,000-bp window centered around the

estimated TSS of the miRNAs. (B) ChIP assays for selected miRNAs showing the binding of NF-κB p65 near the TSS 2 and 4 days after RANKL/M-CSF stimulation of MOs. Each graph contains the relative enrichment of samples immunoprecipitated with the anti-p65 antibody and an IgG as a control. MO samples were tested at 0, 2 and 4 days after M-CSF/RANKL stimulation. On top of each graph the sequence analyzed is indicated. p65 putative binding sites are indicated with a blue dot. Primers used for amplification are indicated with arrows around p65 binding sites. (C) Effects of the two NF-κB inhibitors (10 μM BAY 11-7082 (BAY11) and 100 μM sodium aurothiomalate (SATM) on the phosphorylation levels of p65 as determined by western blotting. p65 and H3 total levels are used as controls. (D) Effects of two NF-κB inhibitors (BAY11 and SATM) on the levels of miRNAs within the miR-99b/125a/let7e and miR-132/212 clusters measured by a time-course analysis of MOs stimulated with RANKL/M-CSF. (E) Effects of treatment with BAY11 and SATM on markers of OC differentiation (ACP5, CTSK, TM7SF4, MMP9) as estimated by qRT-PCR. Data relative to DMSO-treated samples and normalized with RPL38 expression levels. (F) Effects of treatment with BAY 11 and SATM on miRNA targets (IGF1R, TNFAIP3, ITGA4, THBS, IL15 and PTGS2) as estimated by qRT-PCR. Data are relative to DMSO-treated samples and are normalized with respect to RPL38 expression levels. Error bars correspond to the standard deviation of three independent measurements; *corresponds to P-value <0.05; **means P-value <0.01

Figure 6 NF-κB p65 has a direct role in changes in miRNA expression levels. (A) Diagram depicting the region of the p65 gene in exon 11 targeted by the siRNA used in this study. Effects of siRNA experiments on p65 levels in MOs stimulated with RANKL/M-CSF after 1, 2, and 4 days, as analyzed by western blotting (bottom and central panels, normalized with respect to histone H3 levels) and qRT-PCR (left panel, relative to RPL38 expression levels). (B) Effect of p65 depletion on its recruitment near the TSS of the coding sequence of the miRNAs, as demonstrated by ChIP assays. The scheme on top of each graph depicts the region analyzed, indicating the p65 binding site (dot) and the primers used (arrows around the p65 binding site). (C) Effects of p65 siRNA experiments on miR-99b, miR-125a and miR-let7e after 1, 2, and 4 days. Data relative to miR-103 levels. (D) Effects of p65 downregulation on expression of genes upregulated during osteoclastogenesis (CTSK, MMP9, ACP5, TM7SF4).(E) Effects of p65 downregulation on the levels of the miRNA targets TNFAIP3 and IGF1R. Expression data compared with MO samples treated with control siRNA and values relative to RPL38 expression levels. Error bars correspond to the standard deviation of three independent measurements; *corresponds to P-value <0.05; **means P-value <0.01.

Figure 1

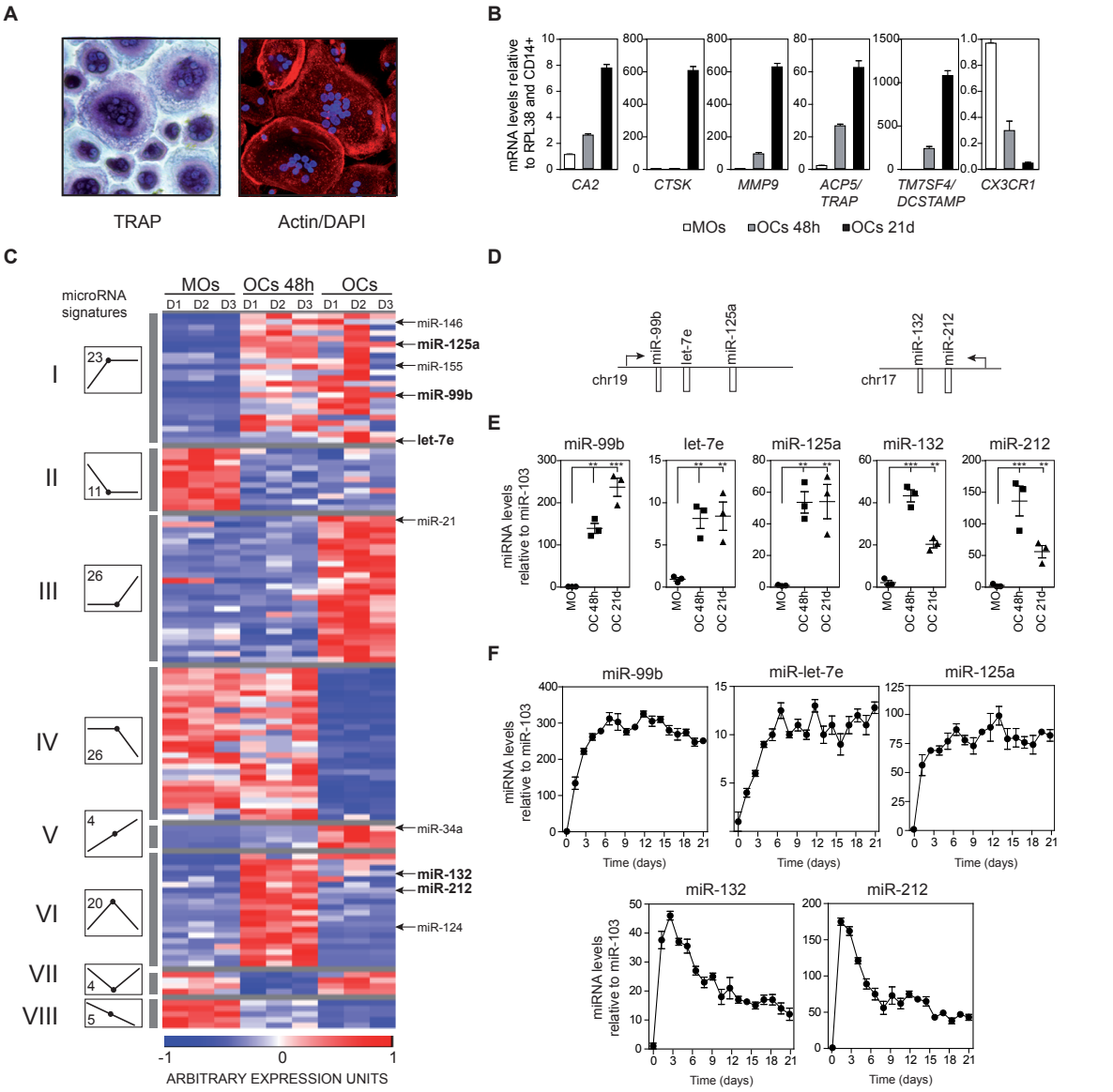
A
TRAP
Actin/DAPI
B
mRNA levels relative to RPL38 and CD14+
CA2
CTSK
MMP9
ACP5/ TRAP
TM7SF4/ DCSTAMP
CX3CR1
MOs
OCs 48h
OCs 21d
C
microRNA signatures
MOs
OCs 48h
OCs
D1 D2 D3 D1 D2 D3 D1 D2 D3
I
II
III
IV
V
VI
VII
VIII
23
11
26
26
4
20
4
5
miR-146
miR-125a
miR-155
miR-99b
let-7e
miR-21
miR-34a
miR-132
miR-212
miR-124
-1
0
1
ARBITRARY EXPRESSION UNITS
D
chr19
miR-99b
let-7e
miR-125a
chr17
miR-132
miR-212
E
miR-99b
let-7e
miR-125a
miR-132
miR-212
miRNA levels relative to miR-103
MO
OC 48h
OC 21d
F
miR-99b
miR-let-7e
miR-125a
miR-132
miR-212
miRNA levels relative to miR-103
Time (days)

Figure 2

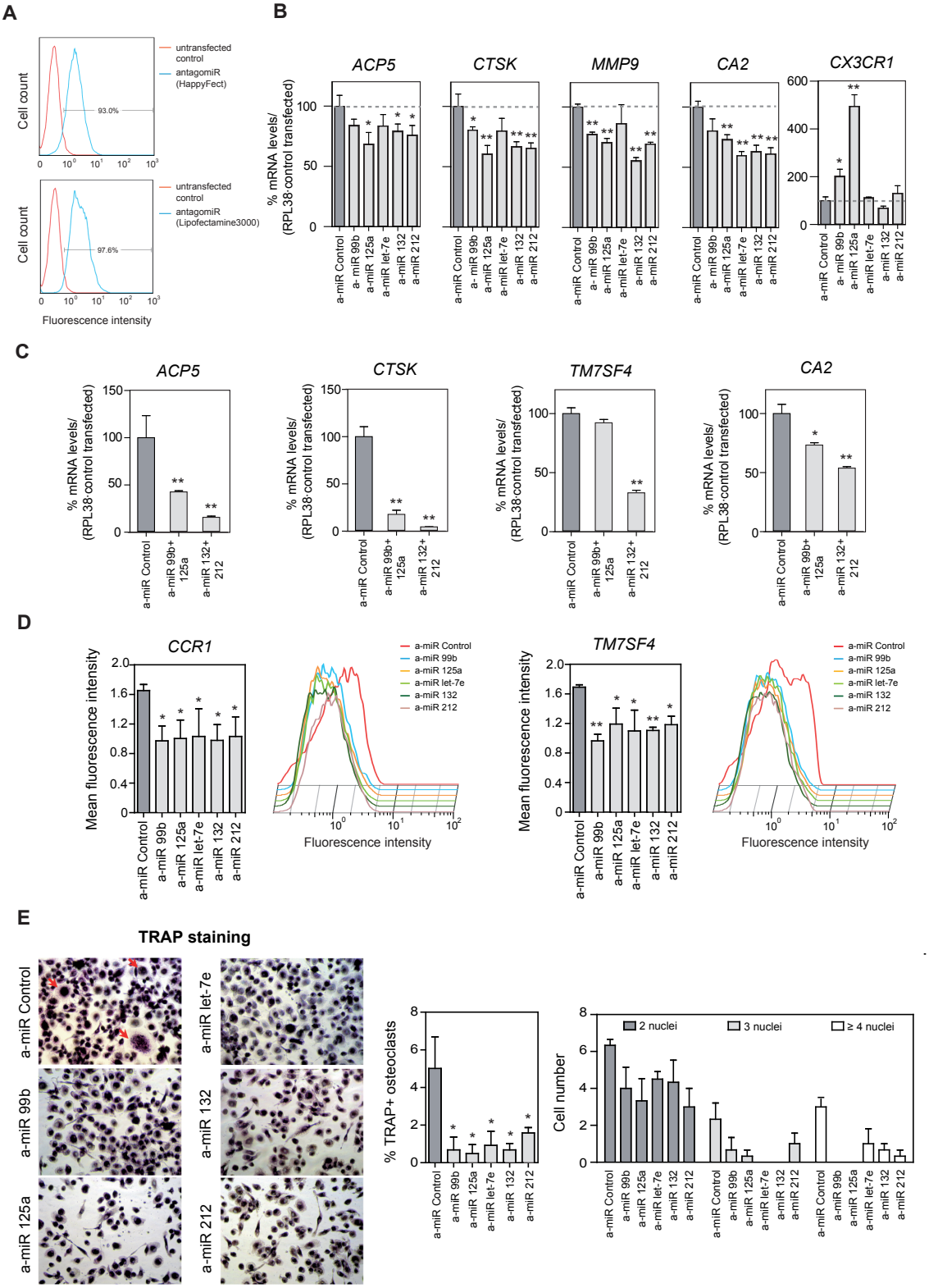

4 days after miRNA inhibition and M-CSF/RANKL stimulation

Figure 3

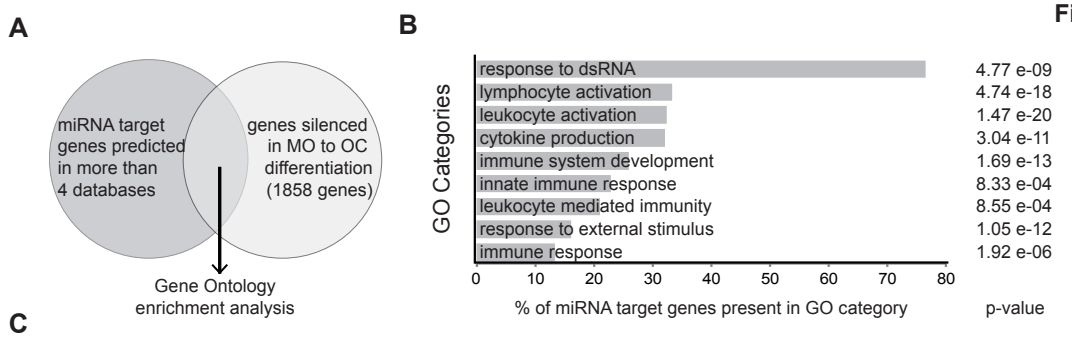

C

miR-125a	*ETV6*	ets variant 6
	IGF1R	insulin-like growth factor 1 receptor
	TNFAIP3	tumor necrosis factor, alpha-induced protein 3
	CX3CR1	chemokine (C-X3-C motif) receptor 1
	IL1A	interleukin 1, alpha
	IRF1	interferon regulatory factor 1
let-7e	*TNFAIP3*	Tumor Necrosis Factor, Alpha-Induced Protein 3
	CD74	CD74 molecule, MHC, class II invariant chain
	CEBPD	CCAAT/enhancer binding protein (C/EBP), delta
	ITGA4	integrin, alpha 4 (antigen CD49D
	THBS1	thrombospondin 1
	PTGS2	prostaglandin-endoperoxide synthase 2
miR-99b	*IGF1R*	insulin-like growth factor 1 receptor

miR-132	*IRF1*	interferon regulatory factor 1
	PTGS2	prostaglandin-endoperoxide synthase 2
	HBEGF	heparin-binding EGF-like growth factor
	NR4A2	nuclear receptor subfamily 4, group A, member 2
miR-212	*CX3CR1*	chemokine (C-X3-C motif) receptor 1
	HBEGF	heparin-binding EGF-like growth factor
	IL15	interleukin 15

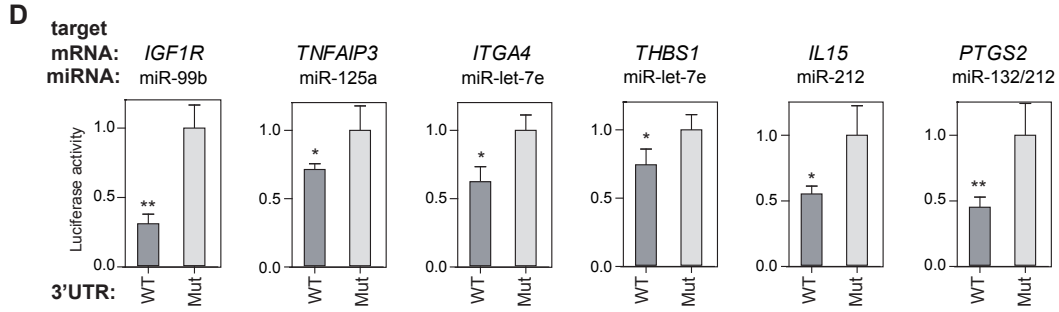

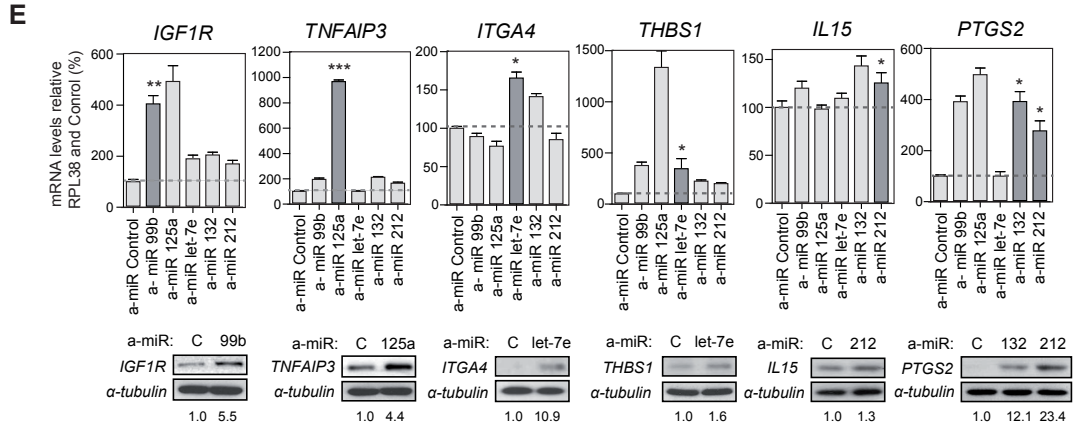

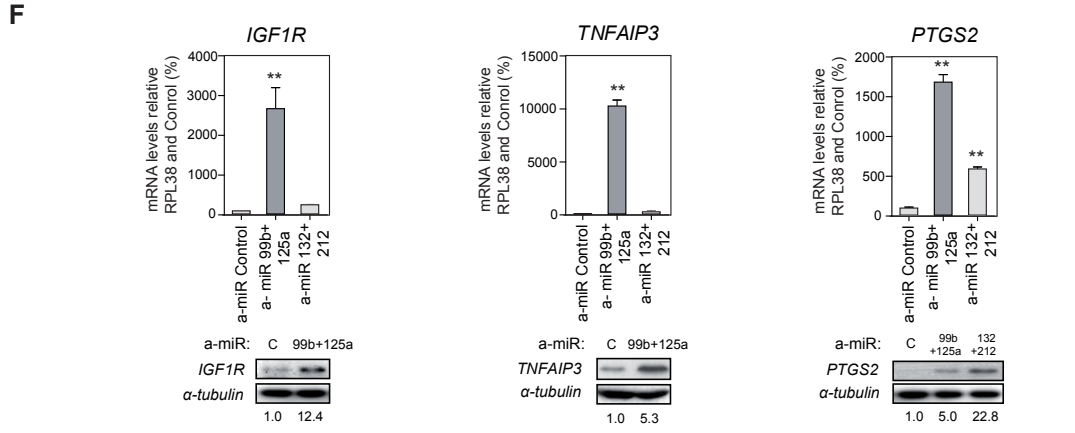

Figure 4

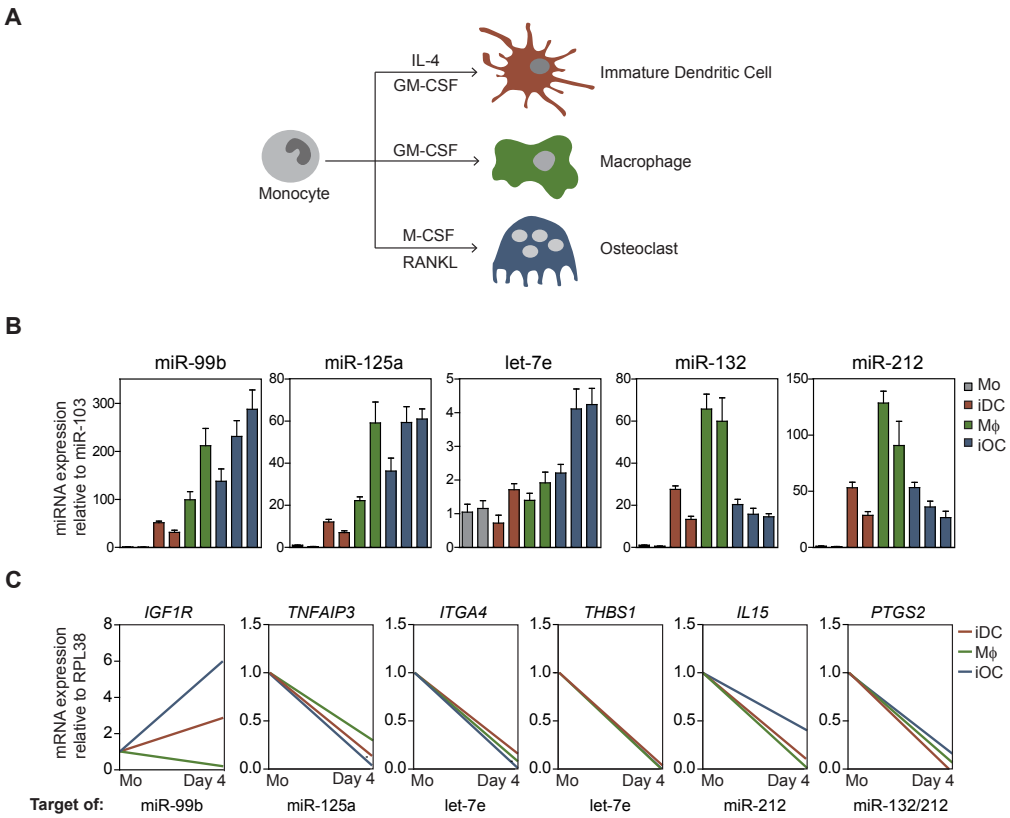
A
IL-4
GM-CSF
Immature Dendritic Cell
GM-CSF
Macrophage
Monocyte
M-CSF
RANKL
Osteoclast
B
miR-99b
miR-125a
let-7e
miR-132
miR-212
miRNA expression relative to miR-103
Mo
iDC
Mϕ
iOC
C
IGF1R
TNFAIP3
ITGA4
THBS1
IL15
PTGS2
mRNA expression relative to RPL38
iDC
Mϕ
iOC
Mo
Day 4
Target of:
miR-99b
miR-125a
let-7e
let-7e
miR-212
miR-132/212

Figure 5

A

p65 binding site presence

NF-kB (V$NFKAPPAB65_01)

miRNA	Chr	Position range	
hsa-miR-126	chr9	139559224	139561224
hsa-let-7e	chr19	52190897	52192897
hsa-miR-125a-5p	chr19	52190897	52192897
hsa-miR-132	chr17	1959152	1961152
hsa-miR-146b-5p	chr10	104178511	104180511
hsa-miR-147	chr9	123018092	123020092
hsa-miR-155	chr21	26945292	26947292
hsa-miR-181d	chr19	13975434	13977434
hsa-miR-199a-5p	chr19	10929651	10931651
hsa-miR-212	chr17	1959152	1961152
hsa-miR-22	chr17	1613805	1615805
hsa-miR-29a	chr7	130595983	130597983
hsa-miR-338-3p	chr17	79090096	79092096
hsa-miR-34a	chr1	9258025	9260025
hsa-miR-365	chr16	14395078	14397078
hsa-miR-370	chr14	101355633	101357633
hsa-miR-409-3p	chr14	101490439	101492439
hsa-miR-449a	chr5	54468005	54470005
hsa-miR-502-5p	chrX	49686225	49688225
hsa-miR-584	chr5	148441737	148443737
hsa-miR-598	chr8	11057875	11059875
hsa-miR-665	chr14	101316552	101318552
hsa-miR-9	chr1	156399493	156401493
hsa-miR-99b	chr19	52190897	52192897

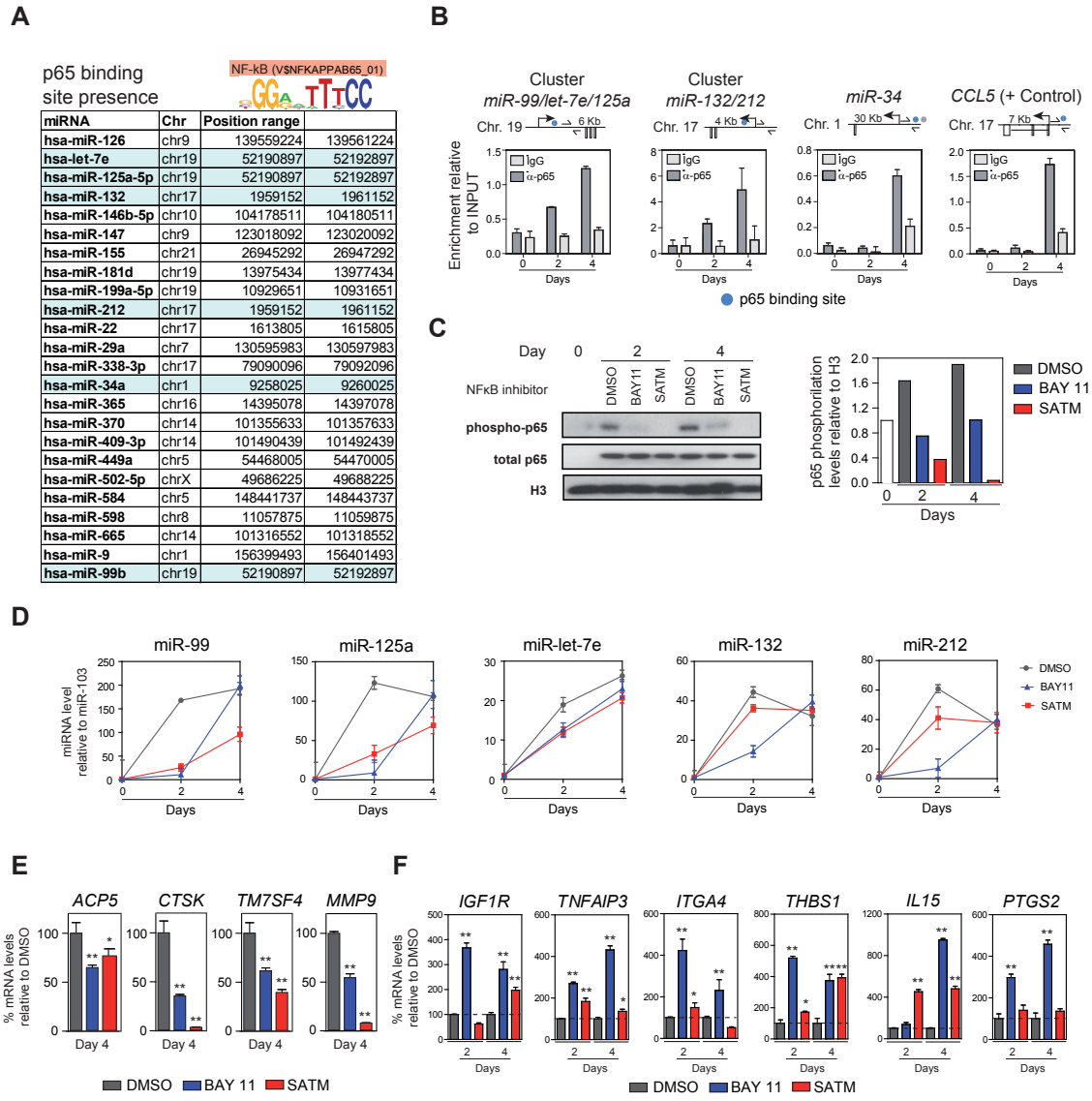

Figure 6

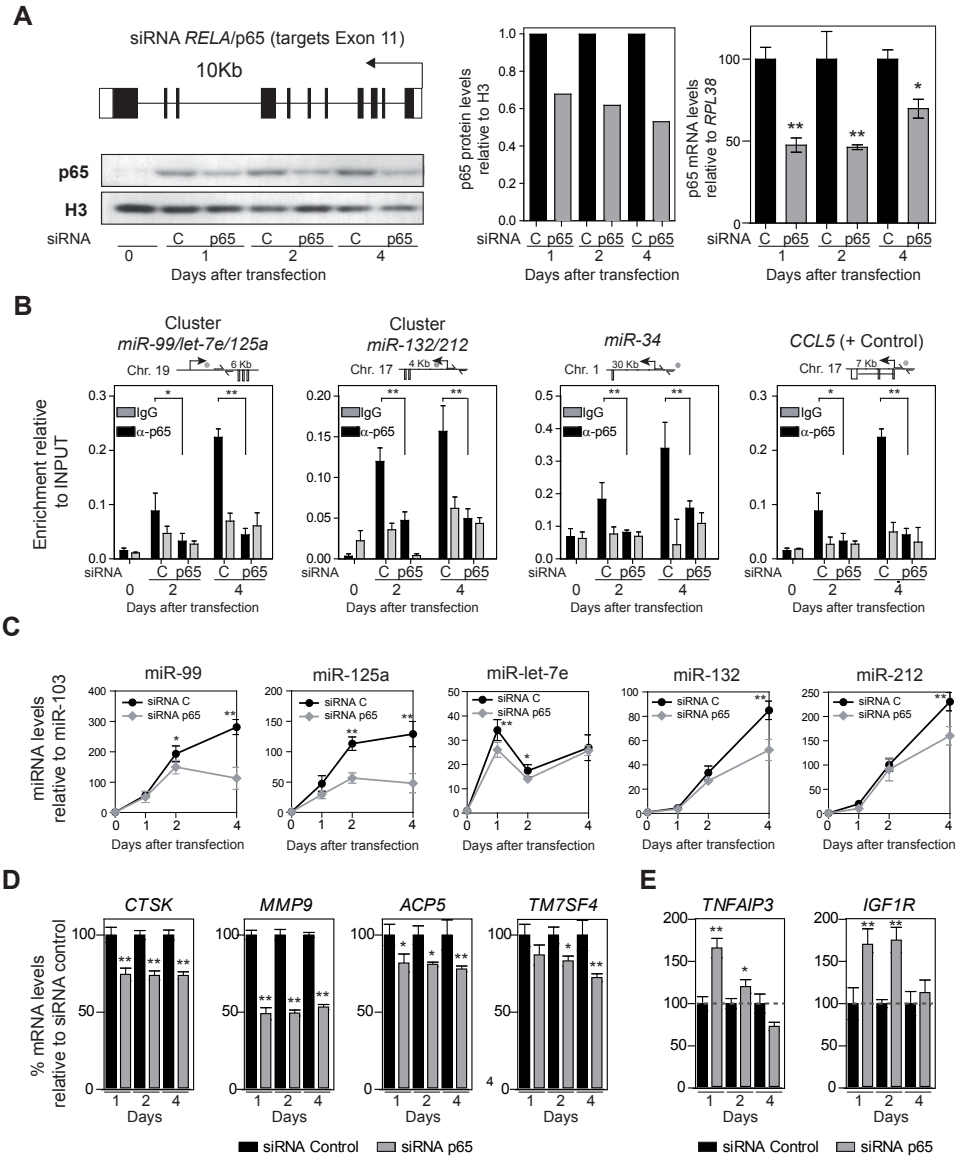
A
siRNA RELA/p65 (targets Exon 11)
10Kb
p65
H3
siRNA C p65 C p65 C p65
0 1 2 4
Days after transfection
p65 protein levels relative to H3
p65 mRNA levels relative to RPL38
B
Cluster miR-99/let-7e/125a
Cluster miR-132/212
miR-34
CCL5 (+ Control)
Enrichment relative to INPUT
IgG
α-p65
C
miR-99
miR-125a
miR-let-7e
miR-132
miR-212
miRNA levels relative to miR-103
siRNA C
siRNA p65
D
CTSK
MMP9
ACP5
TM7SF4
% mRNA levels relative to siRNA control
Days
siRNA Control
siRNA p65
E
TNFAIP3
IGF1R

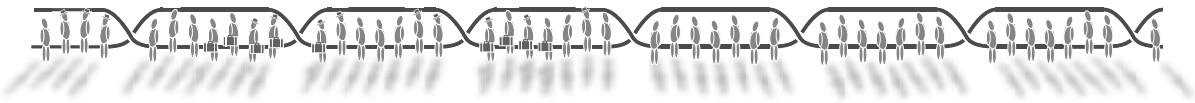

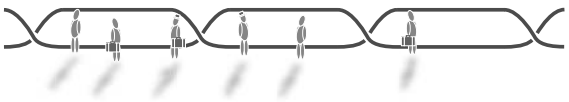

GLOBAL RESULTS AND DISCUSSION

4 GLOBAL RESULTS AND DISCUSSION

In the present doctoral thesis, we have explored the participation and role of epigenetic and non-coding RNA-related mechanisms associated with several differentiation processes that are relevant during inflammation: MO differentiation and maturation to DCs and MACs, and MO activation.

4.1 Global Results

DNA hypomethylation in MO-to-DC and MO-to-MAC differentiation and maturation ***(ARTICLE 1)***

To unravel the DNA methylation changes associated with MO-to-MAC differentiation (GM-CSF-mediated), MO-DC differentiation (GM-CSF + IL-4-mediated) and their correspondent mature phenotype (LPS addition), three sets of matching samples from independent healthy donors were generated and hybridised on a 450k microarray from Illumina.

Statistical analysis of the data illustrates that changes occur mainly during the differentiation process, with few changes happening upon TLR4 engagement by LPS. Moreover, we observed that demethylation is considerably more prevalent than gains in DNA methylation. Most interestingly, although the majority of DNA methylation changes are common for both processes (MAC and DC differentiation), a significant portion of differentially methylated sites are specific for each cell type.

Next, in order to detect the implication of TET2 as the main agent responsible for active demethylation, we silenced it by using specific siRNAs. We observed that TET2 downregulation not only impairs changes in DNA methylation but also in cell identity establishment, as shown by the reduction in the expression of the specific surface markers.

To explore the consequences of DNA methylation during both differentiation processes, we generated global expression profiles from the same samples used for DNA methylation screening. In contrast to variations in DNA methylation patterns which were monodirectional (only demethylation), expression changes occur in both directions (up- and downregulation) and before and after the addition of the LPS.

Once the expression profiles were analysed, we compared the relationship between demethylation and expression changes. A negative correlation was observed between both data sets and this correlation is stronger if the analysis is done in CpGs, located in the TSS200 and the first exon. Most importantly, some of the genes that lost DNA methylation during differentiation

were significantly overexpressed only after the addition of the LPS stimulus. This was the case of two specific MAC genes: *IL1B* and *CCL20*, both with a crucial role in the inflammation response. This suggests that DNA demethylation could be playing a role as a mechanism to prepare the chromatin of specific genes to quickly respond against again an external insult.

IL-4 is the differential external factor between MAC and DC differentiation under our conditions, as it is only crucial for acquiring a DC phenotype, with its absence determining MAC cell identity. As a consequence, it seems plausible that IL-4 signalling through IL-4R triggers or at least contributes to methylation changes for specific DC genes. In order to confirm this hypothesis, we used the specific inhibitor to block JAK3 Tyr kinase activation, which is directly downstream to IL-4R. We then used 450k microarrays from Illumina to detect the genomic effect of this inhibitor at the DNA methylation level. We observed that inhibition of JAK3 impairs DNA demethylation changes of DC-specific genes and induces small but significant DNA demethylation in MAC genes for samples incubated under the conditions for DC differentiation. By contrast, no effect was observed for genes that are demethylated under the conditions for both MAC and DC differentiation, as their demethylation was independent of STAT6 presence. When checking the expression changes in some selected genes, the opposite effect was observed, demonstrating once again the negative correlation between them.

Specific siRNAs against JAK3 and STAT6 were used in order to further dissect the effects that this pathway has on DNA demethylation. As expected, siRNAs against JAK3 partially inhibited the loss of DNA methylation and the same results were observed in STAT6 siRNA experiments. These experiments proved that the JAK3-STAT6 axis is activated only during DC differentiation and furthermore, it is responsible for DNA methylation loss in specific DC genes, as well as the repressor for MAC gene hypomethylation.

TRANSFAC analysis confirmed the existence of binding motifs for STAT6 near CpG sites that become demethylated in specifically in DC differentiation. To test if STAT6 directly binds DC specific genes we performed ChIP experiments, using primers near the CpG site that becomes demethylated and containing a putative STAT binding site. ChIP assays revealed that STAT6 binds to DC specific genes only in DC cells but not in MO, MAC or STAT6 inhibited cells, demonstrating the direct regulation of those genes by the TF STAT6.

In order to demonstrate that STAT6 was able to induce changes in DNA methylation on their own, a constitutive active STAT6 mutant was constructed. Simultaneously, we infected MOs with pCDH-MIG lentiviral vectors carrying STAT6VT and, in parallel, with an empty GFP-expressing MIG vector as a negative control. Following MO infection with STAT6VT, MOs were

differentiated with GM-CSF only (i.e. MAC differentiation conditions) for 9 days and their infection was detected by GFP expression. We then performed BS sequencing of those cells infected with STAT6VT and empty vector and analysed methylation content of specific genes.

We observed that DC specific genes decrease their methylation status when cells were infected with STAT6VT, indicating a crucial role of activated STAT6 in the induction of DNA demethylation changes for DC-specific genes. Furthermore, an impairment of DNA methylation loss for MAC specific genes was observed, revealing a role of STAT6 in preventing DNA demethylation of those genes that should not be activated during DC differentiation. As expected, no change was detected for common genes, demonstrating a mechanism for DNA methylation independent of STAT6 in this case.

Taken together, all these results show a crucial role of the JAK3-STAT6 axis in directing a specific loss of DNA methylation and their correspondent expression changes during DC differentiation, together with the inhibition of MAC-specific genes demethylation.

DNA demethylation of Inflammasome-associated Genes ***(ARTICLE 2)***

Global changes of DNA methylation analysed by 450K hybridisation of MO-to-MAC differentiation experiments described in the above section, revealed that a set of genes involved in the inflammasome activation are demethylated during this process. Moreover, we observed that these genes become upregulated in this process, suggesting a potential regulation of the expression of inflammasome components by DNA methylation.

The analysis of the process dynamics revealed that in all cases, the loss of DNA methylation anticipates the increase in mRNA levels of all these inflammasome-related genes. Loss of DNA methylation was fast (before 72 hours) suggesting an active mechanism of DNA methylation mediated by TET2.

To test active DNA methylation relevance in the inflammasome activity, TET2 was inhibited during MO-to-MAC differentiation using specific siRNAs against TET2, which resulted in impairment of DNA demethylation. We also explored the consequences that TET2 ablation had in changes of 5hmC, one of the oxidized forms in the demethylation process, by using the oxBS method. As expected, the conversion to 5hmC induced during MO-to-MAC differentiation is impaired in the presence of the siRNA against TET2.

To examine the relevance of DNA methylation in the induction of the expression for genes of the inflammasome, we plated MOs for a period between 3 hours and 24 hours in the presence of LPS and IL-1β, which are able to activate MO by their binding to TLR4 and IL-1R

respectively. We also combined LPS with MSU crystals and ATP, both involved in NLRP3 inflammasome induction. We observed a loss of DNA methylation in the inflammasome genes, although only for some of them (*IL1B, IL1RN, IL1A, CASP1)* the expression is induced before 24 hours. In those genes overexpressed during MO activation, gene expression anticipates changes in DNA methylation, indicating a different role of DNA methylation in both biological processes.

As NF-kB is one of the main common pathways induced by IL-1β, LPS and GM-CSF we used an inhibitor of the NF-kB during MO activation and differentiation to analyse the contribution to methylation variations. We detected that NF-kB inhibition is associated with an impairment of DNA methylation and gene expression of the inflammasome-related genes, indicating a relationship between NF-kB and activation of the inflammasome by the regulation of DNA methylation. Moreover, ChIP experiments revealed that p65 subunit from NF-kB complex directly binds to *IL1B, IL1RN, IL1A, CASP-1* promoter region.

CAPS and FMF are two archetypical monogenic autoinflammatory syndromes characterized by the activation of the inflammasome without the presence of an external insult. In order to study the relevance of DNA methylation changes in this context, MOs from patients with CAPS and FMFs were activated and/or differentiated to MACs.

MOs stimulated 24 hours with IL-1β present a small but significant increase of DNA demethylation for genes related to inflammasome in CAPS patients versus healthy controls. Increased demethylation seemed to also occur for FMF samples, although differences were not statistically significant for the selected threshold. The same tendency was observed when MAC differentiation was induced in MO from those patients, but in this case were not significant for the selected threshold.

These results highlight the importance of DNA methylation-mediated upregulation of inflammasome-associated genes in the development of CAPS and FMFs.

DNA hypermethylation in MO-to-DC and MO-to-MAC differentiation ***(ARTICLE 3)***

Despite of the fact that MO-to-DC and MO-to MAC differentiation is primarily associated with a widespread loss of methylation, some of the genes silenced during those differentiation processes undergo gains of DNA methylation. Among others, this set of genes includes *CX3CR1* (a chemokine receptor required for MO homeostasis), *CSF3R* (a receptor for the cytokine CSF3 involved in granulocyte differentiation), and *FYN* (a member of the src-family Tyr kinases involved in myeloid differentiation).

After DNA methylation analysis by BS pyrosequencing, we also tested changes in gene expression for those genes, using quantitative RT-PCR in three independent samples. In all cases,

differentiation correlated with a decrease in gene expression, indicating a possible regulation of gene expression by DNA methylation.

To determine in further detail the role of DNA methylation in gene expression of specific genes during DC differentiation, we performed time-course experiments of those genes. We observed that the loss of gene expression occurs at short intervals while the gain of methylation is progressively increased over time. These results point out that for those genes, in the promoter region, DNA hypermethylation is not the direct cause of gene downregulation.

To find out other possible epigenetic causes involved in the gain of DNA methylation, we examined active and repressive histone modification marks dynamics during DC differentiation by using the ChIP technique near the TSS region. We detected that repressive histone modification marks are concomitant with gains of DNA methylation. Nevertheless, loss of the active histone modifications precedes the very process of gene expression. This therefore indicates the relevance of these histone modification marks in the induction of gene expression.

In order to study the relevance of DNMT3B during the process, we inhibited it by using two inhibitors. A significant reduction in the level of DNA methylation in *CSF3R* and *FYN* was achieved when the inhibitors were present in the media. However, no change in gene expression was observed, once again indicating the independence of methylation in gene expression induction under these conditions. Active histone modifications were also independent of the inhibitors, whereas repressive marks were slightly reduced by the presence of the inhibitors.

To study whether inhibition of DNMTs influenced the acquisition of the DC phenotype, we analysed surface markers. Surprisingly, a dose-dependent effect on the specific DC marker CD209 (DC-SIGN) was observed when using the DNMT3B inhibitor. To confirm these results and examine other DC markers, a quantitative PCR was realised. Surface genes suffer a sharp reduction in gene expression over time, which suggests a mechanism whereby DNA methylation is able to produce changes in DC phenotypes, perhaps by altering the stability of gene expression.

MiRNA changes in MO differentiation models ***(ARTICLE 4)***

A first screening of miRNA expression in MO to OC differentiation revealed that the miR-99b/let-7e/125a and miR-212/132 clusters were upregulated during this process. In order to determine whether the induction of these miRNAs plays a role in repressing critical functions of undifferentiated MOs, that are necessary also in other MO-derived differentiation models, we analysed the expression of these clusters in two other models by using qRT-PCR: MO-to-DC and MO-to-MAC, and compared it to MO-to-OC differentiation. We determined significant

upregulation of both miRNA clusters in the three MO differentiation models studied, suggesting that the repression mediated by these miRNAs is a common mechanism in all these models.

To identify the targets of these miRNAs, we use bioinformatics prediction tools and crossed the predicted data with gene expression public data available during osteoclastogenesis differentiation, assuming an inverse correlation between gene and miRNA expression. The putative identified targets were all genes expressed in other different lineages, a fact that indicates the role of miRNAs as a mechanism to restrict the expression of genes not needed for proper cell function.

To validate the expression data, we performed qRT-PCR of samples from MO-to-DC, MO-to-MAC and MO-to-OC differentiation experiments. A common decrease in the RNA levels of the putative identified targets during the three differentiation processes occurred, indicating the robustness of the mechanisms between all three cell type differentiations.

Luciferase reporter assays were also done to validate the interaction between miRNA and their target. These assays confirmed how the different miRNA from miR-99b/let-7e/125a and miR-212/132 clusters were able to target the putative identified targets previously identified.

Due to the relevance of NF-kB pathway in all MO differentiation models, we explored the potential participation of this pathway in the regulation of the expression of the two miRNA clusters. To this end, we first inspected the presence of consensus binding sites for NF-κB p65 subunit in the promoter region of the miRNAs using bioinformatics tools. This analysis showed that p65 consensus binding site is present in the majority of miRNA TSSs, including the miRNAs within the miR-99b/let-7e/125a and miR-212/132 clusters.

To validate the data, we performed ChIP assays with anti-p65 antibodies during MO differentiation to OC, demonstrating a direct association of NF-κB p65 with the DNA sequence of the upregulated miRNAs. We also detected that p65 inhibition using pharmacological inhibitors and specific siRNAs has a negative effect in the expression of the miRNA and a positive effect on their targets, providing evidence that NF-κB helps repress these targets through miRNAs.

4.2 Global discussion.

In the present thesis, we have investigated the importance of DNA methylation as a regulatory mechanism underlying terminal myeloid differentiation processes. During MO-to-DC and MO-to-MAC differentiation, we observed vast demethylation in thousands of genes, whilst only very few of them underwent gains of methylation.

Due to the large number of genes that become demethylated during MO-to-DC and MO-to-MAC differentiation, and the relevance of those genes in DC and MAC biology, these MO-associated differentiation processes are evidenced as excellent models to study the mechanisms of DNA demethylation in detail **(ARTICLE 1)**. The comparison of the DNA methylation and expression data revealed a complex relationship between these two, however, we detected that the majority of demethylated genes are overexpressed, and the dynamics of the process revealed that demethylation precedes gene upregulation. Loss of DNA methylation occurs rapidly and in the absence of cell proliferation, suggesting that an active mechanism is occurring. This was confirmed by the presence of oxidized 5 mC and also by the impairment of demethylation when TET2 was inhibited, as we and others have demonstrated [219]. TET2 inhibition experiments also highlight the importance of active DNA demethylation in proper differentiation, as the acquisition of DC identity was not properly achieved upon TET2 downregulation. These results coincide with the relevant role of demethylation during myeloid differentiation[136158] , and offer clues related to its role in the proper establishment of the different myeloid cell types.

Apart from those genes where DNA demethylation precedes gene expression in the differentiation process, our study shows a set of genes that, despite being demethylated during the differentiation step, are only overexpressed after LPS-mediated activation. It seems that for those genes, the modification status of the chromatin (particularly DNA methylation) is prepared for the rapid response that cells need once TLR4-mediated activation takes place in order to prompt innate responses against invading pathogens. In this line, it has been described in other cells from the immune system how genome is poised to respond rapidly and efficiently to a stimulus or set of stimuli. For example, Casellas group described how polymerase II was loaded into the genome prior to their activation during the process of B cell activation. [220] Our results emphasize that the mechanism of poising DNA prior to the stimulus is a global way of acting during inflammation.

Most interestingly, our study reveals that there are sets of genes whose DNA methylation status strictly changes in one of the differentiation processes (DC or MAC differentiation) and not the other, thus suggesting a possible role of DNA methylation in the

acquisition of the specific identity of these related cell types. Since IL-4 is the differential factor between *in vitro* human MO-to-DC and MO-to-MAC differentiation, elements downstream to IL-4R should be directing differential methylation patterns between both processes. In our study, we have demonstrated that inhibition of the JAK3-STAT6 axis (located downstream to IL-4R) is able to impair DC methylation and expression in DC specific genes, and have the opposite effect on MAC specific genes (and no effect on common genes). The overexpression of a constitutively activated STAT6 mutant (STAT6VT) during MO differentiation in the presence of GM-CSF only (which would lead to differentiation to MACs) reinforces this hypothesis: DNA demethylation of DC-specific genes was observed during the differentiation under those conditions and the absence of demethylation of specific MAC genes also occurred, with STAT6VT being able to bypass the absence of IL-4R stimulation. Overall, these results reflect how the STAT6-JAK3 axis was responsible of mediating the differential demethylation between DC and MAC. Moreover, these results also suggest that DC identity during MO differentiation not only depends on the demethylation of DC-specific genes (allowing them to be expressed), but also on preventing the expression of MAC-specific genes by impeding them to become demethylated during the process. GM-CSF cell signalling results in large changes to the genomic methylation, whereas the cytokine IL-4 leads to a more limited number of DNA methylation changes by switching on those related with DC function and switching off those genes that define MAC function and are activated by the general activity of GM-CSF. Our results are in line with a recently proposed model of the asymmetric participation of different STATs in response to combinations of cytokines. This study strongly suggests that in response to two cytokine signals, one STAT may provide a wider transcriptional program that is restricted to gain specificity by the superimposed action of another STAT [221]. In our ongoing work, we extend this notion to epigenetic regulation, in particular DNA methylation.

With respect to the mechanisms that STAT6 employs to direct the demethylation of DC-specific genes, we have determined a direct interaction of STAT6 to these genes. Given the participation of TET2 in active demethylation, we speculated whether STAT6 directly interacts and recruits TET2. However, we have been unable to prove such interaction in this context. It is also possible that PU.1 mediates the recruitment of TET2, given that the direct interaction between PU.1 and STAT6 has been already published [222], in addition to the implication of PU.1 in active demethylation via their direct interaction with TET2 [144]. In line with this, we observed that PU.1 silencing results in the impairment of gene methylation in both specific and common genes, which suggests a more general role of PU.1 in DNA demethylation for both processes. PU.1 might act like an adaptor for DNA demethylation. It is possible that PU.1 leads to more specific DNA methylation changes by forming complexes with other sequence specific TFs like

STAT6. It is also possible that STAT6 interacts with other epigenetic enzymes that be involved in the recruitment of TET2 to those specific demethylated DC genes. In this sense, an interaction between STAT6 and CBP/p300 in the context of IL-4 stimulation has been published [223].

Experiments demonstrating the interaction of STAT6 with other factors during MO-to-DC differentiation will be key to better understand the molecular mechanisms behind STAT6-dependent gene demethylation and their consequent gene overexpression. To date, none of the published studies demonstrating an interaction between STAT6 and other factors have been performed in primary human MO, possibly due to the high amounts of the protein required to detect the interaction or by the low quality of the existing STAT6 antibodies. In our experiments, we have not been able to demonstrate the interaction between STAT6 and TET2/PU.1 under MO to DC differentiation in primary cells. Ongoing experiments in this respect include the overexpression of STAT6VT coupled with an HA tag during MO-to-DC differentiation, that will allow us to perform the immunoprecipitations by using an anti-HA antibody and using higher amounts of STAT6 protein. These experiments are challenging due to the big size of the protein and the low efficiency to infect primary MOs.

Given that STAT6 appears to prevent demethylation of MAC-specific genes under the conditions of DC differentiation, another intriguing question is their underlying mechanisms. Perhaps STAT6 is able to directly block upregulation of gene expression of MAC-specific genes through direct interference of the demethylation machinery. In this direction, we have been able to prove STAT6 binding to genes that are specifically demethylated in MACs during MO-to-DC differentiation with the ChIP experiments (not shown in the corresponding article). Consequently, it seems that depending on the context, STAT6 is able to recruit machinery involved in directing or preventing DNA demethylation, and therefore related to opposed processes in relation with gene activation or repression

To summarize this first part of the work, our results show for the first time all the molecular sequential events that take place when a cytokine like IL-4 binds to its receptor and results in activating downstream cell signalling pathways, which eventually result in the specific recruitment of enzymes involved in active DNA methylation.

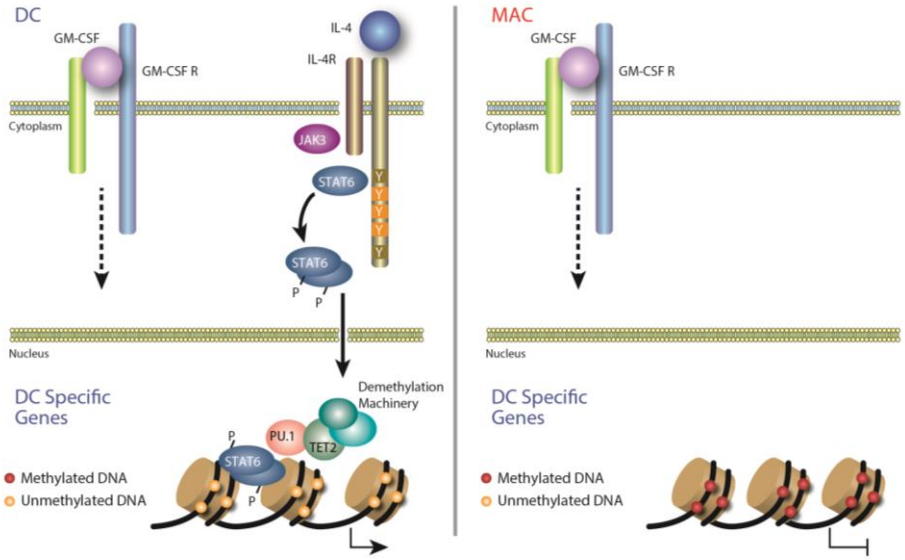

Figure 4-1 Model depicting the participation of the IL-4-JAK3-STAT6 pathway in targeting demethylation of DC-specific genes
IL-4 binding to IL-4R activates JAK3 that is able to phosphorylate STAT6. Once STAT6 is activated, dimerise and enters to the nucleus where mediates the recruitment of TET2 to specific regions coding for genes only expressed in MO derived DC (and not in MO derived MAC). TET2 is the main responsible enzyme to produce demethylation and the consequent gene expression of those genes.

Although demethylation is the most common change regarding DNA methylation in MO-related differentiation processes, significant gains of DNA methylation were also observed for some genes repressed during MO-to-DC and MO-to-MAC differentiation **(ARTICLE 3).** One example of this group of genes is *FYN*, encoding a Tyr-protein kinase related to MO function. Its hypermethylation during MO-to-DC differentiation (also in OC differentiation) occurred after the induction of gene expression, suggesting a possible role of methylation in controlling gene expression stability but not in gene expression induction. Other epigenetic mechanisms involved in gene repression (the acquisition of H3K27me3 or H3K9me3) followed a similar dynamics, which suggests that repressive epigenetic mechanisms are more associated with gene expression stability than with the induction of gene expression itself. In contrast, the loss of active epigenetic marks, H3K4me3 or H3K36me3, precede changes in gene expression, indicating a possible cause-and-effect relationship between the loss of active epigenetics marks and gene expression. Results from the inhibition of the *de novo* DNA methyltransferase DNMT3B are also in the same line. Despite the partial impairment of DNA methylation gains following DNMT3B inhibition, we did not observe an impact on the gene expression changes. However, we observed that some of the surface markers that characterize DCs were not present at the same levels. This result indicates the importance of the gains of DNA methylation for these genes to the acquisition of the DC phenotype during differentiation, which is highly probable to occur

through their role in gene expression stability. This brought up some intriguing questions, as the exact role of DNA methylation in gene expression stability still needs to be studied in depth: what are the long-term consequences of DNA methylation removal? How that could affect the different DNMTs to DNA methylation and genome stability? What are the consequences among other genes that also become hypermethylated during the process? Because DC and MAC are not associated with a high range of hypermethylation changes and because the process of differentiation in both cell types lasts less than one week, we choose the OC model for addressing this questions. OC represent an ideal model to study the effects of DNA methylation in MO differentiation, due to the possibility of long-term experiments (osteoclastogenesis for the last 21 days) and the higher number of hypermethylated genes during differentiation. We are currently inhibiting DNMT3a and DNMT3b using specific siRNAs during osteoclastogenesis at the laboratory, and in agreement with a recently published article [224], we are in the way to better dissect the functional relevance of this factors in the cell .

Analysis of the lists of genes that become demethylated genes in MO-to-MAC and MO-to-DC differentiation revealed the presence of a set of genes involved in the inflammasome pathway **(ARTICLE 2).** Due to the relevance of the inflammasome for the inflammatory properties of MACs we decided to investigate further the role of DNA methylation in this process.

The inflammasome-associated genes identified to be demethylated during MAC differentiation are distributed along the inflammasome signalling cascade. We found demethylation of *NLRC5* and *AIM2*, both members of the NLRs family that comprises a set of genes specialized in detecting danger and/or stress signals within the cell cytoplasm. Namely, NLRC5 is activated by a variety of stimuli including LPS and AIM2 assembles upon sensing foreign cytoplasmic double-stranded DNA (dsDNA). When these proteins detect danger, they are able to oligomerize and form the inflammasome structure that in turn recruits and activates the protease CASP-1. CASP-1 and PYCARD are two of the crucial proteins that form the inflammasome structures, and our data have shown that both genes are also regulated by DNA methylation. PYCARD is an adaptor protein that is able to recruit CASP-1, which is involved in cleaving some inflammatory cytokines like IL-1α or IL-1β. The genes encoding for these cytokines also undergo demethylation in MAC differentiation. Other genes associated with the inflammasome, which were also demethylated include *IL1RN* and *PSTPIP2*. IL1RN is an antagonist of the IL-1β and is overexpressed during inflammation as it tries to compensate for the IL-1β signalling. On the other hand, PSTPIP2 is a negative regulator of CASP-1-autonomous IL-1β production[225] .

In our work, we have studied the dynamics of DNA methylation and gene expression of inflammasome related genes during stimulation, and we have observed that DNA demethylation precedes gene expression upregulation, indicating a possible causal relationship between them.

Given the absence of cell division/DNA replication and the fast decrease of DNA methylation (before 24h) into MO-to-MAC differentiation an active mechanism of methylation seems to be occurring. Our hypothesis is confirmed due to the fact that when TET2 is silenced during MO-to-MAC differentiation, an impairment of demethylation is observed.

On the other hand, loss of DNA methylation in inflammasome-associated genesis also observed during MO activation by IL-1β and LPS and in the presence of ATP and MSU crystals, all of which are activators of the NLRP3 inflammasome. In this case, gene expression anticipates changes in DNA methylation (in contrast with our observations for DNA demethylation in GM-CSF-mediated differentiation), indicating a different and potentially complementary role for DNA methylation in this case.

We have also detected that the inhibition of NF-kB is associated with an impairment of DNA demethylation and gene expression of genes related to inflammasome function during MO activation. This suggests that NF-kB may mediate TET2 recruitment and subsequent DNA demethylation. Additional experiments to elucidate whether NF-kB subunits directly interacts with TET2 (or other enzymes involved in active DNA demethylation) are currently performed in our laboratory.

An interesting experiment would be to investigate whether changes in histone modifications are also associated with the upregulation of inflammasome-related genes. It is possible that differences in the MO-to-MAC differentiation and IL-1 (or LPS)-mediated MO activation could be explained by the dynamics of histone modification changes. It might also be likely that the gain of active histone modifications marks (such as H3K4me3 or H3K36me3) or the loss of repressive histone modification marks (such as H3K27me3 or H3K9me3) anticipate the induction of gene expression in the case of MO activation.

Aberrant hyperactivity of the inflammasome, due to activating mutations, has been shown to causal the development of monogenic autoinflammatory disorders, such as FMF or CAPS. We have demonstrated that exacerbated DNA methylation is associated with CAPS and FMF. No differences in the DNA methylation levels of inflammasome-associated genes between recently isolated MOs from patients and controls was observed. However, when we examined the ability to demethylate these genes in MOs following exposure to IL-1β or GM-CSF, we detected higher DNA demethylation in CAPS and FMF individuals than in healthy donors. These

results suggest that the presence of the IL-1β (which recapitulates the environment of the circulating MOs in these syndormes) primes these genes for increased DNA demethylation-related induction of gene expression in contrast to controls.

It has been demonstrated that IL-1β stimulation induces a positive loop, causing higher rates of IL-1β production [109] . In this work, we propose that DNA demethylation is part of this loop. In other words, the presence of IL-1β induces DNA demethylation of inflammasome genes that are at the same rate stimulating IL-1β production. In patients, MO present a higher rate of IL-1β production, which could be inducing DNA demethylation in these samples that act as an amplifier of the signal.

One potential explanation for the absence of changes in MOs before any type of induction would be that damaged cells are lost during the MO isolation process. In regards to this, inflammasome activation can cause pyroptosis (an inflammatory form of cell death), so these cells would be discarded under separation. Therefore, it is possible that these discarded cells correspond to those ones that have been exposed longer to IL-1β stimulus and consequently, with higher rates of DNA hypomethylation.

To sum up this second part of the thesis, we have demonstrated that NF-kB is able to drive the active loss of DNA methylation in some inflammasome-related genes in both MAC differentiation and MO activation. Moreover, the fact that increased DNA methylation can be involved in the activation of inflammasome-associated genes in autoinflammatory syndromes might explain the different behaviour between patients carrying the same mutation. More interestingly, this finding opens up a number of possibilities from the translational point of view, as new drugs targeting epigenetic and in particular DNA methylation machinery can be designed in order to treat IL-1β mediated diseases.

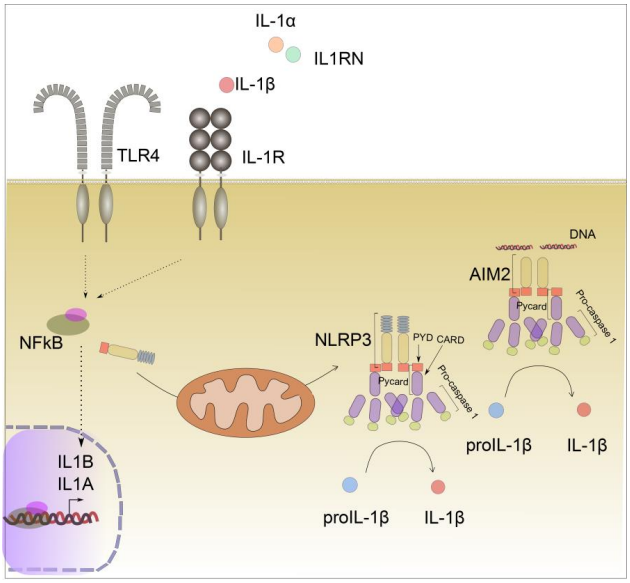

Figure 4-2 Diagram depicting the participation of the active demethylation machinery in driving the expression of inflammasome-related genes.
During MO activation, ligand binding to TLR4 and IL-1R is associated with a DNA demethylation of inflammasome-related genes that is driven by the recruitment of the DNA demethylation machinery by the NF-kB complex.

From the experimental point of view it is worthwhile to comment on some caveats and technical limitations that we tackled while we were performing the experiments presented throughout this thesis. The main technical problem was associated with the use of siRNAs for gene downregulation. Although siRNAs are very specific to downregulate their targets (which gives them an advantage among pharmacological inhibitors), their mechanism of action often starts 48-72 hours post-transfection. In our case, DNA demethylation is a very fast process, with methylation usually decaying before the first 48 hours. In order to partially solve this problem, we did not add cytokines until 24 hours after transfection, which was very useful for the majority of genes but not for those whose methylation decreases completely in 24 hours. Another limitation with siRNAs is that these molecules are not always able to fully silence the targeted protein. In the case of TET2, we were only able to silence 30% of the protein. Consequently, although a reduction in the active mechanism was detected, it was not completely inhibited. Taking this into consideration, we are optimizing the use of CRISPR technology in the laboratory [226] that presents an alternative to siRNAs, due to their specificity and efficiency in the inhibition of their targets. This technique will allow us to determine whether TET2 is the only 5mC dioxygenase involved in the oxidization of 5meC or if TET1 and TET3 are also participating in active demethylation. We will also be able to explore other elements of the active demethylation machinery.

Finally, apart from studying the relevance of DNA methylation in the process of differentiation of MOs to MACs and DCs we were also interested in other regulatory mechanisms involved in MO-associated differentiation **(ARTICLE 4)**. In this sense, the last study presented in this thesis, shows a different implication of NF-kB in the regulation of gene expression. Specifically, we determined that NF-kB plays a role in regulating two miRNA clusters (miR-99b/let-7e/125a and miR-212/132 clusters) that are required for differentiation of MOs to OCs, DCs and MACs. More specifically, we have found that those miRNAs negatively target proteins involved in MO function that are silenced during MO-associated differentiation. The upregulated miRNAs are therefore necessary to ensure the proper silencing of genes that allow MO to differentiate. A previous study from group led to similar conclusions in a model of transdifferentiation based on the ability of the myeloid transcription factor C/EBPa to transdifferentiate pre-B cells into MACs[227]. In that model, upregulation of miRNAs is directly associated with the silencing of the B cell expression programme.

The crucial role of the upregulated miRNA clusters (miR-99b/let-7e/125a and miR-212/132 clusters) during MO-to-OC differentiation, is highlighted by the fact that the use of antagomirs to inhibit the upregulation of these miRNAs impairs differentiation. This reinforces the notion that the silencing of inappropriate genes during differentiation, including those corresponding to the progenitor, is crucial for a proper differentiation. Given the diverse number of potential targets for each miRNA, it seems plausible that the miRNAs within the clusters that we identified to be upreglated perform an inhibitor effect in several of those genes. The bioinformatic analysis to predict the possible targets of each miRNA was performed while ignoring that some of the changes could have been occurring post-transcriptionally, in turn not having any effect on the amount of RNA messenger. Despite this limitation, we found interesting targets with key roles in other lineages, whose inhibition in MO differentiation to DCs, MACs and OCs is essential.

Our study focused on miRNAs that are common for three MO-derived differentiation processes (MO-to-OC, MO-to-DC, and MO-to-MAC). However, it would also be very interesting to concentrate on studying those miRNAs whose changes are exclusive to each of the differentiation processes. This type of approach would be useful in investigating how cell identity is also influenced by miRNAs and how specific pathways of each differentiation are able to regulate miRNA expression changes. The identification of those miRNAs exclusive to each process might be useful for inhibiting in a more specific manner one cell type altered under inflammatory conditions.

In this study, we have also elucidated how NF-kB pathway regulates the miR-99b/let-7e/125a and miR-212/132 upregulation. Accordingly, the NF-kB pathway is activated under inflammation conditions and in all three MO-related differentiation models, inflammation pathways were activated by GM-CSF (MAC and DC) and by M-CSF (OC). Although there were no previous studies describing NF-kB mediated activation of miRNAs in cells of the innate system, it has been recently identified that this pathway is responsible for regulating miRNAs in a primary model of B cell infection by EBV [71]. These results indicates that the NF-kB pathway plays a role in cells of both adaptive and innate immune system to regulate rapid responses to a stimulus through miRNAs.

Altogether, these results show that the NF-kB pathway is able to upregulate a set of miRNAs in the three studied MO-related differentiation models with a critical role in silencing the expression of genes from other lineages. These miRNAs could be potential targets for pharmacological drugs that in one way or another try to inhibit or potentiate the presence of OC, MAC and DC.

To summarize the thesis, we have found how regulatory epigenetic changes are crucial for MO-to-DC and MO-to-MAC differentiation and for MO activation through the regulation of specific transcriptional programmes. In this way, we have demonstrated how cell identity in these processes not only depends on those genes that should be expressed, but also on those that are from other lineages and need to be repressed. Future experiments integrating all epigenetic and transcriptomic data in those models will be helpful in predicting decisions that cells can make under certain circumstances and in unravelling new mechanisms of cellular regulation.

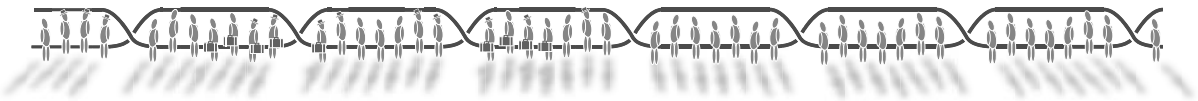

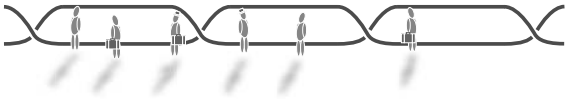

CONCLUSIONS

5 CONCLUSIONS

The conclusions obtained during this doctoral thesis can be summarised as follows

1. *In vitro* differentiation of MOs to DCs and MACs results in predominant loss of DNA methylation, whereas only a few genes undergo gains of DNA methylation. We have determined that 1654 and 2586 CpGs undergo demethylation in in MO-to-DC and MO-to-MAC differentiation, respectively.

2. LPS-mediated maturation of DCs and MACs is associated with very few significant changes in DNA methylation. Specifically, 75 and 27 CpG sites change their DNA methylation status for DC and MAC maturation, respectively.

3. A significant fraction of demethylated CpGs are specific to each differentiation process: 235 genes in MO-to-DC and 1167 genes in MO-to-MAC differentiation. Among them, there are genes involved in DC-specific functions (*DUOX1, SLAMF1)* and MAC unique functions *(IL1B, CCL20).*

4. DNA demethylation in MO-to-MAC and MO-to-DC differentiation is an active process that depends on the activity of the methylcytosine dioxygenase TET2. The activity of TET2 is also responsible for the final DC and MAC phenotype.

5. Expression changes are observed for both differentiation and maturation steps for both DCs and MACs. In addition, a similar proportion of genes are upregulated and downregulated in both steps.

6. Many genes display an inverse relationship between their expression and DNA methylation status. Moreover, some of the genes that lose DNA methylation during differentiation are associated with an increase in expression during the subsequent LPS-mediated maturation step.

7. Inhibition of the JAK3-STAT6 pathway impairs DNA methylation and expression changes of DC-specific genes and have an opposite effect in MAC-specific genes during DC differentiation.

8. STAT6 interacts specifically with genes like *DUOX1* and *SLAMF1*, which are demethylated and overexpressed in DCs. Recruitment to these genes only occurs in DC differentiation, and does not take place in MAC differentiation or when the JAK3 inhibitor is present.

9. A constitutively activated STAT6 form induces demethylation of DC-specific genes and impairs MAC-specific gene demethylation under the conditions of MAC differentiation (in the presence of GM-CSF alone).

10. A small proportion of genes that become silenced during MO-to-DC and MO-to-MAC (*CSF3R, FYN, PRKCE, CXCR1)* differentiation undergo gains of *de novo* DNA methylation.

11. The dynamics of the differentiation process reveals that expression changes precede gains in DNA methylation and in histone modification repressive marks (H3K27me3 and H3K9me3) in specific genes. Loss of activating histone modifications marks H3K36me3 and H3K4me3 parallel specific gene expression changes.

12. Pharmacological inhibition of DNMT3b does not result in impaired gene expression, however it affects the final DC phenotype.

13. Several inflammasome-related genes undergo DNA demethylation during MO-to-MAC differentiation. DNA demethylation occurs in association with upregulation; however for some of these genes (*IL1A, IL1B, AIM2, CASP-1*), upregulation only takes place after LPS exposure.

14. Specific inhibition of TET2 during MO-to-MAC differentiation impaired demethylation, and changes in 5-hydroxymethylcytosine, as well as overexpression of inflammasome genes during MO-to-MAC differentiation.

15. NF-kB is involved in demethylation of inflammasome-related genes, as demonstrated by both NF-kB inhibitors and ChIP assays.

16. LPS or IL-1β mediated activation of MOs *in vitro* stimulates demethylation and overexpression of genes involved in the inflammasome.

17. Patients with autoinflammatory syndromes CAPS and FMF undergo higher DNA methylation in inflammatory-associated genes in *in vitro* activated MOs in comparison to healthy donors.

18. Expression of two miRNA clusters (miR-99b/let-7b/125a and miR-212/132) is increased during MO-to-MAC, MO-to-DC and MO-to-OC differentiation.

19. MiRNA overexpressed during MO differentiation processes are able to reduce the mRNA and protein levels of lineage inappropriate genes like *ITGA4, THBS1* or *IGFR1* and ensure proper differentiation.

20. NF-kB has a direct role in the regulation of miRNAs overexpressed in MO-derived differentiation models.

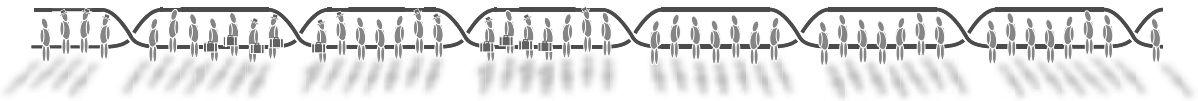

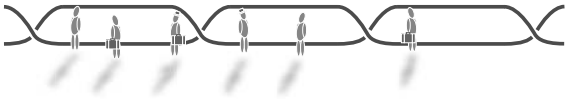

BIBLIOGRAPHY

6 BIBLIOGRAPHY

1. Orkin, S. H. & Zon, L. I. Hematopoiesis and stem cells: plasticity versus developmental heterogeneity. *Nat. Immunol.* **3,** 323–8 (2002).
2. Morrison, S. J. & Scadden, D. T. The bone marrow niche for haematopoietic stem cells. *Nature* **505,** 327–34 (2014).
3. Álvarez-Errico, D., Vento-tormo, R., Sieweke, M. & Ballestar, E. Epigenetic control of myeloid cell differentiation, identity and function. *Nat. Rev. Imm*. **15,** 7–17 (2015).
4. Poltorak, A. *et al.* Defective LPS signaling in C3H/HeJ and C57BL/10ScCr mice: mutations in Tlr4 gene. *Science* **282,** 2085–8 (1998).
5. Medzhitov, R., Preston-Hurlburt, P. & Janeway, C. A. A human homologue of the Drosophila Toll protein signals activation of adaptive immunity. *Nature* **388,** 394–7 (1997).
6. Kärre, K., Ljunggren, H. G., Piontek, G. & Kiessling, R. Selective rejection of H-2-deficient lymphoma variants suggests alternative immune defence. *Nature* **319,** 675–8 (1986)
7. Zeh, H. J. & Lotze, M. T. Addicted to death: invasive cancer and the immune response to unscheduled cell death. *J. Immunother.* **28,** 1–9 (2005)
8. Cella, M., Sallusto, F. & Lanzavecchia, A. Origin, maturation and antigen presenting function of dendritic cells. *Curr. Opin. Immunol.* **9,** 10–6 (1997).
9. Abbas, A. K., Lichtman, A. H. H. & Pillai, S. Cellular and Molecular Immunology. Eighth edition. Philadelphia, PA : Elsevier/Saunders. (2015)
10. Quintin, J., Cheng, S., van der Meer, J. W. & Netea, M. G. Innate immune memory: towards a better understanding of host defense mechanisms. *Curr. Opin. Immunol.* **29C,** 1–7 (2014).
11. Steinman, R. M. Decisions About Dendritic Cells: Past, Present, and Future. *Annu. Rev. Immunol.* **30,** 1–22 (2012).
12. Van Furth, R. & Sluiter, W. Distribution of blood monocytes between a marginating and a circulating pool. *J. Exp. Med.* **163,** 474–9 (1986).
13. Swirski, F. K. *et al.* Identification of splenic reservoir monocytes and their deployment to inflammatory sites. *Science* **325,** 612–6 (2009).
14. Van Furth, R. & Cohn, Z. A. The origin and kinetics of mononuclear phagocytes. *J. Exp. Med.* **128,** 415–35 (1968).
15. Hettinger, J. *et al.* Origin of monocytes and macrophages in a committed progenitor. *Nat. Immunol.* **14,** 821–30 (2013).
16. Robbins, C. S. *et al.* Extramedullary hematopoiesis generates Ly-6C(high) monocytes that infiltrate atherosclerotic lesions. *Circulation* **125,** 364–74 (2012).
17. Ziegler-Heitbrock, L. & Hofer, T. P. J. Toward a refined definition of monocyte subsets. *Front. Immunol.* **4,** 23 (2013).
18. Ingersoll, M. A. *et al.* Comparison of gene expression profiles between human and mouse monocyte subsets. *Blood* **115,** e10–9 (2010).
19. Auffray, C. *et al.* Monitoring of blood vessels and tissues by a population of monocytes with patrolling behavior. *Science* **317,** 666–70 (2007).
20. Carlin, L. M. *et al.* Nr4a1-dependent Ly6C(low) monocytes monitor endothelial cells and orchestrate their disposal. *Cell* **153,** 362–75 (2013).
21. Ginhoux, F. & Jung, S. Monocytes and macrophages: developmental pathways and tissue homeostasis. *Nat. Rev. Immunol.* **14,** 392–404 (2014).
22. Serbina, N. V & Pamer, E. G. Monocyte emigration from bone marrow during bacterial infection requires signals mediated by chemokine receptor CCR2. *Nat. Immunol.* **7,** 311–7 (2006).
23. Lauvau, G., Chorro, L., Spaulding, E. & Soudja, S. M. Inflammatory monocyte effector mechanisms. *Cell. Immunol.* **291,** 32–40 (2014).

24. Steinman, R. M. & Cohn, Z. A. Identification of a novel cell type in peripheral lymphoid organs of mice. I. Morphology, quantitation, tissue distribution. *J. Exp. Med.* **137,** 1142–62 (1973).
25. Steinman, R. M. & Witmer, M. D. Lymphoid dendritic cells are potent stimulators of the primary mixed leukocyte reaction in mice. *Proc. Natl. Acad. Sci. U. S. A.* **75,** 5132–6 (1978).
26. Steinman, R. M. & Idoyaga, J. Features of the dendritic cell lineage. *Immunol. Rev.* **234,** 5–17 (2010).
27. Hashimoto, D., Miller, J. & Merad, M. Dendritic cell and macrophage heterogeneity in vivo. *Immunity* **35,** 323–35 (2011).
28. Reis e Sousa, C. *et al.* In vivo microbial stimulation induces rapid CD40 ligand-independent production of interleukin 12 by dendritic cells and their redistribution to T cell areas. *J. Exp. Med.* **186,** 1819–29 (1997).
29. Satpathy, A. T. *et al.* Notch2-dependent classical dendritic cells orchestrate intestinal immunity to attaching-and-effacing bacterial pathogens. *Nat. Immunol.* **14,** 937–48 (2013).
30. Guilliams, M. *et al.* Dendritic cells, monocytes and macrophages: a unified nomenclature based on ontogeny. *Nat. Rev. Immunol.* **14,** 571–578 (2014).
31. Schraml, B. U. & Reis e Sousa, C. Defining dendritic cells. *Curr. Opin. Immunol.* **32,** 13–20 (2015).
32. Poltorak, M. P. & Schraml, B. U. Fate mapping of dendritic cells. *Front. Immunol.* **6,** 199 (2015).
33. Haniffa, M. *et al.* Human tissues contain CD141hi cross-presenting dendritic cells with functional homology to mouse CD103+ nonlymphoid dendritic cells. *Immunity* **37,** 60–73 (2012).
34. Morelli, A. E. *et al.* CD4+ T cell responses elicited by different subsets of human skin migratory dendritic cells. *J. Immunol.* **175,** 7905–15 (2005).
35. Nakano, H., Yanagita, M. & Gunn, M. D. CD11c(+)B220(+)Gr-1(+) cells in mouse lymph nodes and spleen display characteristics of plasmacytoid dendritic cells. *J. Exp. Med.* **194,** 1171–8 (2001).
36. Martín-Gayo, E., Sierra-Filardi, E., Corbí, A. L. & Toribio, M. L. Plasmacytoid dendritic cells resident in human thymus drive natural Treg cell development. *Blood* **115,** 5366–75 (2010).
37. Steinman, R. M. *et al.* Dendritic cell function in vivo during the steady state: a role in peripheral tolerance. *Ann. N. Y. Acad. Sci.* **987,** 15–25 (2003).
38. León, B., López-Bravo, M. & Ardavín, C. Monocyte-derived dendritic cells formed at the infection site control the induction of protective T helper 1 responses against Leishmania. *Immunity* **26,** 519–31 (2007).
39. Hohl, T. M. *et al.* Inflammatory Monocytes Facilitate Adaptive CD4 T Cell Responses during Respiratory Fungal Infection. *Cell Host Microbe* **6,** 470–481 (2009).
40. Ballesteros-Tato, A., León, B., Lund, F. E. & Randall, T. D. Temporal changes in dendritic cell subsets, cross-priming and costimulation via CD70 control CD8(+) T cell responses to influenza. *Nat. Immunol.* **11,** 216–24 (2010).
41. Segura, E., Albiston, A. L., Wicks, I. P., Chai, S. Y. & Villadangos, J. A. Different cross-presentation pathways in steady-state and inflammatory dendritic cells. *Proc. Natl. Acad. Sci. U. S. A.* **106,** 20377–81 (2009).
42. Wakim, L. M., Waithman, J., van Rooijen, N., Heath, W. R. & Carbone, F. R. Dendritic cell-induced memory T cell activation in nonlymphoid tissues. *Science* **319,** 198–202 (2008).
43. Segura, E. *et al.* Human inflammatory dendritic cells induce Th17 cell differentiation. *Immunity* **38,** 336–48 (2013).

44. Metchinkoff. Leçons sur la pathologie comparée de l'inflammation. *Paris:Masson* (1892)
45. Van Furth, R. *et al.* The mononuclear phagocyte system: a new classification of macrophages, monocytes, and their precursor cells. *Bull. World Health Organ.* **46,** 845–52 (1972).
46. Gordon, S. & Taylor, P. R. Monocyte and macrophage heterogeneity. *Nat. Rev. Immunol.* **5,** 953–64 (2005).
47. Lichanska, A. M. & Hume, D. A. Origins and functions of phagocytes in the embryo. *Exp. Hematol.* **28,** 601–11 (2000).
48. Ginhoux, F. *et al.* Fate mapping analysis reveals that adult microglia derive from primitive macrophages. *Science* **330,** 841–5 (2010).
49. Schulz, C. *et al.* A lineage of myeloid cells independent of Myb and hematopoietic stem cells. *Science* **336,** 86–90 (2012).
50. Yona, S. *et al.* Fate mapping reveals origins and dynamics of monocytes and tissue macrophages under homeostasis. *Immunity* **38,** 79–91 (2013).
51. Epelman, S., Lavine, K. J. & Randolph, G. J. Origin and Functions of Tissue Macrophages. *Immunity* **41,** 21–35 (2014).
52. Hoeffel, G. *et al.* Adult Langerhans cells derive predominantly from embryonic fetal liver monocytes with a minor contribution of yolk sac-derived macrophages. *J. Exp. Med.* **209,** 1167–81 (2012).
53. Zigmond, E. & Jung, S. Intestinal macrophages: well educated exceptions from the rule. *Trends Immunol.* **34,** 162–8 (2013).
54. Coggle, J. E. & Tarling, J. D. The proliferation kinetics of pulmonary alveolar macrophages. *J. Leukoc. Biol.* **35,** 317–27 (1984).
55. Robbins, C. S. *et al.* Local proliferation dominates lesional macrophage accumulation in atherosclerosis. *Nat. Med.* **19,** 1166–72 (2013).
56. Arnold, L. *et al.* Inflammatory monocytes recruited after skeletal muscle injury switch into antiinflammatory macrophages to support myogenesis. *J. Exp. Med.* **204,** 1057–69 (2007).
57. Lawrence, T. & Natoli, G. Transcriptional regulation of macrophage polarization: enabling diversity with identity. *Nat. Rev. Immunol.* **11,** 750–761 (2011).
58. Davies, L. C., Jenkins, S. J., Allen, J. E. & Taylor, P. R. Tissue-resident macrophages. *Nat. Immunol.* **14,** 986–95 (2013).
59. Xue, J. *et al.* Transcriptome-based network analysis reveals a spectrum model of human macrophage activation. *Immunity* **40,** 274–88 (2014).
60. Sallusto, F. & Lanzavecchia, A. Efficient presentation of soluble antigen by cultured human dendritic cells is maintained by granulocyte/macrophage colony-stimulating factor plus interleukin 4 and downregulated by tumor necrosis factor alpha. *J. Exp. Med.* **179,** 1109–18 (1994).
61. Sica, A. & Mantovani, A. Macrophage plasticity and polarization: in vivo veritas. *J. Clin. Invest.* **122,** 787–95 (2012).
62. Verreck, F. A. W. *et al.* Human IL-23-producing type 1 macrophages promote but IL-10-producing type 2 macrophages subvert immunity to (myco)bacteria. *Proc. Natl. Acad. Sci. U. S. A.* **101,** 4560–5 (2004).
63. Boyle, W. J., Simonet, W. S. & Lacey, D. L. Osteoclast differentiation and activation. *Nature* **423,** 337–42 (2003).
64. Netea, M. G., van de Veerdonk, F. L., van der Meer, J. W. M., Dinarello, C. a. & Joosten, L. a. B. Inflammasome-Independent Regulation of IL-1-Family Cytokines. *Annu. Rev. Immunol.* **33,** 141210135520002 (2014).
65. Stegmaier, P., Kel, A. E. & Wingender, E. Systematic DNA-binding domain classification of transcription factors. *Genome Inform.* **15,** 276–86 (2004).

66. Wingender, E., Schoeps, T., Haubrock, M. & Dönitz, J. TFClass: a classification of human transcription factors and their rodent orthologs. *Nucleic Acids Res.* **43,** D97–102 (2015).
67. Wingender, E., Schoeps, T. & Donitz, J. TFClass: an expandable hierarchical classification of human transcription factors. *Nucleic Acids Res.* **41,** D165–D170 (2012).
68. Latchman, D. S. Eukaryotic Transcription Factors. Chapter: Families of DNA Binding Transcription Factors. Elsevier (2007).
69. Gordân, R., Hartemink, A. J. & Bulyk, M. L. Distinguishing direct versus indirect transcription factor-DNA interactions. *Genome Res.* **19,** 2090–100 (2009).
70. Latchman, D. S. Eukaryotic Transcription Factors. Chapter: Activation of gene expression by transcription factors. Elsevier (2007).
71. Vento-Tormo, R. *et al.* NF- B directly mediates epigenetic deregulation of common microRNAs in Epstein-Barr virus-mediated transformation of B-cells and in lymphomas. *Nucleic Acids Res.* **42,** 11025–11039 (2014).
72. Klemsz, M. J., McKercher, S. R., Celada, A., Van Beveren, C. & Maki, R. A. The macrophage and B cell-specific transcription factor PU.1 is related to the ets oncogene. *Cell* **61,** 113–124 (1990).
73. Zhang, D. E. *et al.* Absence of granulocyte colony-stimulating factor signaling and neutrophil development in CCAAT enhancer binding protein alpha-deficient mice. *Proc. Natl. Acad. Sci. U. S. A.* **94,** 569–74 (1997).
74. Tanaka, T. *et al.* Targeted disruption of the NF-IL6 gene discloses its essential role in bacteria killing and tumor cytotoxicity by macrophages. *Cell* **80,** 353–61 (1995).
75. Yamanaka, R. *et al.* Impaired granulopoiesis, myelodysplasia, and early lethality in CCAAT/enhancer binding protein epsilon-deficient mice. *Proc. Natl. Acad. Sci. U. S. A.* **94,** 13187–92 (1997).
76. Hock, H. *et al.* Intrinsic requirement for zinc finger transcription factor Gfi-1 in neutrophil differentiation. *Immunity* **18,** 109–20 (2003).
77. Holtschke, T. *et al.* Immunodeficiency and chronic myelogenous leukemia-like syndrome in mice with a targeted mutation of the ICSBP gene. *Cell* **87,** 307–17 (1996).
78. Okuda, T., van Deursen, J., Hiebert, S. W., Grosveld, G. & Downing, J. R. AML1, the target of multiple chromosomal translocations in human leukemia, is essential for normal fetal liver hematopoiesis. *Cell* **84,** 321–30 (1996).
79. Shivdasani, R. A., Mayer, E. L. & Orkin, S. H. Absence of blood formation in mice lacking the T-cell leukaemia oncoprotein tal-1/SCL. *Nature* **373,** 432–4 (1995).
80. Passegué, E., Jochum, W., Schorpp-Kistner, M., Möhle-Steinlein, U. & Wagner, E. F. Chronic myeloid leukemia with increased granulocyte progenitors in mice lacking junB expression in the myeloid lineage. *Cell* **104,** 21–32 (2001).
81. Yoshida, T., Ng, S. Y.-M., Zuniga-Pflucker, J. C. & Georgopoulos, K. Early hematopoietic lineage restrictions directed by Ikaros. *Nat. Immunol.* **7,** 382–91 (2006).
82. Johansen, L. M. *et al.* c-Myc Is a Critical Target for C/EBP in Granulopoiesis. *Mol. Cell. Biol.* **21,** 3789–3806 (2001).
83. Kelly, L. M., Englmeier, U., Lafon, I., Sieweke, M. H. & Graf, T. MafB is an inducer of monocytic differentiation. *EMBO J.* **19,** 1987–97 (2000).
84. Laouar, Y., Welte, T., Fu, X.-Y. & Flavell, R. A. STAT3 is required for Flt3L-dependent dendritic cell differentiation. *Immunity* **19,** 903–12 (2003).
85. Esashi, E. *et al.* The signal transducer STAT5 inhibits plasmacytoid dendritic cell development by suppressing transcription factor IRF8. *Immunity* **28,** 509–20 (2008).
86. Gilliet, M. *et al.* The development of murine plasmacytoid dendritic cell precursors is differentially regulated by FLT3-ligand and granulocyte/macrophage colony-stimulating factor. *J. Exp. Med.* **195,** 953–8 (2002).
87. Wu, L., Nichogiannopoulou, A., Shortman, K. & Georgopoulos, K. Cell-autonomous defects in dendritic cell populations of Ikaros mutant mice point to a developmental relationship with the lymphoid lineage. *Immunity* **7,** 483–92 (1997).

88. Rosas, M. *et al.* The transcription factor Gata6 links tissue macrophage phenotype and proliferative renewal. *Science* **344,** 645–8 (2014).
89. Gautier, E. L. *et al.* Gene-expression profiles and transcriptional regulatory pathways that underlie the identity and diversity of mouse tissue macrophages. *Nat. Immunol.* **13,** 1118–28 (2012).
90. Suzuki, S. *et al.* Critical roles of interferon regulatory factor 4 in CD11bhighCD8alpha-dendritic cell development. *Proc. Natl. Acad. Sci. U. S. A.* **101,** 8981–6 (2004).
91. Meredith, M. M. *et al.* Expression of the zinc finger transcription factor zDC (Zbtb46, Btbd4) defines the classical dendritic cell lineage. *J. Exp. Med.* **209,** 1153–65 (2012).
92. Ebner, K., Bandion, A., Binder, B. R., de Martin, R. & Schmid, J. A. GMCSF activates NF-kappaB via direct interaction of the GMCSF receptor with IkappaB kinase beta. *Blood* **102,** 192–9 (2003).
93. Hercus, T. R. *et al.* The granulocyte-macrophage colony-stimulating factor receptor: linking its structure to cell signaling and its role in disease. *Blood* **114,** 1289–98 (2009).
94. Jeffrey, K. L., Camps, M., Rommel, C. & Mackay, C. R. Targeting dual-specificity phosphatases: manipulating MAP kinase signalling and immune responses. *Nat. Rev. Drug Discov.* **6,** 391–403 (2007).
95. Witthuhn, B. A. *et al.* Involvement of the Jak-3 Janus kinase in signalling by interleukins 2 and 4 in lymphoid and myeloid cells. *Nature* **370,** 153–7 (1994).
96. Imada, K. & Leonard, W. J. The Jak-STAT pathway. *Mol. Immunol.* **37,** 1–11 (2000)=
97. John, S., Vinkemeier, U., Soldaini, E., Darnell, J. E. & Leonard, W. J. The significance of tetramerization in promoter recruitment by Stat5. *Mol. Cell. Biol.* **19,** 1910–8 (1999).
98. Vinkemeier, U. *et al.* DNA binding of in vitro activated Stat1 alpha, Stat1 beta and truncated Stat1: interaction between NH2-terminal domains stabilizes binding of two dimers to tandem DNA sites. *EMBO J.* **15,** 5616–26 (1996).
99. Mikita, T., Daniel, C., Wu, P. & Schindler, U. Mutational analysis of the STAT6 SH2 domain. *J. Biol. Chem.* **273,** 17634–42 (1998).
100. Daniel, C., Salvekar, A. & Schindler, U. A gain-of-function mutation in STAT6. *J. Biol. Chem.* **275,** 14255–9 (2000).
101. Shimazu, R. *et al.* MD-2, a molecule that confers lipopolysaccharide responsiveness on Toll-like receptor 4. *J. Exp. Med.* **189,** 1777–82 (1999).
102. Park, B. S. *et al.* The structural basis of lipopolysaccharide recognition by the TLR4-MD-2 complex. *Nature* **458,** 1191–5 (2009).
103. Newton, K. & Dixit, V. M. Signaling in innate immunity and inflammation. *Cold Spring Harb. Perspect. Biol.* **4,** a006049– (2012).
104. Horng, T., Barton, G. M., Flavell, R. A. & Medzhitov, R. The adaptor molecule TIRAP provides signalling specificity for Toll-like receptors. *Nature* **420,** 329–33 (2002).
105. Yamamoto, M. *et al.* Essential role for TIRAP in activation of the signalling cascade shared by TLR2 and TLR4. *Nature* **420,** 324–9 (2002).
106. Yamamoto, M. *et al.* TRAM is specifically involved in the Toll-like receptor 4-mediated MyD88-independent signaling pathway. *Nat. Immunol.* **4,** 1144–50 (2003).
107. Yamamoto, M. *et al.* Role of adaptor TRIF in the MyD88-independent toll-like receptor signaling pathway. *Science* **301,** 640–3 (2003).
108. Dunne, A. & O'Neill, L. A. J. The interleukin-1 receptor/Toll-like receptor superfamily: signal transduction during inflammation and host defense. *Sci. STKE* **2003,** re3 (2003).
109. Dinarello, C. A. *et al.* Interleukin 1 induces interleukin 1. I. Induction of circulating interleukin 1 in rabbits in vivo and in human mononuclear cells in vitro. *J. Immunol.* **139,** 1902–10 (1987).
110. Van de Laar, L., Coffer, P. J. & Woltman, A. M. Regulation of dendritic cell development by GM-CSF: molecular control and implications for immune homeostasis and therapy. *Blood* **119,** 3383–93 (2012).

111. Medzhitov, R. & Horng, T. Transcriptional control of the inflammatory response. *Nat. Rev. Immunol.* **9,** 692–703 (2009).
112. Hendrich, B. & Bird, A. Identification and characterization of a family of mammalian methyl-CpG binding proteins. *Mol. Cell. Biol.* **18,** 6538–47 (1998).
113. Blattler, A. & Farnham, P. J. Cross-talk between site-specific transcription factors and DNA methylation states. *J. Biol. Chem.* **288,** 34287–94 (2013).
114. Bird, A. DNA methylation patterns and epigenetic memory. *Genes Dev.* **16,** 6–21 (2002).
115. Booth, M. J., Raiber, E.-A. & Balasubramanian, S. Chemical methods for decoding cytosine modifications in DNA. *Chem. Rev.* **115,** 2240–54 (2015).
116. Irizarry, R. A. *et al.* The human colon cancer methylome shows similar hypo- and hypermethylation at conserved tissue-specific CpG island shores. *Nat. Genet.* **41,** 178–86 (2009).
117. Okano, M., Bell, D. W., Haber, D. A. & Li, E. DNA methyltransferases Dnmt3a and Dnmt3b are essential for de novo methylation and mammalian development. *Cell* **99,** 247–57 (1999).
118. Ito, S. *et al.* Tet proteins can convert 5-methylcytosine to 5-formylcytosine and 5-carboxylcytosine. *Science* **333,** 1300–3 (2011).
119. Hashimoto, H. *et al.* Recognition and potential mechanisms for replication and erasure of cytosine hydroxymethylation. *Nucleic Acids Res.* **40,** 4841–9 (2012).
120. Valinluck, V. & Sowers, L. C. Endogenous cytosine damage products alter the site selectivity of human DNA maintenance methyltransferase DNMT1. *Cancer Res.* **67,** 946–50 (2007).
121. Bransteitter, R., Pham, P., Scharff, M. D. & Goodman, M. F. Activation-induced cytidine deaminase deaminates deoxycytidine on single-stranded DNA but requires the action of RNase. *Proc. Natl. Acad. Sci. U. S. A.* **100,** 4102–7 (2003).
122. He, Y.-F. *et al.* Tet-mediated formation of 5-carboxylcytosine and its excision by TDG in mammalian DNA. *Science* **333,** 1303–7 (2011).
123. Liutkeviciute, Z., Lukinavicius, G., Masevicius, V., Daujotyte, D. & Klimasauskas, S. Cytosine-5-methyltransferases add aldehydes to DNA. *Nat. Chem. Biol.* **5,** 400–2 (2009).
124. Chen, C.-C., Wang, K.-Y. & Shen, C.-K. J. The mammalian de novo DNA methyltransferases DNMT3A and DNMT3B are also DNA 5-hydroxymethylcytosine dehydroxymethylases. *J. Biol. Chem.* **287,** 33116–21 (2012).
125. Smiley, J. A., Kundracik, M., Landfried, D. A., Barnes, V. R. & Axhemi, A. A. Genes of the thymidine salvage pathway: thymine-7-hydroxylase from a Rhodotorula glutinis cDNA library and iso-orotate decarboxylase from Neurospora crassa. *Biochim. Biophys. Acta* **1723,** 256–64 (2005).
126. Branco, M. R., Ficz, G. & Reik, W. Uncovering the role of 5-hydroxymethylcytosine in the epigenome. *Nat. Rev. Genet.* **13,** 7–13 (2012).
127. Frommer, M. *et al.* A genomic sequencing protocol that yields a positive display of 5-methylcytosine residues in individual DNA strands. *Proc. Natl. Acad. Sci. U. S. A.* **89,** 1827–31 (1992).
128. Huang, Y. *et al.* The behaviour of 5-hydroxymethylcytosine in bisulfite sequencing. *PLoS One* **5,** e8888 (2010).
129. Booth, M. J. *et al.* Oxidative bisulfite sequencing of 5-methylcytosine and 5-hydroxymethylcytosine. *Nat. Protoc.* **8,** 1841–51 (2013).
130. Wu, H., Wu, X., Shen, L. & Zhang, Y. Single-base resolution analysis of active DNA demethylation using methylase-assisted bisulfite sequencing. *Nat. Biotechnol.* **32,** 1231–40 (2014).
131. Booth, M. J., Marsico, G., Bachman, M., Beraldi, D. & Balasubramanian, S. Quantitative sequencing of 5-formylcytosine in DNA at single-base resolution. *Nat. Chem.* **6,** 435–40 (2014).

132. Venkatesan, B. M. & Bashir, R. Nanopore sensors for nucleic acid analysis. *Nat. Nanotechnol.* **6,** 615–24 (2011).
133. Bröske, A.-M. *et al.* DNA methylation protects hematopoietic stem cell multipotency from myeloerythroid restriction. *Nat. Genet.* **41,** 1207–1215 (2009).
134. Challen, G. A. *et al.* Dnmt3a and Dnmt3b Have Overlapping and Distinct Functions in Hematopoietic Stem Cells. *Cell Stem Cell* **15,** 350–64 (2014).
135. Li, Z. *et al.* Deletion of Tet2 in mice leads to dysregulated hematopoietic stem cells and subsequent development of myeloid malignancies. *Blood* **118,** 4509–18 (2011).
136. Ji, H. *et al.* Comprehensive methylome map of lineage commitment from haematopoietic progenitors. *Nature* **467,** 338–342 (2010).
137. Accomando, W. P., Wiencke, J. K., Houseman, E. A., Nelson, H. H. & Kelsey, K. T. Quantitative reconstruction of leukocyte subsets using DNA methylation. *Genome Biol.* **15,** R50 (2014).
138. Fischle, W., Wang, Y. & Allis, C. D. Histone and chromatin cross-talk. *Curr. Opin. Cell Biol.* **15,** 172–83 (2003).
139. Rönnerblad, M. *et al.* Analysis of the DNA methylome and transcriptome in granulopoiesis reveals timed changes and dynamic enhancer methylation. *Blood* **123,** (2014).
140. Klug, M. *et al.* Active DNA demethylation in human postmitotic cells correlates with activating histone modifications, but not transcription levels. *Genome Biol.* **11,** R63 (2010).
141. Xie, H., Ye, M., Feng, R. & Graf, T. Stepwise Reprogramming of B Cells into Macrophages. *Cell* **117,** 663–676 (2004).
142. Kallin, E. M. *et al.* Tet2 facilitates the derepression of myeloid target genes during CEBPα-induced transdifferentiation of pre-B cells. *Mol. Cell* **48,** 266–76 (2012).
143. Rodríguez-Ubreva, J. *et al.* Pre-B cell to macrophage transdifferentiation without significant promoter DNA methylation changes. *Nucleic Acids Res.* **40,** 1954–68 (2012).
144. De la Rica, L. *et al.* PU.1 target genes undergo Tet2-coupled demethylation and DNMT3b-mediated methylation in monocyte-to-osteoclast differentiation. *Genome Biol.* **14,** R99 (2013).
145. Young, N. L., Dimaggio, P. A. & Garcia, B. A. The significance, development and progress of high-throughput combinatorial histone code analysis. *Cell. Mol. Life Sci.* **67,** 3983–4000 (2010).
146. Falkenberg, K. J. & Johnstone, R. W. Histone deacetylases and their inhibitors in cancer, neurological diseases and immune disorders. *Nat. Rev. Drug Discov.* **2,** 673–691 (2014).
147. Arrowsmith, C. H., Bountra, C., Fish, P. V, Lee, K. & Schapira, M. Epigenetic protein families: a new frontier for drug discovery. *Nat. Rev. Drug Discov.* **11,** 384–400 (2012).
148. Thurman, R. E. *et al.* The accessible chromatin landscape of the human genome. *Nature* **489,** 75–82 (2012).
149. Grewal, S. I. S. & Moazed, D. Heterochromatin and epigenetic control of gene expression. *Science* **301,** 798–802 (2003).
150. Bannister, A. J. & Kouzarides, T. Regulation of chromatin by histone modifications. *Cell Res.* **21,** 381–95 (2011).
151. Heinz, S., Romanoski, C. E., Benner, C. & Glass, C. K. The selection and function of cell type-specific enhancers. *Nat. Rev. Mol. Cell Biol.* **16,** 144–154 (2015).
152. Wilting, R. H. *et al.* Overlapping functions of Hdac1 and Hdac2 in cell cycle regulation and haematopoiesis. *EMBO J.* **29,** 2586–97 (2010).
153. Wada, T. *et al.* Expression levels of histone deacetylases determine the cell fate of hematopoietic progenitors. *J. Biol. Chem.* **284,** 30673–83 (2009).
154. Barneda-Zahonero, B. *et al.* HDAC7 is a repressor of myeloid genes whose downregulation is required for transdifferentiation of pre-B cells into macrophages. *PLoS Genet.* **9,** e1003503 (2013).

155. Chen, X. *et al.* Requirement for the histone deacetylase Hdac3 for the inflammatory gene expression program in macrophages. *Proc. Natl. Acad. Sci. U. S. A.* **109,** E2865–74 (2012).
156. Ishii, M. *et al.* Epigenetic regulation of the alternatively activated macrophage phenotype. *Blood* **114,** 3244–3254 (2009).
157. Satoh, T. *et al.* The Jmjd3-Irf4 axis regulates M2 macrophage polarization and host responses against helminth infection. *Nat. Immunol.* **11,** 936–944 (2010).
158. Ghisletti, S. *et al.* Identification and characterization of enhancers controlling the inflammatory gene expression program in macrophages. *Immunity* **32,** 317–28 (2010).
159. Netea, M. G., Quintin, J. & Van Der Meer, J. W. M. Trained immunity: A memory for innate host defense. *Cell Host Microbe* **9,** 355–361 (2011).
160. Ostuni, R. *et al.* Latent enhancers activated by stimulation in differentiated cells. *Cell* **152,** 157–71 (2013).
161. Quintin, J. *et al.* Candida albicans infection affords protection against reinfection via functional reprogramming of monocytes. *Cell Host Microbe* **12,** 223–32 (2012).
162. Saeed, S. *et al.* Epigenetic programming of monocyte-to-macrophage differentiation and trained innate immunity. *Science* **345**, (6204)1251086. (2014)
163. Cheng, S.-C. *et al.* mTOR- and HIF-1 -mediated aerobic glycolysis as metabolic basis for trained immunity. *Science* **345**, 345(6204):1250684. (2014).
164. Lavin, Y. *et al.* Tissue-Resident Macrophage Enhancer Landscapes Are Shaped by the Local Microenvironment. *Cell* **159,** 1312–1326 (2014).
165. Ha, M. & Kim, V. N. Regulation of microRNA biogenesis. *Nat. Rev. Mol. Cell Biol.* **15,** 509–24 (2014).
166. Friedman, R. C., Farh, K. K.-H., Burge, C. B. & Bartel, D. P. Most mammalian mRNAs are conserved targets of microRNAs. *Genome Res.* **19,** 92–105 (2009).
167. Chen, C.-Z., Schaffert, S., Fragoso, R. & Loh, C. Regulation of immune responses and tolerance: the microRNA perspective. *Immunol. Rev.* **253,** 112–28 (2013).
168. Huntzinger, E. & Izaurralde, E. Gene silencing by microRNAs: contributions of translational repression and mRNA decay. *Nat. Rev. Genet.* **12,** 99–110 (2011).
169. Lee, Y., Jeon, K., Lee, J.-T., Kim, S. & Kim, V. N. MicroRNA maturation: stepwise processing and subcellular localization. *EMBO J.* **21,** 4663–70 (2002).
170. Lee, Y. *et al.* The nuclear RNase III Drosha initiates microRNA processing. *Nature* **425,** 415–9 (2003).
171. Bohnsack, M. T., Czaplinski, K. & Gorlich, D. Exportin 5 is a RanGTP-dependent dsRNA-binding protein that mediates nuclear export of pre-miRNAs. *RNA* **10,** 185–91 (2004).
172. Bernstein, E., Caudy, A. A., Hammond, S. M. & Hannon, G. J. Role for a bidentate ribonuclease in the initiation step of RNA interference. *Nature* **409,** 363–6 (2001).
173. Chendrimada, T. P. *et al.* TRBP recruits the Dicer complex to Ago2 for microRNA processing and gene silencing. *Nature* **436,** 740–4 (2005).
174. Chien, C.-H. *et al.* Identifying transcriptional start sites of human microRNAs based on high-throughput sequencing data. *Nucleic Acids Res.* **39,** 9345–56 (2011).
175. Kim, S. J., Gregersen, P. K. & Diamond, B. Regulation of dendritic cell activation by microRNA let-7c and BLIMP1. *J. Clin. Invest.* **123,** 823–33 (2013).
176. Undi, R. B., Kandi, R. & Gutti, R. K. MicroRNAs as Haematopoiesis Regulators. *Adv. Hematol.* **2013,** 695754 (2013).
177. Ventura, A. *et al.* Targeted deletion reveals essential and overlapping functions of the miR-17 through 92 family of miRNA clusters. *Cell* **132,** 875–86 (2008).
178. Nahid, M. A., Pauley, K. M., Satoh, M. & Chan, E. K. L. miR-146a is critical for endotoxin-induced tolerance: IMPLICATION IN INNATE IMMUNITY. *J. Biol. Chem.* **284,** 34590–9 (2009).

179. Taganov, K. D., Boldin, M. P., Chang, K.-J. & Baltimore, D. NF-kappaB-dependent induction of microRNA miR-146, an inhibitor targeted to signaling proteins of innate immune responses. *Proc. Natl. Acad. Sci. U. S. A.* **103,** 12481–6 (2006).
180. Mi, Q.-S., Xu, Y.-P., Qi, R.-Q., Shi, Y.-L. & Zhou, L. Lack of microRNA miR-150 reduces the capacity of epidermal Langerhans cell cross-presentation. *Exp. Dermatol.* **21,** 876–7 (2012).
181. Mi, Q.-S. *et al.* Deletion of microRNA miR-223 increases Langerhans cell cross-presentation. *Int. J. Biochem. Cell Biol.* **45,** 395–400 (2013).
182. Guo, H., Callaway, J. B. & Ting, J. P.-Y. Inflammasomes: mechanism of action, role in disease, and therapeutics. *Nat. Med.* **21,** 677–687 (2015).
183. Vanaja, S. K., Rathinam, V. a. K. & Fitzgerald, K. a. Mechanisms of inflammasome activation: recent advances and novel insights. *Trends Cell Biol.* 1–8 (2015).

184. Mailliard, R. B. *et al.* IL-18-induced CD83+CCR7+ NK helper cells. *J. Exp. Med.* **202,** 941–53 (2005).
185. O'Shea, J. J. & Paul, W. E. Mechanisms underlying lineage commitment and plasticity of helper CD4+ T cells. *Science* **327,** 1098–102 (2010).
186. Srinivasula, S. M. *et al.* The PYRIN-CARD protein ASC is an activating adaptor for caspase-1. *J. Biol. Chem.* **277,** 21119–22 (2002).
187. Faustin, B. *et al.* Reconstituted NALP1 inflammasome reveals two-step mechanism of caspase-1 activation. *Mol. Cell* **25,** 713–24 (2007).
188. Bauernfeind, F. G. *et al.* Cutting edge: NF-kappaB activating pattern recognition and cytokine receptors license NLRP3 inflammasome activation by regulating NLRP3 expression. *J. Immunol.* **183,** 787–91 (2009).
189. Py, B. F., Kim, M.-S., Vakifahmetoglu-Norberg, H. & Yuan, J. Deubiquitination of NLRP3 by BRCC3 critically regulates inflammasome activity. *Mol. Cell* **49,** 331–8 (2013).
190. Rodgers, M. A. *et al.* The linear ubiquitin assembly complex (LUBAC) is essential for NLRP3 inflammasome activation. *J. Exp. Med.* **211,** 1333–47 (2014).
191. Lu, A. *et al.* Unified polymerization mechanism for the assembly of ASC-dependent inflammasomes. *Cell* **156,** 1193–206 (2014).
192. Cai, X. *et al.* Prion-like polymerization underlies signal transduction in antiviral immune defense and inflammasome activation. *Cell* **156,** 1207–22 (2014).
193. Netea, M. G. *et al.* Differential requirement for the activation of the inflammasome for processing and release of IL-1beta in monocytes and macrophages. *Blood* **113,** 2324–35 (2009).
194. Piccini, A. *et al.* ATP is released by monocytes stimulated with pathogen-sensing receptor ligands and induces IL-1beta and IL-18 secretion in an autocrine way. *Proc. Natl. Acad. Sci. U. S. A.* **105,** 8067–72 (2008).
195. Davis, B. K. *et al.* Cutting edge: NLRC5-dependent activation of the inflammasome. *J. Immunol.* **186,** 1333–7 (2011).
196. Yao, Y. *et al.* NLRC5 regulates MHC class I antigen presentation in host defense against intracellular pathogens. *Cell Res.* **22,** 836–47 (2012).
197. Jin, T. *et al.* Structures of the HIN domain:DNA complexes reveal ligand binding and activation mechanisms of the AIM2 inflammasome and IFI16 receptor. *Immunity* **36,** 561–71 (2012).
198. Broderick, L., De Nardo, D., Franklin, B. S., Hoffman, H. M. & Latz, E. The inflammasomes and autoinflammatory syndromes. *Annu. Rev. Pathol.* **10,** 395–424 (2015).
199. Kayagaki, N. *et al.* Non-canonical inflammasome activation targets caspase-11. *Nature* **479,** 117–21 (2011).
200. Shi, J. *et al.* Inflammatory caspases are innate immune receptors for intracellular LPS. *Nature* **514,** 187–92 (2014).

201. Carruth, L. M., Demczuk, S. & Mizel, S. B. Involvement of a calpain-like protease in the processing of the murine interleukin 1 alpha precursor. *J. Biol. Chem.* **266,** 12162–7 (1991).
202. Howard, A. D. *et al.* IL-1-converting enzyme requires aspartic acid residues for processing of the IL-1 beta precursor at two distinct sites and does not cleave 31-kDa IL-1 alpha. *J. Immunol.* **147,** 2964–9 (1991).
203. Gross, O. *et al.* Inflammasome activators induce interleukin-1α secretion via distinct pathways with differential requirement for the protease function of caspase-1. *Immunity* **36,** 388–400 (2012).
204. Van Kempen, T. S., Wenink, M. H., Leijten, E. F. A., Radstake, T. R. D. J. & Boes, M. Perception of self: distinguishing autoimmunity from autoinflammation. *Nat. Rev. Rheumatol.* (2015).
205. Russo, R. A. G. & Brogan, P. A. Monogenic autoinflammatory diseases. *Rheumatology (Oxford).* **53,** 1927–39 (2014).
206. Jesus, A. A. & Goldbach-Mansky, R. IL-1 blockade in autoinflammatory syndromes. *Annu. Rev. Med.* **65,** 223–44 (2014).
207. Marek-Yagel, D. *et al.* Clinical disease among patients heterozygous for familial Mediterranean fever. *Arthritis Rheum.* **60,** 1862–6 (2009).
208. Misawa, T. *et al.* Microtubule-driven spatial arrangement of mitochondria promotes activation of the NLRP3 inflammasome. *Nat. Immunol.* **14,** 454–60 (2013).
209. Balci-Peynircioglu, B. *et al.* Pyrin, product of the MEFV locus, interacts with the proapoptotic protein, Siva. *J. Cell. Physiol.* **216,** 595–602 (2008).
210. Taskiran, E. Z., Cetinkaya, A., Balci-Peynircioglu, B., Akkaya, Y. Z. & Yilmaz, E. The effect of colchicine on pyrin and pyrin interacting proteins. *J. Cell. Biochem.* **113,** 3536–46 (2012).
211. Waite, A. L. *et al.* Pyrin and ASC co-localize to cellular sites that are rich in polymerizing actin. *Exp. Biol. Med. (Maywood).* **234,** 40–52 (2009).
212. Hoffman, H. M., Wright, F. A., Broide, D. H., Wanderer, A. A. & Kolodner, R. D. Identification of a locus on chromosome 1q44 for familial cold urticaria. *Am. J. Hum. Genet.* **66,** 1693–8 (2000).
213. Aróstegui, J. I. *et al.* Clinical and genetic heterogeneity among Spanish patients with recurrent autoinflammatory syndromes associated with the CIAS1/PYPAF1/NALP3 gene. *Arthritis Rheum.* **50,** 4045–50 (2004).
214. Aksentijevich, I. *et al.* De novo CIAS1 mutations, cytokine activation, and evidence for genetic heterogeneity in patients with neonatal-onset multisystem inflammatory disease (NOMID): a new member of the expanding family of pyrin-associated autoinflammatory diseases. *Arthritis Rheum.* **46,** 3340–8 (2002).
215. Aksentijevich, I. *et al.* The clinical continuum of cryopyrinopathies: novel CIAS1 mutations in North American patients and a new cryopyrin model. *Arthritis Rheum.* **56,** 1273–85 (2007).
216. Hoffman, H. M. *et al.* Prevention of cold-associated acute inflammation in familial cold autoinflammatory syndrome by interleukin-1 receptor antagonist. *Lancet (London, England)* **364,** 1779–85 (2004)
217. Tanaka, N. *et al.* High incidence of NLRP3 somatic mosaicism in patients with chronic infantile neurologic, cutaneous, articular syndrome: results of an International Multicenter Collaborative Study. *Arthritis Rheum.* **63,** 3625–32 (2011).
218. Dinarello, C. A., Novick, D., Kim, S. & Kaplanski, G. Interleukin-18 and IL-18 binding protein. *Front. Immunol.* **4,** 289 (2013).
219. Klug, M., Schmidhofer, S., Gebhard, C., Andreesen, R. & Rehli, M. 5-Hydroxymethylcytosine is an essential intermediate of active DNA demethylation processes in primary human monocytes. *Genome Biol.* **14,** R46 (2013).

220. Kouzine, F. *et al.* Global regulation of promoter melting in naive lymphocytes. *Cell* **153,** 988–99 (2013).
221. Hirahara, K. *et al.* Asymmetric Action of STAT Transcription Factors Drives Transcriptional Outputs and Cytokine Specificity. *Immunity* **42,** 877–89 (2015).
222. Litterst, C. M. & Pfitzner, E. Transcriptional Activation by STAT6 Requires the Direct Interaction with NCoA-1. *J. Biol. Chem.* **276,** 45713–45721 (2001).
223. McDonald, C. & Reich, N. C. Cooperation of the transcriptional coactivators CBP and p300 with Stat6. *J. Interferon Cytokine Res.* **19,** 711–22 (1999).
224. Nishikawa, K. *et al.* DNA methyltransferase 3a regulates osteoclast differentiation by coupling to an S-adenosylmethionine-producing metabolic pathway. *Nat. Med.* **21,** 281–7 (2015).
225. Drobek, A. *et al.* PSTPIP2, a Protein Associated with Autoinflammatory Disease, Interacts with Inhibitory Enzymes SHIP1 and Csk. *J. Immunol.* **195,** 3416–26 (2015).
226. Sander, J. D. & Joung, J. K. CRISPR-Cas systems for editing, regulating and targeting genomes. *Nat. Biotechnol.* **32,** 347–55 (2014).
227. Rodriguez-Ubreva, J. *et al.* C/EBPa-mediated activation of microRNAs 34a and 223 inhibits Lef1 expression to achieve efficient reprogramming into macrophages. *Mol. Cell. Biol.* **34,** 1145–57 (2014).

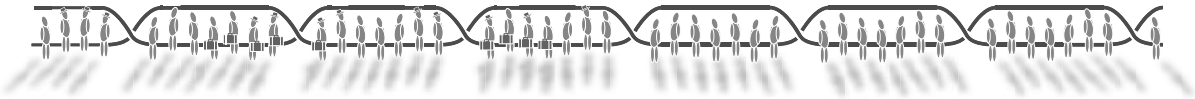

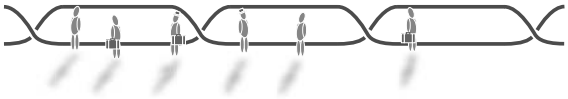

SUPPLEMENTARY INFORMATION

Epigenetic control of myeloid cell differentiation, identity and function

Damiana Álvarez-Errico[1], Roser Vento-Tormo[1], Michael Sieweke[2] and Esteban Ballestar[1]

Abstract | Myeloid cells are crucial effectors of the innate immune response and important regulators of adaptive immunity. The differentiation and activation of myeloid cells requires the timely regulation of gene expression; this depends on the interplay of a variety of elements, including transcription factors and epigenetic mechanisms. Epigenetic control involves histone modifications and DNA methylation, and is coupled to lineage-specifying transcription factors, upstream signalling pathways and external factors released in the bone marrow, blood and tissue environments. In this Review, we highlight key epigenetic events controlling myeloid cell biology, focusing on those related to myeloid cell differentiation, the acquisition of myeloid identity and innate immune memory.

Histones
A family of basic proteins found in the nuclei of eukaryotic cells that package and organize DNA into repetitive structural units named nucleosomes.

[1]Chromatin and Disease Group, Cancer Epigenetics and Biology Programme (PEBC), Bellvitge Biomedical Research Institute (IDIBELL), 08908 L'Hospitalet de Llobregat, Barcelona, Spain. [2]Stem Cell and Macrophage Biology, Centre d'Immunologie de Marseille-Luminy, Campus de Luminy, Case 906, 13288 Marseille Cedex 09, France. Correspondence to E.B. e-mail: eballestar@idibell.cat
doi:10.1038/nri3777

Cell differentiation across the myeloid lineage provides an excellent model for defining the intricate gene-regulatory mechanisms that confer identity and function on immune cells. The initial steps of myeloid cell differentiation take place in the bone marrow, and they are determined by cytokine signals that are mainly provided by stromal cells[1] and that promote the progressive activation of the myeloid-specifying transcriptional programme. Later on, terminal differentiation processes that lead to the generation of mature myeloid cells occur in the blood or peripheral tissues and depend on the exposure of precursor cells to cytokines, antigens and other factors[2].

The control of differentiation from progenitor and intermediate cell types to fully differentiated myeloid cells requires the timely regulation of gene expression, the basis of which depends on the interplay of a variety of elements, including transcription factors, epigenetic regulation and post-transcriptional control mechanisms. Epigenetic regulation, comprising the post-translational modification of histones and DNA methylation, is not only coupled with transcription factor-mediated regulation, but is also linked with upstream signalling pathways that connect external signals and gene function to shape the identity and function of immune cells. In light of recent data obtained by high-throughput epigenomic techniques, we now possess detailed information concerning how the myeloid compartment develops in association with epigenetic changes.

In this Review, we discuss the role of epigenetic regulation in determining cell fate decisions within the myeloid compartment, as well as during the generation of functional myeloid cell responses. In particular, we focus on the prominent role of DNA demethylation events in myeloid cell differentiation and the relevance of the ten-eleven-translocation (TET) protein methylcytosine dioxygenase TET2, an enzyme that promotes DNA demethylation. Finally, we describe the newly emerging data that point to an important role for epigenetic mechanisms in controlling memory-type responses in monocytes and macrophages.

Epigenetics and gene expression control

Histone modifications are important for the regulation of chromatin function and enable the recruitment of specific nuclear factors that promote different cellular functions. We now know of more than 100 post-translational modification sites that can be found in histones as a result of the acetylation, methylation, phosphorylation or ubiquitylation of different lysine, arginine, serine and other amino acid residues[3]. Specific sites within histone tails — in particular, lysine and arginine residues — are targeted by different families of histone-modifying enzymes depending on the specific signals and conditions that a cell is exposed to[4]. Histone acetylation is one of the best-studied modifications and it generally correlates with the levels of gene expression[5]. The overall acetylation status is determined by the relative activity of histone acetyltransferases (HATs) and histone deacetylases (HDACs). Similarly, the methylation status of lysine or arginine residues depends on the relative activity of lysine and arginine methyltransferases on one hand, and lysine demethylases, arginine deiminases and

arginine demethylases on the other. The effect of methylation status on transcription depends on the exact residue targeted and the degree of methylation; that is, whether a residue is monomethylated (me1), dimethylated (me2) or trimethylated (me3)[3]. For instance, considering histone H3, H3K4me3 is associated with transcriptional activation, whereas H3K27me3 is linked with gene repression[3].

DNA methylation has a central role in cell differentiation and function by driving and stabilizing gene activity states during cell fate decisions. Addition of a methyl group to the 5′ position of the pyrimidine ring of certain cytosines that are adjacent to guanines in the DNA (known as CpG dinucleotides) directly modulates the binding of particular transcription factors to their cognate sites or influences the binding of other nuclear factors that display higher or lower affinity for methylated cytosines[6,7], which eventually modifies transcription factor accessibility or chromatin structure. Most CpG dinucleotides are methylated throughout the mammalian genome, and 5-methylcytosine (5meC) is evenly distributed, except for in CpGs that are densely clustered in areas called CpG islands (CGIs)[8,9]. CGIs have long been thought to be the primary DNA methylation-dependent regulatory regions. However, they exhibit low levels of methylation in many cell types, and the greatest variation in DNA methylation levels among different cell types occurs primarily at the borders of CGIs, in regions termed 'shores', which are also hotspots for hypermethylation and hypomethylation in malignant cells[10]. More recently, high-throughput DNA methylation analysis has led to the identification of potential regulatory hypomethylated regions that are located either partially or completely outside CGIs, in shores (within 2 kb upstream or downstream of CGIs), 'shelves' (within 2 kb upstream or downstream from shores) or in the 'open sea'. Moreover, a substantial proportion of regulatory hypomethylated regions are located either partially or fully within gene bodies, reflecting the importance of intragenic methylation in the regulation of gene transcription[11,12]. Studies of whole-genome DNA methylation are leading to the identification of new regulatory hypomethylated regions beyond CGIs that have important regulatory functions[13]. The analysis of the DNA methylome of mouse stem cells has confirmed that the majority of CpGs behave in a bimodal way[14]. Most CpGs show a high level of methylation and some are unmethylated; however, there is also a group of CpGs that show an intermediate level of methylation, and these correspond to distal regulatory regions[14].

Methylation of cytosines silences certain genomic regions during cell fate determination, including imprinted genes and X chromosome inactivation genes, as well as some cell-type-specific genes[9]. DNA methyltransferases (DNMTs) mediate the methylation of cytosines and are well characterized in mammals. DNMT1 maintains pre-existing DNA methylation profiles throughout DNA replication cycles, whereas DNMT3A and DNMT3B are mainly responsible for *de novo* methylation[15]. By contrast, the mechanisms that control DNA demethylation have proven to be more elusive. Methyl groups can be lost from DNA by enzymatic inhibition or exclusion of DNMTs in dividing cells. This replication-dependent loss of 5meC — known as passive DNA demethylation — has been described in several biological processes and is a commonly used mechanism to pharmacologically demethylate cells[16]. DNA methylation can also be rapidly lost independent of DNA replication. In the past 15 years, a variety of enzymes and mechanisms have been proposed to participate in this so-called active demethylation[17]. We now know that active DNA demethylation involves the activity of TET proteins; this family of methylcytosine dioxygenases sequentially oxidizes 5meC to 5-hydroxymethylcytosine (5hmC), 5-formylcytosine (5fC) and 5-carboxycytosine (5caC), which are then excised by G/T mismatch-specific thymine DNA glycosylase (TDG). In turn, this two-step process of oxidation and excision generates abasic sites that are then used by the base excision repair machinery to regenerate unmodified cytosines, changing the DNA methylation patterns and locally decreasing DNA methylation[18–21]. Whether these oxidized nucleotides (such as 5hmC) are themselves bona fide epigenetic marks with direct functional consequences or just transient intermediates remains controversial. The relevance of TET proteins and 5hmC is evident from the fact that embryonic stem cells from mice that are triple deficient for *Tet1*, *Tet2* and *Tet3* show severely compromised differentiation and development[22]. Surprisingly, long conserved stretches of low-methylated DNA with a regulatory function, known as 'canyons', have recently been discovered. These are maintained by DNMT3A and their borders are flanked by 5hmC[23].

Epigenetics of immune cell differentiation

Early epigenetic events in haematopoiesis. Epigenetic changes are crucial in haematopoiesis as they regulate the successive gene-expression programmes that give rise to all immune cell populations. Haematopoietic cell differentiation is initiated and maintained in the bone marrow by haematopoietic stem cells (HSCs), a rare cell population that gives rise to the entire population of circulating blood cells and immune cells that are found in the peripheral tissues[24]. HSCs have self-renewal capacity and are multipotent, allowing the immune and haematopoietic compartments to be maintained and repopulated. Investigation into the participation of epigenetic events in haematopoiesis has revealed that both DNA and histone modifications are important in this process. For instance, the ablation of *Hdac1* and *Hdac2* in mouse bone marrow progenitor cells impedes the development of erythrocytes and megakaryocytes[25]. In addition, mice with reduced DNMT1 activity have a myeloerythroid bias as they cannot suppress key myeloerythroid regulators, and thus can generate myeloerythroid, but not lymphoid, progeny[26].

Haematopoiesis is a tightly regulated process during which there is a subsequent appearance of restrictive nodes. An in depth study of the transcriptome associated with lineage commitment in early progenitors of human blood cells has revealed a layer of regulation that relies on

Shores
Regions that are located within 2 kb of CpG islands and are usually methylation hotspots.

Shelves
Regions that flank CpG island shores and are located 2–4 kb from CpG islands.

Open sea
CpG sites that are located outside of the CpG island context.

Imprinted genes
Genes for which the expression status is determined by the parent that contributed them.

great transcriptional diversity, including transcriptional isoforms that control protein levels[27]. The first ramification of this is that multipotent progenitors (MPPs) differentiate into two branches: one deriving from the common myeloid progenitor (CMP) and the other from the common lymphoid progenitor (CLP)[28]. Downstream of CMPs, specific growth factors sustain the generation of the granulocyte–macrophage lineage (which gives rise to monocytes, neutrophils, eosinophils, basophils and mast cells) and the megakaryocyte–erythroid lineage[24] (which gives rise to erythrocytes and platelets). By contrast, CLPs have the capacity to generate B cells, T cells and natural killer (NK) cells[28]. The participation of epigenetic events in these decisions is highlighted, for instance, by the finding that committed CMPs differentiate into megakaryocyte–erythroid lineages when HDAC1 expression is sustained by the GATA-binding protein 1 (GATA1; also known as erythroid transcription factor 1), whereas when HDAC1 expression is downregulated by CCAAT/enhancer-binding protein (C/EBP) transcription factors, committed CMPs give rise to myeloid cells, in particular granulocytes[29].

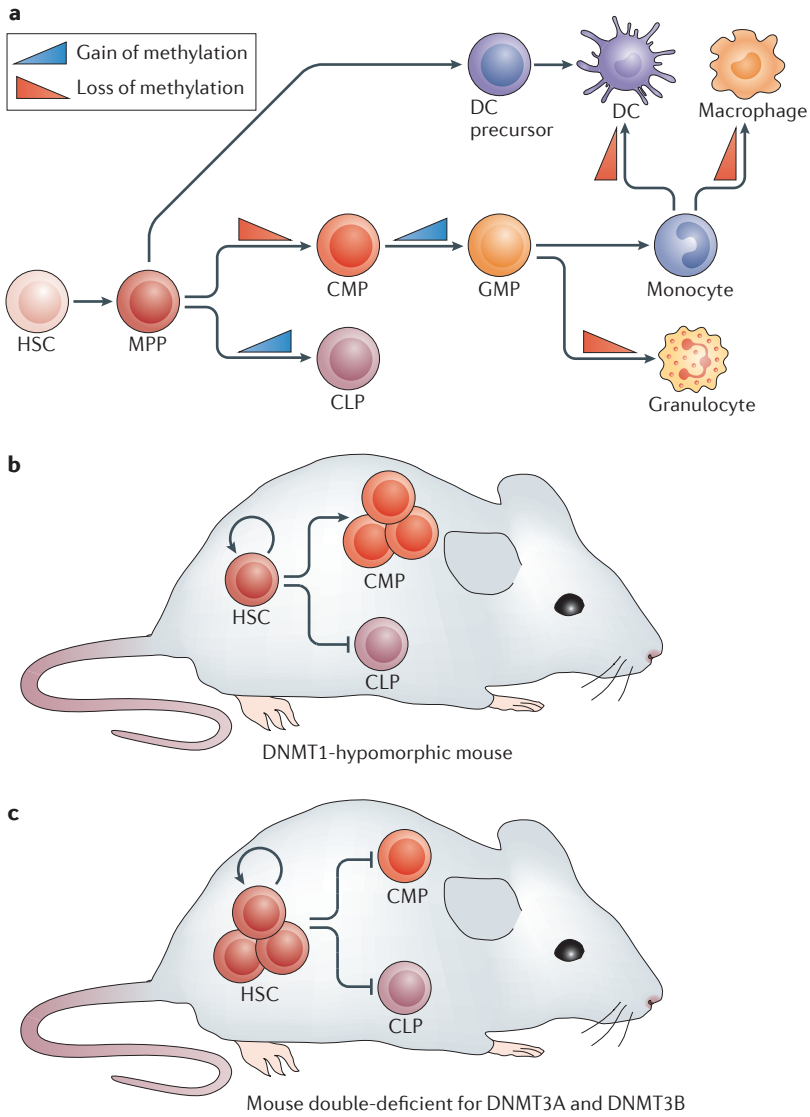

Figure 1 | **DNA methylation events in the early stages of haematopoiesis.** **a** | The figure shows the main patterns of methylation that occur during adult haematopoiesis, summarizing data obtained from studies using primary cells from humans and mice, as well as cell lines. The key changes in DNA methylation that are associated with each step are indicated, with the blue triangles representing an overall increase in methylation and the red triangles representing a loss of methylation[36,40,41,43]. **b** | The figure depicts how haematopoiesis is deregulated in DNA methyltransferase 1 (DNMT1)-hypomorphic mice, which only possess one allele encoding a functional DNMT1 protein . Haematopoietic stem cells (HSCs) in these mice are biased towards myeloerythroid lineage differentiation to the detriment of lymphoid development. **c** | HSCs from mice that are double-deficient for DNMT3A and DNMT3B expression show enhanced self-renewal capacity, but are subsequently blocked from undergoing further differentiation into common myeloid progenitors (CMPs) or common lymphoid progenitors (CLPs). A similar, although less severe, phenotype is seen in mice with a single deficiency of either DNMT3A or DNMT3B (not shown), with this phenotype being more pronounced in HSCs with a single deficiency of DNMT3A than in HSCs with a single deficiency of DNMT3B. DC, dendritic cell; GMP, granulocyte–macrophage progenitor; MPP, multipotent progenitor.

Distinct DNA methylation patterns characterize myeloid and lymphoid cell differentiation. DNA methylation events help to regulate HSC self-renewal during haematopoiesis, facilitating the commitment to a lymphoid or myeloid fate, and finally establishing the identities of differentiated cell types[30]. DNMT1 is indispensable for protecting HSCs from the premature activation of predominant differentiation programmes[26] (FIG. 1), and DNMT3A and DNMT3B are required to silence the expression of transcription factors related to self-renewal and multipotency, such as RUNT-related transcription factor 1 (RUNX1) and GATA3, allowing differentiation to proceed[31]. In addition, analysis of the epigenome of HSCs has revealed that genes encoding transcription factors that are important for haematopoietic cell differentiation, such as C/EBPα, EBF1 and paired box protein PAX5 (PAX5), display low levels of DNA methylation and are enriched in both activating H3K4me3 and repressive H3K27me3 marks (also known as bivalent domains), showing coordination of epigenetic regulatory mechanisms[32]. Myelomonocytic cells are more evolutionarily ancient than the lymphoid compartment[33]; perhaps reflecting this, the DNA methylation patterns of HSCs more closely resemble those seen in myeloid cells than those in lymphoid cells[34], suggesting an intrinsic myeloid bias of the HSC methylome[35,36]. This connection between the myeloid lineage and HSCs is reinforced by the recent finding that macrophage colony-stimulating factor (M-CSF; also known as CSF1) — a myeloid cytokine released during infection and inflammation — can activate the transcription factor PU.1 in HSCs, thereby promoting a myeloid-specifying gene signature and myeloid differentiation potential[37].

DNA methylation levels increase upon lymphoid commitment, but decrease sharply as myeloid differentiation progresses[36]. This is consistent with the observation that HSCs are unable to differentiate into lymphoid cells in mice with reduced DNMT1 activity, as myeloerythroid regulators cannot be silenced[26]. Cells from *Dnmt1*-hypomorphic mice show higher expression levels and lower DNA methylation levels of signature myeloerythroid progenitor genes, including the genes

that encode the transcription factors GATA1, inhibitor of DNA binding 2 (ID2) and C/EBPα[26]. Compared with the DNA methylation profiles of $CD34^+$ progenitor cells, terminally differentiated monocytes and granulocytes show a marked trend towards DNA hypomethylation[38]. In addition, when the DNA methylation signatures of terminally differentiated human blood cells — including B cells, NK cells, T cells, monocytes, basophils, eosinophils and neutrophils — were assessed, a marked hypomethylation pattern was found in myeloid cells compared with in lymphoid cells[36,39]. Notably, regulatory hypomethylated regions are more common in monocytes than in lymphoid cells[12].

Although DNA hypomethylation is a general feature of myeloid cells, it is important to note that DNA methylation is dynamically regulated during granulopoiesis and varies with the stage of differentiation. During neutrophil development, there is an increase in DNA methylation during the transition of CMPs into granulocyte–macrophage progenitors (GMPs), followed by a reduction in methylation between the GMP and promyelocyte stages of development[40] (FIG. 1). However, differences in methylation levels between promyelocytes and the polymorphonuclear neutrophils that they give rise to seem to be very small[40]. Possibly, the initial increase in DNA methylation seen during the CMP to GMP transition is related to the silencing of pluripotency-related genes, thereby generating a first 'wave' of commitment and a reduction in self-renewal capacity. This may then be followed by a DNA demethylation-dependent derepression of myeloid-specific genes in the second stage of development. Finally, the small but significant changes in 5meC levels during the transition from promyelocytes to neutrophils could be associated with specific and rapid response genes, suggesting that DNA methylation is a more dynamic regulatory mechanism than previously thought. TET2 — the most abundant TET family member in myeloid cells — is likely to participate in the observed changes towards demethylation during myeloid differentiation.

The aforementioned findings, comparing the DNA methylation profiles of myeloid cells that were analysed *ex vivo* at various stages of development, are generally consistent with those obtained from differentiation models. For instance, the *in vitro* differentiation of monocytes into macrophages or dendritic cells involves active DNA demethylation throughout the entire process[41–43]. Various studies have identified differentially methylated gene regions that are methylated in monocytes and undergo active demethylation during their differentiation into macrophages and dendritic cells[41–43]. However, *de novo* DNA methylation has rarely been detected during these two differentiation processes[41,43].

Epigenetic control of myeloid cell identity

Lessons from transcription factor-mediated transdifferentiation models. In the myeloid compartment, the differentiation and establishment of inflammatory cells depends on the instructive effects of several lineage-specific transcription factors, including PU.1, C/EBPα and GATA1 (REFS 44,45) (FIG. 2). Transcription factor-mediated reprogramming and transdifferentiation experiments have not only been useful for investigating the specific contribution of transcription factors to myeloid cell identity, but have also shed light on their association with the epigenetic machinery. One example is the demonstration of the ability of PU.1 and C/EBPα to promote the conversion of fibroblasts into macrophages[46], which reinforces the key role of these two transcription factors as modulators of macrophage-specific gene expression. Another key model is represented by the C/EBPα-induced transdifferentiation of B cells into macrophages[47,48]. In this process, C/EBPα expression in pre-B cells coordinates the acquisition of the macrophage-specific gene-expression programme leading to the generation of functional macrophages. It has been demonstrated that HDAC7 has a role in repressing macrophage-specific genes, and its expression is strongly downregulated during C/EBPα-mediated transdifferentiation, allowing the induction of the macrophage-specifying programme[49].

Surprisingly, C/EBPα-mediated transdifferentiation of pre-B cells into macrophages occurs without noticeable changes in DNA methylation, and reprogrammed macrophages retain the DNA methylation profile of pre-B cells[95]. Neither a gain in the methylation of lymphoid-specific genes nor the demethylation of myeloid-specific genes occurs during this process. However, C/EBPα activates TET2 during the C/EBPα-mediated reprogramming of B cells into macrophages[50]. Specifically, TET2 promotes hydroxymethylation and facilitates the derepression of myeloid target genes during this process. This suggests that TET2-mediated hydroxymethylation may have a direct positive role in gene expression, without necessarily leading to demethylation. In line with this, *in vitro* studies have shown that methyl-CpG binding proteins have a reduced binding affinity for 5hmC compared with 5mC[51], reinforcing the possibility that this oxidized nucleotide may itself have a direct effect on gene expression.

These findings highlight the relevance of C/EBPα and TET2 in the acquisition of cell identity in macrophages, despite the inability of this system to proceed further towards demethylation. The importance of C/EBPα and TET2 is also indicated by the finding that the ectopic expression of C/EBPα, together with transduction of the Yamanaka factors OCT4 (also known as POU5F1), SOX2, Krüppel-like factor 4 (KLF4) and MYC — which are collectively referred to as OSKM — allows the direct reprogramming of terminally differentiated mature B cells towards a pluripotent state[52]. More recently, it has been shown that the efficiency of this process can be increased 100-fold if C/EBPα is transfected before the introduction of the Yamanaka factors in a mechanism that involves TET2 and 5hmC, and presumably favours a more open chromatin conformation, which allows the transcription factors greater accessibility[53]. In fact, the sole overexpression of TET2 enhances OSKM-induced B cell reprogramming[53]. All of these findings indicate that TET2 is a key enzyme in the acquisition of myeloid cell identity. It is also tempting to speculate that TET2 may be a key factor in

Methyl-CpG binding proteins
A family of proteins characterized by the presence of the methyl-CpG binding domain, several of which are integral components of or are involved in the recruitment of different histone deacetylase complexes and chromatin remodelling factors of different nuclear complexes that have a role in gene expression.

Yamanaka factors
A set of transcription factors that are highly expressed in embryonic stem cells. Their overexpression induces pluripotency in somatic cells.

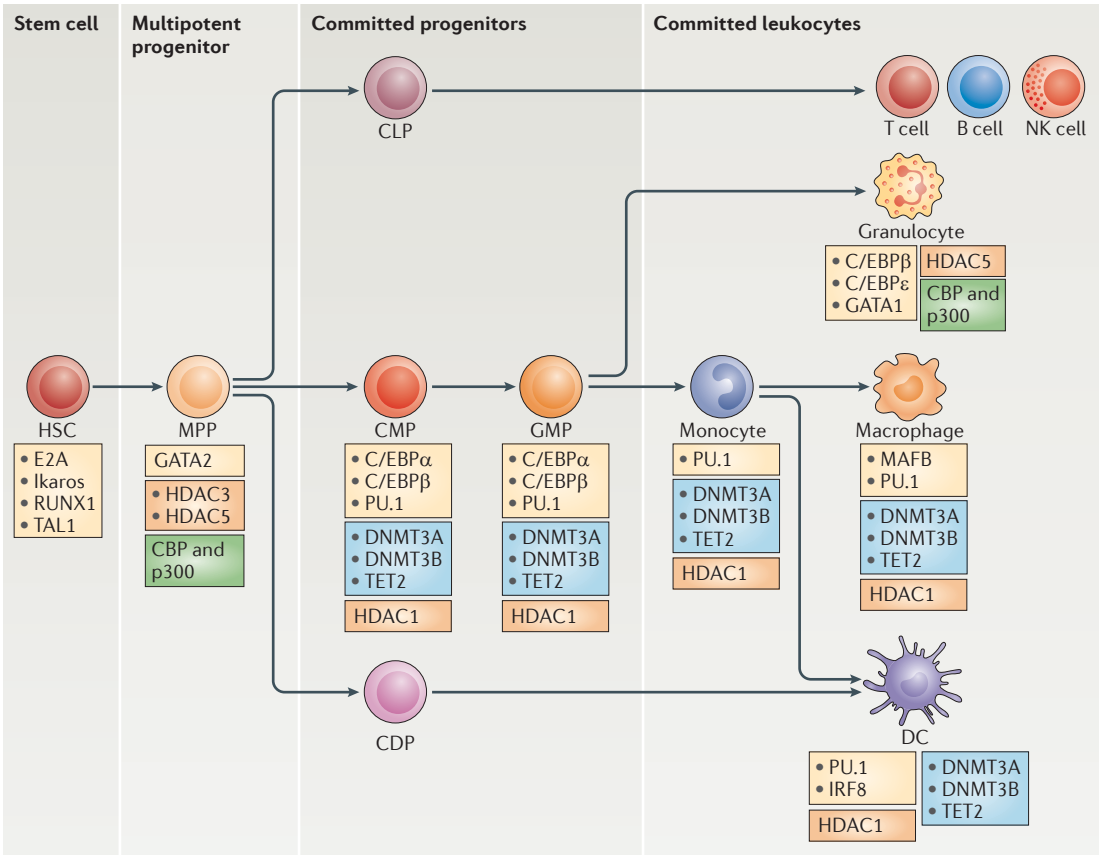

Figure 2 | **Transcription factors and epigenetic regulators of haematopoietic cell differentiation.** The figure focuses on the main stages of myeloid differentiation (in the central horizontal axis) and indicates the key transcription factors (yellow boxes) and epigenetic enzymes that could be involved at each stage. Enzymes that participate in DNA demethylation events are shown in blue boxes, histone deacetylases (HDACs) are shown in orange boxes and histone acetyltransferases are shown in green boxes. Progenitor cells involved at each stage include haematopoietic stem cells (HSCs), multipotent progenitors (MPPs), common myeloid progenitor (CMPs), common lymphoid progenitor (CLPs) and granulocyte–monocyte progenitors (GMPs). These progenitors ultimately give rise to various terminally differentiated cell types, such as dendritic cells (DCs) and macrophages. In pluripotent cells, self-renewal is controlled by Ikaros and E2A, and progression into increasingly committed myeloid cells types is dependent on the expression and dose of PU.1 that is already present at the CMP stage. In human monocytes, PU.1 has been reported to interact with DNA methylation enzymes such as methylcytosine dioxygenase TET2 and DNA methyltransferase 3B (DNMT3B), and may potentially recruit them to their target genes. CCAAT/enhancer binding protein-α (C/EBPα) is also an important regulatory transcription factor that cooperates with PU.1 to promote myeloid identity. In inflamed tissues, monocytes undergo terminal differentiation into macrophages in a process that is controlled by the transcription factor MAFB, or into inflammatory DCs in a process controlled by interferon-regulatory factor 8 (IRF8) expression. IRF8 also blocks granulocytic transcriptional programmes. CBP, CREB-binding protein; CDP, common DC precursor; GATA1, GATA-binding protein 1; NK, natural killer; p300, histone acetyltransferase p300; RUNX1, RUNT-related transcription factor 1; TAL1, T cell acute lymphocytic leukaemia protein 1.

determining the closer relationship of myeloid cells to HSCs, compared with their relationship to lymphocytes. At any rate, these results have useful applications in the field of reprogramming and regenerative biology.

***TET2* and the relevance of active demethylation in myeloid cells.** *TET2* is mutated in several myeloid malignancies, suggesting a central role for TET2 in the control of myeloid cell proliferation and differentiation[54]. Myeloid cancers with mutant forms of *TET2* display impaired hydroxylation of 5meC[19], and this may be related to the altered methylation that is observed in these cells; however, it is difficult to establish a direct relationship as hypermethylation is a hallmark of human cancers. TET2-deficient mice have an enhanced repopulation capacity that is linked to lower levels of 5hmC in HSCs, demonstrating a role for TET2 in maintaining haematopoietic homeostasis[55]. Interestingly, knockdown of *TET2* in human $CD34^+$ progenitors skews their differentiation toward the granulomonocytic lineage, at the expense of the lymphoid and erythroid lineages[56]. These results seem to contradict the C/EBPα-mediated pre-B cell to macrophage transdifferentiation model, in which TET2 was shown to have a key role in driving differentiation towards the myeloid lineage. However, these results may indicate cell-stage-dependent

'M1' or 'classical' activation
Lipopolysaccharide- or interferon-γ-mediated stimulation of macrophages leading to a pro-inflammatory phenotype.

'M2' or 'alternative' activation
Interleukin-4-dependent stimulation of macrophages that leads to an anti-inflammatory phenotype.

differences in TET2 dependency and reflect the complexity of the DNA methylation events that are involved in myeloid differentiation. TET2 could link environmental conditions, including nutrient availability, to developmental fate, as suggested by experiments showing that the cellular metabolite 2-hydroxyglutarate inhibits TET2 and affects the differentiation of haematopoietic and myeloid cells[57]. Deletion of *Tet2* in the haematopoietic compartment leads to the development of a chronic myelomonocytic leukaemia-like disease in young mice that is associated with the expansion of myeloid progenitor populations and the activation of myeloid and self-renewal programmes[58]. Mice in which all haematopoietic cells, or specifically myeloid lineage cells, are engineered to express a mutant form of the metabolic enzyme isocitrate dehydrogenase 1 (IDH1) show an accumulation of pluripotent progenitor cells and lineage-restricted cell progenitors owing to 2-hydroxyglutarate-induced DNA hypermethylation, with TET2 affecting proliferation and possibly differentiation[59]. The participation of TET2 in haematopoiesis is also evident in studies using TET2 knockdown, in which cells show self-renewal and there is a bias towards differentiation of monocytic lineage cells, with diminished granulopoiesis[19,60].

It is likely that PU.1 is an important mediator of these demethylation processes. In a related monocyte-derived differentiation process, it has been demonstrated that PU.1 binds TET2 and recruits it to the promoters of genes that become demethylated[61]. Interestingly, PU.1 is also able to recruit DNMT3B to target the deposition of *de novo* DNA methylation[61], which strongly suggests that PU.1 could act as a rheostat that regulates DNA methylation changes in both directions to facilitate and/or block gene expression. A recent report indicates that many other myeloid transcription factors can recruit DNMTs, and perhaps DNA demethylating enzymes, which subsequently promote methylation changes at specific CpG sites[62].

Epigenetic remodelling in myeloid activation

A key feature of myeloid cells is their ability to rapidly respond to intracellular and extracellular signals. It has been suggested that the activation of macrophages, for instance, may involve a complex array of stimulus- and microenvironment-dependent expression programmes that result in a spectrum of functional states that could extend beyond the clearly defined, polarized phenotypes resulting from 'M1' or 'classical' activation and 'M2' or 'alternative' activation[63] (BOX 1). The importance of epigenetic regulation in the context of myeloid cell activation is exemplified by the effects of the loss of HDAC3 in mouse macrophages, which renders them hyperresponsive to interleukin-4 (IL-4) and skewed towards an M2 phenotype, highlighting the relevance of histone acetylation status for controlling the functional responses of macrophages[64]. HDAC3 is required for inflammatory M1 activation of certain lipopolysaccharide (LPS)-induced inflammatory genes, such as *Il6* (which encodes IL-6), in mouse bone marrow-derived macrophages[65]. HDAC3 is also required for the expression of *Ifnb* (which encodes interferon-β (IFNβ)) in both resting and LPS-stimulated bone marrow-derived macrophages[65]. In line with this, M2 activation of macrophages *in vivo* depends on the removal of repressive marks at M2-activating genes, such as *Irf4* (which encodes IFN-regulatory factor 4), by the histone demethylase Jumonji domain-containing 3 (JMJD3)[66,67].

The interplay between the epigenetic changes that occur at promoters located close to transcriptional start sites and those that occur at enhancers located at distant intergenic and intragenic regions ensures that responses are cell-type-specific and stimulus-specific. Compared with promoters, the epigenetic hallmark of regulatory distal regions is the presence of higher levels of H3K4me1 and H3K4me2, and lower levels of H3K4me3 (REF. 68). In contrast to M2-like macrophage activation, LPS-mediated M1-like activation of macrophages has been widely studied in order to dissect the molecular basis of macrophage activation. Of note, in the absence of Toll-like receptor (TLR) signalling, inflammatory gene loci are occupied by repressors such as B cell lymphoma 6 (BCL-6)[69], and HDACs and histone demethylases are recruited[70]. Chromatin immunoprecipitation followed by sequencing (ChIP–seq) analysis has revealed that the histone acetyltransferase p300 (also known as EP300) binds to enhancers of genes that are activated upon LPS stimulation[71]. Consistent with this, these enhancers are enriched in binding sites for inflammatory type transcription factors, such as nuclear factor-κB (NF-κB), IRFs and activator protein 1, in addition to the constitutively

Box 1 | **Determinants of epigenetic regulation in macrophage polarization**

Macrophages, together with dendritic cells, are responsible for phagocytosis, cytokine production and antigen presentation. Macrophages display a high heterogeneity not only because of their own intrinsic terminal differentiation pathways, but also in response to environmental stimuli. On the basis of their phenotype, macrophages are often classified into two distinct polarized phenotypes that are identified as M1 macrophages and M2 macrophages. However, macrophages can undergo a transition between different functional states, and the stability of these two phenotypes and other phenotypic states is still unclear. M1 macrophages are associated with pro-inflammatory responses, as they develop in response to pattern recognition receptor activation and are able to secrete large amounts of pro-inflammatory cytokines, such as tumour necrosis factor, as well as nitric oxide. By contrast, M2 macrophages develop in response to type 2-associated immune mediators, such as interleukin-4 (IL-4) and IL-13, and are implicated in responses to parasite infection, tissue remodelling, angiogenesis and tumour progression. M2 macrophages are characterized by the production of specific sets of enzymes, such as arginase 1. The environmental signals that determine macrophage polarization activate stimulus-specific transcription factors, such as signal transducer and activator of transcription (STAT) family members, interferon-regulatory factors (IRFs) and nuclear factor-κB (NF-κB) family members, thereby inducing a transcriptional response that shapes the functional phenotype of the cell[63]. ETS family transcription factors, such as PU.1, also have a primary role in macrophage diversification. Some of these transcription factors recruit or associate with epigenetic enzymes. A proper transcriptional response during macrophage polarization is dependent on changes in the epigenome, including both DNA methylation and chromatin modification changes. Several studies point towards the importance of epigenetic regulation in macrophage polarization. For example, overexpression of DNA methyltransferase 3B (DNMT3B) skews macrophages towards an M2 phenotype[85]. Other examples indicate the importance of histone modifications in macrophage polarization. For instance, the H3K27 demethylase Jumonji domain-containing 3 (JMJD3) is crucial for M2 macrophage polarization but is dispensable for M1 macrophage polarization[67], whereas the absence of HDAC3 biases macrophages towards an M2 phenotype[64].

bound lineage-determining transcription factor PU.1. Notably, this combination of binding sites provides cell specificity as well as signal specificity to responsive target genes[71]. In addition to the recruitment of epigenetic modifiers to pre-existing enhancers, the engagement of TLR4 by LPS promotes chromatin modification changes, with the establishment of *de novo* enhancers due to H3K4 methylation by the histone methyltransferases MLL1 (also known as KMT2A), MLL3 (also known as KMT2C) and MLL4 (also known as KMT2B and KMT2D), and the collaboration of transcription factors such as NF-κB and PU.1 (REF. 72). In addition, the K4 methyltransferase MLL4 is required for the expression of subunit P of phosphatidylinositol *N*-acetylglucosaminyltransferase, the enzyme that catalyses the first step of glycosylphosphatidylinositol (GPI) anchor synthesis, which is necessary for the expression of the LPS co-receptor CD14 (REF. 73). Interestingly enough, transcription of enhancer RNAs (eRNAs) precedes the appearance of H3K4me1 and H3K4me2 marks[72]. Notably, the transcription and activity of eRNAs is repressed in a cell-type-specific manner in macrophages by the nuclear receptors REV-ERBα (also known as NR1D1) and REV-ERBβ (also known as NR1D2), which provide a mechanism for repression or negative regulation[74].

Epigenetics in host defence and inflammation

The innate defensive responses that are mediated by myeloid cells are powerful and potentially harmful if misplaced in time or space. Therefore, the ability to respond readily must be balanced with the capacity to do so only when needed. Two main strategies of host defence against pathogens — namely, resistance and tolerance — help to achieve effective host protection. Resistance reduces the pathogen burden, whereas tolerance ensures the minimal possible tissue damage that is compatible with defensive action[75,76]. Although immune memory has classically been considered as an exclusive trait of the adaptive immune system, a paradigm shift is revealing the existence of memory-type behaviour in innate immune cells. The phenomena of trained immunity and endotoxin tolerance are examples of such innate-type memory (FIG. 3a). The decision to respond with enhanced (trained) or decreased (tolerance) cytokine production depends on the type and concentration of ligand that monocytes encounter. Upon priming with *Candida albicans* or fungal cell wall β-glucans, monocytes respond with increased cytokine production upon restimulation. By contrast, the prestimulation of monocytes with endotoxins, such as LPS, induces tolerance. Notably, chromatin structure and epigenetic modifications are crucial for such processes to occur and to be sustained[75].

Epigenetics in trained immunity. The term trained immunity has been used to refer to nonspecific memory-type responses that are seen in the innate immune system, in which the priming of monocytes or macrophages by an initial challenge (such as an infection or vaccine) results in their enhanced responsiveness to a secondary challenge[77,78] (FIG. 3a). We still know little about the mechanisms mediating trained immunity in vertebrates. Recent studies have described a new class of enhancers, termed latent enhancers, that are inactive and unmarked in the basal state, but undergo H3K4 methylation and H3K27 acetylation during the first encounter with a stimulus. When the stimulus has ceased, transcription is terminated, and H3K27 acetylation and H3K4me3 disappear, whereas H3K4me1 persists at the latent enhancers for at least 24 hours and constitutes the basis for a faster and enhanced response after restimulation[79] (FIG. 3b).

Monocyte training with β-glucans is associated with stable changes in H3K4me3 at the promoters of important genes, such as those encoding the pro-inflammatory cytokines tumour necrosis factor (TNF), IL-6 and IL-18 (REF. 80); however, no changes have been observed in H3K27me3. More recently, it has been demonstrated that β-glucan-mediated macrophage training results in a gain in *de novo* H3K27 acetylation in 17% of dynamic promoters and 40% of enhancers[81]. Finally, experiments in which monocytes were trained with *C. albicans*-derived β-glucan showed that both histone methylation and acetylation patterns define a metabolic gene signature that underlies the metabolic switch required for monocyte activation and training[82].

Epigenetics in endotoxin tolerance. In contrast to trained immunity, endotoxin tolerance is a form of innate memory in which the initial stimulation of monocytes or macrophages with the TLR4 ligand LPS causes these cells to enter a long-term refractory state, such that they do not mount a pro-inflammatory response to subsequent TLR4 stimulation (FIG. 3a). Understanding the mechanisms behind this response is relevant for extreme inflammatory conditions, such as sepsis. For example, when myeloid blood cells from patients with sepsis enter a suppressed state (also known as compensatory anti-inflammatory response syndrome) as a result of endotoxin tolerance, there is a high risk of life-threatening infection[83]. The restimulation of tolerant macrophages with LPS produces two main types of gene-expression programmes; one set of 'tolerized' genes show diminished or abolished expression, whereas the expression of a second group of 'non-tolerized' genes is increased or remains unchanged. The transcription-activating H3K4me3 mark is imprinted on the promoters of both tolerized and non-tolerized genes, but H3K4me3 methylation is only maintained on the promoters of the non-tolerized genes[84]; the tolerized genes, including those encoding inflammatory cytokines, remain devoid of this mark (FIG. 3b).

The contribution of DNA methylation changes to innate memory processes has been less explored, given the presumed stability of this type of modification. Therefore, 5meC deposition or removal has been considered to be unlikely to support the rapid changes required for immune responses. However, the recent description of transitions from stable 5meC into more labile oxidized intermediates — such as 5hmC, 5fC and 5caC — could provide a suitable mechanism to support rapid response genes. Given that monocytes are already considered to have undergone a terminal differentiation step, DNA demethylation could be related

Enhancer RNAs
(eRNAs). A class of relatively short non-coding RNA molecules (50–2000 nucleotides in length) that are transcribed from the DNA sequence of enhancer regions.

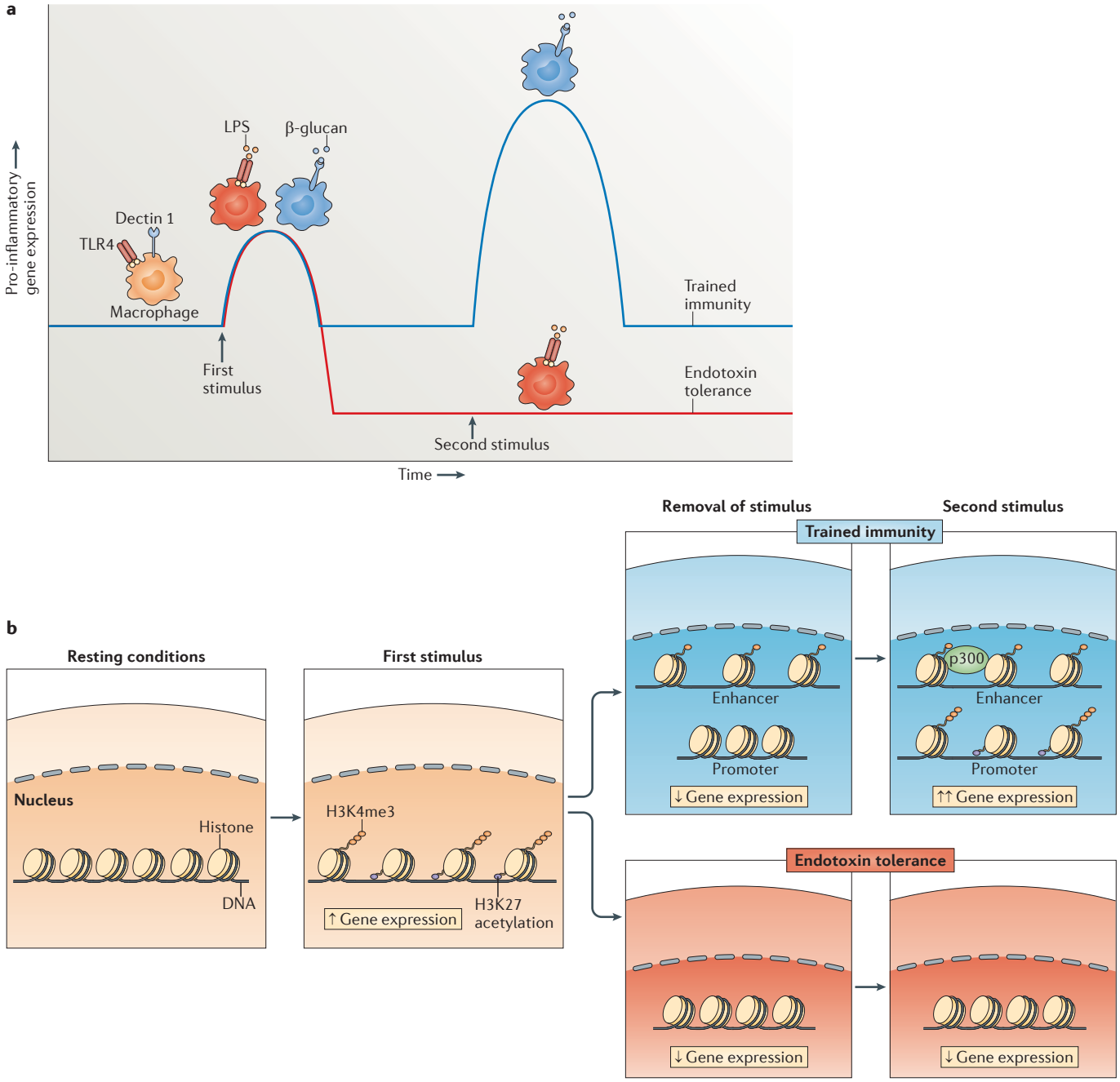

Figure 3 | **Epigenetic regulation of memory-like activity in monocytes and macrophages.** **a** | The biological phenomena of endotoxin tolerance and trained immunity are depicted in the graph. Stimulation of monocytes and/or macrophages via pattern recognition receptors (PRRs), such as Toll-like receptor 4 (TLR4) or dectin 1 (also known as CLEC7A), leads to increased expression of pro-inflammatory genes. Decreased or increased responsiveness of these cells to subsequent PRR stimulation may then occur, depending on the initial type of stimulus that the cell received. TLR4 stimulation with lipopolysaccharide (LPS) can induce a state of endotoxin tolerance (represented by the red line and red macrophages), whereas the stimulation of dectin 1 with β-glucan from *Candida albicans* leads to a state of trained immunity (represented by the blue line and blue macrophages). The red line indicates tolerized genes that remain refractory to a second stimulus and the blue line represents trained genes that show enhanced expression in response to subsequent stimulation. **b** | The epigenetic changes underlying endotoxin tolerance and trained immunity are depicted (methylation is represented by orange ovals and acetylation by purple ovals). Initial PRR stimulation leads to trimethylation of histone H3K4 (H3K4me3) and global acetylation of histones H4 on promoters of pro-inflammatory genes. In the case of endotoxin tolerance (red boxes), the removal of the stimulus results in the loss of activating marks and gene expression returns to basal levels. Following a second encounter with the stimulus, some of these genes (that is, tolerized genes) will not regain the H3K4me3 mark or acetylation, and will remain silent and refractory to stimulation. By contrast, non-tolerized genes will conserve H3K4me3 and be expressed to the same level or to a greater extent (not shown in the figure). In the case of trained immunity (blue boxes), pro-inflammatory genes will retain enhancers marked with monomethylation of histone H3K4. A second stimulus will induce transcription factors to bind to both the enhancers and the promoters of these genes, and will facilitate the recruitment of chromatin modifiers such as the histone acetyltransferase p300, thereby promoting an increased in H3K4me3 and enhancing the expression of trained genes.

to the preparation for a set of possible responses to a variety of stimuli rather than to the establishment of a closed identity per se. The high levels of TET2 in myeloid cells and, as a result, their ability to demethylate DNA suggest that such a regulatory mechanism confers a functional plasticity that depends on the stimuli more than on the cell history. The maintenance of a memory-like phenotype in immune cells is most likely to be induced by reprogramming the transcriptional profile of the cells through epigenetic changes, as happens with the TLR-induced chromatin modifications underlying endotoxin-induced tolerance. As previously mentioned, DNMT3B affects the control of the inflammatory response of macrophages[85], which is compatible with the idea of activation beyond dual polarization (for instance, M1-like and M2-like states for macrophages, or tolerogenic and activating phenotypes for dendritic cells) into a more complex variety of expression programmes than clearly defined, polarized and fixed phenotypes[86]. However, the contribution of DNA methylation to these processes remains to be investigated.

Myeloid cell epigenetics and disease

As discussed above, *TET2* is mutated in several myeloid malignancies. Defects in other epigenetic regulators have also been associated with the development of myeloproliferative disorders such as myelodysplastic syndrome, which is the most common form of acute myeloid leukaemia. These disorders develop as a result of altered myelopoiesis, which leads to the uncontrolled expansion of progenitor cell populations and blockage of further cell differentiation. The recurrence of genetic alterations in epigenetic enzymes in acute myeloid leukaemia highlights their relevance to myeloid differentiation. Other examples of genetic susceptibility factors in myeloid malignancies include *DNMT3A*, *IDH1* and *IDH2* (as reviewed in REF. 87). Remarkably, azanucleosides — such as 5-azacytidine and decitabine — constitute the core therapy in the management of myelodysplastic syndrome[88], presumably owing to their ability to induce demethylation. In addition to epigenetic-based therapies, the presence of mutations of DNA methylation modifiers, such as *DNMT3A,* may constitute useful biomarkers for predicting the success of classical cytotoxic treatments[89]. Regarding mutations in chromatin-modifying enzymes, it has been shown that loss-of-function mutations in *EZH2* and *ASXL1* are present in a variety of myeloid malignancies, including myelodysplastic syndrome[87].

Defective epigenetic regulation of terminally differentiated myeloid cells may also contribute to disease. For example, silencing of the H3K4 methyltransferase ASH1-like (*Ash1l*) in innate immune cells in mice leads to increased susceptibility to endotoxin shock and sepsis, and the development of autoimmune disease[90]. Another example of inflammatory disease is atherosclerosis, where macrophages are part of atherosclerotic plaques and are key players in disease progression[91]. It has been shown that HDAC3 is upregulated in human atherosclerosis and that deletion of *Hdac3* in mouse macrophages promotes a transforming growth factor-β-mediated anti-inflammatory phenotype and a better disease outcome[92]. HDAC9 also shapes the macrophage phenotype and represses alternative activation programmes in these cells, thereby promoting the development of atherogenic lesions. The deletion of *Hdac9* results in the downregulation of pro-inflammatory gene expression and promotes an anti-inflammatory macrophage phenotype, resulting in an overall amelioration of atherosclerosis in a mouse model[93].

Together, these results suggest that manipulation of the chromatin landscape and the use of HDAC inhibitors could provide complementary therapeutic approaches. In line with this, an inhibitor of the H3K27me3 demethylase JMJD3 has been shown to reduce LPS-induced cytokine production in human macrophages[94]. This opens up the possibility of using such inhibitors for the treatment of inflammatory diseases in humans.

Conclusions

The differentiation and functional specialization of myeloid cells must be tightly regulated to ensure that these cells execute their proper function. The acquisition of a unique cell identity (for example, a monocyte, macrophage or dendritic cell) during the differentiation from myeloid precursors is coordinated and controlled by several regulatory elements that shape gene-expression programmes, including transcription factors, epigenetic regulators and post-transcriptional mechanisms. Epigenetic regulation that is based on histone modifications and DNA methylation provides stable, yet reversible, marks that bestow flexibility on the process. In this Review, we have discussed the relevance of epigenetic changes to myeloid differentiation. The high expression of TET2 (which is crucial for active demethylation of DNA) and its demonstrated role as a key determinant of myeloid cell identity highlight the importance of the dynamics of DNA methylation changes in these cells. Active deposition or removal of methyl groups establishes a dynamic crosstalk with transcription factors, such as PU.1, which is involved in targeting DNMTs and TET2 to specific genomic sites. Upon differentiation, innate immune cell function is coordinated by regulation of the chromatin modification landscape in the context of enhancers, promoters and rapid response genes. This is particularly true for inflammatory macrophage responses, in which the recruitment of stimulus-specific transcription factors is coordinated by PU.1-driven chromatin remodelling and the marking of specific DNA sites. Epigenetic control mechanisms may have a role in providing a flexible mechanism for the stable preactivation of cells that ensures myeloid cells mount the correct level of response under inflammatory conditions. Given that epigenetic regulation is both reversible and highly dynamic, developing an understanding the molecular details is of great interest from a therapeutic point of view, as it would allow the development of drugs that target specific epigenetic modifications. In addition, the identification of epigenetic alterations in innate immune cells that could be used as biomarkers of disease or predictors of treatment success could lead to a novel era of personalized medicine.

1. De Kleer, I., Willems, F., Lambrecht, B. & Goriely, S. Ontogeny of myeloid cells. *Front. Immunol.* **5**, 423 (2014).
2. Geissmann, F. *et al.* Development of monocytes, macrophages, and dendritic cells. *Science* **327**, 656–661 (2010).
3. Kouzarides, T. Chromatin modifications and their function. *Cell* **128**, 693–705 (2007).
4. Fischle, W., Wang, Y. & Allis, C. D. Histone and chromatin cross-talk. *Curr. Opin. Cell Biol.* **15**, 172–183 (2003).
5. Turner, B. M. Histone acetylation and an epigenetic code. *Bioessays* **22**, 836–845 (2000).
6. Hendrich, B. & Bird, A. Identification and characterization of a family of mammalian methyl-CpG binding proteins. *Mol. Cell. Biol.* **18**, 6538–6547 (1998).
7. Blattler, A. & Farnham, P. J. Cross-talk between site-specific transcription factors and DNA methylation states. *J. Biol. Chem.* **288**, 34287–34294 (2013).
8. Bird, A., Taggart, M., Frommer, M., Miller, O. J. & Macleod, D. A fraction of the mouse genome that is derived from islands of nonmethylated, CpG-rich DNA. *Cell* **40**, 91–99 (1985).
9. Zemach, A., McDaniel, I. E., Silva, P. & Zilberman, D. Genome-wide evolutionary analysis of eukaryotic DNA methylation. *Science* **328**, 916–919 (2010).
10. Irizarry, R. A. *et al.* The human colon cancer methylome shows similar hypo- and hypermethylation at conserved tissue-specific CpG island shores. *Nature Genet.* **41**, 178–186 (2009).
11. Maunakea, A. K. *et al.* Conserved role of intragenic DNA methylation in regulating alternative promoters. *Nature* **466**, 253–257 (2010).
12. Zilbauer, M. *et al.* Genome-wide methylation analyses of primary human leukocyte subsets identifies functionally important cell-type-specific hypomethylated regions. *Blood* **122**, e52–e60 (2013).
13. Schlesinger, F., Smith, A. D., Gingeras, T. R., Hannon, G. J. & Hodges, E. *De novo* DNA demethylation and noncoding transcription define active intergenic regulatory elements. *Genome Res.* **23**, 1601–1614 (2013).
14. Stadler, M. B. *et al.* DNA-binding factors shape the mouse methylome at distal regulatory regions. *Nature* **480**, 490–495 (2011).
15. Goll, M. G. & Bestor, T. H. Eukaryotic cytosine methyltransferases. *Annu. Rev. Biochem.* **74**, 481–514 (2005).
16. Piccolo, F. M. & Fisher, A. G. Getting rid of DNA methylation. *Trends Cell Biol.* **24**, 136–143 (2014).
17. Wu, H. & Zhang, Y. Reversing DNA methylation: mechanisms, genomics, and biological functions. *Cell* **156**, 45–68 (2014).
18. Tahiliani, M. *et al.* Conversion of 5-methylcytosine to 5-hydroxymethylcytosine in mammalian DNA by MLL partner TET1. *Science* **324**, 930–935 (2009).
This article demonstrates that TET1 oxidizes 5meC to 5hmC *in vivo,* indicating its potential role in epigenetic regulation.
19. Ko, M. *et al.* Impaired hydroxylation of 5-methylcytosine in myeloid cancers with mutant TET2. *Nature* **468**, 839–843 (2010).
20. Ito, S. *et al.* Tet proteins can convert 5-methylcytosine to 5-formylcytosine and 5-carboxylcytosine. *Science* **333**, 1300–1303 (2011).
21. He, Y. F. *et al.* Tet-mediated formation of 5-carboxylcytosine and its excision by TDG in mammalian DNA. *Science* **333**, 1303–1307 (2011).
22. Dawlaty, M. M. *et al.* Loss of tet enzymes compromises proper differentiation of embryonic stem cells. *Dev. Cell* **29**, 102–111 (2014).
23. Jeong, M. *et al.* Large conserved domains of low DNA methylation maintained by Dnmt3a. *Nature Genet.* **46**, 17–23 (2014).
24. Laiosa, C. V., Stadtfeld, M. & Graf, T. Determinants of lymphoid-myeloid lineage diversification. *Annu. Rev. Immunol.* **24**, 705–738 (2006).
25. Wilting, R. H. *et al.* Overlapping functions of Hdac1 and Hdac2 in cell cycle regulation and haematopoiesis. *EMBO J.* **29**, 2586–2597 (2010).
26. Broske, A. M. *et al.* DNA methylation protects hematopoietic stem cell multipotency from myeloerythroid restriction. *Nature Genet.* **41**, 1207–1215 (2009).
27. Chen, L. *et al.* Transcriptional diversity during lineage commitment of human blood progenitors. *Science* **345**, 1251033 (2014).
28. Kondo, M., Weissman, I. L. & Akashi, K. Identification of clonogenic common lymphoid progenitors in mouse bone marrow. *Cell* **91**, 661–672 (1997).
29. Wada, T. *et al.* Expression levels of histone deacetylases determine the cell fate of hematopoietic progenitors. *J. Biol. Chem.* **284**, 30673–30683 (2009).
30. Trowbridge, J. J., Snow, J. W., Kim, J. & Orkin, S. H. DNA methyltransferase 1 is essential for and uniquely regulates hematopoietic stem and progenitor cells. *Cell Stem Cell* **5**, 442–449 (2009).
31. Challen, G. A. *et al.* Dnmt3a and Dnmt3b have overlapping and distinct functions in hematopoietic stem cells. *Cell Stem Cell* **15**, 350–364 (2014).
32. Sun, D. *et al.* Epigenomic profiling of young and aged HSCs reveals concerted changes during aging that reinforce self-renewal. *Cell Stem Cell* **14**, 673–688 (2014).
33. Boehm, T. Evolution of vertebrate immunity. *Curr. Biol.* **22**, R722–R732 (2012).
34. Hodges, E. *et al.* Directional DNA methylation changes and complex intermediate states accompany lineage specificity in the adult hematopoietic compartment. *Mol. Cell* **44**, 17–28 (2011).
35. Mansson, R. *et al.* Molecular evidence for hierarchical transcriptional lineage priming in fetal and adult stem cells and multipotent progenitors. *Immunity* **26**, 407–419 (2007).
36. Ji, H. *et al.* Comprehensive methylome map of lineage commitment from haematopoietic progenitors. *Nature* **467**, 338–342 (2010).
This article represents the first genome-wide analysis of DNA methylation during differentiation, identifying gene-specific hypomethylation in the myeloid lineage and an increase in methylation in the lymphoid lineage.
37. Mossadegh-Keller, N. *et al.* M-CSF instructs myeloid lineage fate in single haematopoietic stem cells. *Nature* **497**, 239–243 (2013).
38. Bocker, M. T. *et al.* Genome-wide promoter DNA methylation dynamics of human hematopoietic progenitor cells during differentiation and aging. *Blood* **117**, e182–e189 (2011).
39. Accomando, W. P., Wiencke, J. K., Houseman, E. A., Nelson, H. H. & Kelsey, K. T. Quantitative reconstruction of leukocyte subsets using DNA methylation. *Genome Biol.* **15**, R50 (2014).
40. Ronnerblad, M. *et al.* Analysis of the DNA methylome and transcriptome in granulopoiesis reveal timed changes and dynamic enhancer methylation. *Blood* **123**, e79– e89 (2014).
41. Klug, M. *et al.* Active DNA demethylation in human postmitotic cells correlates with activating histone modifications, but not transcription levels. *Genome Biol.* **11**, R63 (2010).
42. Klug, M., Schmidhofer, S., Gebhard, C., Andreesen, R. & Rehli, M. 5-Hydroxymethylcytosine is an essential intermediate of active DNA demethylation processes in primary human monocytes. *Genome Biol.* **14**, R46 (2013).
43. Zhang, X. *et al.* DNA methylation dynamics during *ex vivo* differentiation and maturation of human dendritic cells. *Epigenet. Chromatin* **7**, 21 (2014).
44. Scott, E. W., Simon, M. C., Anastasi, J. & Singh, H. Requirement of transcription factor PU.1 in the development of multiple hematopoietic lineages. *Science* **265**, 1573–1577 (1994).
45. Laslo, P. *et al.* Multilineage transcriptional priming and determination of alternate hematopoietic cell fates. *Cell* **126**, 755–766 (2006).
46. Feng, R. *et al.* PU.1 and C/EBPα/β convert fibroblasts into macrophage-like cells. *Proc. Natl Acad. Sci. USA* **105**, 6057–6062 (2008).
47. Xie, H., Ye, M., Feng, R. & Graf, T. Stepwise reprogramming of B cells into macrophages. *Cell* **117**, 663–676 (2004).
48. Bussmann, L. H. *et al.* A robust and highly efficient immune cell reprogramming system. *Cell Stem Cell* **5**, 554–566 (2009).
49. Barneda-Zahonero, B. *et al.* HDAC7 is a repressor of myeloid genes whose downregulation is required for transdifferentiation of pre-B cells into macrophages. *PLoS Genet.* **9**, e1003503 (2013).
50. Kallin, E. M. *et al.* Tet2 facilitates the derepression of myeloid target genes during CEBPα-induced transdifferentiation of pre-B cells. *Mol. Cell* **48**, 266–276 (2012).
This article demonstrates a direct role for TET2 in the 5hmC-mediated activation of myeloid-specific genes during the acquisition of myeloid identity.
51. Hashimoto, H. *et al.* Recognition and potential mechanisms for replication and erasure of cytosine hydroxymethylation. *Nucleic Acids Res.* **40**, 4841–4849 (2012).
52. Hanna, J. *et al.* Direct reprogramming of terminally differentiated mature B lymphocytes to pluripotency. *Cell* **133**, 250–264 (2008).
53. Di Stefano, B. *et al.* C/EBPα poises B cells for rapid reprogramming into induced pluripotent stem cells. *Nature* **506**, 235–239 (2014).
54. Delhommeau, F. *et al.* Mutation in TET2 in myeloid cancers. *N. Engl. J. Med.* **360**, 2289–2301 (2009).
55. Li, Z. *et al.* Deletion of Tet2 in mice leads to dysregulated hematopoietic stem cells and subsequent development of myeloid malignancies. *Blood* **118**, 4509–4518 (2011).
56. Pronier, E. *et al.* Inhibition of TET2-mediated conversion of 5-methylcytosine to 5-hydroxymethylcytosine disturbs erythroid and granulomonocytic differentiation of human hematopoietic progenitors. *Blood* **118**, 2551–2555 (2011).
57. Losman, J. A. *et al.* (R)-2-hydroxyglutarate is sufficient to promote leukemogenesis and its effects are reversible. *Science* **339**, 1621–1625 (2013).
58. Moran-Crusio, K. *et al.* Tet2 loss leads to increased hematopoietic stem cell self-renewal and myeloid transformation. *Cancer Cell* **20**, 11–24 (2011).
59. Sasaki, M. *et al.* IDH1(R132H) mutation increases murine haematopoietic progenitors and alters epigenetics. *Nature* **488**, 656–659 (2012).
60. Ko, M. *et al.* Ten-eleven-translocation 2 (TET2) negatively regulates homeostasis and differentiation of hematopoietic stem cells in mice. *Proc. Natl Acad. Sci. USA* **108**, 14566–14571 (2011).
61. de la Rica, L. *et al.* PU.1 target genes undergo Tet2-coupled demethylation and DNMT3b-mediated methylation in monocyte-to-osteoclast differentiation. *Genome Biol.* **14**, R99 (2014).
62. Hervouet, E., Vallette, F. M. & Cartron, P. F. Dnmt3/transcription factor interactions as crucial players in targeted DNA methylation. *Epigenetics* **4**, 487–499 (2009).
63. Lawrence, T. & Natoli, G. Transcriptional regulation of macrophage polarization: enabling diversity with identity. *Nature Rev. Immunol.* **11**, 750–761 (2011).
64. Mullican, S. E. *et al.* Histone deacetylase 3 is an epigenomic brake in macrophage alternative activation. *Genes Dev.* **25**, 2480–2488 (2011).
65. Chen, X. *et al.* Requirement for the histone deacetylase Hdac3 for the inflammatory gene expression program in macrophages. *Proc. Natl Acad. Sci. USA* **109**, E2865–E2874 (2012).
66. Ishii, M. *et al.* Epigenetic regulation of the alternatively activated macrophage phenotype. *Blood* **114**, 3244–3254 (2009).
67. Satoh, T. *et al.* The Jmjd3–Irf4 axis regulates M2 macrophage polarization and host responses against helminth infection. *Nature Immunol.* **11**, 936–944 (2010).
68. Heintzman, N. D. *et al.* Distinct and predictive chromatin signatures of transcriptional promoters and enhancers in the human genome. *Nature Genet.* **39**, 311–318 (2007).
69. Barish, G. D. *et al.* Bcl-6 and NF-κB cistromes mediate opposing regulation of the innate immune response. *Genes Dev.* **24**, 2760–2765 (2010).
70. Adelman, K. *et al.* Immediate mediators of the inflammatory response are poised for gene activation through RNA polymerase II stalling. *Proc. Natl Acad. Sci. USA* **106**, 18207–18212 (2009).
71. Ghisletti, S. *et al.* Identification and characterization of enhancers controlling the inflammatory gene expression program in macrophages. *Immunity* **32**, 317–328 (2010).
72. Kaikkonen, M. U. *et al.* Remodeling of the enhancer landscape during macrophage activation is coupled to enhancer transcription. *Mol. Cell* **51**, 310–325 (2013).
73. Austenaa, L. *et al.* The histone methyltransferase Wbp7 controls macrophage function through GPI glycolipid anchor synthesis. *Immunity* **36**, 572–585 (2012).
74. Lam, M. T. *et al.* Rev-Erbs repress macrophage gene expression by inhibiting enhancer-directed transcription. *Nature* **498**, 511–515 (2013).
75. Medzhitov, R., Schneider, D. S. & Soares, M. P. Disease tolerance as a defense strategy. *Science* **335**, 936–941 (2012).
76. Medzhitov, R. Origin and physiological roles of inflammation. *Nature* **454**, 428–435 (2008).

77. Netea, M. G., Quintin, J. & van der Meer, J. W. Trained immunity: a memory for innate host defense. *Cell Host Microbe* **9**, 355–361 (2011).
78. Quintin, J., Cheng, S. C., van der Meer, J. W. & Netea, M. G. Innate immune memory: towards a better understanding of host defense mechanisms. *Curr. Opin. Immunol.* **29C**, 1–7 (2014).
79. Ostuni, R. *et al.* Latent enhancers activated by stimulation in differentiated cells. *Cell* **152**, 157–171 (2013).
This article identifies latent enhancers as key elements of innate immune memory; these are characterized by being marked with H3K4me3 following an initial stimulus.
80. Quintin, J. *et al. Candida albicans* infection affords protection against reinfection via functional reprogramming of monocytes. *Cell Host Microbe* **12**, 223–232 (2012).
This article describes the H3K4me3 mark as a mediator of trained immunity in monocytes.
81. Saeed, S. *et al.* Epigenetic programming of monocyte-to-macrophage differentiation and trained innate immunity. *Science* **345**, 1251086 (2014).
82. Cheng, S. C. *et al.* mTOR- and HIF-1α-mediated aerobic glycolysis as metabolic basis for trained immunity. *Science* **345**, 1250684 (2014).
83. Adib-Conquy, M. & Cavaillon, J. M. Compensatory anti-inflammatory response syndrome. *Thromb. Haemost.* **101**, 36–47 (2009).
84. Foster, S. L., Hargreaves, D. C. & Medzhitov, R. Gene-specific control of inflammation by TLR-induced chromatin modifications. *Nature* **447**, 972–978 (2007).
This study characterizes the two types of TLR-induced responses and provides an epigenetic basis for the acquisition of endotoxin tolerance.
85. Yang, X. *et al.* Epigenetic regulation of macrophage polarization by DNA methyltransferase 3b. *Mol. Endocrinol.* **28**, 565–574 (2014).
86. Sica, A. & Mantovani, A. Macrophage plasticity and polarization: *in vivo* veritas. *J. Clin. Invest.* **122**, 787–795 (2012).
87. Shih, A. H., Abdel-Wahab, O., Patel, J. P. & Levine, R. L. The role of mutations in epigenetic regulators in myeloid malignancies. *Nature Rev. Cancer* **12**, 599–612 (2012).
88. Quintas-Cardama, A., Santos, F. P. & Garcia-Manero, G. Therapy with azanucleosides for myelodysplastic syndromes. *Nature Rev. Clin. Oncol.* **7**, 433–444 (2010).
89. Patel, J. P. *et al.* Prognostic relevance of integrated genetic profiling in acute myeloid leukemia. *N. Engl. J. Med.* **366**, 1079–1089 (2012).
90. Xia, M. *et al.* Histone methyltransferase Ash1l suppresses interleukin-6 production and inflammatory autoimmune diseases by inducing the ubiquitin-editing enzyme A20. *Immunity* **39**, 470–481 (2013).
91. Moore, K. J., Sheedy, F. J. & Fisher, E. A. Macrophages in atherosclerosis: a dynamic balance. *Nature Rev. Immunol.* **13**, 709–721 (2013).
92. Hoeksema, M. A. *et al.* Targeting macrophage histone deacetylase 3 stabilizes atherosclerotic lesions. *EMBO Mol. Med.* **6**, 1124–1132 (2014).
93. Cao, Q. *et al.* Histone deacetylase 9 represses cholesterol efflux and alternatively activated macrophages in atherosclerosis development. *Arterioscler Thromb. Vasc. Biol.* **34**, 1871–1879 (2014).
94. Kruidenier, L. *et al.* A selective jumonji H3K27 demethylase inhibitor modulates the proinflammatory macrophage response. *Nature* **488**, 404–408 (2012).
95. Rodríguez-Ubreva, J. *et al.* Pre-B cell to macrophage transdifferentiation without significant promoter DNA methylation changes. *Nucleic Acids Res.* **40**, 1954–1968 (2012).

Acknowledgements
This work was supported by grant SAF2011-29635 from the Spanish Ministry of Science and Innovation, grant CIVP16A1834 from the Fundación Ramón Areces and grant Precisesads 115565–3 of the Innovative Medicines Initiative (IMI) Programme.

Competing interests statement
The authors declare no competing interests.

the FEBS Journal

Gains of DNA methylation in myeloid terminal differentiation are dispensable for gene silencing but influence the differentiated phenotype

Roser Vento-Tormo, Damiana Álvarez-Errico, Javier Rodríguez-Ubreva and Esteban Ballestar

Chromatin and Disease Group, Cancer Epigenetics and Biology Programme (PEBC), Bellvitge Biomedical Research Institute (IDIBELL), L'Hospitalet de Llobregat, Barcelona, Spain

Keywords
dendritic cell; differentiation; DNA methylation; histone modifications; monocyte

Correspondence
E. Ballestar, Chromatin and Disease Group, Cancer Epigenetics and Biology Programme (PEBC), Bellvitge Biomedical Research Institute (IDIBELL), Avda. Gran Via 199-203, 08908 L'Hospitalet de Llobregat, Barcelona, Spain
Fax: +34 932607219
Tel: +34 932607133
E-mail: eballestar@idibell.cat

(Received 16 June 2014, revised 4 September 2014, accepted 9 September 2014)

doi:10.1111/febs.13045

DNA methylation-mediated regulation drives and stabilizes transcription states throughout development. In myeloid differentiation, DNA methylation changes occur predominantly in the direction towards hypomethylation. Also, *in vitro* differentiation of monocytes to dendritic cells and macrophages is characterized by DNA demethylation. In this study, we identified the existence of methylation changes in the direction of hypermethylation among genes that become repressed during monocyte-to-dendritic cell differentiation. We identified the acquisition of DNA methylation in genes such as *CSF3R*, *FYN*, and *CX3CR1*, but not in others, such as *CD14*. Analysis of the dynamics of methylation and expression changes of these genes revealed that loss of expression was rapid and was associated with the loss of H3K4me3 and H3K36me3, whereas gains of DNA methylation were progressive and partially concomitant with increases in H3K9me3 and H3K27me3. Inhibition of DNA methyltransferases, with the DNA replication-independent drug nanaomycin A, revealed that there were no effects on expression and H3K4me3 changes, despite the partial impairment of DNA methylation and H3K27me3 acquisition. However, cells treated with the DNA methyltransferase inhibitor showed lower levels of dendritic cell surface markers, suggesting a potential effect on the stability of the differentiated phenotype. Our data give rise to a novel perspective on the functional relevance and mechanisms of the acquisition of DNA methylation in myeloid cell differentiation.

Introduction

DNA methylation is a major epigenetic mechanism involved in determining and stabilising cell-fate decisions. Differentiation changes during haematopoiesis are directional; cells become less methylated as differentiation progresses in the myeloid branch [1–4], and this is accompanied by the upregulation of lineage-specific genes. Comparison of progenitors and cells at the various stages of differentiation in the lymphoid and myeloid branches has confirmed this hypomethylation trend in the latter, in contrast to the changes observed in lymphoid differentiation. Demethylation also characterizes myeloid cell terminal differentiation processes that lead to functional mature cell types. The findings obtained with *in vitro* models that recapitulate terminal differentiation in the myeloid lineage are consistent with the findings obtained from comparing cells

Abbreviations
5azadC, 5-aza-2′-deoxycytidine; BrdU, bromodeoxyuridine; ChIP, chromatin immunoprecipitation; DC, dendritic cell; DNMT, DNA methyltransferase; FACS, fluorescence-activated cell sorting; GM-CSF, granulocyte–macrophage colony-stimulating factor; iDC, immature dendritic cell; IL, interleukin; iMAC, immature macrophage; LPS, lipopolysaccharide; MAC, macrophage; MO, monocytes; PBMC, peripheral blood mononuclear cell; TSS, transcription start site.

isolated at different stages of differentiation. For instance, monocyte (MO)-to-dendritic cell (DC) and MO-to-macrophage (MAC) differentiation are also accompanied by DNA demethylation [5,6], although other MO-related differentiation models, such as MO-to-osteoclast differentiation, show acquisition of DNA methylation to a similar extent as demethylation events [7]. However, this latter differentiation process might be an exception, given that it is accompanied by massive cellular fusion and generation of polykaryons, in which the genetic material is redundant and high levels of repression are required. The restricted occurrence of hypermethylation events in myeloid differentiation processes raises questions about the functional relevance and mechanisms involved in silencing inappropriate genes during lineage commitment. In fact, examining the dynamics of DNA methylation changes in both directions reveals that the timing is different for DNA demethylation and gene activation than for acquisition of DNA methylation and gene silencing [7].

The establishment of *de novo* DNA methylation has been well studied in oocytes and during development [8,9], and also in the context of cancer, where many CpG islands become hypermethylated [10]. Findings in recent years have revealed that DNA hypermethylation in cancer is mainly driven by instructive mechanisms [11]. On the other hand, hypermethylation in cancer cells constitutes a mechanism leading to the inappropriate silencing of genes, particularly when it involves cell cycle or tumour suppressor genes. This has given rise to an interest in the generation of drugs that can reverse aberrant hypermethylation.

As this process is rather limited in the context of differentiation, e.g. in myeloid cells, where DNA demethylation seems to predominate, little is known about the roles and mechanisms associated with genes that become hypermethylated. We do not know whether hypermethylation occurs mainly in a passive manner. Also, we do not fully understand why certain genes that are repressed become hypermethylated, whereas others do not. It is likely that acquisition of DNA methylation during differentiation occurs through instructive mechanisms as well.

Here, we investigated the dynamics of the setting of DNA methylation during MO-to-DC and MO-to-MAC differentiation, and its potential functional relevance to these differentiation processes. To this end, we chose several genes that are repressed when MOs differentiate to DCs and MACs. We identified changes towards hypermethylation in a few CpG sites near the transcription start sites (TSSs) of genes such as the granulocyte-specific gene *CSF3R* and the kinase gene *FYN*. In contrast, *CD14*, which is also repressed during these two differentiation processes, showed no changes in DNA methylation. These changes occurred after a decrease in histone H3K4me3 and H3K36me3, but were coincident with the increase in repressive markers such as H3K9me3 and H3K27me3. Inhibition of DNA methyltransferases (DNMTs) with nanaomycin A, a replication-independent specific inhibitor of DNMT3b, did not alter the repression of these genes, even though the acquisition of hypermethylation was partially abolished. Flow cytometry analyses indicated that such decreases in the acquisition of DNA methylation affected the expression levels of DC-characteristic surface markers, suggesting a potential role in establishing the phenotype of these cells. Our results indicate that acquisition of DNA methylation has little effect on the direct expression changes of hypermethylated genes, although a general role in stabilising the differentiated phenotype cannot be discounted.

Results

Acquisition of DNA methylation in genes that are repressed during the MO-derived differentiation processes

DNA methylation changes in MO-to-MAC and MO-to-DC differentiation mainly occur in the direction of demethylation [5,6]. This is consistent with the results

Fig. 1. Identification of DNA methylation changes in candidate genes during MO-to-DC and MO-to-MAC differentiation. (A) Depiction of the differentiation system. MOs from peripheral blood were exposed to either G-MSF or GM-CSF + IL-4 to generate iMACs or iDCs, respectively. Maturation of these two cell types to give mature MACs (mMACs) and mature DCs (mDCs) was achieved following incubation with LPS. (B) Flow cytometry analysis of cell types to test changes in surface markers, including CD14, CD209 (specific to DCs), and CD83 (specific to mDCs). MFI, median fluorescence intensity. (C) Real-time quantitative PCR analysis of selected gene markers and their levels in MOs, iDCs, mDCs, iMACs and mMACs. (D) BrdU assay showing the percentages of replicating cells at different times during MO-to-DC and MO-to-MAC differentiation. From day 1 to day 3, only ~ 10% of cells divided. Ctrl, control. (E) Schematic representation of the six genes analysed in this study. The analysed CpG sites (vertical black line), the TSS (arrow) and the location of primers for ChIP (blue), expression (red, real-time quantitative PCR) and methylation (green, bisulfite pyrosequencing) analysis are indicated. Exons are marked as boxes, but look like lines (given the length of the genes) in all cases except for *CD14*, which is shorter. (F) Real-time quantitative PCR analysis of selected genes that become repressed during differentiation. (G) Bisulfite pyrosequencing data showing the DNA methylation changes.

obtained from comparing the DNA methylation profiles of isolated cells at different stages of myeloid differentiation, in which demethylation occurs as differentiation progresses. The above-referenced analyses on MO-to-MAC and MO-to-DC differentiation were performed with a low-resolution method [5] or an array-based method [6], which, although having a coverage of 99% of RefSeq genes, allows the analysis of

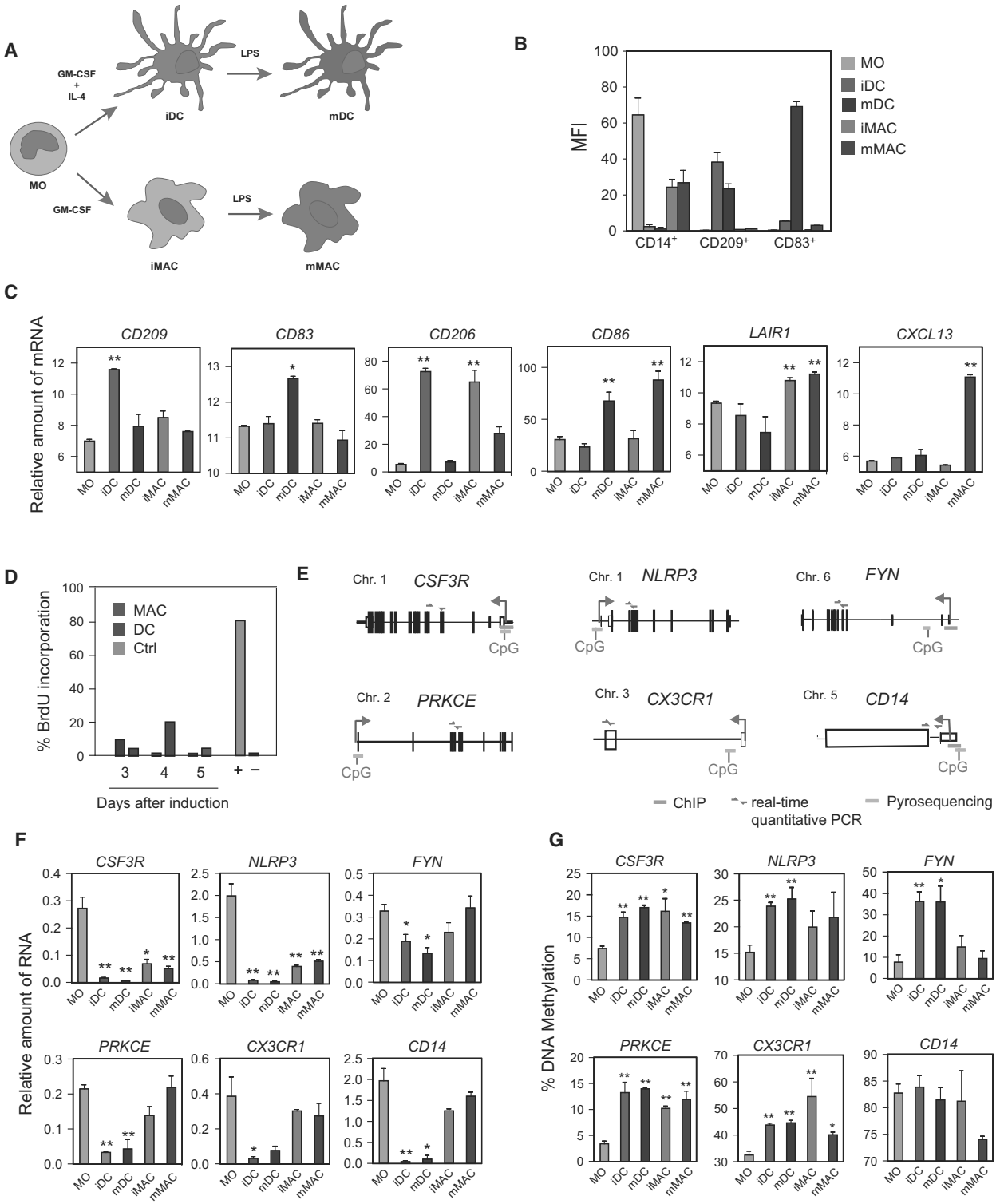

~ 480 000 of the 28 million CpG sites (~ 1.5%) of the human methylome. This means that, despite the overall prevalence of DNA demethylation events, the acquisition of DNA methylation at individual CpG sites in these differentiation processes might have been underestimated. To investigate the potential acquisition of DNA methylation at CpGs in genes that are repressed during these processes, we focused on a selection of genes. To this end, we first derived MACs and DCs from MOs by stimulating peripheral blood monocytes with granulocyte–MAC colony-stimulating factor (GM-CSF) and GM-CSF + interleukin (IL)-4, respectively. We also stimulated immature MACs (iMACs) and immature DCs (iDCs) with lipopolysaccharide (LPS) to generate their mature counterparts (Fig. 1A). These cells showed the expected changes in surface markers such as CD14, the level of which decreased during differentiation towards DCs, whereas the decrease in CD14 level in MACs was less marked (Fig. 1B). On the other hand, the level of CD209 increased in DCs, but not in MACs, as expected. Finally, the level of the mature DC surface marker CD83 increased only DCs after exposure to LPS, but not in MACs (Fig. 1B), as revealed by fluorescence-activated cell sorting (FACS) analysis. We also used quantitative RT-PCR to determine the mRNA levels of these and specific markers of DCs and MACs (Fig. 1C). These included not only *CD209* and *CD83*, but also *CD206* (common to DCs and MACs), *CD86* (characteristic of mature DCs and MACs), *LAIR1* (specific to MACs), and *CXCL13* (specific to mature MACs) (Fig. 1C). We then tested the occurrence of cell division during these two differentiation processes. We measured the levels of cell proliferation by incubating cells with bromodeoxyuridine (BrdU). Fewer than 10% were found to be BrdU-positive between 1 and 5 days, confirming the low replication rate of these cells (Fig. 1D). This supports the notion that any DNA methylation changes observed in this period are independent of DNA replication.

We next investigated changes in the DNA methylation status of selected CpG sites around the TSSs of selected genes during MO-to-DC and MO-to-MAC differentiation. To this end, we chose genes that are known to become totally or partially silenced during these differentiation processes. Genes in this selection included the granulocyte-specific gene *CSF3R*, which codes for a cytokine that controls the production, differentiation and function of granulocytes, and *CX3CR1*, another MO-specific gene. We also included *CD14*, which codes for the membrane receptor, and is downregulated in DCs and, to a lesser extent, in MACs. Previous DNA methylation studies had reported no changes for this gene. Other genes included *NLRP3*, which codes for a member of the Nod-like receptor family that is involved in recognising the molecular patterns expressed by invading pathogens, and *FYN*, a gene encoding a member of the src-family tyrosine kinases. Finally, we looked at *PRKCE*, on the basis of our own expression array data (unpublished results by Vento-Tormo and colleagues). A schematic representation of these genes and the locations of primers for the expression and DNA methylation analysis is shown in Fig. 1E. We performed real-time quantitative PCR and compared the expression levels of all the aforementioned genes between peripheral blood MOs and derived iDCs and iMACs (Fig. 1F). In all of these comparisons, we found lower levels of expression in the differentiated cells than in the originating MOs.

To test the potential increase in the DNA methylation levels in these genes between MOs and DCs, we first performed bisulfite pyrosequencing of CpG sites located near the TSSs for all of the genes. Our analysis revealed significantly higher methylation levels in DCs for *CSF3R*, *FYN*, *NLRP3* and *PRKCE*, although no differences were observed for *CD14* (Fig. 1G). Changes were relatively small, and genes such as *CSF3R* experienced an increase in methylation from 20% in MOs to 40% in DCs. However, these changes were reproducible in different experiments. The expression data for these genes in MOs and DCs confirmed an inverse relationship in all cases.

We found changes in almost all cases in the transition from MOs to iDCs and iMACs, with no further increase in the transition to their mature counterparts following exposure to LPS. In all cases, except for *FYN*, DNA methylation was acquired during differentiation to both DCs and MACs. For this reason, we

Fig. 2. Dynamics of DNA methylation, expression and histone modification changes for *CSF3R*, *FYN* and *CD14* during MO-to-DC differentiation. (A) Depiction of the structure of *CSF3R*, *FYN* and *CD14* including the TSS (arrow), the exons (black boxes). (B) Real-time quantitative PCR analysis of the genes during MO-to-DC differentiation. Values are relative to RPL38 levels. (C) Bisulfite pyrosequencing data over time showing the acquisition of DNA methylation changes during differentiation. (D) Changes in H3K36me3, H3K4me3, H3K9me3 and H3K27me3. Relative enrichment is the fraction of the input immunoprecipitated for each antibody. Data for each antibody are accompanied by IgG as a negative control.

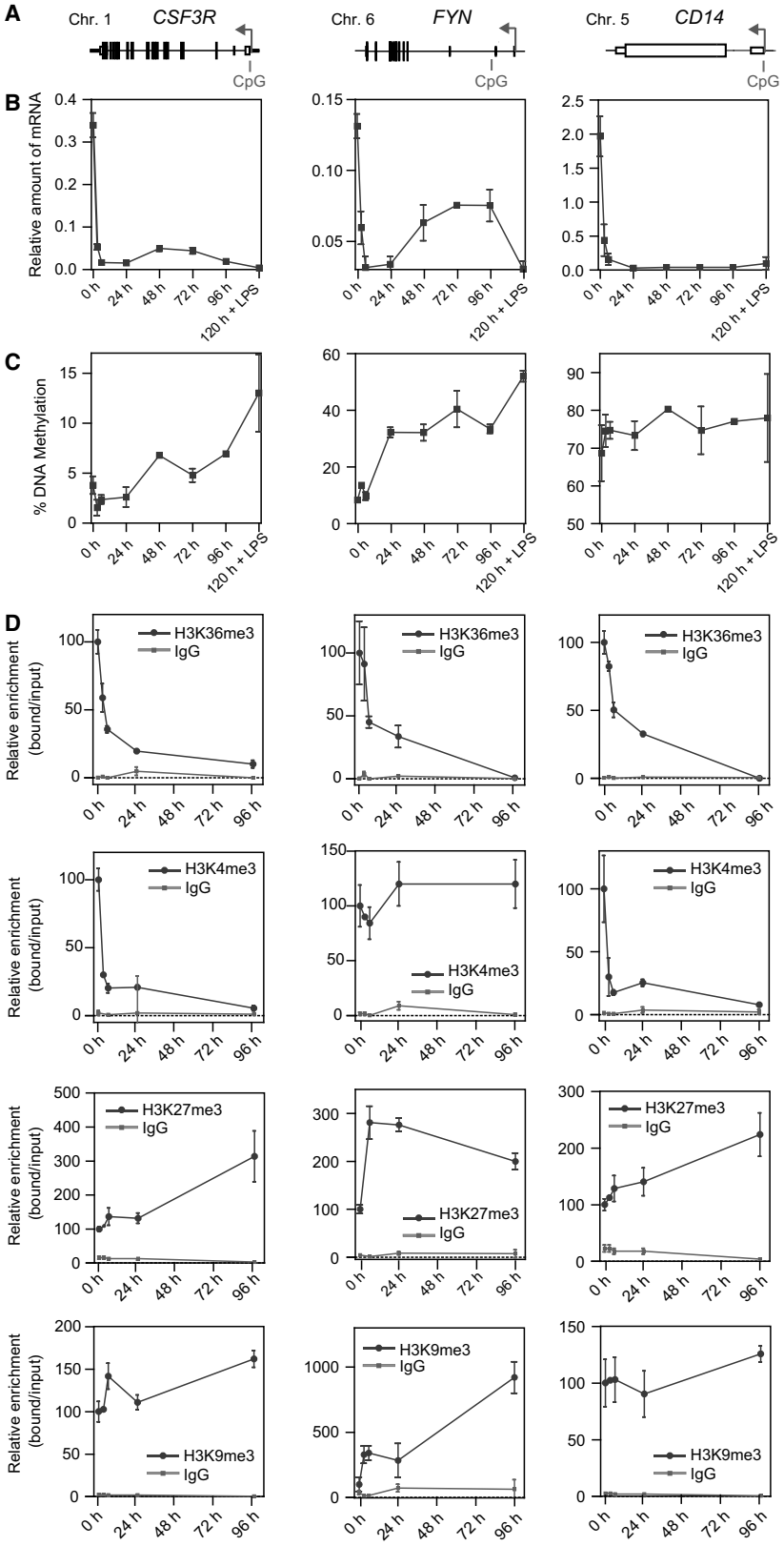
A
Chr. 1
CSF3R
Chr. 6
FYN
Chr. 5
CD14
CpG
B
Relative amount of mRNA
C
% DNA Methylation
D
Relative enrichment (bound/input)
H3K36me3
H3K4me3
H3K27me3
H3K9me3
IgG
0 h
24 h
48 h
72 h
96 h
120 h + LPS

focused on the MO-to-iDC conversion in the subsequent experiments.

Silencing and loss of activating histone modifications precede hypermethylation during MO-to-DC differentiation

We observed acquisition of DNA methylation in various genes that become repressed during differentiation from MOs. Experiments in a related model of MO-to-osteoclast differentiation had revealed that genes that become hypermethylated are silenced before acquiring DNA methylation [7], indicating that expression changes are driven by other mechanisms. In this context, DNA methylation changes in such genes would be more likely to play a stabilising role than be a driving mechanism. This contrasts with the concomitant demethylation associated with activation that was observed in the same differentiation model [7]. We explored the dynamics of expression and DNA methylation changes through differentiation to DCs by focusing on three of the above genes: *CSF3R* and *FYN*, in which DNA methylation increases, and *CD14*, in which it does not. *CSF3R* and *FYN* were chosen because they were among those showing the greatest changes, and also because of their physiological relevance in the context of DC-to-MAC differentiation. We found that *CSF3R* and *FYN* showed a sharp decrease in expression during the first 6 h following the addition of GM-CSF and IL-4 (Fig. 2B), whereas DNA methylation increased more gradually and was delayed with respect to silencing (Fig. 2C).

Our results suggest that expression changes, which occur earlier than DNA methylation changes, are associated with other regulatory mechanisms, perhaps those related to transcription factor binding, and possibly with specific histone modifications. Changes in DNA methylation could also be associated with the subsequent acquisition of other histone modifications. This prompted us to perform chromatin immunoprecipitation (ChIP) experiments with four histone modifications, including H3K4me3 and H3K36me3, which are characteristic of active transcription at the TSS and downstream of the TSS, respectively, and H3K9me3 and H3K27me3, which are generally associated with repression. We observed that H3K4me3 and H3K36me3 decreased early on, whereas changes in H3K9me3 and H3K27me3 coincided in time with the increase in DNA methylation (Fig. 2D). Remarkably, the transient re-expression of *FYN* at intermediate time points during DC differentiation was also reflected by the histone modifications, with an increase in H3K4me3 and a decrease in H3K27me3 (see the central panel in Fig. 2). In general, histone modification changes occurred in the proximity of the TSS and were less apparent when the region from –500 to +500 bp relative to the TSS was analysed (not shown). Interestingly, we observed that changes in these histone modifications occurred in the three studied genes, *CSF3R*, *FYN*, and *CD14*, regardless of the acquisition of DNA methylation, indicating that DNA methylation may not be functionally relevant in the silencing of these genes.

Functional relevance of DNA methylation changes during MO-to-DC differentiation

To test the functional relevance of DNA methylation in MO-to-DC differentiation, we investigated the potential effects of inhibiting DNMTs throughout the process. We used two DNMT inhibitors, 5-aza-2′-deoxycytidine (5azadC) and nanaomycin A. 5azadC induces DNA demethylation in a replication-coupled manner, and therefore should have a limited effect in this model, given that ~ 10% of the cells divide during differentiation. Nanaomycin A directly inhibits DNMT3b activity [12,13]. We used two different concentrations for both inhibitors: 50 and 500 nM for 5azadC, and 100 nM and 500 nM for nanaomycin A. In the case of 5azadC, we used these concentrations to minimize unwanted secondary effects, including cell death of primary MOs, which we had tested in pilot studies. These concentrations are slightly lower than the standard ones used for

Fig. 3. Effects of the DNMT inhibitors 5azadC and nanaomycin A on DNA methylation, expression and histone modification changes during MO-to-DC differentiation. (A) Effects of two concentrations of 5azadC (50 and 500 nM) and nanaomycin A (100 and 500 nM) on the acquisition of DNA methylation changes in *CSF3R* and *FYN* over time with respect to untreated control cells. (B) Effects of 5azadC and nanaomycin A (conditions as above) on the expression changes for the same genes as above. (C) Effects of 5azadC and nanaomycin A (conditions as above) on the changes in H3K4me3 (red bars) and H3K27me3 (blue bars). (D) Effects of 5azadC and nanaomycin A on the levels of the surface markers CD209 (specific to DCs) and CD83 [specific to mature DCs (mDCs)]. The viabilities of cells in the presence of these concentrations of drugs are also shown. (E) Real-time quantitative PCR analysis of the selected DC surface markers CD209, CD206 and CD83 during DC differentiation. The effects of two concentrations of DNMT inhibitors, i.e. nanaomycin A (100 and 500 nM) and 5azadC (50 and 500 nM), are compared with those on control cells, in the absence of these inhibitors. Ctrl, control.

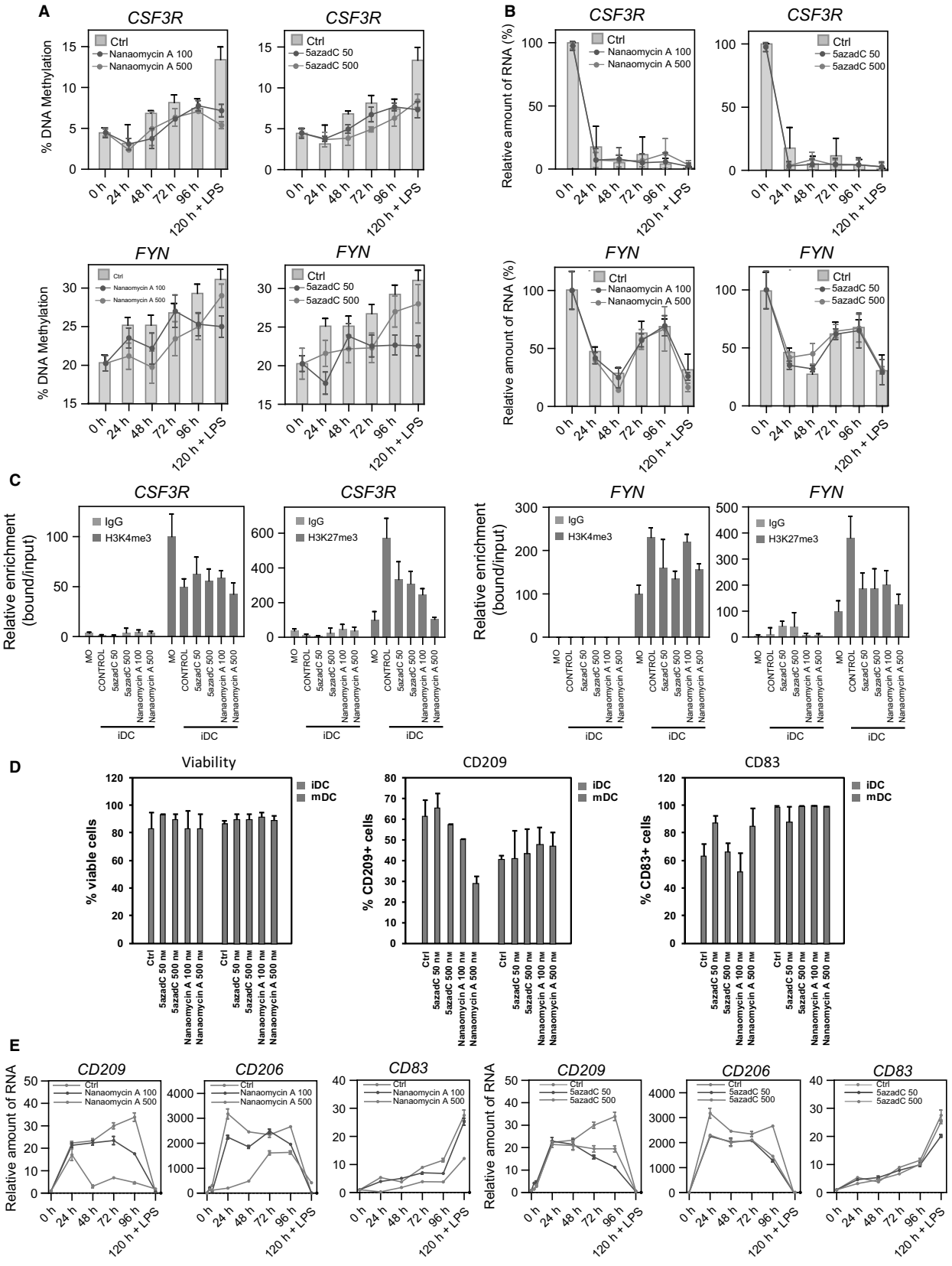
A
CSF3R
FYN
% DNA Methylation
Ctrl
Nanaomycin A 100
Nanaomycin A 500
5azadC 50
5azadC 500
0 h
24 h
48 h
72 h
96 h
120 h + LPS
B
Relative amount of RNA (%)
C
Relative enrichment (bound/input)
IgG
H3K4me3
H3K27me3
MO
CONTROL
iDC
D
Viability
CD209
CD83
% viable cells
% CD209+ cells
% CD83+ cells
iDC
mDC
E
CD209
CD206
CD83
Relative amount of RNA

cancer cell lines. We then investigated the ability of these drugs to inhibit the acquisition of DNA methylation by the aforementioned genes, and the ability of these genes to become silenced during differentiation. In addition, we investigated whether these compounds caused changes in surface markers that can be tested by FACS, but found no effects on cell viability over the entire differentiation time frame at the concentrations used.

Analysis of the DNA methylation changes during differentiation with pyrosequencing revealed that both 5azadC and nanaomycin A affected the ability of genes such as *CSF3R* and *FYN* to become hypermethylated (Fig. 3A). The results were more evident for *CSF3R*, where the acquisition of methylation was reduced by half, than for *FYN*, which also has a more complex pattern of expression and histone modifications over time. We observed that 5azadC had a moderate effect on the acquisition of DNA methylation, which is likely to be related to the low division rate of these cells, as cell division is essential for the effect of this drug.

We then tested the effects of these drugs on the expression levels of *CSF3R* and *FYN*. We found that neither 5azadC nor nanaomycin A influenced the loss of expression or the dynamics of this, reinforcing the notion that expression changes of these genes occur before the acquisition of DNA methylation, and that inhibition of DNMTs does not affect their ability to be silenced (Fig. 3B). We also compared the expression levels of DNMT3b in cells treated with nanaomycin A and untreated cells by using real-time quantitative PCR, and found no differences (not shown). This is consistent with the findings of others that specific inhibition by nanaomycin A does not involve changes in the levels of DNMT3b [12].

We also investigated the levels of H3K4me3, H3K36me3, H3K9me3 and H3K27me3 in the genes in MOs and iDCs and mDCs in the absence or presence of these DNMT inhibitors. Whereas we did not find differences in the pattern of H3K4me3 for *CSF3R*, and only moderate differences for *FYN*, with respect to control cells, we observed that the acquisition of H3K27me3 was significantly impaired (Fig. 3C); this may be associated with the existing links between this histone modification and DNA methylation [14], which is affected by treatment with these DNMT inhibitors. For H3K36me3 and H3K9me3, as for H3K4me3, we did not see any differences in cells treated with demethylating agents (not shown).

We then investigated whether the two compounds influenced the ability of cells to differentiate by studying the surface markers CD209, which is characteristic of DCs, and CD83, which is characteristic of mature DCs. We observed that, although the numbers of viable cells were similar in 5azadC-treated and nanaomycin A-treated cells, the levels of CD209 were significantly lower in those treated with nanaomycin A (Fig. 3D), indicating that inhibition of DNMT3B affects the stability of the differentiated phenotype of these cells. In parallel, we used real-time quantitative PCR to analyse these two markers and CD206, as an additional iDC marker. We found that both CD209 and CD206 levels were decreased in both 5azadC-treated and nanaomycin A-treated cells, although, again, nanaomycin A had a greater effect than 5azadC (Fig. 3E).

Discussion

Our results provide evidence for the *de novo* acquisition of DNA methylation in certain genes that become repressed during MO-to-MAC and MO-to-DC differentiation. These changes occur progressively, and are delayed with respect to the loss of expression of such genes. The changes in expression appear to be more closely correlated with the loss of active histone modifications such as H3K4me3 and H3K36me3, and are perhaps associated with the direct control of specific transcriptional repressors. On the other hand, gains of DNA methylation are associated with the acquisition of repressive markers such as H3K27me3 and H3K9me3. We assessed the functional relevance of these DNA methylation changes in the genes considered here by using two DNMT inhibitors. The results suggest that partial impairment of DNA methylation acquisition does not alter the ability of these genes to become repressed. However, we did note an effect of DNMT inhibition on the phenotype of the DCs, which suggests that it has a role in stabilizing the differentiated phenotype.

There is compelling evidence that differentiation in the myeloid lineage is associated with changes in DNA methylation biased towards demethylation [2,3]. This is compatible with the observation that postmitotic terminal differentiation from MOs to DCs and MACs is accompanied by demethylation [5,6]. These analyses were performed by combining methyl-CpG immunoprecipitation with hybridization on promoter microarrays or by using 450K arrays. These are robust methods, but are insufficient for full coverage of individual CpG sites. Despite the predominance of changes in the direction of demethylation, it seems to us that acquisition of DNA methylation at specific CpG sites could have been underestimated. Our analy-

sis has shown that certain CpG sites near the TSSs of genes that become repressed undergo acquisition of DNA methylation. In principle, this is consistent with a repressive role.

Comparison of the dynamics of expression and DNA methylation changes in another MO-related differentiation model [7] revealed that demethylation and increased mRNA levels occur concomitantly, suggesting a causal relationship between the loss of DNA methylation and gene activation. However, analysis of this relationship in genes that become repressed and have their DNA methylation levels increased led to different conclusions [7]. In fact, gene silencing occurs before the acquisition of DNA methylation. This also occurs in MO-to-DC differentiation, where repression of certain genes also precedes their hypermethylation. These findings imply that the roles of demethylation and acquisition of DNA methylation are somewhat different, at least in these myeloid-related differentiation processes, and are just not antagonistic mechanisms. Cells in the myeloid lineage, in particular MOs, express high levels of Tet2 [15,16], a member of the TET family of methylcytosine dioxygenases, which generates intermediates in the route towards DNA demethylation. In fact, myeloid cells constitute an excellent system in which active DNA demethylation appears to play a key role in activating specific genes. In contrast, the delay in the changes to the acquisition of DNA methylation for those genes that become repressed suggests a different role. In fact, DNA methylation in these genes might be passively acquired, and might only play a role in stabilizing gene repression, rather than being a primary driver of expression changes.

The final experiment in our study, which tested the functional effects of two DNMT inhibitors, addressed the functional relevance of the acquisition of DNA methylation by these genes. Our results provide evidence that DNA methylation changes in genes such as *CSF3R* and *FYN* are not necessary for their repression. *CSF3R* is the receptor for granulocyte colony-stimulating factor, which is essential for granulocyte development [17], and so its silencing is required for MAC versus granulocyte commitment. FYN is a tyrosine kinase from the Src family that promotes proliferation and is upregulated in chronic myeloid leukaemia [18]. Its silencing may reflect the need for cell cycle arrest in MO-to-DC differentiation. Therefore, we cannot rule out the possibility that DNA methylation stabilizes this expression status once it has been achieved, at least over the long term. On the other hand, we found that the expression of DC-specific surface markers is reduced following treatment with these DNMT inhibitors. Specifically, we observed that DC-SIGN (CD209) expression declined following treatment with nanaomycin A. DC-SIGN is a well-recognized DC marker that mediates several DC functions, including antigen uptake, intercellular adhesion, and signalling [19]. Given the decrease in expression observed for this molecule upon *de novo* methylation inhibition, our data indicate that DNA methylation may play a role in the stabilization of the differentiated phenotype of DCs.

Our results introduce a novel concept concerning the role of DNA methylation changes. Our current view of the role of DNA methylation takes into account that the location of a CpG site determines the functionality of its methylation (differing according to its location in a CpG island, shore, open sea, or enhancer, or in the context of a transcription factor-binding site), but our experiments also indicate that the directionality of the change, i.e. the gain or loss of DNA methylation at specific genes, can have different roles. Whereas loss of DNA methylation is associated with the concomitant activation of certain genes, acquisition of DNA methylation by other genes is not necessarily associated with their immediate silencing, and it seems rather to have a longer-term effect related to the stabilization of the phenotype.

Experimental procedures

Differentiation of DCs from peripheral blood mononuclear cells (PBMCs)

For this study, we obtained human blood samples (buffy coats) from anonymous donors through the Catalan Blood and Tissue Bank (Barcelona). The donors were informed about the potential use of their blood for research, and had any questions arising during the interview answered. The donors signed a consent form at the Catalan Blood and Tissue Bank before samples were obtained. This Blood Bank follows the WMA Declaration of Helsinki principles. Blood samples were carefully deposited on Ficoll-Paque gradients (Amersham, Buckinghamshire, UK), and then centrifuged at 800 ***g*** (30 min) with minimum deceleration. Following centrifugation, we collected PBMCs, and washed them twice with ice-cold $NaCl/P_i$ at 600 ***g*** for 5 min. We then used positive selection with MACS magnetic CD14 antibody (Miltenyi Biotec, Bergisch Gladbach, Germany) to isolate pure $CD14^+$ cells from PBMCs. We then resuspended $CD14^+$ cells in RPMI Medium 1640 (1X) + GlutaMAXTM-1 (Gibco, Life Technologies, Carlsbad, CA, USA) supplemented with 10% fetal bovine serum, 100 units·mL^{-1} penicillin, and 100 μg·mL^{-1} streptomycin. For DC differentiation, the medium was supplemented with 500 U of human IL-4 and 800 U of GM-CSF (Gentaur

Molecular Products, Kampenhout, Belgium). For MAC differentiation, the medium was supplemented with 800 U of GM-CSF (Gentaur Molecular Products).

We seeded the cells at different densities, depending on the cell numbers required for specific techniques. These numbers were 3×10^5 cells per well (96-well plates), 5×10^6 cells per well (six-well plates), and 40×10^6 cells (10-mm plates). We cultured these cells for 4 days, and changed the media and cytokines every 2 days. To induce maturation on day 4, we supplemented cells with 5 $\mu g \cdot mL^{-1}$ LPS (Sigma-Aldrich, St Louis, MO, USA) for 24 h.

Bisulfite sequencing and pyrosequencing

We carried out bisulfite modification of genomic DNA isolated from MOs, and derived DCs and MACs with the protocol described by Herman *et al.* [20]. We then used 2 μL of the modified DNA (20–30 ng) as a template for the subsequent analysis. We designed primers for amplification and sequencing with PYROMARK ASSAY DESIGN 2.0 software (Qiagen, Venlo, Limburg, The Netherlands). We performed PCR amplifications with the HotStart Taq DNA polymerase PCR kit (Qiagen), and then tested the quality of the amplified products by agarose gel electrophoresis. We pyrosequenced the PCR products with the Pyromark Q24 system (Qiagen). The list of all primer sequences is included in Table S1.

ChIP assays

We crosslinked $CD14^+$ cells at 0, 3, 6, 24 and 96 h after treatment with GM-CSF + IL-4 with 1% formaldehyde, and performed ChIP assays after sonication. We used the standard protocol for ChIP experiments, and the results were analysed with real-time quantitative PCR. For each specific antibody/sample, we represented data as the ratio of the bound fraction versus the input. We used the following antibodies: anti-H3K4me3 IgG rabbit monoclonal (ref. 17-614; Millipore, Billerica, MA, USA), anti-H3K36me3 serum (ref. ab9050; Abcam, Cambridge, UK), anti-H3K9me3 serum (ref. ab8898; Abcam), and anti-H3K27me3 serum (ref. 07-449; Millipore). We used IgG as a negative control. We designed primer sequences to overlap with regions showing hypermethylation at given CpG sites, generally close to the TSS. Primer sequences are shown in Table S1. Three biological replicates of these experiments were carried out.

BrdU proliferation assays

We used BrdU at a final concentration of 300 μM, and BrdU pulses were applied to each well for 2 days. For flow cytometry assays, we seeded $CD14^+$ cells on six-well plates, and cultured them in differentiation medium. In this case, we added BrdU to the medium at different times. We then fixed cells after 2 days with 4% paraformaldehyde (30 min, room temperature), permeabilized them with $NaCl/P_i$/BSA/Triton X-100 0.8% (10 min, room temperature), and treated them with 2 M HCl for 30 min. We then neutralized the HCl with two 5-min washes with NaBo (0.1 M, pH 8.5) and two 5-min washes with $NaCl/P_i$. Cells were incubated with anti-BrdU mouse IgG1 (18 h at 4 °C, 1 : 1000 dilution), and anti-mouse Alexa-488-conjugated serum was added to detect the BrdU-positive nuclei.

FACS staining

For FACS analysis, we directly stained $CD14^+$ MOs and DCs with phycoerythrin-conjugated mAbs against CD14 (Miltenyi), Horizon V450-conjugated mAbs against CD209 (BD), and allophycocyanin-conjugated mAbs against CD83 (Miltenyi). We incubated 0.3×10^6 cells with the indicated antibodies for 30 min at 4 °C, and washed them once with ice-cold $NaCl/P_i$BSA 0.1%. We analysed cells with a Gallios Flow Cytometer (Beckman Coulter, Brea, CA, USA) and FLOWJO software (Tree Star, Ashland, OR, USA).

Acknowledgements

This study was funded by grant SAF2011-29635 (Spanish Ministry of Science and Innovation), grant CIVP16A1834 (Fundación Ramón Areces), and grant 2009SGR184 (AGAUR, Catalan Government). R. Vento-Tormo is supported by a PFIS predoctoral fellowship.

Author contributions

E. Ballestar and R. Vento-Tormo designed the research, R. Vento-Tormo and J. Rodríguez-Ubreva performed the experiments, E. Ballestar, R. Vento-Tormo, J. Rodríguez-Ubreva and D. Álvarez-Errico analysed the data and E. Ballestar wrote the paper.

References

1 Broske AM, Vockentanz L, Kharazi S, Huska MR, Mancini E, Scheller M, Kuhl C, Enns A, Prinz M, Jaenisch R *et al.* (2009) DNA methylation protects hematopoietic stem cell multipotency from myeloerythroid restriction. *Nat Genet* **41**, 1207–1215.

2 Ji H, Ehrlich LI, Seita J, Murakami P, Doi A, Lindau P, Lee H, Aryee MJ, Irizarry RA, Kim K *et al.* (2010) Comprehensive methylome map of lineage commitment from haematopoietic progenitors. *Nature* **467**, 338–342.

3 Hodges E, Molaro A, Dos Santos CO, Thekkat P, Song Q, Uren PJ, Park J, Butler J, Rafii S, McCombie WR

et al. (2011) Directional DNA methylation changes and complex intermediate states accompany lineage specificity in the adult hematopoietic compartment. *Mol Cell* **44**, 17–28.
4 Ronnerblad M, Andersson R, Olofsson T, Douagi I, Karimi M, Lehmann S, Hoof I, de Hoon M, Itoh M, Nagao-Sato S *et al*. (2014) Analysis of the DNA methylome and transcriptome in granulopoiesis reveal timed changes and dynamic enhancer methylation. *Blood* **123**, 79–89.
5 Klug M, Heinz S, Gebhard C, Schwarzfischer L, Krause SW, Andreesen R & Rehli M (2010) Active DNA demethylation in human postmitotic cells correlates with activating histone modifications, but not transcription levels. *Genome Biol* **11**, R63.
6 Zhang X, Ulm A, Somineni HK, Oh S, Weirauch MT, Zhang HX, Chen X, Lehn MA, Janssen EM & Ji H (2014) DNA methylation dynamics during ex vivo differentiation and maturation of human dendritic cells. *Epigenetics Chromatin* **7**, 21.
7 de la Rica L, Rodriguez-Ubreva J, Garcia M, Islam AB, Urquiza JM, Hernando H, Christensen J, Helin K, Gomez-Vaquero C & Ballestar E (2013) PU.1 target genes undergo Tet2-coupled demethylation and DNMT3b-mediated methylation in monocyte-to-osteoclast differentiation. *Genome Biol* **14**, R99.
8 Okano M, Bell DW, Haber DA & Li E (1999) DNA methyltransferases Dnmt3a and Dnmt3b are essential for de novo methylation and mammalian development. *Cell* **99**, 247–257.
9 Sasaki H & Matsui Y (2008) Epigenetic events in mammalian germ-cell development: reprogramming and beyond. *Nat Rev Genet* **9**, 129–140.
10 Esteller M (2007) Cancer epigenomics: DNA methylomes and histone-modification maps. *Nat Rev Genet* **8**, 286–298.
11 Ohm JE & Baylin SB (2007) Stem cell chromatin patterns: an instructive mechanism for DNA hypermethylation? *Cell Cycle* **6**, 1040–1043.
12 Kuck D, Caulfield T, Lyko F & Medina-Franco JL (2010) Nanaomycin A selectively inhibits DNMT3B and reactivates silenced tumor suppressor genes in human cancer cells. *Mol Cancer Ther* **9**, 3015–3023.
13 Caulfield T & Medina-Franco JL (2011) Molecular dynamics simulations of human DNA methyltransferase 3B with selective inhibitor nanaomycin A. *J Struct Biol* **176**, 185–191.
14 Schlesinger Y, Straussman R, Keshet I, Farkash S, Hecht M, Zimmerman J, Eden E, Yakhini Z, Ben-Shushan E, Reubinoff BE *et al*. (2007) Polycomb-mediated methylation on Lys27 of histone H3 pre-marks genes for de novo methylation in cancer. *Nat Genet* **39**, 232–236.
15 Klug M, Schmidhofer S, Gebhard C, Andreesen R & Rehli M (2013) 5-Hydroxymethylcytosine is an essential intermediate of active DNA demethylation processes in primary human monocytes. *Genome Biol* **14**, R46.
16 Kallin EM, Rodriguez-Ubreva J, Christensen J, Cimmino L, Aifantis I, Helin K, Ballestar E & Graf T (2012) Tet2 facilitates the derepression of myeloid target genes during CEBPalpha-induced transdifferentiation of pre-B cells. *Mol Cell* **48**, 266–276.
17 Demetri GD & Griffin JD (1991) Granulocyte colony-stimulating factor and its receptor. *Blood* **78**, 2791–2808.
18 Ban K, Gao Y, Amin HM, Howard A, Miller C, Lin Q, Leng X, Munsell M, Bar-Eli M, Arlinghaus RB *et al*. (2008) BCR-ABL1 mediates up-regulation of Fyn in chronic myelogenous leukemia. *Blood* **111**, 2904–2908.
19 Garcia-Vallejo JJ & van Kooyk Y (2013) The physiological role of DC-SIGN: a tale of mice and men. *Trends Immunol* **34**, 482–486.
20 Herman JG, Graff JR, Myohanen S, Nelkin BD & Baylin SB (1996) Methylation-specific PCR: a novel PCR assay for methylation status of CpG islands. *Proc Natl Acad Sci USA* **93**, 9821–9826.

Supporting information

Additional supporting information may be found in the online version of this article at the publisher's web site:
Table S1. List of primers.

de la Rica et al. Genome Biology (2015)16:2
DOI 10.1186/s13059-014-0561-5

Genome Biology

RESEARCH Open Access

NF-κB-direct activation of microRNAs with repressive effects on monocyte-specific genes is critical for osteoclast differentiation

Lorenzo de la Rica[1,2†], Antonio García-Gómez[1†], Natalia R Comet[1], Javier Rodríguez-Ubreva[1], Laura Ciudad[1], Roser Vento-Tormo[1], Carlos Company[1], Damiana Álvarez-Errico[1], Mireia García[3], Carmen Gómez-Vaquero[3] and Esteban Ballestar[1*]

Abstract

Background: Monocyte-to-osteoclast conversion is a unique terminal differentiation process that is exacerbated in rheumatoid arthritis and bone metastasis. The mechanisms implicated in upregulating osteoclast-specific genes involve transcription factors, epigenetic regulators and microRNAs (miRNAs). It is less well known how downregulation of osteoclast-inappropriate genes is achieved.

Results: In this study, analysis of miRNA expression changes in osteoclast differentiation from human primary monocytes revealed the rapid upregulation of two miRNA clusters, miR-212/132 and miR-99b/let-7e/125a. We demonstrate that they negatively target monocyte-specific and immunomodulatory genes like *TNFAIP3*, *IGF1R* and *IL15*. Depletion of these miRNAs inhibits osteoclast differentiation and upregulates their targets. These miRNAs are also upregulated in other inflammatory monocytic differentiation processes. Most importantly, we demonstrate for the first time the direct involvement of Nuclear Factor kappa B (NF-κB) in the regulation of these miRNAs, as well as with their targets, whereby NF-κB p65 binds the promoters of these two miRNA clusters and NF-κB inhibition or depletion results in impaired upregulation of their expression.

Conclusions: Our results reveal the direct involvement of NF-κB in shutting down certain monocyte-specific genes, including some anti-inflammatory activities, through a miRNA-dependent mechanism for proper osteoclast differentiation.

Background

The successful generation of differentiated cell types from their progenitors depends on the highly coordinated regulation of gene expression by transcription factors, epigenetic enzymes, and small non-coding RNAs, of which microRNAs (miRNAs) are the best studied. These regulate gene expression through sequence complementarity with their target mRNAs by mediating their decay or interfering with their translation [1]. miRNAs are known to have a major role in cell differentiation. However, their specific contribution in terminal differentiation processes remains poorly understood.

One such process is monocyte (MO)-to-osteoclast (OC) differentiation. OCs are giant, multinucleated cells that degrade bone [2] and differentiate from monocytic progenitors under inflammatory conditions. Their deregulation is associated with several diseases, either through deficient function that results in osteopetrosis [3] or aberrant hyperactivation that gives rise to generalized bone loss in osteoporosis [4] and rheumatoid arthritis [5]. Moreover, OCs cause bone complications in multiple myeloma [6] and in cancer metastasis, including prostate and breast cancers [7]. OCs differentiate from MO/macrophage progenitors [8] after macrophage colony-stimulating factor (M-CSF) [9] and receptor activator of nuclear factor kappa-B ligand (RANKL) [10] stimulation. *In vitro* generation of OCs from peripheral blood MOs allows differentiation to be studied

* Correspondence: eballestar@idibell.cat
†Equal contributors
[1]Chromatin and Disease Group, Cancer Epigenetics and Biology Programme (PEBC), Bellvitge Biomedical Research Institute (IDIBELL), 08908 L'Hospitalet de Llobregat, Barcelona, Spain
Full list of author information is available at the end of the article

in this model, since isolation of primary bone OCs can otherwise be challenging [11]. During osteoclastogenesis, progenitor cells fuse, reorganize their cytoskeleton [12] and activate the gene expression profile necessary for bone destruction. Several signaling pathways activate nuclear factor-kappa B (NF-κB), mitogen-activated protein kinase (MAPK) and c-Jun [13], which coordinately turn on NFATc1 [14], the osteoclastogenesis master transcription factor. NFATc1 acts in conjunction with PU.1 and MITF [15], activating OC-specific genes such as those encoding tartrate-resistant acid phosphatase (*TRAP* or *ACP5*) [16], cathepsin K (*CTSK*) [17], dendritic cell-specific transmembrane protein (*DC-STAMP* or *TM7SF4*) [18], matrix metallopeptidase 9 (*MMP9*) [19] and carbonic anhydrase 2 (*CA2*). Most importantly, other genes like *CX3CR1*, a MO-specific gene, and *TNFAIP3*, a deubiquitinating protease that mediates TRAF6 degradation and impairs NF-κB activation [20], need to be silenced during OC differentiation. It is not well understood how the silencing program is established during MO-to-OC differentiation. The importance of miRNAs in OC differentiation has been established through the observation that knock-out models for the miRNA processing machinery impair OC formation and reduced expression of TRAP and NFATc1 [21]. In addition, silencing of miRNAs, such as miR-29b [22] and miR-124 [23], is essential for the upregulation of pro-osteoclastic genes.

In this study, we investigated the role of miRNAs in establishing and maintaining a repressive program during OC differentiation. To this end, we performed high-throughput miRNA expression profiling of human peripheral blood MOs before and 2 and 20 days after stimulation with RANKL and M-CSF. We identified different dynamics in miRNA expression changes. Two miRNA clusters, miR-212/132 and miR- 99b/let-7e/125a, are highly upregulated during the early stages of osteoclastogenesis. Functional analysis of these miRNAs revealed that their depletion impairs proper OC differentiation. Interestingly, these miRNAs target MO-specific and anti-inflammatory genes that are downregulated during differentiation, such as *TNFAIP3*, *IGF1R*, *THBS1*, *ITGA4*, *IL15* and *PTGS2*. We investigated the potential involvement of the NF-κB transcription factor in the upregulation of these miRNAs. We demonstrated the direct association of p65 NF-κB with the transcription start site (TSS) of these miRNA clusters. Most importantly, we found that the pharmacological inhibition of the p65 subunit of NF-κB or its depletion results in impaired overexpression of these miRNAs and affects the downregulation of their targets. Our results demonstrate the direct relationship between p65 NF-κB and miRNA-mediated repression of several MO-specific and anti-inflammatory genes that is key for proper osteoclastogenesis and reveal novel potential pathways for therapeutic intervention in the treatment of bone complications in diseases such as rheumatoid arthritis and bone metastases.

Results

The miRNA expression profile changes drastically during osteoclastogenesis

To determine the dynamics of miRNA expression during human osteoclastogenesis, we first generated three sets of matching samples corresponding to peripheral blood MOs (CD14+ cells), MOs 48 hours after RANKL/M-CSF treatment, and mature OCs obtained from the same sets of MOs, 21 days after RANKL/M-CSF stimulation. The quality of the OCs was confirmed microscopically by the presence of three or more nuclei in TRAP-positive cells and the formation of the actin ring (Figure 1A). At the molecular level, we confirmed the upregulation of osteoclastic markers (*CA2*, *CTSK*, *MMP9*, *ACP5*/*TRACP* and *TM7SF4/DCSTAMP*) and the silencing of the MO-specific gene *CX3CR1* (Figure 1B). We then performed miRNA expression profiling during the differentiation of MOs to OCs using the three sets of samples. Statistical analysis of the combined expression data from three biological replicates showed 115 miRNAs that were differentially expressed at one or more of the times analyzed (Figure 1C; Additional file 1). miRNAs displayed different expression profiles over time that enabled them to be classified into eight groups (Figure 1C) according to the combination of upregulation or downregulation at the initial or late stages of OC differentiation. Of particular interest were the miRNAs whose expression increased rapidly in the initial stages (groups I, V and VI; Figure 1C), regardless of their subsequent changes over time. miRNAs that become upregulated immediately after M-CSF and RANKL stimulation are potentially more important for the differentiation process than for the function of fully differentiated OCs. miRNAs within two clusters ranked top in terms of the coefficient of change and relative expression levels, specifically miR-99b/let-7e/125a (group I, average fold change = 49.4 between MOs and 48 h post-MCSF/RANKL stimulation) and miR-212/132 (group VI, average fold change = 50.57 between MOs and 48 h post-MCSF/RANKL stimulation) (Figure 1D). Several other activated miRNAs identified in our analysis have already been described in human and mouse experiments concerning OC differentiation (Figure 1C) like miR-124, a negative regulator of NFATc1 expression [23], and miR-155, also upregulated in bone marrow macrophage-derived OCs [24,25].

We confirmed the overexpression of all the miRNAs within the miR-99b/let-7e/125a and miR-212/132 clusters using quantitative RT-PCR (qRT-PCR) (Figure 1E). This analysis also confirmed that individual miRNAs from each of the two clusters do not reach the same expression levels. For example, miR-99b and miR-125a levels are increased by 300-fold and 100-fold respectively, whereas

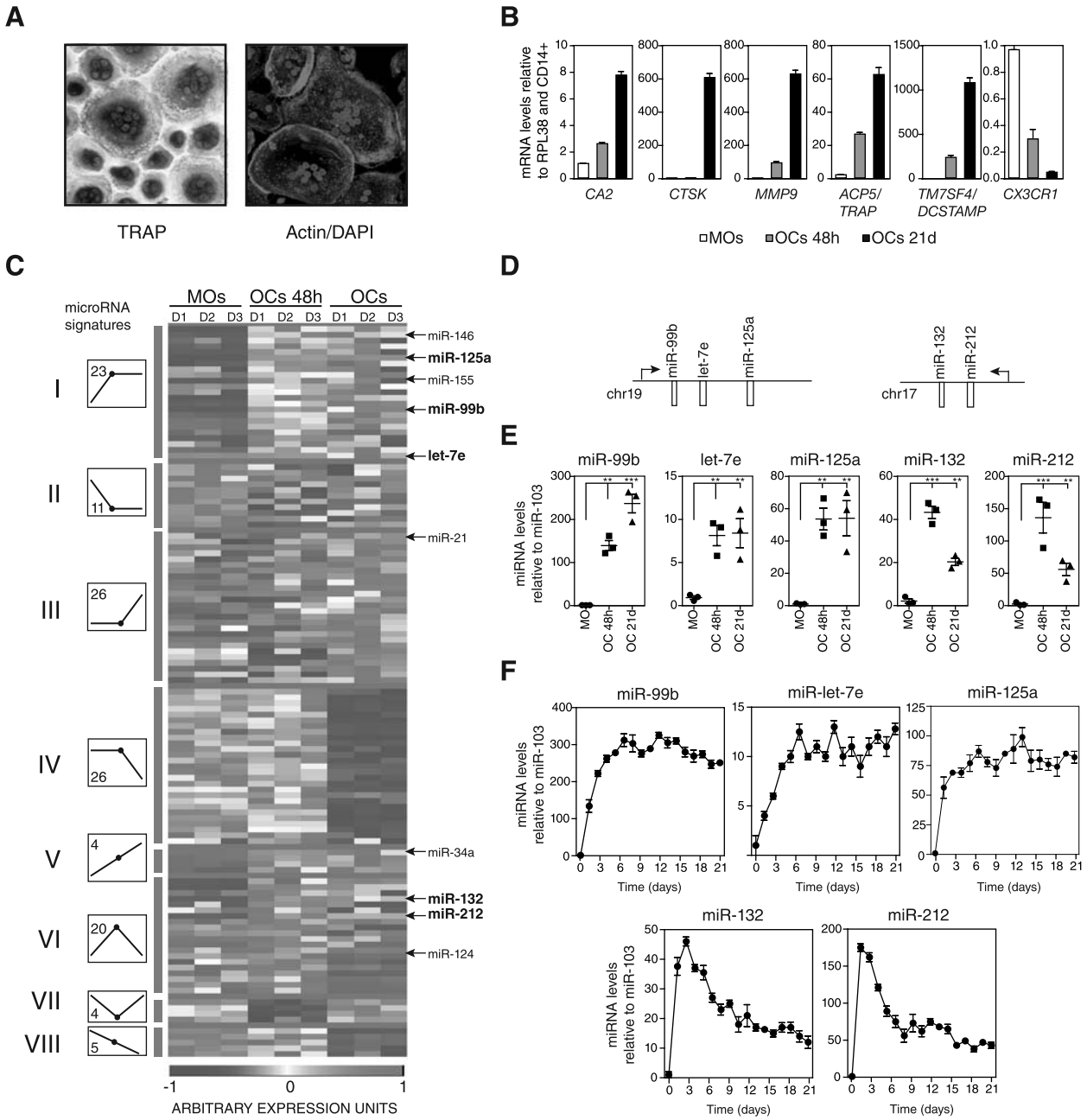

Figure 1 MicroRNA expression profiling during monocyte-to-osteoclast differentiation. (A) Validation of the presence of OCs by TRAP and phalloidin staining, showing the presence of TRAP activity/multiple nuclei and the actin ring, respectively. **(B)** Molecular characterization of OC differentiation. Several OC markers are upregulated (*CA2*, *CTSK*, *MMP9*, *ACP5/TRAP*, and *TM7SF4/DCSTAMP*), and the MO marker *CX3CR1* is silenced. Data for MOs, MOs 48 h after M-CSF and RANKL treatment and OCs at 21 days are presented. RPL38 gene expression levels were used for normalization. Error bars correspond to the standard deviation of three individual measurements. **(C)** Heatmap showing expression array data from the miRNA expression screening. miRNAs were subdivided into eight groups (I to VIII) according to their expression profile (diagram); the number of miRNAs in each group is indicated inside the expression dynamics diagram. Scale shown at the bottom, whereby normalized expression units ranges from -1 (blue) to +1 (red). **(D)** Representation of the genomic distribution of miR-99b/125a/let7e and miR-132/212 clusters, including the TSS (indicated with an arrow). **(E)** Validation of array data by quantitative PCR in independent biological replicates. Analysis in MOs, MOs incubated 48 h with RANKL/M-CSF and fully differentiated OCs. Data normalized with respect to miR-103. **(F)** Expression dynamics of the indicated miRNAs during OC differentiation, also normalized with respect to miR-103.

miR-let-7e induction is only increased by 10- to 12-fold. This strongly suggests that miRNAs in these clusters are regulated not only transcriptionally but also post-transcriptionally during MO-to-OC differentiation, as it has previously been observed for other miRNAs in other differentiation programs [26]. To refine the expression dynamics of these miRNAs during the differentiation process further, we generated a time course of osteoclastogenesis from three different healthy donors, and checked the miRNA levels at several times during the entire differentiation process. The two clusters showed different dynamics when we analyzed their expression levels over time. Specifically, after RANKL/M-CSF stimulation, the miR-99b/let-7e/125a cluster miRNAs underwent rapid overexpression during the first four days and the levels remained stably high until day 21 (Figure 1F, top). In contrast, miR-212/132 cluster miRNAs peaked at day 3, displaying an increase of around 50-fold (miR132) to 170-fold (miR-212), followed by an approximately 5-fold drop (Figure 1F, bottom). This suggests that the functions of miR-132 and miR-212 are involved in the early events of osteoclastogenesis, since their expression levels are tightly regulated and constrained to the first four days of differentiation.

Inhibition of miRNAs within the miR-99b/let-7e/125a and miR-212/132 clusters impairs osteoclastogenesis

To investigate the role of the individual miRNAs within the two aforementioned clusters in OC differentiation, we performed loss of function experiments. We transfected primary MOs with specific inhibitors or antagomirs for each of the individual miRNAs contained in the miR-99b/let-7e/125a and miR-212/132 clusters. In these experiments, transfections with miRNA inhibitors were performed simultaneously with RANKL/M-CSF stimulation. We collected samples at 4 days. Then we tested the expression of OC markers to assess the impact of depleting these miRNAs on the differentiation process. Simultaneously, we checked the efficiency of transfection by flow cytometry of cells transfected with a control antagomir fluorescein-conjugate, recording efficiencies of 93% and 97.6% depending on the reagent used for transfection (Figure 2A). qRT-PCR analysis revealed that individual inhibition of each of the miRNAs within the two clusters results in a delay and decrease in the levels of OC markers like *ACP5*, *CA2*, *CTSK* and *MMP9* (Figure 2B) at 4 days after RANKL/M-CSF stimulation. An opposite effect was observed for the MO-specific gene *CX3CR1* with miR-99b and miR-125a (Figure 2B). We also performed double-transfection experiments with two combinations of miRNA inhibitors, containing two miRNAs within each cluster. In these experiments with two miRNA inhibitors we observed higher inhibition of OC markers than in single transfections (Figure 2C), further demonstrating the functional role of these miRNAs in the proper differentiation of OCs.

We then investigated the effects of depleting these miRNAs on the acquisition of two essential OC membrane proteins, CCR1 [27] and TM7SF4/DCSTAMP [28] (Figure 2D). Flow cytometry analysis of these two surface markers revealed that the depletion of any of the individual miRNAs within the two clusters decreases their levels 4 days after RANKL/M-CSF stimulation.

Finally, we tested whether depletion of these miRNAs impacts the ability of MOs to fuse and form OCs following RANKL/M-CSF stimulation. To this end, we performed TRAP staining 4 days after RANKL/M-CSF treatment on cells transfected with power inhibitors for each of the miRNAs, when the first multinucleated OCs start to be apparent. We observed a delay in OC formation in all cases, proving the relevance of these miRNAs for the differentiation and fusion in TRAP+ OCs (Figure 2E). These effects were less obvious at longer differentiation times; however, this is not surprising given the medium/long-term instability of antagomirs transfected into cells. In summary, all these results indicate that the high levels of the miRNAs from these two clusters are necessary for proper differentiation of OCs.

Upregulated miRNAs target monocyte-specific and immunomodulatory genes that need to be silenced during osteoclastogenesis

Our results demonstrated that the miRNAs within the most strongly activated miRNA clusters have a functional effect on OC differentiation when inhibited in MOs, as reflected by the decrease and delay in the upregulation of OC markers, including OC-specific surface proteins, as well as in the ability to form multinuclear cells. To identify the targets of these miRNAs, we retrieved a list of putative targets using miRWalk [29], which contains prediction databases like TargetScan [30], miRDB [31] and others, as well as information about validated targets. We then linked the list of potential targets with previously reported high-throughput data on expression changes during OC differentiation [32], assuming an inverse relationship between the levels of a given miRNA and the expression levels of its targets. For this analysis, we imposed the criteria that the targets should be predicted by at least four databases (Figure 3A) and that downregulation was defined as a minimum 0.5-fold change. Applying these conditions we identified a number of putative downregulated targets for each overexpressed miRNA (Additional file 2). We then used the Database for Annotation, Visualization and Integrated Discovery (DAVID) to identify functional categories. This tool revealed a highly significant enrichment of categories related to the immune system (Figure 3B), including immune system development

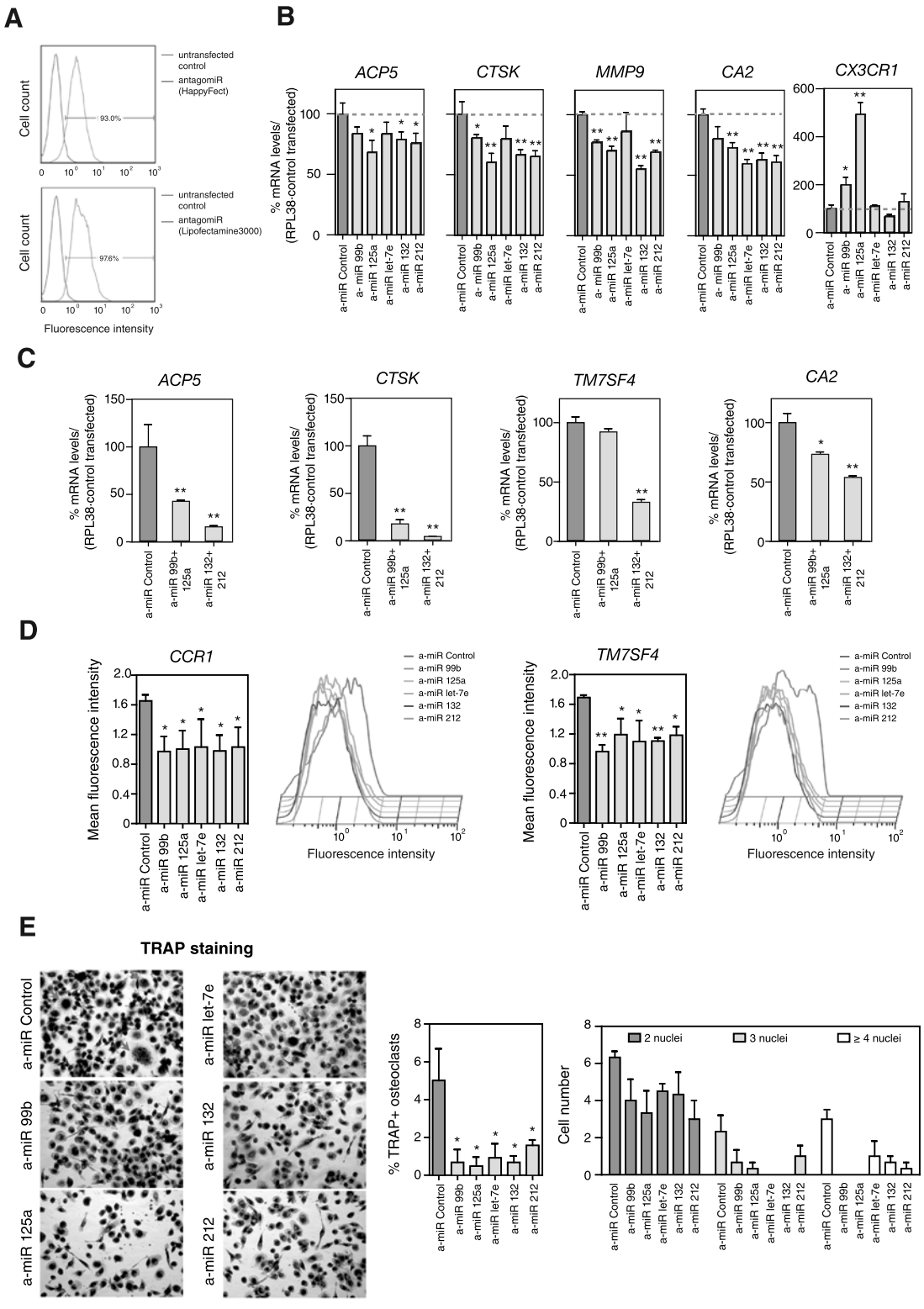

Figure 2 (See legend on next page.)

(See figure on previous page.)
Figure 2 Influence of miRNAs in modulating monocyte-to-osteoclast differentiation. (A) Quantification by flow cytometry of the transfection efficiency using a fluorescent control power inhibitor or antagomir. **(B)** Functional effect of miRNA inhibition using power inhibitors (or antagomirs) for the individual miRNAs in the miR-99b/125a/let7e and miR-132/212 clusters on *CA2*, *CTSK*, *MMP9*, *ACP5* and *CX3CR1* expression levels 4 days after M-CSF/RANL stimulation. Quantification was done using qRT-PCR with specific primers for each gene and using the *RPL38* gene for normalization. **(C)** Functional effect of miRNA inhibition using double transfections with power inhibitors for two miRNAs within the miR-99b/125a/let7e and miR-132/212 clusters. Quantification was carried out using qRT-PCR with specific primers for each gene and using the *RPL38* gene for normalization. **(D)** Effect of miRNA inhibition on the levels of surface markers CCR1 and TM7SF4. A bar diagram summarizing the results of the individual inhibition of each miRNA of the two clusters is presented. Also, a plot of the fluorescence-activated cell sorting (FACS) analysis is presented. **(E)** Effect of miRNA inhibition on the ability of cells to differentiate in OCs. Cells were arrested at 4 days after inducing differentiation. OCs were stained with TRAP. Cells with three or more nuclei were counted as OCs. In the images, multinuclear OCs are indicated with a red arrow. On the right, a bar diagram showing the percentage of OCs under each condition (center) and a bar diagram showing the number of cells with two, three or four or more nuclei under each condition (right). Error bars correspond to the standard deviation of three independent measurements; *corresponds to P-value <0.05; **means P-value <0.01.

(*P*-value 1.69 E-11) and cytokine production (*P*-value 3.04 E-11). We identified a number of critical factors from among these (Figure 3C). For instance, miR-99b was found to target the 3′ UTRs of *IGF1R*, miR-125a targeted *ETV6*, *TNFAIP3* and *CX3CR1*, and let7e targeted *TNFAIP3* and *ITGA4*. In the case of the miRNAs in the miR-212/132 cluster, miR-212 was found to target *CX3CR1* and *HBEGF*, and miR-132 targeted *IRF1* and *NR4A2*. Some of these genes are also silenced by other mechanisms during OC differentiation. Two examples are the MO-specific gene *CX3CR1* and the anti-inflammatory gene *TNFAIP3*, which are rapidly silenced after MCSF/RANKL stimulation, and their promoters are hypermethylated [33].

To validate the putative targets, we performed luciferase reporter assays using a vector containing the renilla luciferase coding region plus the wild type or a mutant form (Mut) of the putative 3′ UTR target sites of each potentially targeted gene. We carried out these assays in HeLa cells, in which we had previously estimated the expression of high levels of miRNAs of the miR-99b/let-7e/125a and miR-212/132 clusters. These assays confirmed that miR-99b targets *IGF1R*, miR-125a targets *TNFAIP3*, and let-7e targets *ITGA4* and *THBS1*. On the other hand, miR-132 targets *PTGS2*, and miR-212 also targets *PTGS2* and *IL15* (Figure 3D).

To obtain further evidence of the *in vivo* effect of the miRNAs on their putative targets, we performed qRT-PCR and western blotting in MOs transfected with each of the miRNA inhibitors. In the case of the miR-99b/let-7e/125a cluster, inhibition of miR-99, miR-125a and let-7e resulted in the specific upregulation of *IGF1R*, *TNFAIP3* and *IGF1R*, and of *ITGA4* and *THBS1*, respectively. With respect to the miR-212/132 cluster, inhibition of miR-132 and miR-212 gave rise to the upregulation of *PTGS2* and the inhibition of miR-212 resulted in the upregulation of *IL15* (Figure 3E). We also observed crossover effects between some miRNAs and targets. For instance, inhibition of miR-99b and miR-125a also affected *PTGS2*, which was not validated in luciferase assays but also contains putative recognition sites at its 3′ UTR for miR-99b and miR-125. We observed increased mRNA and protein levels for some of these targets in double transfection experiments with antagomirs (Figure 3F). Together with the luciferase assays, all these results confirmed the essential role of the miRNAs in the downregulation of these genes during OC differentiation.

Changes in the miRNA cluster expression levels in related inflammatory-driven monocyte differentiation processes

We also investigated whether the observed miRNA expression changes occurring in OC differentiation constitute a more general regulatory mechanism also operating in another two related differentiation processes involving MOs, specifically MO-to-dendritic cell differentiation and MO-to-macrophage differentiation. These two processes are triggered following stimulation with granulocyte-macrophage CSF/IL4 or granulocyte-macrophage CSF alone (Figure 4A). Analysis of the expression changes of all miRNAs within the miR-99b/let-7e/125a and miR-212/132 clusters showed these are common to all three processes (Figure 4B). Specifically, we observed that all these miRNAs increased more markedly in macrophages than in dendritic cells, suggesting a bias towards the ability to generate a strong NF-κB-mediated response, such as TLR4-initiated signals occurring in inflammatory macrophages. Given the negative relationship between these miRNAs and the regulation of their targets, it is feasible that they have a key role in the extinction of mRNAs that are characteristic of a less inflammatory prone state. This prompted us to investigate the relationship between the increase in these miRNAs and the expression levels of their validated targets in MO-to-dendritic cell and MO-to-macrophage differentiation. We also noted a decrease in the mRNA levels of *TNFAIP3*, *ITGA4*, *THBS*, *IL5*, and *PTGS2* during the three differentiation processes (Figure 4C). The only exception was *IGF1R*, which appeared to increase over time in OC and dendritic cell differentiation, consistent with the findings of others [34]. This could perhaps be due to the predominant effect of other regulatory mechanisms, probably at the transcription level (Figure 4C). In this case, the

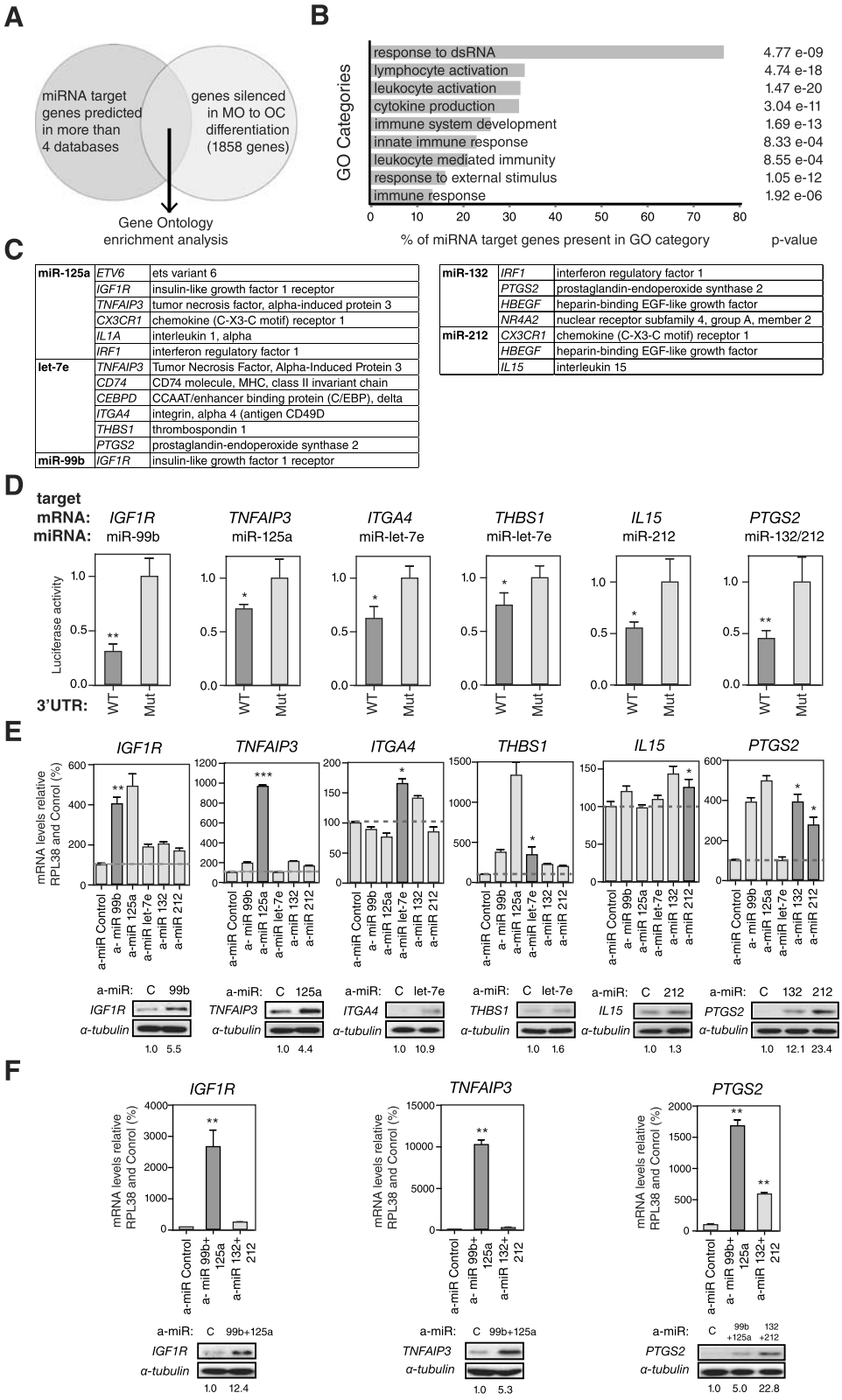

Figure 3 (See legend on next page.)

(See figure on previous page.)
Figure 3 Analysis of miRNA targets. (A) Venn diagram summarizing the rationale for selecting putative miRNA targets by combining the lists generated with prediction algorithms with those generated from expression datasets (1,858 genes with a fold change <0.5). **(B)** Gene Ontology (GO) enrichment analysis of putative miRNA targets from the previous analysis. **(C)** Summary of putative targets and their corresponding miRNA matches among the miR-99b/125a/let7e and miR-132/212 clusters. **(D)** Luciferase assays of HeLa cells cotransfected with different luciferase reporter psiCheck2 constructs containing the 3' UTR of putative targeted transcription factors (wild type (WT) or mutant (Mut) forms). **(E)** Effects on validated targets of the single transfection with miRNA power inhibitors in MOs 4 days after being stimulated with RANKL/M-CSF, as assessed by qRT-PCR and western blotting. Expression data are relative to the levels obtained for the samples transfected with control power inhibitor or antagomir (a-miR) and are normalized to the *RPL38* gene. Protein data have been normalized against α-tubulin, using the sample transfected with the control power inhibitor as a reference. At the bottom, quantification of the levels of protein relative to the control for each antagomir. **(F)** Effects on validated targets of the double transfection with miRNA power inhibitors in MOs 4 days after being stimulated with RANKL/M-CSF, as assessed by qRT-PCR and western blotting. Data analyzed as above. Error bars correspond to standard deviation of three independent experiments; *corresponds to P-value <0.05; **means P-value <0.01; ***means P-value < 0.001.

upregulation of miR-99b, which targets *IGF1R*, could be related more to fine-tuning regulation in order to achieve the proper levels of this protein instead of blocking the expression of it.

A direct role for NF-κB in the upregulation of miRNAs?

Our results supported the notion that miRNAs play a role in the efficiency of OC differentiation and enabled us to identify two upregulated miRNA clusters whose participation in downregulating genes is key to this process. As explained above, MO-to-OC differentiation is induced by RANKL, which ultimately stimulates NF-κB, a transcription factor once it has been translocated into the nucleus. NF-κB acts in concert with PU.1, Jun and the OC-specific transcription factor NFATc1. NF-κB helps regulate many OC-specific genes. The transcription factor NF-κB is also likely to participate in shutting down MO-specific genes through the activation of miRNAs. To explore the potential involvement of NF-κB in the changes in miRNAs during MO-to-OC differentiation, we first investigated the enrichment of the consensus binding site for the p65 NF-κB subunit in a window of 500 bp upstream and downstream of the TSS of the miRNAs (determined from the miRStart database) [35]. This analysis showed that the p65 NF-κB consensus binding site is present in the majority of miRNA TSSs, including the miRNAs within the miR-99b/let-7e/125a and miR-212/132 clusters (Figure 5A). We then investigated the presence of p65 NF-κB around the TSSs of these two miRNA clusters by performing chromatin immunoprecipitation (ChIP) assays with anti-p65 antibodies in MOs before and 48 h and 96 h after induction with RANKL/M-CSF. We also used primers near the TSS of *CCL5* as a positive control. We noted specific enrichment of p65 at 48 h and 96 h after RANKL/M-CSF stimulation in the two upregulated miRNA clusters (Figure 5B), demonstrating a direct association of NF-κB p65 with the encoding sequence of the upregulated miRNAs. We also found that p65 bound near the TSSs of other miRNAs, such as miR-34a (Figure 5B), suggesting that this may be a general mechanism of miRNA upregulation in OC differentiation.

To investigate the involvement of the NF-κB pathway in the activation of these miRNAs in greater depth, we treated MOs with two NF-κB inhibitors, Bay 11-7082 and sodium aurothiomalate (SATM), and investigated the effects on the expression of the aforementioned miRNAs following induction by RANKL/M-CSF. SATM inhibits the activity of IκB kinase by modifying cysteine residues within its catalytic domain. Bay 11-7082 selectively and irreversibly inhibits the tumor necrosis factor-α-inducible phosphorylation of IκBα, resulting in reduced expression of NF-κB and adhesion molecules. Both inhibitors eventually reduce the levels of phosphorylated Ser536 of p65, which correspond to its active form. To test the toxicity of these two inhibitors, we first performed MTT assays over a wide range of concentrations with primary MOs (not shown), and selected 10 μM for Bay 11-7082 and 100 μM for SATM. Consistent with a relevant role of the NF-κB pathway in the activation of these miRNAs, we observed that phosphorylation of p65 increases following RANKL/M-CSF stimulation of MOs (Figure 5C). Under our conditions we observed potent inhibition of p65, as reflected by the reduced levels of phospho-Ser536 p65, especially at 2 days, whereas at 4 days the inhibitory effects of Bay 11-7082 were significantly reduced, perhaps due to its instability in the culture medium (Figure 5C). We then investigated the effects of these two inhibitors on miRNA expression. Both inhibitors decreased expression of upregulated miRNAs (Figure 5D), reinforcing the notion of the direct role of NF-κB in mediating their upregulation. Consistent with the results obtained with the western blotting (Figure 5C), the reduction in miRNA upregulation was more obvious only at 2 days, whereas at 4 days the miRNAs of cells treated with Bay 11-7082 had reached the levels of cells treated with the vehicle. As mentioned above, this is perhaps due to the stability of the inhibitors in the culture medium, which are added only at the beginning. It could also be due to the contribution of additional regulatory mechanisms that could be compensating for the inhibition of the NF-κB pathway. We also checked the

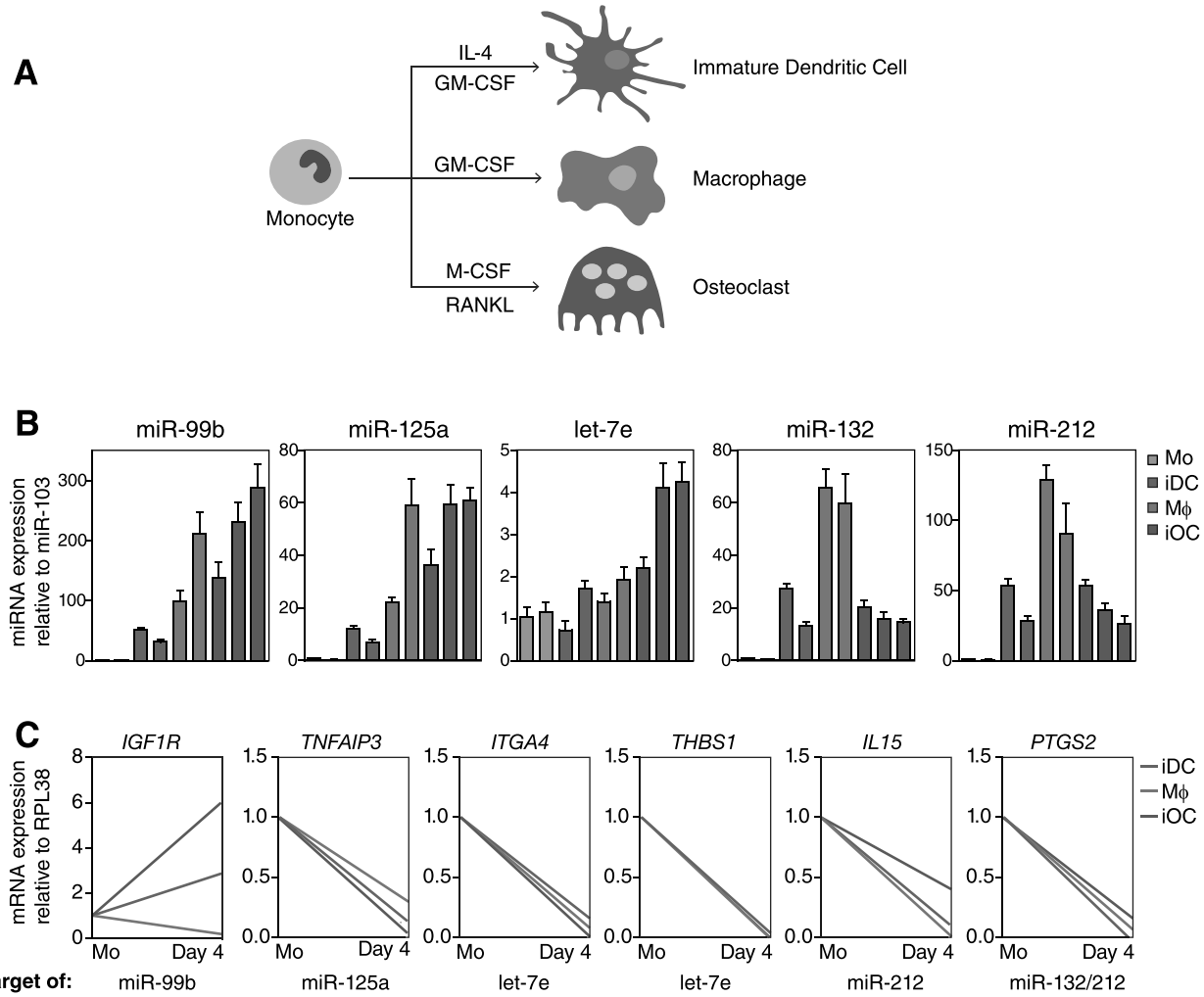

Figure 4 Comparison of changes in the expression levels of the miRNAs within the miR-99b/125a/let7e and miR-132/212 clusters during osteoclast differentiation, and changes during monocyte-to-macrophage and monocyte-to-dendritic cell differentiation. (A) Diagram depicting the three differentiation models used in this experiment. GM-CSF, granulocyte-macrophage colony-stimulating factor. **(B)** Relative expression levels of the miRNAs in matching samples of MOs (grey), immature dendritic cells (iDC, red), macrophages (green,) and monocytes stimulated with RANKL/M-CSF after 1, 2 and 4 days (immature OCs (iOC) (blue)). qRT-PCR data were normalized with respect to miR-103. **(C)** Relative expression levels of miRNA targets in the same set of samples. qRT-PCR data were normalized with respect to the *RPL38* gene. Error bars correspond to standard deviation of three independent measurements.

effects on both classical OC markers and miRNA-validated targets. The two inhibitors reduced the levels of OC markers, as determined by qRT-PCR after 4 days (Figure 5E). Conversely, both SATM and Bay 11-7082 had an overall positive effect on miRNA targets, providing evidence that NF-κB helps repress these targets through miRNAs (Figure 5F). We observed different effects in terms of which of the two drugs was more effective or whether the effect was more evident at 2 or 4 days, but we cannot discard the occurrence of pleiotropic effects, or interference with other regulatory mechanisms.

Therefore, as an unequivocal test of a potential causal relationship between NF-κB and miRNA expression changes in MO-to-OC differentiation, we investigated the consequences of ablating p65 expression in MOs. To this end, we downregulated p65 levels in MOs using transient transfection experiments with a small interfering RNA (siRNA) that targets exon 11 of p65 (Figure 6A). In parallel, we used a control siRNA. Following transfection we stimulated differentiation with RANKL/M-CSF. Under these conditions, we used qRT-PCR and western blotting to check the effects on p65 levels 1, 2 and 4 days after RANKL/M-CSF stimulation of MOs. By this means, we were able to confirm that the level of p65 downregulation was close to 50% (Figure 6A). siRNA-mediated downregulation of p65 resulted in decreased binding of the miRNAs to TSSs (Figure 6B). We also examined the expression levels of these miRNAs following p65 depletion and found that the RANKL/M-CSF-stimulated upregulation of the miRNAs within the miR-99b/let-7e/125a cluster was

A

p65 binding site presence

NF-kB (V$NFKAPPAB65_01)

miRNA	Chr	Position range	
hsa-miR-126	chr9	139559224	139561224
hsa-let-7e	chr19	52190897	52192897
hsa-miR-125a-5p	chr19	52190897	52192897
hsa-miR-132	chr17	1959152	1961152
hsa-miR-146b-5p	chr10	104178511	104180511
hsa-miR-147	chr9	123018092	123020092
hsa-miR-155	chr21	26945292	26947292
hsa-miR-181d	chr19	13975434	13977434
hsa-miR-199a-5p	chr19	10929651	10931651
hsa-miR-212	chr17	1959152	1961152
hsa-miR-22	chr17	1613805	1615805
hsa-miR-29a	chr7	130595983	130597983
hsa-miR-338-3p	chr17	79090096	79092096
hsa-miR-34a	chr1	9258025	9260025
hsa-miR-365	chr16	14395078	14397078
hsa-miR-370	chr14	101355633	101357633
hsa-miR-409-3p	chr14	101490439	101492439
hsa-miR-449a	chr5	54468005	54470005
hsa-miR-502-5p	chrX	49686225	49688225
hsa-miR-584	chr5	148441737	148443737
hsa-miR-598	chr8	11057875	11059875
hsa-miR-665	chr14	101316552	101318552
hsa-miR-9	chr1	156399493	156401493
hsa-miR-99b	chr19	52190897	52192897

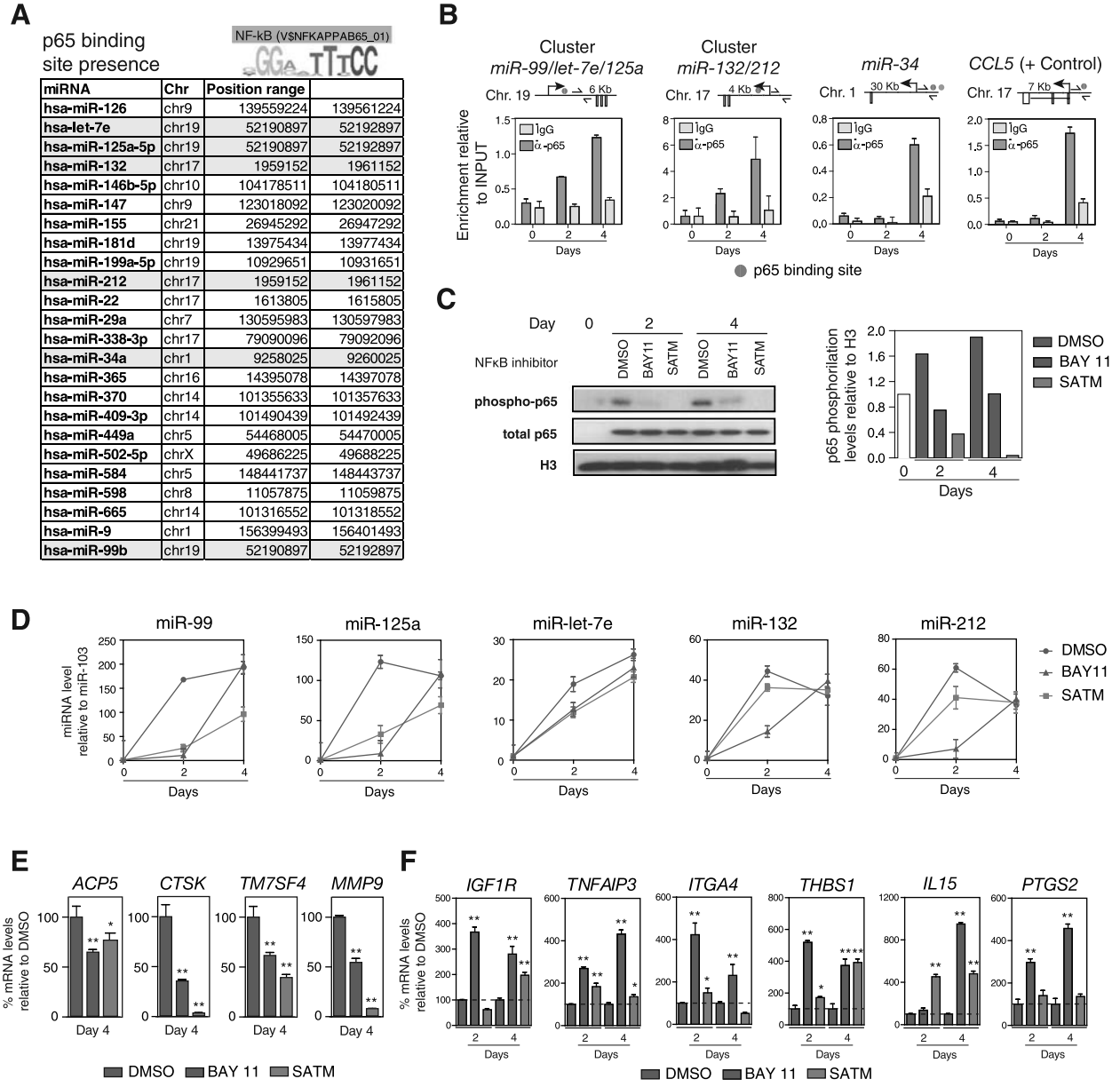

Figure 5 NF-κB dependence of miRNA expression changes. (A) Analysis of the presence of NF-κB subunit binding motifs (from TRANSFAC database) in a 1,000-bp window centered around the estimated TSS of the miRNAs. **(B)** ChIP assays for selected miRNAs showing the binding of NF-κB p65 near the TSS 2 and 4 days after RANKL/M-CSF stimulation of MOs. Each graph contains the relative enrichment of samples immunoprecipitated with the anti-p65 antibody and an IgG as a control. MO samples were tested at 0, 2 and 4 days after M-CSF/RANKL stimulation. On top of each graph the sequence analyzed is indicated. p65 putative binding sites are indicated with a blue dot. Primers used for amplification are indicated with arrows around p65 binding sites. **(C)** Effects of the two NF-κB inhibitors (10 μM BAY 11-7082 (BAY11) and 100 μM sodium aurothiomalate (SATM) on the phosphorylation levels of p65 as determined by western blotting. p65 and H3 total levels are used as controls. **(D)** Effects of two NF-κB inhibitors (BAY11 and SATM) on the levels of miRNAs within the miR-99b/125a/let7e and miR-132/212 clusters measured by a time-course analysis of MOs stimulated with RANKL/M-CSF. **(E)** Effects of treatment with BAY11 and SATM on markers of OC differentiation (*ACP5*, *CTSK*, *TM7SF4*, *MMP9*) as estimated by qRT-PCR. Data relative to DMSO-treated samples and normalized with *RPL38* expression levels. **(F)** Effects of treatment with BAY 11 and SATM on miRNA targets (*IGF1R*, *TNFAIP3*, *ITGA4*, *THBS*, *IL15* and *PTGS2*) as estimated by qRT-PCR. Data are relative to DMSO-treated samples and are normalized with respect to *RPL38* expression levels. Error bars correspond to the standard deviation of three independent measurements; *corresponds to *P*-value <0.05; **means *P*-value <0.01.

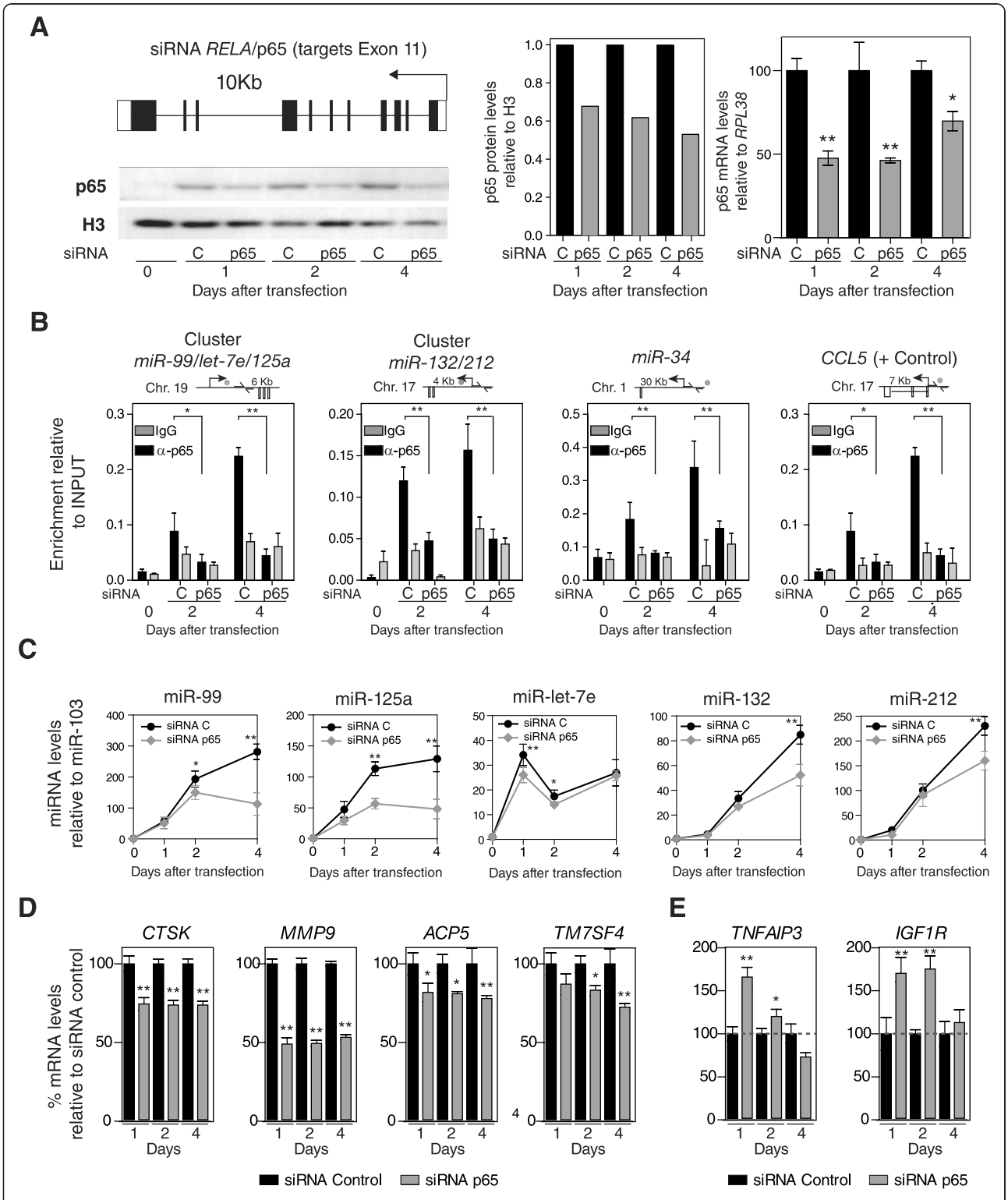

Figure 6 (See legend on next page.)

(See figure on previous page.)
Figure 6 NF-κB p65 has a direct role in changes in miRNA expression levels. (A) Diagram depicting the region of the p65 gene in exon 11 targeted by the siRNA used in this study. Effects of siRNA experiments on p65 levels in MOs stimulated with RANKL/M-CSF after 1, 2, and 4 days, as analyzed by western blotting (bottom and central panels, normalized with respect to histone H3 levels) and qRT-PCR (left panel, relative to RPL38 expression levels). **(B)** Effect of p65 depletion on its recruitment near the TSS of the coding sequence of the miRNAs, as demonstrated by ChIP assays. The scheme on top of each graph depicts the region analyzed, indicating the p65 binding site (dot) and the primers used (arrows around the p65 binding site). **(C)** Effects of p65 siRNA experiments on miR-99b, miR-125a and miR-let7e after 1, 2, and 4 days. Data relative to miR-103 levels. **(D)** Effects of p65 downregulation on expression of genes upregulated during osteoclastogenesis (*CTSK*, *MMP9*, *ACP5*, *TM7SF4*). **(E)** Effects of p65 downregulation on the levels of the miRNA targets *TNFAIP3* and *IGF1R*. Expression data compared with MO samples treated with control siRNA and values relative to *RPL38* expression levels. Error bars correspond to the standard deviation of three independent measurements; *corresponds to *P*-value <0.05; **means *P*-value <0.01.

partially impaired following p65 depletion (Figure 6C). We also analyzed two miRNAs that are not direct p65 targets and observed no effect on their levels following p65 depletion (not shown).

We investigated the effects of depleting p65 on the expression of OC markers (*ACP5*, *CTSK* and *TM7SF4*) as well as on miRNA targets. Whereas depletion of p65 led to a decrease in the upregulation of OC markers (Figure 6D), it resulted in an increase in miRNA targets (Figure 6E), thereby confirming the direct role of p65 in regulating this process.

Taken together, our findings are the first demonstration that NF-κB is directly associated with and activates miRNAs that are essential for the regulation of critical targets whose downregulation is essential for proper OC differentiation.

Discussion

Our results provide novel insights into the role and mechanisms of the fine-tuned control of expression and its relation with inflammatory pathways in MO-to-OC differentiation. Firstly, we identified a set of miRNAs that are required for OC differentiation. Most importantly, these miRNAs target and repress OC-inappropriate genes, including several MO-specific and immunomodulatory genes. Secondly, our results reinforce the key role of the NF-κB transcription factor as a direct regulator of miRNA upregulation, specifically focusing on the miR-99b/let-7e/125a and miR-212/132 clusters.

Screening miRNA expression changes at two points during differentiation revealed different groups of miRNAs based on their expression profiles over time. Overall, our data show prevalent upregulation of miRNAs in OC differentiation. Twenty-three miRNAs displayed fast upregulation followed by sustained expression levels, 20 miRNAs had a rapid increase followed by downregulation over a longer period following induction until day 21, and 26 miRNAs were upregulated only at later stages. In contrast, there were significantly fewer miRNAs whose expression levels decreased over time. The predominance of upregulated miRNAs may suggest that their primary role is to repress or ensure the maintenance of low levels of OC-inappropriate genes that could also be repressed through other mechanisms. Previous data from our group have already shown this type of behavior in B cell-to-macrophage transdifferentiation [36]. Our analysis of the functional effects of the depletion of the miRNAs within the miR-99b/let-7e/125a and miR-212/132 clusters, as well the analysis of their targets, shows that these molecules have a direct role in repressing MO-specific and immunomodulatory genes like *TNFAIP3*, *IGF1R* and *IL15*. In addition, loss of function experiments using specific inhibitors for the above miRNAs influences the efficiency of osteoclastogenesis, as determined by analyzing expression changes of standard markers of OC differentiation at the RNA and protein levels, the effects on validated targets of these miRNAs and the ability of cells to fuse to yield multinucleated OCs.

Our results suggest that fine-tuning modulation through miRNA-mediated repression drives the monocytic steady state program into an NF-κB-driven proinflammatory differentiation program. This idea is reinforced by the observation that the upregulation of these miRNAs also occurs in related inflammatory-related monocytic differentiation processes, including MO-to-dendritic cell differentiation and MO-to-macrophage differentiation. MOs are heterogeneous circulating progenitors that can either patrol the resting endothelium or migrate into tissues in response to inflammatory signals. Regulation of switching between these different states requires the ability to respond rapidly to changes that may include silencing of undesired response pathways, and the commitment to ensure proper outcomes. miRNAs may contribute to this process as a flexible regulatory mechanism, as it has been described for miR146a and Relb pathway Ly6Chigh inflammatory MO responses [37]. Our analysis on the functional effects of depletion of the miRNAs within the miR-99b/let-7e/125a cluster reveals a possible common pathway of commitment into cells with strong NF-κB-dependent responses, suggesting the targeting of the anti-inflammatory molecule TNFAIP3 (A20) by these microRNAs, which are upregulated in the conversion into OCs, dendritics cells and macrophages. In addition, depletion of the miR-212/132 cluster, as well as the analysis of their targets, shows that these elements have a

direct role in repressing genes like *IRF1* or *IL15*, which could also shape inflammation.

Ly6Chigh MO conversion to Ly6Clo anti-inflammatory macrophages with a restorative phenotype in murine hepatic fibrosis requires the upregulation of genes encoding molecules of the anti-inflammatory macrophage program, like *CX3CR1*, or with anti-fibrotic effects, like *CD74* [38]. Interestingly, both genes are targeted by the miR-212/132 cluster in our MO-based differentiation models that converge on the set-up of inflammatory or NF-κB programs in different cell types. In addition, an immunosuppresive role has also been assigned to the IGF1R-IGF1 axis, and cord blood mononuclear cells as well as peripheral blood mononuclear cells (PBMCs) treated with IGF1 show a decrease NF-κB binding activity [39]. Our results show that *IGF1R* is targeted by miR99b and miR125a also suggesting a coordinated shutdown of signal transduction that block NF-κB pathways.

The second major conclusion of our study is the role of NF-κB in directly upregulating the miR-212/132 and miR-99b/let-7e/125a clusters, and perhaps other miRNAs. Multiple genes implicated in inflammation, including pro-inflammatory cytokines and their receptors, are under the transcriptional control of the transcription factor NF-κB [40]. A few reports have recently proved that NF-κB has a direct role in regulating miRNA expression [41,42]. To the best of our knowledge, however, this is the first report demonstrating a direct role for NF-κB in miRNA control in OC differentiation. NF-κB is a major target of RANKL, which is used together with M-CSF to stimulate differentiation of MOs into OCs. However, only a few direct NF-κB targets have so far been described. For instance, it has been shown that NF-κB cooperates with NFATc2 to induce expression of NFATc1, with NFkB p50 and p65 being recruited to the NFATc1 promoter within 1 hour of treatment of OCPs with RANKL, resulting in transient auto-amplification of NFATc1 expression, which is crucial for OC formation [14]. To date, the participation of NF-κB in this context had been restricted to an activator of genes that are necessary for OC differentiation. Our findings reveal a novel role for NF-κB in activating miRNAs that repress the expression of OC-inappropriate genes that are not required for differentiation. This perhaps includes not only MO-to-OC differentiation, but also other related MO-related differentiation processes where NF-κB plays a key role. Several papers have come out showing regulatory programs of Ly6Chigh inflammatory MOs/macrophages versus Ly6Clo resting cells [37,38,43]. Nonetheless, unraveling the mechanisms that delineate NF-κB versus other programs in human MOs has been more difficult and this issue is directly addressed by the present work.

The results of our study constitute the first clear evidence that NF-κB directly regulates miRNAs, showing together with our findings on the miRNA targets and the impact on OC differentiation that this is a novel mechanism of gene repression of OC-inappropriate genes in this differentiation process. In addition, our conclusions open up possibilities for exploiting novel pathways for therapeutic intervention.

Conclusions

Our study on miRNA expression changes during MO-to-OC differentiation reveals the occurrence of rapid upregulation of two miRNA clusters. We have demonstrated that miRNAs within these two clusters are necessary for MOs to differentiate into OCs. These miRNAs are key to repressing OC-inappropriate genes, including certain anti-inflammatory genes, and are needed for proper OC differentiation. We demonstrate that these changes and their functional effects also occur in other MO differentiation processes, indicating that these miRNAs are needed for the downregulation of OC-inappropriate genes in MOs. Most importantly, we demonstrate for the first time that NF-κB directly regulates these miRNAs and is thus directly implicated in the inhibition of the less differentiated monocytic expression program.

Materials and methods

Differentiation of osteoclasts from peripheral blood mononuclear cells

Human blood samples came from anonymous blood donors through the Catalan Blood and Tissue Bank in Barcelona as thrombocyte concentrates (buffy coats). The anonymous blood donors received oral and written information about the possibility that their blood would be used for research purposes, and any questions that arose were then answered. Before giving their first blood sample the donors signed a consent form at the Banc de Teixits, which adheres to the principles set out in the WMA Declaration of Helsinki. The blood was carefully layered on a Ficoll-Paque gradient (Amersham, Buckinghamshire, UK) and centrifuged at 2,000 rpm for 30 minutes without braking. After centrifugation, PBMCs at the interface between the plasma and the Ficoll-Paque gradient were collected and washed twice with ice-cold phosphate-buffered saline, followed by centrifugation at 2,000 rpm for 5 minutes. Pure CD14+ cells were isolated from PBMCs using positive selection with MACS magnetic CD14 antibody (Miltenyi Biotec, Bergisch Gladbach, Germany). Cells were then resuspended in α-minimal essential medium (α-MEM GlutaMAX Supplement, no nucleosides; Invitrogen, Carlsbad, CA, USA) containing 10% fetal bovine serum, 100 units/ml penicillin, 100 μg/ml streptomycin and antimycotic, supplemented with 25 ng/ml human M-CSF and 50 ng/ml soluble hRANKL (PeproTech EC, London, UK). Depending on the amount needed, cells were seeded at a density of 3×10^5 cells/well in 96-well plates, 5×10^6 cells/well in 6-well plates or 40×10^6 cells in 10-mm plates and cultured for 21 days

(unless otherwise noted); media and cytokines were changed twice a week. The presence of OCs was checked by TRAP staining using the Leukocyte Acid Phosphatase Assay Kit (Sigma-Aldrich, St. Louis, Missouri, USA) according to the manufacturer s instructions. Phalloidin/DAPI staining enabled us to confirm that the populations were highly enriched in multinuclear cells, some of which contained more than 40 nuclei. We used several methods to determine that on day 21 almost 85% of the nuclei detected were osteoclastic nuclei (in polykaryons; nuclei, rather than cells, were quantified). OCs (TRAP-positive cells with three or more nuclei) were also analyzed at the mRNA level: upregulation of key OC markers (*CA2*, *CTSK*, *MMP9*, *ACP5/TRAP* and *TM7SF4/DCSTAMP*) and downregulation of the MO marker *CX3CR1* were confirmed.

Visualization of osteoclasts with phalloidin and DAPI staining

Pure isolated CD14+ cells were seeded and cultured in glass Lab-Tek Chamber Slides (Thermo Fisher Scientific, Waltham, MA, USA) for 21 days in the presence of human M-CSF and human RANKL. OCs were then washed twice with phosphate-buffered saline and fixed (3.7% paraformaldehyde, 15 minutes). Cells were permeabilized with 0.1% (V/V) Triton X-100 for 5 minutes and stained for F-actin with 5 U/ml Alexa Fluor® 647-Phalloidin (Invitrogen). Cells were then mounted in Mowiol-DAPI mounting medium. Cultures were visualized by confocal laser scanning microscopy (Leica TCP SP2 AOBS confocal microscope).

Flow cytometry

Cells were stained with fluorochrome-conjugated antibodies against CCR1 (R&D Systems, reference FAB145A-100) and TM7SF4 (R&D Systems, reference FAB7824-A) (Both antibodies are from R&D Systems, Minneapolis, MN, USA) 0 and 4 days after RANKL/M-CSF stimulation. CCR1 and TM7SF4 expression were monitored on a Gallios Flow Cytometer (Beckman Coulter, Pasadena, California, USA) and analyzed by FlowJo software (Tree Star, Inc., Ashland, Oregon, USA). All experiments were performed in triplicate and bar graphs correspond to independent biological samples.

MicroRNA expression screening and target prediction

Total RNA was extracted with TriPure (Roche, Basel, Switzerland) following the manufacturer s instructions. Ready-to-use miRNA PCR Human Panel I V2.R from Exiqon (reference 203608) was used according to the instruction manual (Exiqon, Vedbeak, Denmark). Total RNA (30 ng) was used for each RT-PCR reaction. Paired samples of MOs at 0 (MO), 2 (OC 48 h) and 21 (OC) days after M-CSF and RANKL stimulation were obtained from three female healthy donors (aged 25 to 28 years), and were analyzed with a Roche LightCycler® 480 real-time PCR system. Results were converted to relative values using the inter-plate calibrators included in the panels ($\log_2$ ratios). Average expression values of MO, OC 48 h and OC were normalized with respect to the reference gene miR-103. A *t*-test was then performed and differentially expressed miRNAs (fold change >2 or <0.5), with a significant *P*-value ($P < 0.05$) in at least one of the comparisons, were selected and represented on a heatmap. The raw expression data are listed in full in Additional file 1. The array expression data were validated in the samples used (validation set), and in a larger cohort of samples obtained from independent donors (replication set) using Exiqon microRNA LNA™ PCR primer sets (hsa-miR-99b-5p, reference 204367; hsa-miR-125a-5p, reference 204339; hsa-miR-132-3p, reference 204129; hsa-miR-212-3p, reference 204170; hsa-miR-103a-3p, reference 204063).

To predict the potential targets of the deregulated miRNAs, we used the algorithms from several databases: TargetScan, PicTar, PITA, miRBase, microRNA.org, miRDB/MirTarget2, TarBase, miRecords and StarBase/CLIPseq. Only targets predicted by at least four of these databases were retained for further analysis.

Bioinformatics analysis of expression data

To compare the expression data with the methylation data, we used CD14+ and OC expression data from the ArrayExpress database [44] (accession EMEXP-2019) from a previous publication [32]. Affymetrix GeneChip Human Genome U133 Plus 2.0 expression data were processed using the limma and affy packages from Bioconductor. The pre-processing stage was divided into three main steps: background correction, normalization and reporter summarization. We chose the expresso function of the affy package for preprocessing. Thus, the robust multi-array average (RMA) method was used for background correction. Quantile normalization was then done. We also introduced a specific step for PM (perfect matchprobes) adjustment, using the PM-only model-based expression index (option pmonly). Finally, for the summarization step, the median polish method was used. Next, variance filtering by IQR (interquartile range) was carried out, taking 0.50 as the threshold value. After preprocessing, data were analyzed using the empirical Bayes moderated *t*-test available in the limma statistics package. Expression data were validated by qRT-PCR.

Transfection of primary human monocytes with miRNA inhibitors and p65 NF-κB siRNA

To perform the miRNA inhibitor experiments, we used unlabeled miRCURY LNA™ microRNA Power inhibitors to inhibit miR-99b (reference 4101513), miR-let-7e (reference 4103550), miR-125a (reference 4103094), miR-

132 (reference 4103093), miR-212 (reference 4104787) or a control (Negative Control A, reference 199006) Exiqon, Vedbaek, Denmark. Power inhibitors (5 or 10 nM) were transfected into CD14+ MOs using HappyFect Transfection Reagent (Tecan, Weymouth, UK) or Lipofectamine ®3000 (Life Technologies). Cells were simultaneously incubated in the presence of RANKL/M-CSF in the conditions previously described. The efficiency of transfection was quantified by flow cytometry using the 5′-fluorescein-labeled Negative Control A. For samples collected at 4 days or after, we added a fresh aliquot of miRNA inhibitors after 48 h. To silence p65, we used Silencer® Select Pre-Designed siRNA (Life Technologies) against human RELA (p65), targeting exon 11 (reference s11916) in parallel with a Silencer® Select negative control in purified CD14+ MOs in the presence of M-CSF, followed by stimulation with RANKL (and M-CSF) 24 h after siRNA transfection. We used Lipofectamine RNAiMAX Transfection Reagent (Invitrogen) for efficient siRNA transfection. mRNA and protein levels were examined by qRT-PCR and western blotting 1, 2, and 4 days after siRNA transfection. These experiments were performed with at least three biological replicates.

Luciferase assays

The putative miRNA binding sites in the 3′ UTRs of *IGF1R*, *TNFAIP3*, *ITGA4*, *THBS1*, *IL15*, and *PTGS2* were amplified by PCR from genomic DNA derived from CD14 + cells. The PCR products were cloned into pGEM®-T Easy Vector (Promega, Madison, Wisconsin, USA) and four to seven point mutations were introduced into each target site by site-directed mutagenesis. Each of the fragments containing the 3′ UTR of putative miRNA binding sites was cloned into psiCHECK-2 vector (Promega). 293 T cells were cultured for 24 h and then co-transfected using lipofectamine RNAimax with 10 ng of psiCHECK-2 vector containing wild-type or mutant 3′ UTR plus 50 nM of miRNA power inhibitors per well. The luciferase analysis was performed 48 h later using the Dual-Luciferase Reporter Assay (Promega). Primers to clone the 3′ UTR of putative miRNA binding sites are listed in Additional file 3.

Chromatin immunoprecipitation assays

For ChIP assays, CD14+ cells 0, 2 and 4 days after treatment with M-CSF and RANKL were crosslinked with 1% formaldehyde and subjected to immunoprecipitation after sonication. ChIP experiments were performed as described elsewhere [33]. Analysis involved real-time qPCR. Data are represented as the ratio of bound fraction to input for each specific factor. We used a mouse monoclonal antibody against the carboxyl terminus of human NF-κB p65 (sc-372, Santa Cruz Biotechnology, Dallas, Texas, USA). Primer sequences are shown in Additional file 3. Experiments included three biological replicates.

Quantitative RT-PCR and western blotting

RNA was isolated by TRIzol extraction (Invitrogen) and reverse-transcribed using SuperScriptTM II Reverse Transcriptase (Invitrogen). Primers for conventional and qRT-PCR were designed using Primer3 v.0.4.0 (Table S1 in Additional file 1). qRT-PCR was performed in triplicate using LightCycler 480 SYBR Green Mix (Roche). PCR reactions were run and analyzed using the LightCycler 480 II System (Roche). Expression values were normalized against the expression of the endogenous gene controls *RPL38*, *HPRT1* and *GAPDH*. Primers are listed in Additional file 3.

For western blots, protein lysates were generated and western blotting performed using standard procedures using antibodies against phospho-Ser536 p65 (Cell Signaling, 3033 Danvers, Massachusetts, USA), p65 (Santa Cruz Biotechnologies, sc-372), IGF1R (Abcam, ab32823, Cambridge, UK), PTGS2 (Abcam, ab15191), TNFAIP3 (Abcam, ab92324), IL15 (Abcam, ab7213), ITGA4 (Abcam, ab81280), THBS1 (Thermo Scientific, MA5-13398), α-tubulin (Sigma, 1142) and total histone 3 (Abcam, ab1791).

Graphs and heatmaps

All graphs were created using Prism5 Graphpad (GraphPad Software, San Diego, California, USA). Heatmaps were generated from expression or methylation data using the Genesis program (Graz University of Technology).

Data access

Raw data for microRNA expression profiling as obtained following qRT-PCR amplification of Ready-to-use microRNA PCR Human Panel I V2.R from Exiqon (reference 203608) is available in Additional file 1. It is also available in NCBI s Gene Expression Omnibus through GEO Series accession number GSE63773.

Additional files

Additional file 1: Raw data of miRNA expression profiling following quantitative RT-PCR (qRT-PCR) amplification of Ready-to-use microRNA PCR Human Panel I V2.R from Exiqon (reference 203608) in a Roche LC480 II corresponding to pure CD14+ cells (MOs), and these cells at 48 h and 21 d after RANKL/M-CSF stimulation from three anonymous individuals (D1, D2 and D3). Data are as follows: RAW crossing point (Cp) values as produced by the qPCR system (columns B, D, F, N, P, R, Z, AB, AD), RAW concentration (Conc) as produced by the qRT-PCR system (columns C, E, G, O, Q, S, AA, AC, AE), concentration values relative to miR103 (housekeeping) levels (columns H, I, J, T, U, V, AF, AG, AH). The average of the three samples for each cell type (MOs, OCs 48 h, OCs 21 d) (column K, W, AI), standard deviation (column L, X, AJ).

Additional file 2: (A) Heatmaps corresponding to putative targets for all miRNAs within the miR-99b/125a/let7e and miR-132/212 clusters using miRWalk. For a given prediction database (DIANAmT, miRanda, miRDB, miRWalk, PICTAR4, PICTAR5, PITA, RNA22, TargetScan)

red corresponds to a positive match and blue indicates that it is not predicted. Only those putative targets predicted with at least four algorithms were used. **(B)** Overlap between the analysis with miRWAlk and expression data [32], using those genes that are downregulated in OC differentiation at least 0.5-fold. **(C)** Schematic representations of the pairing between different miRNAs and the 3′ UTR of different putative target genes.

Additional file 3: Primer sequences.

Abbreviations

bp: base pair; ChIP: chromatin immunoprecipitation; IL: interleukin; M-CSF: macrophage colony-stimulating factor; miRNA: microRNA; MO: monocyte; NF-κB: nuclear factor-kappa B; OC: osteoclast; PBMC: peripheral blood mononuclear cell; qRT-PCR: quantitative RT-PCR; RANKL: receptor activator of nuclear factor kappa-B ligand; SATM: sodium aurothiomalate; siRNA: small interfering RNA; TSS: transcription start site; UTR: untranslated region.

Competing interests

The authors declare that they have no competing interests.

Authors' contributions

LR and EB conceived experiments; LR, AGG, NC, JRU, LC and RVT performed experiments; CC performed biocomputing analysis; LR, AGG, JRU, DAE, MG, CGV and EB analyzed the data; EB wrote the paper. All authors read and approved the final manuscript.

Acknowledgements

We thank Dr Mercedes Garayoa for her helpful suggestions about protocols and providing antibodies. We thank Dr Lluís Espinosa and Dr Anna Bigas for advice on inhibition of the NF-κB pathway and for sharing reagents. We also thank Dr Pura Muñoz-Cánoves and Dr Maribel Parra for critical reading of the manuscript. This work was supported by grant SAF2011-29635 from the Spanish Ministry of Science and Innovation, grant CIVP16A1834 from the Fundación Ramón Areces, and EU FP7 306000 STATegra project. CGV is funded by FIS grant (PI13/00222). LR is supported by a PFIS predoctoral fellowship.

Author details

[1]Chromatin and Disease Group, Cancer Epigenetics and Biology Programme (PEBC), Bellvitge Biomedical Research Institute (IDIBELL), 08908 L'Hospitalet de Llobregat, Barcelona, Spain. [2]Present address: Barts and The London School of Medicine and Dentistry, Centre for Neuroscience & Trauma, Blizard Institute, Queen Mary University of London, 4 Newark Street, London E1 2AT, UK. [3]Rheumatology Service, Bellvitge University Hospital (HUB), 08908 L'Hospitalet de Llobregat, Barcelona, Spain.

Received: 7 November 2014 Accepted: 4 December 2014
Published online: 05 January 2015

References

1. Ambros V: **microRNAs: tiny regulators with great potential.** *Cell* 2001, **107:**823–826.
2. Blair HC, Teitelbaum SL, Ghiselli R, Gluck S: **Osteoclastic bone resorption by a polarized vacuolar proton pump.** *Science* 1989, **245:**855–857.
3. Tolar J, Teitelbaum SL, Orchard PJ: **Osteopetrosis.** *N Engl J Med* 2004, **351:**2839–2849.
4. Rachner TD, Khosla S, Hofbauer LC: **Osteoporosis: now and the future.** *Lancet* 2011, **377:**1276–1287.
5. Scott DL, Wolfe F, Huizinga TW: **Rheumatoid arthritis.** *Lancet* 2010, **376:**1094–1108.
6. Mundy GR, Raisz LG, Cooper RA, Schechter GP, Salmon SE: **Evidence for the secretion of an osteoclast stimulating factor in myeloma.** *N Engl J Med* 1974, **291:**1041–1046.
7. Yoneda T: **Cellular and molecular mechanisms of breast and prostate cancer metastasis to bone.** *Eur J Cancer* 1998, **34:**240–245.
8. Yasuda H, Shima N, Nakagawa N, Yamaguchi K, Kinosaki M, Mochizuki S, Tomoyasu A, Yano K, Goto M, Murakami A, Tsuda E, Morinaga T, Higashio K, Udagawa N, Takahashi N, Suda T: **Osteoclast differentiation factor is a ligand for osteoprotegerin/osteoclastogenesis-inhibitory factor and is identical to TRANCE/RANKL.** *Proc Natl Acad Sci U S A* 1998, **95:**3597–3602.
9. Wiktor-Jedrzejczak W, Bartocci A, Ferrante AW Jr, Ahmed-Ansari A, Sell KW, Pollard JW, Stanley ER: **Total absence of colony-stimulating factor 1 in the macrophage-deficient osteopetrotic (op/op) mouse.** *Proc Natl Acad Sci U S A* 1990, **87:**4828–4832.
10. Lacey DL, Timms E, Tan HL, Kelley MJ, Dunstan CR, Burgess T, Elliott R, Colombero A, Elliott G, Scully S, Hsu H, Sullivan J, Hawkins N, Davy E, Capparelli C, Eli A, Qian YX, Kaufman S, Sarosi I, Shalhoub V, Senaldi G, Guo J, Delaney J, Boyle WJ: **Osteoprotegerin ligand is a cytokine that regulates osteoclast differentiation and activation.** *Cell* 1998, **93:**165–176.
11. Nicholson GC, Malakellis M, Collier FM, Cameron PU, Holloway WR, Gough TJ, Gregorio-King C, Kirkland MA, Myers DE: **Induction of osteoclasts from CD14-positive human peripheral blood mononuclear cells by receptor activator of nuclear factor kappaB ligand (RANKL).** *Clin Sci (Lond)* 2000, **99:**133–140.
12. Saltel F, Chabadel A, Bonnelye E, Jurdic P: **Actin cytoskeletal organisation in osteoclasts: a model to decipher transmigration and matrix degradation.** *Eur J Cell Biol* 2008, **87:**459–468.
13. Ikeda F, Nishimura R, Matsubara T, Tanaka S, Inoue J, Reddy SV, Hata K, Yamashita K, Hiraga T, Watanabe T, Kukita T, Yoshioka K, Rao A, Yoneda T: **Critical roles of c-Jun signaling in regulation of NFAT family and RANKL-regulated osteoclast differentiation.** *J Clin Invest* 2004, **114:**475–484.
14. Takayanagi H, Kim S, Koga T, Nishina H, Isshiki M, Yoshida H, Saiura A, Isobe M, Yokochi T, Inoue J, Wagner EF, Mak TW, Kodama T, Taniguchi T: **Induction and activation of the transcription factor NFATc1 (NFAT2) integrate RANKL signaling in terminal differentiation of osteoclasts.** *Dev Cell* 2002, **3:**889–901.
15. Sharma SM, Bronisz A, Hu R, Patel K, Mansky KC, Sif S, Ostrowski MC: **MITF and PU.1 recruit p38 MAPK and NFATc1 to target genes during osteoclast differentiation.** *J Biol Chem* 2007, **282:**15921–15929.
16. Yu M, Moreno JL, Stains JP, Keegan AD: **Complex regulation of tartrate-resistant acid phosphatase (TRAP) expression by interleukin 4 (IL-4): IL-4 indirectly suppresses receptor activator of NF-kappaB ligand (RANKL)-mediated TRAP expression but modestly induces its expression directly.** *J Biol Chem* 2009, **284:**32968–32979.
17. Matsumoto M, Kogawa M, Wada S, Takayanagi H, Tsujimoto M, Katayama S, Hisatake K, Nogi Y: **Essential role of p38 mitogen-activated protein kinase in cathepsin K gene expression during osteoclastogenesis through association of NFATc1 and PU.1.** *J Biol Chem* 2004, **279:**45969–45979.
18. Kim K, Lee SH, Ha Kim J, Choi Y, Kim N: **NFATc1 induces osteoclast fusion via up-regulation of Atp6v0d2 and the dendritic cell-specific transmembrane protein (DC-STAMP).** *Mol Endocrinol* 2008, **22:**176–185.
19. Sundaram K, Nishimura R, Senn J, Youssef RF, London SD, Reddy SV: **RANK ligand signaling modulates the matrix metalloproteinase-9 gene expression during osteoclast differentiation.** *Exp Cell Res* 2007, **313:**168–178.
20. Mabilleau G, Chappard D, Sabokbar A: **Role of the A20-TRAF6 axis in lipopolysaccharide-mediated osteoclastogenesis.** *J Biol Chem* 2011, **286:**3242–3249.
21. Mizoguchi F, Izu Y, Hayata T, Hemmi H, Nakashima K, Nakamura T, Kato S, Miyasaka N, Ezura Y, Noda M: **Osteoclast-specific Dicer gene deficiency suppresses osteoclastic bone resorption.** *J Cell Biochem* 2010, **109:**866–875.
22. Rossi M, Pitari MR, Amodio N, Di Martino MT, Conforti F, Leone E, Botta C, Paolino FM, Del Giudice T, Iuliano E, Caraglia M, Ferrarini M, Giordano A, Tagliaferri P, Tassone P: **miR-29b negatively regulates human osteoclastic cell differentiation and function: Implications for the treatment of multiple myeloma-related bone disease.** *J Cell Physiol* 2013, **228:**1506–1515.
23. Lee Y, Kim HJ, Park CK, Kim YG, Lee HJ, Kim JY, Kim HH: **MicroRNA-124 regulates osteoclast differentiation.** *Bone* 2013, **56:**383–389.
24. Bluml S, Bonelli M, Niederreiter B, Puchner A, Mayr G, Hayer S, Koenders MI, van den Berg WB, Smolen J, Redlich K: **Essential role of microRNA-155 in the pathogenesis of autoimmune arthritis in mice.** *Arthritis Rheum* 2011, **63:**1281–1288.
25. Zhang J, Zhao H, Chen J, Xia B, Jin Y, Wei W, Shen J, Huang Y: **Interferon-beta-induced miR-155 inhibits osteoclast differentiation by targeting SOCS1 and MITF.** *FEBS Lett* 2012, **586:**3255–3262.
26. Nowak JS, Choudhury NR, de Lima AF, Rappsilber J, Michlewski G: **Lin28a regulates neuronal differentiation and controls miR-9 production.** *Nat Commun* 2014, **5:**3687.

27. Hoshino A, Iimura T, Ueha S, Hanada S, Maruoka Y, Mayahara M, Suzuki K, Imai T, Ito M, Manome Y, Yasuhara M, Kirino T, Yamaguchi A, Matsushima K, Yamamoto K: **Deficiency of chemokine receptor CCR1 causes osteopenia due to impaired functions of osteoclasts and osteoblasts.** *J Biol Chem* 2010, **285:**28826–28837.
28. Kukita T, Wada N, Kukita A, Kakimoto T, Sandra F, Toh K, Nagata K, Iijima T, Horiuchi M, Matsusaki H, Hieshima K, Yoshie O, Nomiyama H: **RANKL-induced DC-STAMP is essential for osteoclastogenesis.** *J Exp Med* 2004, **200:**941–946.
29. Dweep H, Sticht C, Pandey P, Gretz N: **miRWalk–database: prediction of possible miRNA binding sites by 'walking' the genes of three genomes.** *J Biomed Inform* 2011, **44:**839–847.
30. Lewis BP, Burge CB, Bartel DP: **Conserved seed pairing, often flanked by adenosines, indicates that thousands of human genes are microRNA targets.** *Cell* 2005, **120:**15–20.
31. Wang X: **miRDB: a microRNA target prediction and functional annotation database with a wiki interface.** *RNA* 2008, **14:**1012–1017.
32. Gallois A, Lachuer J, Yvert G, Wierinckx A, Brunet F, Rabourdin-Combe C, Delprat C, Jurdic P, Mazzorana M: **Genome-wide expression analyses establish dendritic cells as a new osteoclast precursor able to generate bone-resorbing cells more efficiently than monocytes.** *J Bone Miner Res* 2009, **25:**661–672.
33. de la Rica L, Rodriguez-Ubreva J, Garcia M, Islam AB, Urquiza JM, Hernando H, Christensen J, Helin K, Gomez-Vaquero C, Ballestar E: **PU.1 target genes undergo Tet2-coupled demethylation and DNMT3b-mediated methylation in monocyte-to-osteoclast differentiation.** *Genome Biol* 2013, **14:**R99.
34. Moreaux J, Hose D, Kassambara A, Reme T, Moine P, Requirand G, Goldschmidt H, Klein B: **Osteoclast-gene expression profiling reveals osteoclast-derived CCR2 chemokines promoting myeloma cell migration.** *Blood* 2011, **117:**1280–1290.
35. Chien CH, Sun YM, Chang WC, Chiang-Hsieh PY, Lee TY, Tsai WC, Horng JT, Tsou AP, Huang HD: **Identifying transcriptional start sites of human microRNAs based on high-throughput sequencing data.** *Nucleic Acids Res* 2011, **39:**9345–9356.
36. Rodriguez-Ubreva J, Ciudad L, van Oevelen C, Parra M, Graf T, Ballestar E: **C/EBPa-mediated activation of miR-34a and miR-223 inhibits Lef1 expression to achieve efficient reprogramming into macrophages.** *Mol Cell Biol* 2014, **34:**1145–1157.
37. Etzrodt M, Cortez-Retamozo V, Newton A, Zhao J, Ng A, Wildgruber M, Romero P, Wurdinger T, Xavier R, Geissmann F, Meylan E, Nahrendorf M, Swirski FK, Baltimore D, Weissleder R, Pittet MJ: **Regulation of monocyte functional heterogeneity by miR-146a and Relb.** *Cell Rep* 2012, **1:**317–324.
38. Ramachandran P, Pellicoro A, Vernon MA, Boulter L, Aucott RL, Ali A, Hartland SN, Snowdon VK, Cappon A, Gordon-Walker TT, Williams MJ, Dunbar DR, Manning JR, van Rooijen N, Fallowfield JA, Forbes SJ, Iredale JP: **Differential Ly-6C expression identifies the recruited macrophage phenotype, which orchestrates the regression of murine liver fibrosis.** *Proc Natl Acad Sci U S A* 2012, **109:**E3186–E3195.
39. Puzik A, Rupp J, Troger B, Gopel W, Herting E, Hartel C: **Insulin-like growth factor-I regulates the neonatal immune response in infection and maturation by suppression of IFN-gamma.** *Cytokine* 2012, **60:**369–376.
40. Baeuerle PA, Baltimore D: **NF-kappa B: ten years after.** *Cell* 1996, **87:**13–20.
41. Taganov KD, Boldin MP, Chang KJ, Baltimore D: **NF-kappaB-dependent induction of microRNA miR-146, an inhibitor targeted to signaling proteins of innate immune responses.** *Proc Natl Acad Sci U S A* 2006, **103:**12481–12486.
42. Vento-Tormo R, Rodriguez-Ubreva J, Lisio LD, Islam AB, Urquiza JM, Hernando H, Lopez-Bigas N, Shannon-Lowe C, Martinez N, Montes-Moreno S, Piris MA, Ballestar E: **NF-kappaB directly mediates epigenetic deregulation of common microRNAs in Epstein-Barr virus-mediated transformation of B-cells and in lymphomas.** *Nucleic Acids Res* 2014, **42:**11025–11039.
43. Hanna RN, Shaked I, Hubbeling HG, Punt JA, Wu R, Herrley E, Zaugg C, Pei H, Geissmann F, Ley K, Hedrick CC: **NR4A1 (Nur77) deletion polarizes macrophages toward an inflammatory phenotype and increases atherosclerosis.** *Circ Res* 2012, **110:**416–427.
44. Rustici G, Kolesnikov N, Brandizi M, Burdett T, Dylag M, Emam I, Farne A, Hastings E, Ison J, Keays M, Kurbatova N, Malone J, Mani R, Mupo A, Pedro Pereira R, Pilicheva E, Rung J, Sharma A, Tang YA, Ternent T, Tikhonov A, Welter D, Williams E, Brazma A, Parkinson H, Sarkans U: **ArrayExpress update–trends in database growth and links to data analysis tools.** *Nucleic Acids Res* 2013, doi:10.1093/nar/gks1174. Pubmed ID 23193272.

Published online 08 September 2014 *Nucleic Acids Research, 2014, Vol. 42, No. 17* ***11025–11039***
doi: 10.1093/nar/gku826

NF-κB directly mediates epigenetic deregulation of common microRNAs in Epstein-Barr virus-mediated transformation of B-cells and in lymphomas

Roser Vento-Tormo[1], Javier Rodríguez-Ubreva[1], Lorena Di Lisio[2], Abul B. M. M. K. Islam[3], Jose M. Urquiza[1], Henar Hernando[1], Nuria López-Bigas[4,5], Claire Shannon-Lowe[6], Nerea Martínez[2], Santiago Montes-Moreno[2], Miguel A. Piris[2] and Esteban Ballestar[1,*]

[1]Chromatin and Disease Group, Cancer Epigenetics and Biology Programme (PEBC), Bellvitge Biomedical Research Institute (IDIBELL), 08908 L'Hospitalet de Llobregat, Barcelona, Spain, [2]Pathology Department, Hospital Universitario Marques de Valdecilla, Cancer Genomics, IFIMAV, 39008 Santander, Spain, [3]Department of Genetic Engineering and Biotechnology, University of Dhaka, Dhaka 1000, Bangladesh, [4]Department of Experimental and Health Sciences, Barcelona Biomedical Research Park, Universitat Pompeu Fabra (UPF), 08003 Barcelona, Spain, [5]Catalan Institution for Research and Advanced Studies (ICREA), 08003 Barcelona, Spain and [6]CR-UK Institute for Cancer Studies, University of Birmingham, Birmingham B15 2TT, UK

Received October 31, 2013; Revised August 26, 2014; Accepted September 1, 2014

ABSTRACT

MicroRNAs (miRNAs) have negative effects on gene expression and are major players in cell function in normal and pathological conditions. Epstein-Barr virus (EBV) infection of resting B lymphocytes results in their growth transformation and associates with different B cell lymphomas. EBV-mediated B cell transformation involves large changes in gene expression, including cellular miRNAs. We performed miRNA expression analysis in growth transformation of EBV-infected B cells. We observed predominant downregulation of miRNAs and upregulation of a few miRNAs. We observed similar profiles of miRNA expression in B cells stimulated with CD40L/IL-4, and those infected with EBNA-2- and LMP-1-deficient EBV particles, suggesting the implication of the NF-kB pathway, common to all four situations. In fact, the NF-kB subunit p65 associates with the transcription start site (TSS) of both upregulated and downregulated miRNAs following EBV infection This occurs together with changes at histone H3K27me3 and histone H3K4me3. Inhibition of the NF-kB pathway impairs changes in miRNA expression, NF-kB binding and changes at the above histone modifications near the TSS of these miRNA genes. Changes in expression of these miRNAs also occurred in diffuse large B cell lymphomas (DLBCL), which are strongly NF-kB dependent. Our results highlight the relevance of the NF-kB pathway in epigenetically mediated miRNA control in B cell transformation and DLBCL.

INTRODUCTION

The Epstein-Barr virus (EBV) is one of the best studied oncogenic human herpesvirus. The vast majority of the human population is infected by EBV. Fortunately, the most common pattern of EBV infection is a clinically silent childhood infection and, generally, EBV establishes a permanent latent infection without further complications. However, EBV has oncogenic potential, reflected by its ability to growth transform B lymphocytes *in vivo*. EBV is associated with different tumors, including several B cell lymphomas, and carcinomas of the stomach and the nasopharyngeal cavity. EBV is considered to play a causative role in Burkitt lymphomas although the mechanism remains elusive (1). EBV has a less strict association with Hodgkin's lymphoma and diffuse large B cell lymphoma (DLBCL). However, the great prevalence of these latter two lymphoma types makes the study of the changes associated with EBV infection of B-cells and biology particularly relevant to our understanding of lymphoma pathogenesis.

In vitro, EBV efficiently immortalizes primary resting B lymphocytes (RBLs), converting them into permanently growing lymphoblastoid cell lines (LCLs). *In vitro* infection results in the activation of a specific viral gene expression program that involves expression of six nuclear antigens (EBNA-1, -2, 3A, -3B, -3C and -LP), three membrane proteins (LMP-1, -2A and -2B) and a set of 25 microRNAs (miRNAs). Five of these proteins and several of the miRNAs are essential for transformation. For instance, LMP-1

*To whom correspondence should be addressed. Tel: +34 932607133; Fax: +34 932607219; Email: eballestar@idibell.cat

is required to establish cell transformation *in vitro* (2) and is required for continuous proliferation (3). It has also been reported that members of the EBV miRNA cluster cooperate to transform B lymphocytes (4). Infection of B cells with EBV is similar to the physiological stimulation with CD40L plus IL-4 (5), T cell-derived mitogens and in both cases involves the activation of the NF-kB pathway. Dissection of the cell pathways has shown that EBV can also make use of the NF-kB pathway through LMP-2A in EBV-associated epithelial carcinoma (6) and it is likely that LMP-2A could have similar effects following infection of B cells.

EBV-mediated growth-transformation of B cells results in major changes in gene expression and nuclear reorganization. Changes in gene expression levels depend on a variety of mechanisms including not only transcription factor-mediated and epigenetic control (7) but also post-transcriptional regulation, such as those dependent on viral but also cellular miRNAs. We and other researchers have previously investigated the effects of experimental infection with EBV on epigenetic marks. For instance, EBV infection leads to demethylation of genes within the B cell transcription program (8) and contributes to the overexpression of genes essential for transformation. Also, analyses of histone modifications have shown that EBV infection results in both global and gene-specific changes in different modifications, which also contribute to key changes in gene expression during the growth-transformation of B cells (9).

MicroRNAs are a class of non-coding genes with broad influences on cellular signal transduction pathways. They function by inhibiting translation of select groups of mRNA transcripts containing imperfect annealing sequences in their 3′ untranslated regions (3′ UTRs) and, less frequently, through other regions of the transcript. Previous studies have shown that EBV infection results in upregulation of several miRNAs. For instance, miR-34a is strongly induced by EBV (10) and is associated with growth promotion. It has also been demonstrated that miR-155 is upregulated following EBV infection. These miRNAs are also strongly upregulated in B cell lymphomas (11,12) and it has been proposed that miRNAs misregulation in lymphomas could be used for diagnosis, prognosis or prediction of response to specific therapies (13). As aforementioned, DLBCL is one of the B cell lymphoma types associated with EBV (14) and also the most common type of lymphoma, accounting for 30–40% of lymphomas in western countries. On the basis of the correlation between microarray gene expression profiling and clinical outcome, it is now possible to classify the majority of DLBCLs into molecular variants called activated B cell-like DLBCL (ABC-DLBCL) and germinal center-like DLBCL (GC-DLBCL). A distinguishing feature of DLBCL is a signature of genes that are induced by NF-kB, which is upregulated in ABC-DLBCL (15) but not in GC-DLBCL.

We currently know little about the overall relevance of miRNAs in EBV-mediated transformation of B cells and about how much of the miRNA expression footprint in B cell lymphomas is associated with EBV primary infection. In this study, we investigated the deregulation of human miRNAs during EBV-mediated transformation of RBLs to LCLs, using a high-throughput strategy. We observed significant upregulation of several miRNAs, although miRNA downregulation was highly predominant. Time-course analysis indicated that miRNA deregulation occurs before cell proliferation, particularly for those that become upregulated. Also, analysis of B cells infected with EBV deficient in EBNA-2 and LMP-1, and with B cells stimulated with IL-4/CD40L, revealed that similar changes in miRNA expression occur, suggesting a potential role of the stimulation of the NF-kB pathway that is common to all these conditions. We showed that changes in miRNA expression occur in parallel with changes in histone H3K4me3 and H3K27me3. The involvement of NF-kB in miRNA deregulation was demonstrated by the enrichment of the binding motifs of the NF-kB complex subunits among the genomic sequences of the miRNAs undergoing expression changes, NF-kB p65 binding to miRNA promoters from ChIP-seq data and the finding that p65 binds the promoters of miRNAs following EBV infection. Moreover, we showed that the use of NF-kB inhibitors impairs the expression changes of these miRNAs, and abrogates both the association of the NF-kB subunit p65 as well as changes in histone modifications near the transcription start site (TSS) of these miRNAs. We also observed a large overlap in miRNA expression changes when comparing the profiles associated with EBV-mediated transformation of B cells with the profiles obtained for DLBCL primary samples. miRNA expression changes are related to changes in the levels of targets relevant to B cell transformation and in DLBCL. Our findings identify a novel mechanistic link between NF-kB and epigenetic regulation of miRNAs in EBV-mediated transformation of B cells and their implications in this model and in DLBCLs.

MATERIALS AND METHODS

Ethics statement

Human blood samples used in this study came from anonymous blood donors and were obtained from the Catalan blood donation center (Banc de Sang i Teixits). The anonymous blood donors received oral and written information about the possibility that their blood would be used for research purposes, and any questions that arose were then answered. Before giving their first blood sample the donors signed a consent form at the Banc de Teixits, which adheres to the principles set out in the WMA Declaration of Helsinki. The protocol used to transform B cells from these anonymous donors with EBV was approved by IDIBELL's Committee of Biosecurity (CBS) on 5 May 2011 and the Ethics Committee of the University Hospital of Bellvitge (CEIC) on 28 May 2011.

The study population consisted of a retrospective series of *de novo* cases of DLBCL obtained from various centers in Spain. The study was reviewed and approved as being of minimal or no risk or as being exempt by each of the participating institutional review boards, and the overall collaborative study was approved by the institutional review board of the Spanish National Cancer Research Centre (CNIO), Madrid, Spain. The study protocol and sampling methods were approved by the Instituto de Salud Carlos III institutional review board in de-identified anonymous format. All cases positively stained for CD20. Cases diagnosed as

T cell histiocyte-rich B cell lymphoma, primary mediastinal B cell lymphoma cases, cutaneous LBCL, intravascular LBCL and those histologically associated with a follicular lymphoma component were excluded.

Cells

Viable peripheral blood mononuclear cells were isolated by Lymphoprep density gradient centrifugation from buffy coats from anonymous blood donors. Resting B cells were isolated by positive selection using CD19 MicroBeads (Miltenyi Biotec), or by depletion using a B Cell Isolation Kit (Miltenyi Biotec). For EBV-mediated transformation, isolated B cells were immortalized with the supernatant of the marmoset cell line B95.8 and with the EBV variant 2089 made from 293 cells carrying a recombinant B95.8 EBV genome (16). Preparations of the 2089 recombinant wild-type EBV with a GFP (green fluorescent protein) vinsert or viruses deleted for LMP-1 and EBNA-2 (17) were made from 293 cells carrying the recombinant B95.8 EBV genomes, and transfected with 0.5 μg BZLF1 (p509) + 0.5 μg gp110 (pRA). For B cell activation, isolated B cells were cultured 5×10^6/3 ml per well of a 6-well plate with 50 ng/ml CD40L (Enzo Life Sciences) and 50 ng/ml IL-4 (Gentaur) and the B cell blasts were split weekly in a 1:2 ratio. The percentages of activated and proliferating B-cells were detected by CD86 expression measured by flow cytometry and tritiated thymidine incorporation, respectively.

miRNA profiling and individual assays

For the miRNA expression analysis, cDNA synthesis and real-time quantitative polymerase chain reaction (qPCR) were performed using the miRCURY LNA Universal RT microRNA PCR system (Exiqon, Denmark) according to the manufacturer's instructions. miRNAs were screened using Ready-to-Use microRNA PCR Human Panel I V2.R from Exiqon. For each reverse transcriptase-PCR (RT-PCR) reaction, 30 ng of total RNA were used. Samples from RBLs and LCLs were analyzed in triplicates on a Roche LightCycler 480 real-time PCR system. Results were converted to relative values using the inter-plate calibrators included in the panels (log 2 ratios). Samples with Cp values equal or higher than 37 were considered as having the same value (i.e. 37 Cp), considering that above that threshold the amount of a particular miRNA is negligible. RBL and LCL average expression values were normalized with respect to the reference miRNA miR-103. Differentially expressed miRNAs (log FC > 2 or log FC < -2) were selected. Individual assays were also performed using probes from Exiqon. Nucleolar RNAs RNU44 and RNU48 were used for frozen samples assays.

Quantitative RT-PCR (qRT-PCR)

For qRT-PCR of cellular genes, cDNA was produced with the SuperScript II Reverse Transcriptase (Invitrogen Co). Quantitative real-time PCR was done on a LightCycler 480 II System using LightCycler 480 SYBR Green Mix (Roche). Reactions were carried out in triplicate and qRT-PCR data were analyzed using the standard curve method. We used the housekeeping gene RPL38 and HPRT1 as a control. All primer sequences are listed in Supplementary Table S1.

Chromatin immunoprecipitation (ChIP) assays

To test the binding of p65 NF-kB to miRNA promoters, as well as changes in histone H3K4me3 and histone H3K27me3, we performed ChIP assays as previously described (18). We used a rabbit polyclonal against the C-t of NF-kB p65 (sc-372, Santa Cruz Biotechnology), anti-histone H3K4me3 (17–614, Millipore) and anti-histone H3K27me3 (07–449, Millipore). Immunoprecipitated material was used for analyses of specific sequences by qRT-PCR (see primers sequences in Supplementary Table S1).

DNA methylation analysis

Bisulfite pyrosequencing (BPS) was performed according to standard protocols and evaluated with the Pyro Q-CpG 1.0.9 program (Biotage, Uppsala, Sweden). Primer sequences for BPS PCR reactions are shown in Supplementary Table S1.

ChIP-seq analysis

ChIP-seq sources and data processing. Sources of ChIP-seq data are detailed in Supplementary Table S2. We downloaded either aligned BED or BAM format files from public databases. BAM files were converted to BED format using BETools (bamToBed function) (19). When there was more than one replicate, they were concatenated to obtain wider coverage and greater sequence depth.

Analysis of differential association of histone modifications. Differential association (increased or decreased genomic location) of H3K4me3, H3K27me3 and H3K9me3 was analyzed using the MACS program (version 2.0.9; macs2diff function) (20) using the parameter settings: -g hs -nomodel -shiftsize = 75 -bdg -a 4 -q 0.005. Therefore, the q-value cutoff was established as 0.005. MACS' macs2diff function establishes differential regions by comparing two treatment files corresponding to two conditions (in this case, lymphoblastoid cells and resting B cells), and comparing each of them against corresponding control 'Input' files. This comparison generates an output containing a list of 'differentially bound locations' with a 'differential score' ($-\log_{10}$ q-value), where a positive number means that the signal in lymphoblastoid cells is higher than in resting B cells, and a negative number means the opposite. Higher scores indicate a greater difference between the two cell types. Unique and consistently found differentially bound locations were considered for further analysis, e.g. correlation with expression. However, differential locations with a score ($-\log_{10}$ q-value) of exactly zero were excluded from the analysis. When more than one replicate of the aligned file was present, they were merged to ensure wider coverage and greater sequencing depth. Significantly differentially bound locations were annotated to the closest EnsEMBL (version-65) transcripts and genes (21) using BEDTools (closestBed function) (19). We calculated the Pearson's correlation coefficient between the differentially bound location scores, in which negative

and positive values respectively indicate decreased and increased location scores in lymphoblastoid cells/resting B cells comparisons. Normalized read density wig files were produced using JavaGenomics Toolkit (http://palpant.us/java-genomics-toolkit/) and were used in UCSC (University of California, Santa Cruz) genome browser (http://genome.ucsc.edu/) to visualize read-density peaks around miRNA TSS.

Transfection with miRNA mimics and siRNAs

A total of 5 nM miRNA mimics (Ambion) were transfected into LCLs using Lipofectamine RNAiMAX reagent (Invitrogen) following the manufacturer's protocol. Experiments were also performed using 5 nM control mimic. To silence p65, we used Silencer Select Pre-Designed siRNA (Life Technologies) against human RELA (p65), targeting exon 11 (ref. s11916) in parallel with a Silencer Select negative control in purified CD19+ cells, followed by addition of the EBV-containing supernatant 4 h after the cells were transfected with the siRNA. We used Lipofectamine RNAiMAX Transfection Reagent (Invitrogen) for efficient siRNA transfection. mRNA and protein levels were examined by qRT-PCR and western blot 2 and 3 days after siRNA transfection.

Cell proliferation and apoptosis assays

To test the effects of transfection of specific mimics on DNA synthesis, we measured incorporation of 5′-bromo-2′-deoxyuridine (BrdU) 48 h after miRNA transfection. Cells were incubated in 15 μM BrdU during 30 min. Cells were fixed with 70% ethanol 1 h and permeabilized (phosphate buffered saline (PBS)-bovine serum albumin-Triton X-100 0.8% (PBT), 10 min, RT) and treated with 2 M HCl for 30 min, After DNA opening, HCl was neutralized by two 5-min washed with NaBo (0.1 M, pH 8.5) and two 5-min washes with PBT. Cells were incubated with anti-BrdU antibody (18 h at 4C, 1:1000 dilution) and anti-mouse Alexa-488 conjugated antibody was added to visualize the BrdU-positive nuclei. Cells were analyzed using fluorescence-activated cell sorting (FACS) (Beckman Coulter) and FlowJo software (Tree Star, Inc.). We also measured [3H]-thymidine incorporation, 48 h after miRNA transfection, cells were pulsed with 1 ml [3H]-thymidine (0.4 mCi/ml) for 4 h at 37C°. After washing three times with PBS, cells were incubated with 1 ml ice-cold 5% trichloroacetic acid (TCA) for 15 min at 4C°, washed three times with absolute methanol, air dried and the TCA-precipitable fraction was solubilized in 500 ml of 0.1 M NaOH-1% sodium dodecyl sulphate. [3H]-thymidine incorporation was determined with a scintillation counter. We used tetramethylrhodamine methyl ester (TMRM) to measure apoptosis. Forty eight hours after transfection with mimics, cells were incubated during 4 h with etoposide. Cells were washed two times with PBS and incubated 30 min at 37C° with TMRM. Cells were analyzed using FACS (Beckman Coulter) and FlowJo software (Tree Star, Inc.).

Differential analysis from expression beadchips

Expression data were downloaded from NCBI (National Center for Biotechnology Information) GEO database (22) with accession number GSE30196 (23). Authors investigated global gene expression profiles in peripheral blood; hence, in this paper we focused on the samples of LCLs, and CD19-specific B cell subsets. Data analysis was performed on statistical environment R (24), using Bioconductor Package Genefilter with the purpose of applying non-specific filtering by IQR (interquartile range). Then first, processed data was utilized directly, the threshold for IQR was set to 0.5 and a Welch's *t*-test was carried out. Subsequently, data were selected taking a cut-off of *P*-value below 0.01, FDR (False Discovery Rate) below 0.05 and establishing fold-change value above 1.4 for overexpressed data and below 1/1.4 for downregulated genes.

miRNA target prediction

To predict the potential targets of the dysregulated miRNAs, we used the algorithms available in miRWalk database (25), including information produced by eight established miRNA prediction programs on 3′ UTRs of all known genes of Human: RNA22, miRanda, miRDB, TargetScan, RNAhybrid, PITA, PICTAR and Diana-microT. Only those targets predicted by at least three databases were considered for further analysis.

Differential expression analysis of microRNA microarrays

Microarray Expression data are Agilent Human MicroRNA microarray and come from a study by Martin-Pérez *et al.* (26) and data for lymph nodes (LN) (GSE23026) from the same research team. Data were processed and analyzed in R environment (24), using package AgimicroRNA (27) for processing microarrays and limma (28) for differential analysis. Thus, the workflow would be: (i) Preprocessing microarray using background method 'half', which establishes a value for negative data. (ii) Quantile normalization (iii) and default filtering method removing control and non-quality probes. (iv) An experimental Bayes moderated *t*-statistics test was carried out from limma package in order to observe differential expression in such data.

Putative binding of NF-kB motifs

Possible occurrence of NF-kB subunit binding motifs in the region comprising 1000 bp upstream and 1000 bp downstream with respect to TSS was inspected using TRANSFAC matrices. The matches of the sequences against the set of TRANSFAC matrices were performed using R environment, specifically the functions countsPWM and matchPWM contained in the Bioconductor package Biostrings.

Graphics and heatmaps

All graphs were created using Prism5 Graphpad. Heatmaps were generated from the expression data using the Genesis program from Graz University of Technology.

RESULTS

Screening of miRNAs during EBV-mediated conversion of RBLs to LCLs

To investigate the participation and role of miRNAs in EBV-mediated transformation of RBLs we first performed miRNA profiling with a qPCR-based panel containing over 375 miRNAs. The analysis included CD19+ samples before and after EBV infection, once they had become LCLs. For this analysis, we performed two independent sets of experiments with two forms of the EBV, the B95.8 strain and the 2089 form of EBV that infects B cells very efficiently (16), performing both in duplicate. Analysis of the results showed significant changes in expression of 34 miRNAs (Figure 1A and Supplementary Table S3). Remarkably, we observed predominant downregulation of miRNA expression. Specifically, 24 miRNAs displayed significant downregulation (including miR150, miR199a-5p, miR-223, miR-28-5p, miR451), whereas only 10 miRNAs became upregulated (including miR-551b, miR-34a, miR-155, miR-193b, miR-365).

Several of the upregulated and downregulated miRNAs have been previously described as being involved in the transformation of B cells or in lymphomagenesis. For instance, miR-155 is overexpressed during the acquisition of EBV-mediated latency III (29,30), and selective inhibition of miR-155 function specifically inhibits the growth of LCLs and DLBCL (31). Also, miR-34a has been shown to be strongly induced by EBV infection and expressed in many EBV and Kaposi's sarcoma-associated herpesvirus-infected lymphoma cell lines (10) and its inhibition impairs the growth of EBV-transformed cells. Of the downregulated miRNAs we identified miR-150, previously described as displaying an extremely low level of expression in Burkitt lymphoma cells and as inducing differentiation when ectopically expressed in Burkitt lymphoma lines (32).

We then performed qRT-PCR with specific LNA probes to test individual expression changes of those miRNAs displaying the largest changes between RBL and LCL, considering their potential relevance in the transformation process based on previous data. Comparing the levels of these miRNAs between RBLs and LCLs confirmed the results obtained in the high-throughput screening (Figure 1B). To determine the dynamics of changes in expression of these miRNAs we used the 2089 EBV strain (16), given that this strain yields a high level of infection and over 90% of B cells are positive for EBV transcription factor EBNA-2 a few hours after being exposed to the virus. Time-course analysis of expression showed that several of the miRNAs displayed changes even 24 h post-infection (for instance, miR-155 and miR-34a), before proliferation had started (Figure 1C), indicating that at least changes in these miRNAs might be related to the activation process or initial transformation steps.

To test the specificity of the changes in miRNA expression associated with EBV-mediated proliferation as well as the potential role of EBV proteins we screened in three additional conditions. First, we screened for B cells stimulated with IL-4 and CD40L, given that EBV-mediated transformation and B cell activation share common pathways (33). We found similar levels of cell activation, measured by cytometry analysis of the CD86 surface marker in IL-4/CD40L-stimulated cells and EBV-infected B cells (results not shown, but similar to those previously shown, see (9)). In parallel, we stimulated B cells with two recombinant forms of EBV in which the LMP-1 and EBNA-2 genes, the two best characterized EBV-encoded proteins, are deleted. Under these conditions, cells undergo a few divisions but do not acquire the capability of unlimited growth. Comparison of the miRNA expression levels of these three sample sets yielded similar profiles to those obtained with wild-type EBV (Figure 1D and Supplementary Table S4). In all cases, we observed a very similar profile for the set of upregulated miRNAs. In the case of downregulated miRNAs, we observed more variability, but in general the majority of miRNAs displayed changes in the same direction than the ones observed for wild-type EBV. These results suggest that all four conditions share a common pathway. It is well known that NF-kB is a common pathway for both IL-4/CD40L-stimulation and EBV infection, making it a strong candidate, even as a direct transcriptional regulator for some of them, to be that responsible for the changes observed in the panel of miRNAs. In fact, some of the misregulated miRNAs, like miR-155 (34), have previously been associated with the NF-kB pathway. It is also known that EBNA-1- and LMP-1-deficient EBV can still make use of the NF-kB pathway through LMP-2A (6). We also performed individual qRT-PCR analysis of the top upregulated and downregulated miRNAs at 24 h and 7 days post-infection of samples generated with wild-type EBV, EBNA-2- and LMP-1-deficient viral particles and samples generated through IL-4/CD40L activation. This enabled us to confirm that all four conditions have very similar effects on the changes that these miRNAs underwent (Figure 1E).

Transcriptional and epigenetic control of miRNAs associated with EBV-mediated transformation of B cells

To determine whether miRNA expression changes observed during RBL to LCL conversion are a consequence of transcriptional regulation or due to modulation of miRNA stability, we determined by qRT-PCR the levels of long miRNA precursors, termed primary miRNAs (pri-miRNAs), during this process. The analysis of these precursors revealed similar dynamics in the changes to mature miRNAs levels, and most of the pri-miRNAs showed increased or decreased levels even before 24 h, indicating that these miRNAs are subject to transcriptional activation control (or repression). In the case of miR-199a we checked the pri-miRNAs corresponding to its two genomic locations, and only miR-199a1 (located in chromosome 19) displayed the expected changes in expression, discarding the other one as responsible for the observed changes in the mature form of this miRNA (Figure 2A).

The existence of transcriptional control in mediating the observed changes in miRNA expression suggests the potential participation of epigenetic mechanisms, together with changes in association of transcription factors. Previous results from our team had demonstrated the existence of DNA demethylation events in association with EBV-mediated transformation (8) as well as changes in his-

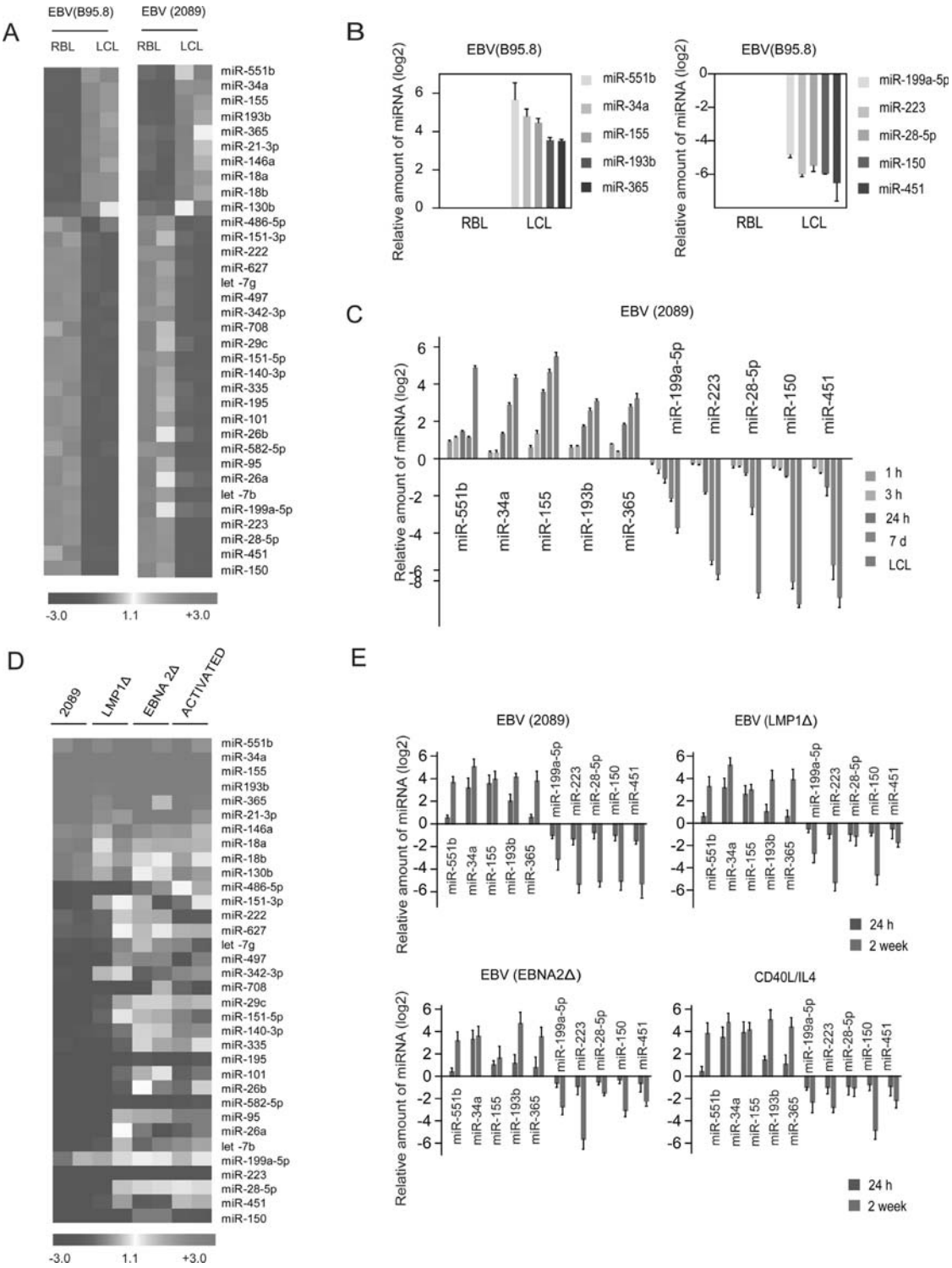

Figure 1. MicroRNA expression profiling during RBL-to-LCL transformation. (A) Heatmap including the data for the two RBL/LCL pairs of samples showing differential expression of miRNAs for each of the EBV systems (B95.8 EBV strain, left, and 2089 EBV strain, right). Only those miRNAs with an FC > 2 or FC < 0.5 were selected. Similar patterns of miRNA expression changes were obtained in the two situations. (B) Individual analysis of the top five upregulated and downregulated miRNAs upon B95.8 EBV infection using LNA probes and qRT-PCR. (C) Time-course analysis of the miRNA expression changes in the top upregulated and downregulated miRNAs using LNA probes and qRT-PCR. In this case we used the 2089 EBV strain, which has a very high yield of infection. (D) Heatmap showing differential expression of miRNAs between B cells after four different treatments (infected with wild-type 2089 EBV, EBV deficient for LMP-1, EBV deficient for EBNA-2 and stimulated with IL-4 /CD40L) with respect to resting B cells. The data represented in the heatmap correspond to the average of the fold change for each case. Similar patterns of miRNA expression were found in all samples. (E) Individual analysis of previously selected miRNAs using LNA probes and qRT-PCR for all four situations, as in the previous section.

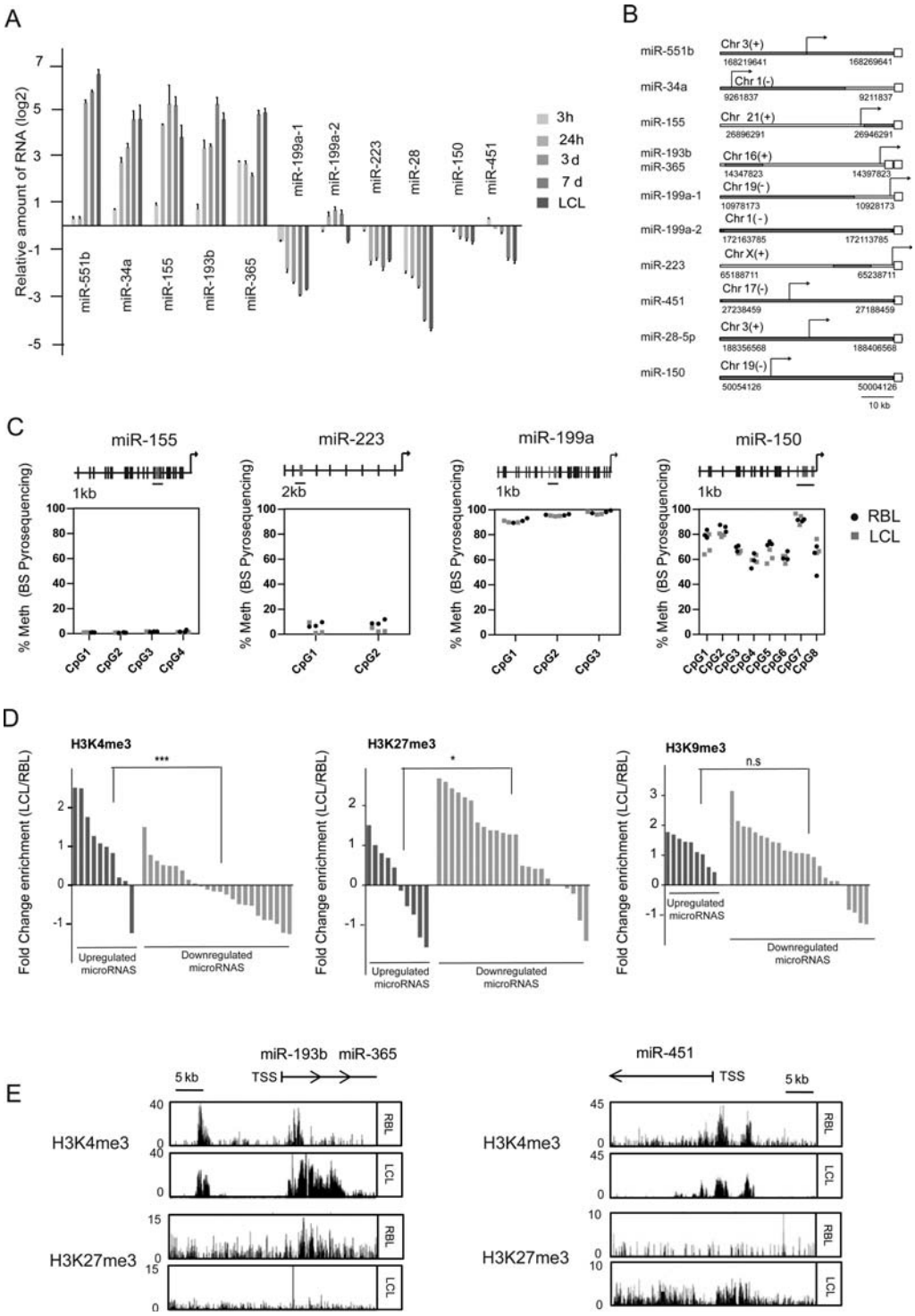

Figure 2. Transcriptional and epigenetic control of miRNAs in EBV-mediated transformation of RBLs. (A) qRT-PCR analysis of miRNA precursors (primary miRNAs) for the top five upregulated and downregulated miRNAs at different times (3 h, 1, 3, 7 days and LCLs) following infection of RBLs with EBV (2089 EBV strain). (B) Scheme depicting the genomic localization of selected miRNAs. Each empty square represents the mature form of a given miRNA. TSSs are indicated with an arrow. TSS locations were predicted using miRStart (http://mirstart.mbc.nctu.edu.tw/) (25). (C) Analysis of DNA methylation changes in CpGs by pyrosequencing. For each miRNA 2–8 consecutive CpGs were analyzed in RBLs and LCLs. The location of the analyzed CpGs is represented on top in relation with the TSS (indicated by an arrow). (D) Comparison of the ChIP-seq profiles for H3K4me3, H3K27me3 and H3K9me3 between RBLs and LCLs for all miRNAs of our study. A window of 5000 bp was inspected. The values correspond to the ratio between LCL and RBL of the average value using 50 bp segments within the 5000 bp window of each miRNA. Log2 values are represented. (E) Examples of the comparison of the ChIP-Seq profiles of two histone modifications (H3K4me3, active transcription; H3K27me3, repression) for one upregulated miRNA (miR-193b/miR-365) and one downregulated miRNA (miR-451) in RBLs and LCLs.

tone modifications like H3K27me3 and H3K9me3 (9). We therefore tested the epigenetic profile around the TSS of several upregulated and downregulated miRNAs. To this end we first determined the TSS of all miRNAs displaying expression changes using miRStart (Figure 2B) (25). We then investigated the possible existence of DNA methylation changes near the TSS using BPS. For instance, for miR-155, one of the upregulated miRNAs, we found no detectable levels of methylation in the four CpG sites near its TSS in either RBLs or LCLs (Figure 2C). Other examples of miRNAs tested for methylation near the corresponding TSS included downregulated miRNAs like miR-223, miR-199a and miR-150, in which we observed variable levels of DNA methylation but no differences were found between RBL and LCL (Figure 2C). In summary, we did not observe any changes in DNA methylation at the TSS associated with miRNAs.

We also tested the levels of histone modifications like histone H3K4me3, H3K27me3 and H3K9me3, which are associated with transcriptional activation and repression, respectively. To this end, we compared ChIP-seq data between RBLs and LCLs (GSE19465 for RBLs, ENCODE data for GM12878 for LCLs, described in detail in the Materials and Methods). We noted changes in these marks that were compatible with those observed in the expression of these miRNAs. A general analysis across all up- and downregulated miRNAs revealed that both H3K4me3 and H3K27me3 show significant changes that are consistent with the change in expression (Figure 2D and Supplementary Table S5). Specifically, upregulated miRNAs generally displayed an increase in histone H3K4me3 and a decrease in histone H3K27me3, whereas downregulated miRNAs exhibited higher levels of histone H3K27me3 and lower levels of histone H3K4me3 (Figure 2D). In contrast, changes in H3K9me3 are less associated with the miRNA expression changes. For instance, we observed that miRNAs like miR-193b/miR-365, which become upregulated during RBL-to-LCL transformation, display an increase in H3K4me3 and a decrease in H3K27me3 (Figure 2E). For downregulated miRNAs, such as miR-223, miR-150 and miR-451 (Figure 2E and Supplementary Figure S1), the decrease in H3K4me3 was more evident than the increase in H3K27me3. In summary, our findings reinforce the notion of the existence of mechanisms that control gene transcription, which might complement the effects of direct control by transcription factors, including those involved in the NF-kB pathway.

NF-kB is directly involved in regulation of both upregulation and downregulation of miRNAs in RBL-to-LCL transformation

To explore the potential involvement of the NF-kB pathway in the observed changes in miRNAs during the transformation of B cells we did several analyses. First, we investigated the enrichment of the consensus sites for NF-kB subunits (p65, p50, c-rel, etc.) in a window of 1000 bp upstream and downstream with respect to the TSS of miRNAs (determined from the miRStart database) (25). This showed these consensus binding sites to be present in the majority of miRNA TSSs (Supplementary Figure S2). We then determined the presence of peaks of p65 subunit of NF-kB and RNA pol II binding from ChIP-seq experiments in the proximity of the TSSs of all miRNAs using public data sets (see Supplementary Table S2). This revealed the presence of p65 peaks in 7 out of 10 upregulated miRNAs and 11 out of 24 downregulated miRNAs, indicating that p65 NF-kB is physically associated with the TSS of both upregulated and downregulated miRNAs and, therefore, perhaps involved both in activation and repression of miRNAs (Figure 3A and Supplementary Figure S3). To further explore the involvement of the NF-kB pathway in the activation and repression of these miRNAs, we treated RBLs with two different NF-κB inhibitors: Bay 11–7082 and sodium aurothiomalate (SATM) and investigated the effects on the expression changes on the aforementioned miRNAs. Bay 11–7082 has been commonly used as a specific NF-kB inhibitor, although recent data have questioned its specificity (35,36). SATM forms gold adducts with the cysteine residues of IKK (37) although its use as a NF-kB inhibitor has been more restricted. We first set up the concentration for each inhibitor by using LCLs and a wide range of concentrations. We selected 10 μM for Bay 11–7082 and 500 μM for SATM. Both compounds were able to impair changes in expression of upregulated and downregulated miRNAs, although Bay 11–7082 has a higher effect (Supplementary Figure S4 and Figure 3B), reinforcing the notion of the role of this pathway in mediating misregulation of these miRNAs.

We then confirmed the presence of p65 NF-kB at the TSS of these miRNAs, by performing ChIP assays with anti-p65 antibodies in CD19+ cells before and 72 h after infection with EBV and investigated the association of p65 at the genomic sequence around the TSS of both miRNAs that become upregulated (miR-155, miR-34a and miR-193b) (34) and downregulated (miR-199a, miR-150 and miR-451), focusing on sequences that display binding motifs for NF-kB. We also used the *TSH2B* as negative control. Interestingly, we observed specific enrichment of p65 at 72 h after EBV infection in both upregulated and downregulated miRNAs genes (Figure 3C), demonstrating the EBV-dependent association of p65 to both sets of miRNAs. Interestingly, binding of p65 was abrogated upon treatment with the NF-kB pathway inhibitor SATM (Figure 3C). For this and the following experiments we used SATM instead of Bay 11–7082, because the latter induces cell death, as also reported by others (38).

Finally, to test the implication of NF-kB in the histone modification-mediated regulation of these miRNAs we performed ChIP assays with the two histone modifications which had displayed significant changes in relation with their increase or decrease at the TSS of these miRNAs, i.e. histone H3K4me3 and histone H3K27me3. ChIP assays confirmed the decrease of histone H3K27me3 in miRNAs that become upregulated and their increase in miRNAs that are downregulated (Figure 3D, top). In contrast, we observed and increase of histone H3K4me3 in miRNAs that become upregulated, although changes in miRNAs that become downregulated were less strict (Figure 3D, bottom). These changes were partially or totally abrogated in the presence of NF-kB pathway inhibitor SATM (Figure 3D). These changes were not observed at control genes that are not targeted by p65 (Figure 3D).

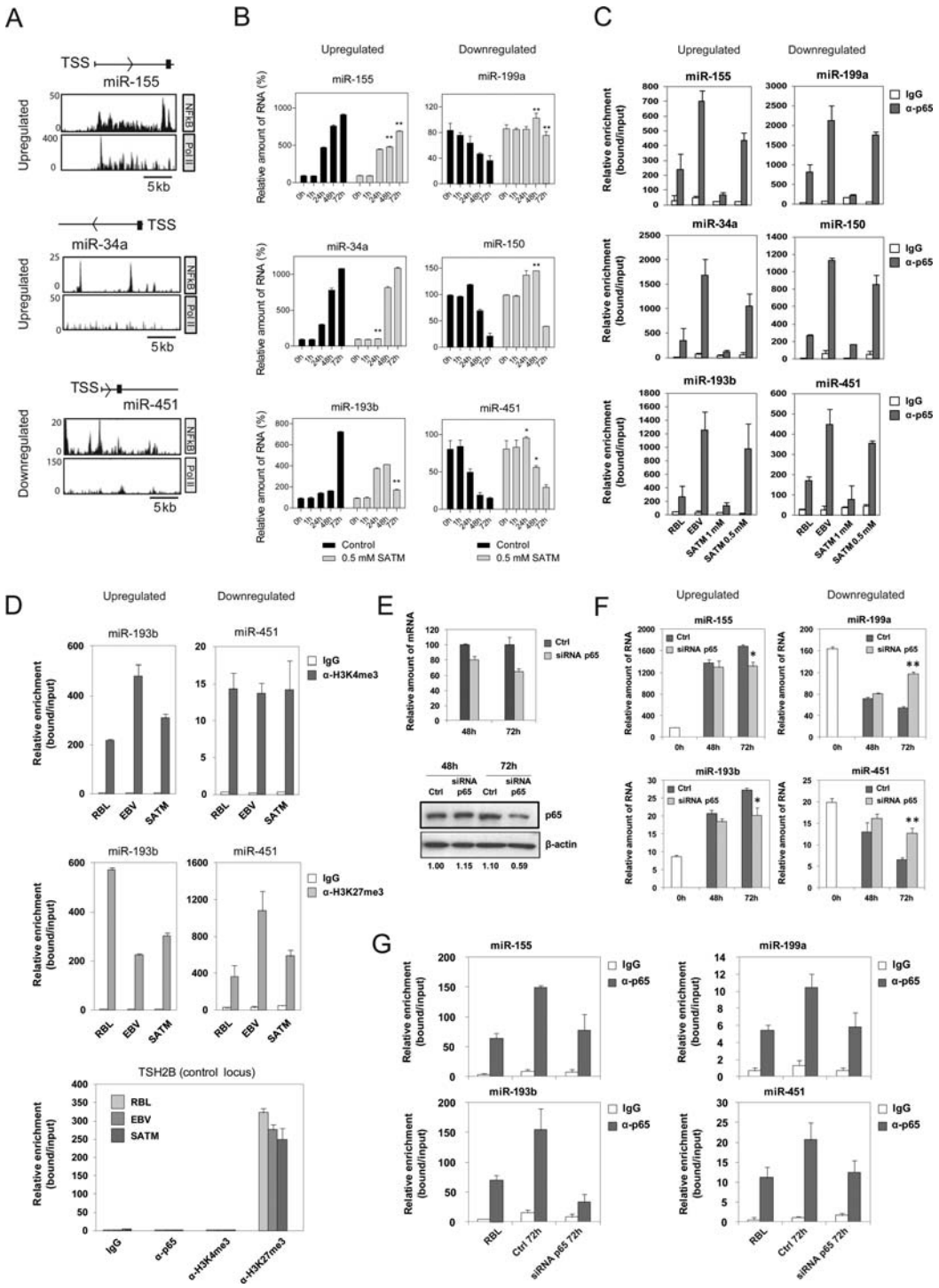

Figure 3. NF-kB dependence of miRNA expression changes. (A) ChIP-Seq analysis for NF-kB p65 and pol II in LCLs around the TSS of selected miRNAs, one upregulated (miR-155) and two downregulated (miR-34a and miR-451). (B) Effects of one of the NF-κB pathway inhibitors, SATM (at 500 μM), in the levels of selected upregulated and downregulated miRNAs in a time-course analysis of B cells infected with EBV. (C) ChIP assays for the above miRNAs showing the binding of the NF-kB p65 and pol II in B cells infected with EBV after 3 days and once they have become LCLs, as well as the effect following treatment with NF-kB pathway inhibitor SATM at two concentrations (500 μM and 1 mM). (D) ChIP assays demonstrating changes in histone H3K4me3 and histone H3K27me3 at the TSS of upregulated and downregulated miRNAs, as well as the effect following treatment with 1 mM SATM. (E) Effects of siRNA on p65 levels in B lymphocytes following transfection and EBV infection after 2 and 3 days, as analyzed by qRT-PCR (relative to the combined levels of the RPL38 and HPRT1 genes) and western blot (β-actin as loading control). Control samples correspond to B lymphocytes transfected with a control siRNA and were also infected with EBV. (F) Effect of p65 depletion on the expression changes of selected upregulated and downregulated miRNAs in a time-course analysis of B cells infected with EBV. (G) Effect of p65 depletion on their recruitment near the TSS of miRNAs, as demonstrated by ChIP assays.

Given the limited specificity of the two above inhibitors, as an unequivocal test of a potential causal relationship between NF-kB and miRNA expression changes in EBV-mediated B lymphocyte transformation, we investigated the consequences of ablating p65 expression in RBLs. To this end, we downregulated p65 levels in RBLs using transient transfection experiments with an siRNA that targets exon 11 of p65. In parallel, we used a control siRNA. Following transfection we infected both control siRNA- and p65 siRNA-treated cells with EBV. Under these conditions, we used qRT-PCR and western blot to check the effects on p65 levels 48 and 72 h after EBV infection. By this means, we were able to confirm that the level of p65 downregulation was close to 40% at 72 h at both mRNA and protein levels (Figure 3E). We examined the expression levels of these miRNAs following p65 depletion and found that both upregulation and downregulation of the miRNAs was partially impaired following siRNA-mediated p65 depletion (Figure 3F). We confirmed that siRNA-mediated downregulation of p65 resulted in decreased binding of p65 to the miRNAs-associated TSS (Figure 3G).

Together, our findings indicate that NF-kB is involved in both activation and repression of miRNAs, and that this process is mediated by changes in histone H3K4me3 and histone H3K27me3. Most of the reports have demonstrated a role for NF-kB as a transcriptional activator, although it has also been reported that it can act as a repressor (39).

Analysis of miRNA expression in B cell lymphomas

As indicated, the pathogenic role of EBV and lymphomas is well established for Burkitt, Hodgkin and DLBCL, although the latter two have a less strict association than Burkitt lymphomas. On the other hand, of the lymphoid malignancies, those most clearly associated with NF-κB pathway are the ABC subgroup of DLBCL (40), Hodgkin lymphomas, primary mediastinal B cell lymphomas, gastric MALT lymphomas and multiple myeloma. Given these two facts, we decided to explore the relationship between the miRNAs whose expression changes in EBV-mediated transformation of RBLs and those obtained when comparing DLBCLs with normal LN, which are enriched in B cells. To this end, we first compared the expression status of the selection of the upregulated and downregulated miRNAs analyzed above and compared a cohort of 18 samples corresponding to DLBCL and 17 samples corresponding to control LN (Figure 4A). This comparison revealed that miR-155 is also upregulated in DLBCLs compared with LN and that miR-150, miR-199 and miR-28 are significantly downregulated in DLBCL with respect to LN. In parallel, we also used the miRNA expression data for DLBCL obtained by Martin-Pérez *et al.* (26); and LN (GSE23026) from the same research team and obtained the expression changes between these two groups. This comparison allowed us to confirm the data obtained by individual analysis of selected miRNA and identified additional miRNAs displaying a significant change in expression when comparing DLBCLs with LN similar to that observed during the EBV-mediated transformation of RBLs (Figure 4B and Supplementary Table S6). We also performed this analysis by separating the two DLBCL subgroups, ABC DLBCL and GC DLBCL. Interestingly, for the miRNAs that are misregulated in response to EBV-mediated transformation, we observed similar patterns of miRNA expression for both groups (Supplementary Figure S5).

Functional effects of miRNAs in EBV-mediated transformation of B cells and in DLBCLs

Changes in the levels of miRNAs are likely to affect the levels of their targets. To identify miRNA targets, we retrieved a list of putative targets using miRWalk (41), which contains prediction databases like TargetScan (42), miRDB (43) and others, as well as information about validated targets. We then linked the list of potential targets with expression data from RBL versus LCL comparisons (GSE30916) (23) and with expression data corresponding to a cohort of 17 DLBCL samples and 7 control LN (44), assuming an inverse relationship between the levels of a given miRNA and the expression levels of its targets. To select targets we chose those predicted with a minimum of three hits in different databases from miRWalk and at least 2-fold change for overexpressed genes or 0.5-fold change for downregulated genes (Figure 5A and Supplementary Table S7). We concentrated our efforts on those miRNAs for which we had observed changes in the same direction when comparing RBL versus LCLs and DLBCL versus LN, i.e. miR-155, among the tested upregulated miRNAs, and downregulated miRNAs mir-199a-5p, miR-28-5p and miR-150. We observed a number of putative targets relevant to B cell transformation. For instance, *MKI67* and *TRAF1* are targeted by miR-150, miR-199a-5p and miR-28-5p. *MKI67* encodes for a protein that is considered a classical marker for cell proliferation (45) and TRAF1 is a key factor in EBV-mediated transformation (46) and in lymphomagenesis (47). Other examples include *MCM10* and *CCND1* also targeted by miR-199a-5p, *PBK*, that promotes tumour cell proliferation through p38 MAPK activity (48) that is targeted by miR-28-5p and cyclin genes *CCND1* and *CCND2* targeted by miR-150. We confirmed changes in expression of these targets over a time course in B cells following EBV infection (Figure 5B).

To confirm the direct effects of the aforementioned miRNAs on the levels of their putative targets, we focused on the downregulated miRNAs. We transfected mimics for miR-150, miR-199 and miR-28 in LCLs. The transfection efficiency of mature miRNAs was assessed by FACS analysis using control fluorophore-labeled miRNAs, which revealed that over 88% of LCLs became positive (Figure 5C). qRT-PCR of each miRNA showed peak high expression levels with respect to untransfected LCLs at 24 and 48 h (Figure 5C). We then investigated the effects on the mRNA levels of their targets. Several of these targets had significantly reduced mRNA levels following mimic transfection (Figure 5E), indicating a role of the changes in these miRNAs with respect to their levels.

Finally, we tested the effects of these miRNAs on cell proliferation and apoptosis. We first tested the impact of transfecting DLBCL cell line MD901 with mimics for miR-155 (upregulated during EBV-mediated B cell transformation), miR-150, miR-199 and miR-28 (downregulated) measuring incorporation of BrdU or tritiated thymidine. We were unable to observe any significant effect on cell proliferation

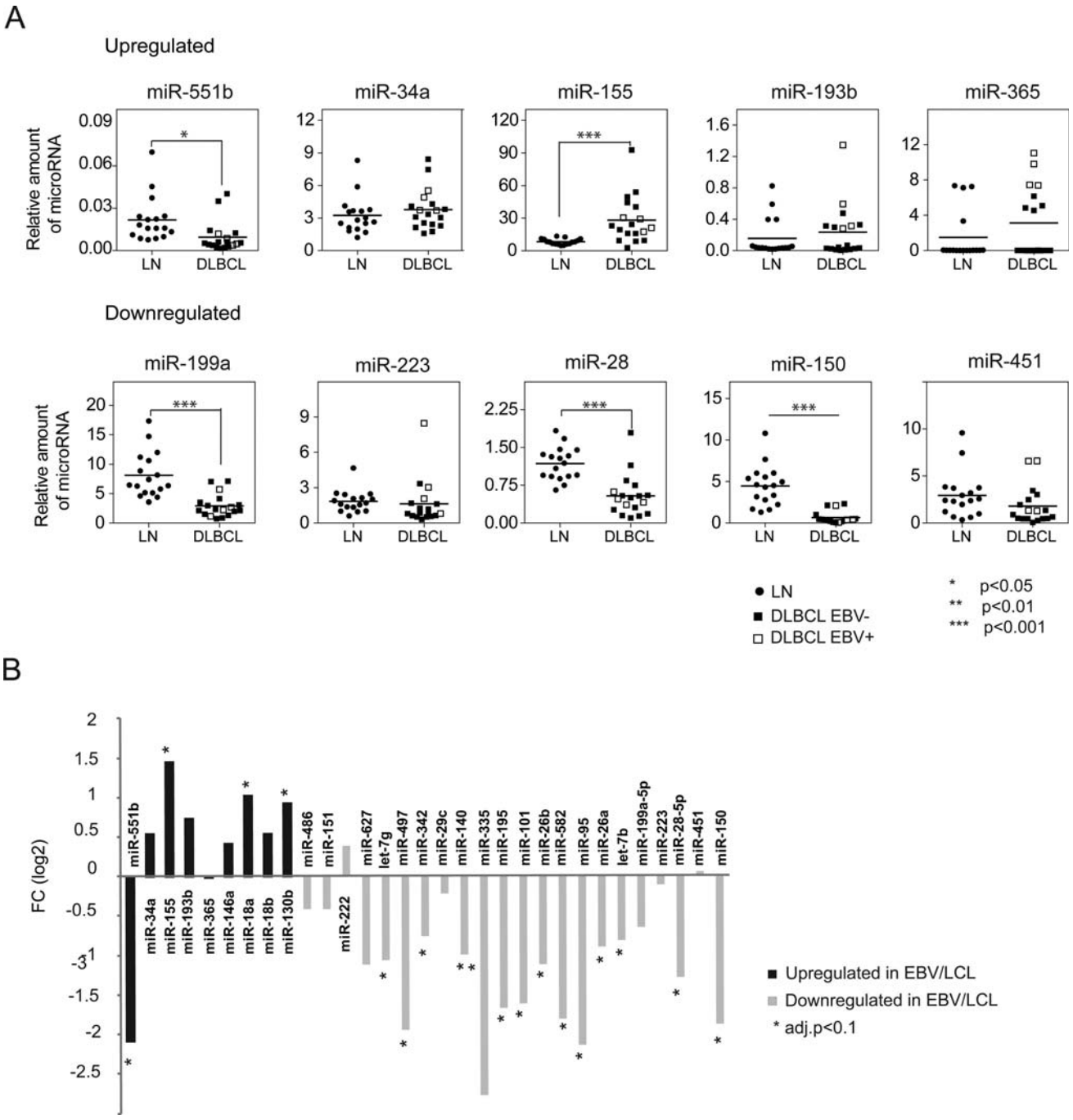

Figure 4. Comparison of the miRNA expression changes in primary DLBCLs. (A) Individual analysis of selected miRNAs in DLBCL and LN (negative control) cases using LNA probes and qRT-PCR. EBV positive and negative DLBCL cases are indicated. Fold changes were statistically significant for one upregulated miRNA (miR-155) and three downregulated miRNAs (miR-199a, miR-28 and miR-150) (***$P < 0.0001$). (B) Comparison of the miRNA expression data obtained by using a high-throughput analysis for miRNAs in a cohort of DLBCLs (26) and controls (LN) (GSE23026). Black and light gray bars correspond to upregulated and downregulated miRNAs respectively from the RBL versus LCL comparison.

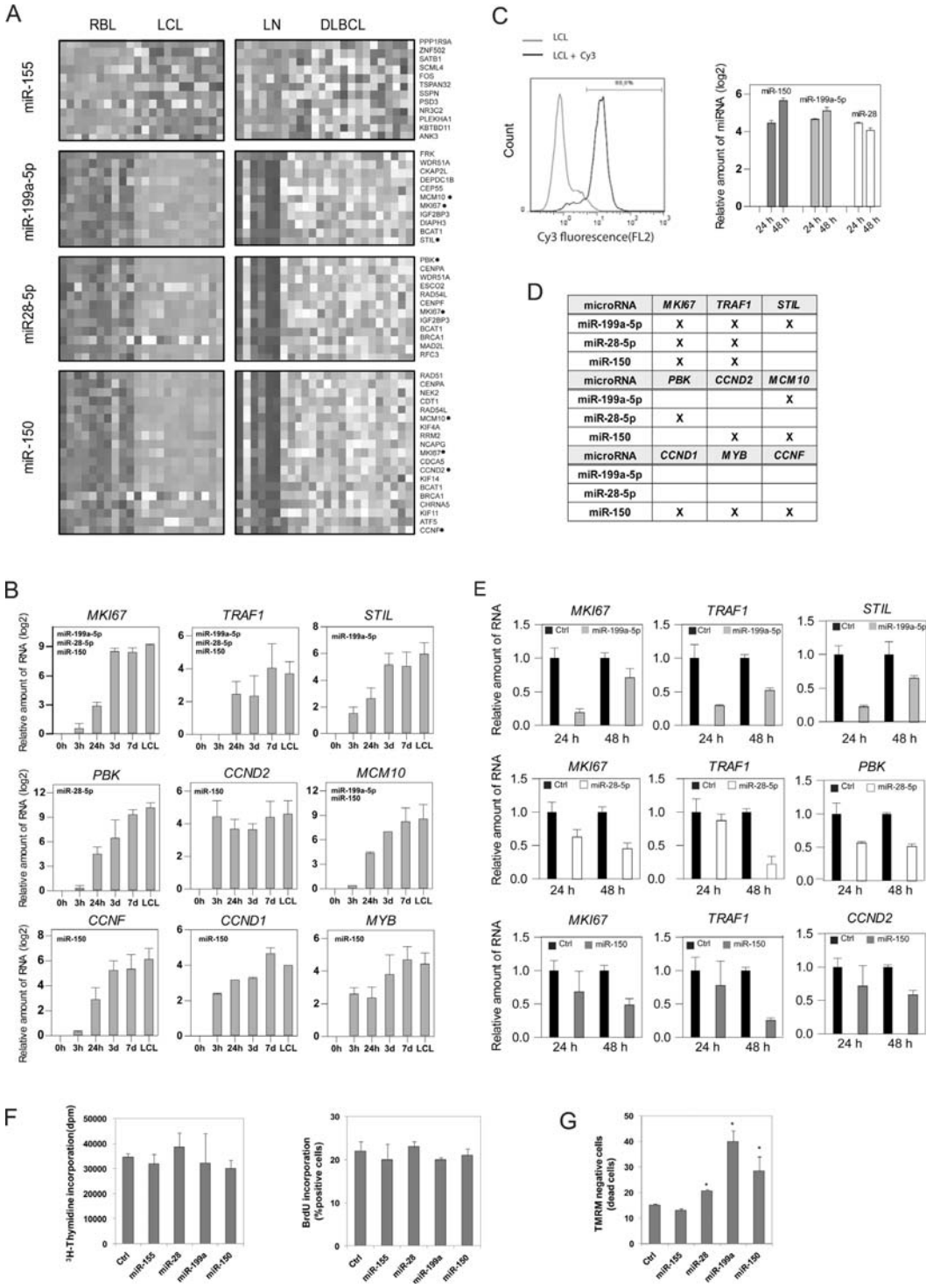

Figure 5. Expression changes of miRNA targets in EBV-mediated transformation of B cells and DLBCL. (A) Heatmap including expression data of putative targets in the RBL versus LCL and DLBCL versus LN comparisons. Represented targets include those predicted for at least 3 of 10 prediction algorithms (DIANA-mT, miRanda, miRDB, miRWalk, RNAhybrid, PCTAR4, PICTAR5, PITA, RNA22, TargetScan) in the miRWAlk program. Putative targets were compared with expression data from microarray data of RBL versus LCL (FC > 2, $P < 0.05$) and DLBCL versus LN (FC > 1.3, $P < 0.05$). Only targets common to both processes were represented. (B) Individual analysis for selected targets using qRT-PCR and a time-course series of B cells following EBV infection. (C) Efficiency of the experiments of miRNA mimic transfections. (D) Summary table indicating the miRNA/targets analyzed in functional experiments. (E) Effects of the introduction of mimics in LCLs for selected miRNAs (miR-150, miR-199a-5p and miR-28-5p) in the expression levels of their targets. (F) Analysis of tritiated thymidine and BrdU incorporation on MD209 cells following transfection with selected miRNA mimics (miR-155, miR-150, miR-199a-5p and miR-28-5p) and a control miRNA mimic (G) Analysis of apoptosis levels following transfection with the aforementioned selected miRNA mimics and measured by TMRM fluorescence.

(Figure 5F). In contrast, when we investigated the effects on induced apoptosis following transfection with these mimics, we observed that ectopic expression of miR-155 increased the resistance to apoptosis, whereas overexpression of miR-150, miR-199 and miR-28 increased the levels of apoptotic cells (Figure 5G), indicating that their downregulation following infection with EBV reduces the propensity to undergo apoptosis during EBV-mediated transformation of B cells.

DISCUSSION

Our results provide evidence of the existence of widespread changes of miRNA expression in association with EBV-mediated transformation of RBLs. It is notable that downregulation of miRNAs is predominant with respect to miRNA overexpression. In addition, comparison of these results with those obtained by activating and inducing proliferation with the T cell-derived mitogens CD40L and IL-4, as well as with EBV particles deficient for EBNA-2 and LMP-1, suggests that the process is driven by a pathway that is common to all four situations, i.e. the stimulation of the NF-kB pathway. This hypothesis is reinforced by our findings on the presence of binding motifs of NF-kB subunits, NF-kB p65 ChIP-seq data near the TSS of miRNAs, ChIP assays on selected up- and downregulated miRNAs, as well as results about the inhibition of this pathway and the effects on miRNA levels and reduced p65 binding. Several of the miRNA targets are related to cell transformation or proliferation. In addition, the significant overlap between the miRNA expression changes in EBV-related B cell transformation and DLBCL versus LN reinforces the notion of the relevance of this pathway to B cell transformation and especially in lymphomagenesis.

Several studies have previously addressed the effects of EBV infection on the miRNAs of host B cells. Changes in various miRNAs have been described, including upregulation of miRNAs like miR-155 (29,30) and miR-34a (10), and downregulation of miRNAs like miR-150 (32). Our own data have shown changes in these miRNAs as well. The global analysis shows that miRNA downregulation is predominant with respect to miRNA upregulation. miRNAs have negative effects on gene expression, so an overall decrease in miRNA levels suggests that some of the constraints for gene repression are relaxed. This observation is compatible with the general notion that transformation of RBLs to LCLs results in overexpression of many genes. These data are also consistent with our own observations about epigenetic control when analyzing DNA methylation and histone modification changes during the EBV-mediated transformation of B cells. In the case of DNA methylation we found that hypomethylation, and not hypermethylation, occurs during this process (8) again reinforcing the idea of relaxation of gene control. For histone modifications and accessibility to endonucleases we also observed changes that are compatible with increased gene expression, specifically a decrease in heterochromatic histone modifications and increased accessibility (9).

Our findings also indicate that the changes observed for RBL transformed with wild-type EBV are common to other similar situations. We noted a similar pattern of miRNA misregulation in B cells stimulated with IL-4/CD40L and in B cells infected with EBV deficient for LMP-1 and EBNA-2, the best characterized EBV proteins. In the first case, cells are stimulated to proliferate at a similar rate to cells infected with EBV. In B cells infected with these defective EBV particles, the initial steps toward transformation take place but proliferation rates are much lower. However, all situations share the stimulation of the NF-kB pathway and the commonalities in the misregulation of miRNAs suggest the role of this pathway. Although our study has focused on the elements within the canonical pathway, EBV and CD40L also stimulated the non-canonical pathway (49,50), which may also be involved in miRNA misregulation. It is then likely that LMP-1-deficient EBV make use of the non-canonical NF-kB pathway and this could explain stimulation of common sets of miRNAs. This had been previously demonstrated for miR-155 (34), in which the two binding sites at the miR-155 promoter recruit NF-kB, which is stimulated by LMP-1. In the case of EBNA-2- and LMP-1-deficient EBV particles, it is thought that stimulation of the NF-kB pathway occurs through LMP2A (6). The direct role of NF-kB in the regulation of these miRNAs is supported by the results obtained with both ChIP-seq data and individual ChIP assays and the observation that inhibitors for the NF-kB pathway impair both miRNA expression changes, as well as the binding of p65 and the changes in histone modifications at the mRNA genomic sites during the transformation of RBL with EBV. The implication of the NF-kB in directly targeting miRNAs has previously reported (34), however, to the best of our knowledge, our study is the first evidence demonstrating a direct role of this pathway in both targeting up- and downregulated miRNAs, as well as the finding of direct changes in the histone modification marks around the TSS of both groups of miRNAs. Previous studies have shown the ability of EBV and LMP-2 to upregulate DNMT3b and drive hypermethylation in gastric cancer (51), however, during infection of B cells from peripheral blood, we have been able to identify demethylation events (8) and there are no changes at the miRNA genomic sites.

The NF-kB pathway is relevant in the context of EBV-transformation of B cells and is considered to be a major pathway in lymphomagenesis, particularly in certain types of lymphomas, including DLBCL, which are also known to be associated with EBV infection. Comparing the miRNA displaying significant change during the EBV-mediated transformation of RBLs and those from the DLBCL and LN analysis revealed striking resemblances, suggesting that the type of changes in miRNAs are common to the two processes. This also applies to large sets of the predicted targets for these miRNAs, reinforcing the notion of the relevance of EBV and NF-kB in the pathogenesis of DLBCL. Earlier studies have shown that ABC DLBCL are more dependent on the NF-kB pathway (40). In this sense, it was relevant to compare the miRNA expression profiles of ABC DLBCL versus those from GC DLBCL. However, we did not observe a significant difference between these two. Recent studies have demonstrated that mutations in NF-kB related genes account for deregulation of the NF-kB pathway also in GC DLBCL (52).

There is increasing evidence of a role for miRNAs in proper B cell differentiation and in relation with the pathogenesis of B cell lymphomas (13). Interestingly, among the misregulated miRNAs in our model, i.e. the EBV-mediated transformation of B cells, there are several well studied miRNAs known for their relevance in the biology and cell cycle within the B cell compartment. For instance, miR-150 is associated with B cell differentiation and its upregulation is negatively associated with the expression of C-MYB (53). MiR-34a, one of the top upregulated miRNAs in EBV-mediated B cell transformation, is known to target Foxp1 required for B cell differentiation (54). In this context, miR-155 has also been associated with B cell differentiation (55). Quiescent differentiated B cells have a restricted transcription program in which only a limited set of genes (ubiquitously expressed and cell type-specific genes) are expressed. This progressive restriction of the transcription program, is well known to occur during differentiation. EBV-mediated transformation could therefore be viewed as a process inverse to that occurring during differentiation, and some of the mechanisms involved are likely to act in an opposite direction to those driving differentiation. Therefore, the activation of the aforementioned miRNAs, and the downregulation of a large number of miRNAs leading to the loosening of repression of many genes would be consistent with the type of changes occurring in transformed B cells. Our analysis of miRNA targets has led to the identification of genes that may play a key role in the transformation process and in maintaining the phenotype in lymphoma cells, including *MKI67* and *TRAF*, targeted by at least three of the downregulated miRNAs, and others like *CCND1*, *STIL* and *PBK* targeted by miR-150, miR-199a-5p and miR-28, respectively. Overall, our findings indicate a close relationship in the miRNA-mediated acquisition of the phenotype in B cells and a connection between the transformation process and the phenotype in lymphomas.

SUPPLEMENTARY DATA

Supplementary Data are available at NAR Online.

ACKNOWLEDGEMENTS

We thank the Spanish National Tumour Bank Network, especially Dr. María Jesús Artiga, for providing us with primary samples. We also thank Dr. Lluís Espinosa and Dr. Anna Bigas for advice on inhibition of the NF-kB pathway and for sharing reagents.

FUNDING

Spanish Ministry of Economy and Competitiveness (MINECO) [SAF2011-29635]; Fundación Ramón Areces [CIVP16A1834]; Catalan Agency for Management of University and Research Grants (AGAUR) [2009SGR184]; STATegra project [EU FP7 306000]. RTICC [RD06/0020/0107 to L.D.L.]. Funding for open access charge: Spanish Ministry ofEconomy and Competitiveness (MINECO) [SAF2011-29635].
Conflict of interest statement. None declared.

REFERENCES

1. Bornkamm,G.W. (2009) Epstein-Barr virus and its role in the pathogenesis of Burkitt's lymphoma: an unresolved issue. *Semin. Cancer Biol.*, **19**, 351–365.
2. Kaye,K.M., Izumi,K.M. and Kieff,E. (1993) Epstein-Barr virus latent membrane protein 1 is essential for B-lymphocyte growth transformation. *Proc. Natl. Acad. Sci. U.S.A.*, **90**, 9150–9154.
3. Kilger,E., Kieser,A., Baumann,M. and Hammerschmidt,W. (1998) Epstein-Barr virus-mediated B-cell proliferation is dependent upon latent membrane protein 1, which simulates an activated CD40 receptor. *EMBO J.*, **17**, 1700–1709.
4. Feederle,R., Haar,J., Bernhardt,K., Linnstaedt,S.D., Bannert,H., Lips,H., Cullen,B.R. and Delecluse,H.J. (2011) The members of an Epstein-Barr virus microRNA cluster cooperate to transform B lymphocytes. *J. Virol.*, **85**, 9801–9810.
5. Hollyoake,M., Stuhler,A., Farrell,P., Gordon,J. and Sinclair,A. (1995) The normal cell cycle activation program is exploited during the infection of quiescent B lymphocytes by Epstein-Barr virus. *Cancer Res.*, **55**, 4784–4787.
6. Stewart,S., Dawson,C.W., Takada,K., Curnow,J., Moody,C.A., Sixbey,J.W. and Young,L.S. (2004) Epstein-Barr virus-encoded LMP2A regulates viral and cellular gene expression by modulation of the NF-kappaB transcription factor pathway. *Proc. Natl. Acad. Sci. U.S.A.*, **101**, 15730–15735.
7. Niller,H.H., Wolf,H. and Minarovits,J. (2009) Epigenetic dysregulation of the host cell genome in Epstein-Barr virus-associated neoplasia. *Semin. Cancer Biol.*, **19**, 158–164.
8. Hernando,H., Shannon-Lowe,C., Islam,A.B., Al-Shahrour,F., Rodriguez-Ubreva,J., Rodriguez-Cortez,V.C., Javierre,B.M., Mangas,C., Fernandez,A.F., Parra,M. *et al.* (2013) The B cell transcription program mediates hypomethylation and overexpression of key genes in Epstein-Barr virus-associated proliferative conversion. *Genome Biol.*, **14**, R3.
9. Hernando,H., Islam,A.B., Rodriguez-Ubreva,J., Forne,I., Ciudad,L., Imhof,A., Shannon-Lowe,C. and Ballestar,E. (2013) Epstein-Barr virus-mediated transformation of B cells induces global chromatin changes independent to the acquisition of proliferation. *Nucleic Acids Res.*, **42**, 249–263.
10. Forte,E., Salinas,R.E., Chang,C., Zhou,T., Linnstaedt,S.D., Gottwein,E., Jacobs,C., Jima,D., Li,Q.J., Dave,S.S. *et al.* (2012) The Epstein-Barr virus (EBV)-induced tumor suppressor microRNA MiR-34a is growth promoting in EBV-infected B cells. *J. Virol.*, **86**, 6889–6898.
11. Eis,P.S., Tam,W., Sun,L., Chadburn,A., Li,Z., Gomez,M.F., Lund,E. and Dahlberg,J.E. (2005) Accumulation of miR-155 and BIC RNA in human B cell lymphomas. *Proc. Natl. Acad. Sci. U.S.A.*, **102**, 3627–3632.
12. Arribas,A.J., Gomez-Abad,C., Sanchez-Beato,M., Martinez,N., Dilisio,L., Casado,F., Cruz,M.A., Algara,P., Piris,M.A. and Mollejo,M. (2013) Splenic marginal zone lymphoma: comprehensive analysis of gene expression and miRNA profiling. *Mod. Pathol.*, **26**, 889–901.
13. Di Lisio,L., Martinez,N., Montes-Moreno,S., Piris-Villaespesa,M., Sanchez-Beato,M. and Piris,M.A. (2012) The role of miRNAs in the pathogenesis and diagnosis of B-cell lymphomas. *Blood*, **120**, 1782–1790.
14. Campo,E., Swerdlow,S.H., Harris,N.L., Pileri,S., Stein,H. and Jaffe,E.S. (2011) The 2008 WHO classification of lymphoid neoplasms and beyond: evolving concepts and practical applications. *Blood*, **117**, 5019–5032.
15. Rosenwald,A., Wright,G., Leroy,K., Yu,X., Gaulard,P., Gascoyne,R.D., Chan,W.C., Zhao,T., Haioun,C., Greiner,T.C. *et al.* (2003) Molecular diagnosis of primary mediastinal B cell lymphoma identifies a clinically favorable subgroup of diffuse large B cell lymphoma related to Hodgkin lymphoma. *J. Exp. Med.*, **198**, 851–862.
16. Delecluse,H.J., Hilsendegen,T., Pich,D., Zeidler,R. and Hammerschmidt,W. (1998) Propagation and recovery of intact, infectious Epstein-Barr virus from prokaryotic to human cells. *Proc. Natl. Acad. Sci. U.S.A.*, **95**, 8245–8250.
17. Feederle,R., Bartlett,E.J. and Delecluse,H.J. (2010) Epstein-Barr virus genetics: talking about the BAC generation. *Herpesviridae*, **1**, 6.

18. Ballestar,E., Paz,M.F., Valle,L., Wei,S., Fraga,M.F., Espada,J., Cigudosa,J.C., Huang,T.H. and Esteller,M. (2003) Methyl-CpG binding proteins identify novel sites of epigenetic inactivation in human cancer. *EMBO J.*, **22**, 6335–6345.
19. Quinlan,A.R. and Hall,I.M. (2010) BEDTools: a flexible suite of utilities for comparing genomic features. *Bioinformatics*, **26**, 841–842.
20. Zhang,Y., Liu,T., Meyer,C.A., Eeckhoute,J., Johnson,D.S., Bernstein,B.E., Nusbaum,C., Myers,R.M., Brown,M., Li,W. *et al.* (2008) Model-based analysis of ChIP-Seq (MACS). *Genome Biol.*, **9**, R137.
21. Hubbard,T.J., Aken,B.L., Beal,K., Ballester,B., Caccamo,M., Chen,Y., Clarke,L., Coates,G., Cunningham,F., Cutts,T. *et al.* (2007) Ensembl 2007. *Nucleic Acids Res.*, **35**, D610–D617.
22. Barrett,T., Wilhite,S.E., Ledoux,P., Evangelista,C., Kim,I.F., Tomashevsky,M., Marshall,K.A., Phillippy,K.H., Sherman,P.M., Holko,M. *et al.* (2013) NCBI GEO: archive for functional genomics data sets–update. *Nucleic Acids Res.*, **41**, D991–D995.
23. Min,J.L., Barrett,A., Watts,T., Pettersson,F.H., Lockstone,H.E., Lindgren,C.M., Taylor,J.M., Allen,M., Zondervan,K.T. and McCarthy,M.I. (2010) Variability of gene expression profiles in human blood and lymphoblastoid cell lines. *BMC Genom.*, **11**, 96.
24. Dessau,R.B. and Pipper,C.B. (2008) ["R"–project for statistical computing]. *Ugeskr Laeger*, **170**, 328–330.
25. Chien,C.H., Sun,Y.M., Chang,W.C., Chiang-Hsieh,P.Y., Lee,T.Y., Tsai,W.C., Horng,J.T., Tsou,A.P. and Huang,H.D. (2011) Identifying transcriptional start sites of human microRNAs based on high-throughput sequencing data. *Nucleic Acids Res.*, **39**, 9345–9356.
26. Martin-Perez,D., Vargiu,P., Montes-Moreno,S., Leon,E.A., Rodriguez-Pinilla,S.M., Lisio,L.D., Martinez,N., Rodriguez,R., Mollejo,M., Castellvi,J. *et al.* (2012) Epstein-Barr virus microRNAs repress BCL6 expression in diffuse large B-cell lymphoma. *Leukemia*, **26**, 180–183.
27. Lopez-Romero,P. (2011) Pre-processing and differential expression analysis of Agilent microRNA arrays using the AgiMicroRna Bioconductor library. *BMC Genom.*, **12**, 64.
28. Lymma,G.K. (2005) Limma: linear models for microarray data. In: Gentleman,R., Carey, V., Dudoit, S., Irizarry, R. and Huber, W. (eds.). *Bioinformatics and Computational Biology Solutions using R and Bioconductor*. Springer, New York. pp. 397–420.
29. Yin,Q., McBride,J., Fewell,C., Lacey,M., Wang,X., Lin,Z., Cameron,J. and Flemington,E.K. (2008) MicroRNA-155 is an Epstein-Barr virus-induced gene that modulates Epstein-Barr virus-regulated gene expression pathways. *J. Virol.*, **82**, 5295–5306.
30. Jiang,J., Lee,E.J. and Schmittgen,T.D. (2006) Increased expression of microRNA-155 in Epstein-Barr virus transformed lymphoblastoid cell lines. *Genes Chromosomes Cancer*, **45**, 103–106.
31. Linnstaedt,S.D., Gottwein,E., Skalsky,R.L., Luftig,M.A. and Cullen,B.R. (2010) Virally induced cellular microRNA miR-155 plays a key role in B-cell immortalization by Epstein-Barr virus. *J. Virol.*, **84**, 11670–11678.
32. Chen,S., Wang,Z., Dai,X., Pan,J., Ge,J., Han,X., Wu,Z., Zhou,X. and Zhao,T. (2013) Re-expression of microRNA-150 induces EBV-positive Burkitt lymphoma differentiation by modulating c-Myb in vitro. *Cancer Sci.*, **104**, 826–834.
33. Thorley-Lawson,D.A. (2001) Epstein-Barr virus: exploiting the immune system. *Nat. Rev. Immunol.*, **1**, 75–82.
34. Gatto,G., Rossi,A., Rossi,D., Kroening,S., Bonatti,S. and Mallardo,M. (2008) Epstein-Barr virus latent membrane protein 1 trans-activates miR-155 transcription through the NF-kappaB pathway. *Nucleic Acids Res.*, **36**, 6608–6619.
35. Strickson,S., Campbell,D.G., Emmerich,C.H., Knebel,A., Plater,L., Ritorto,M.S., Shpiro,N. and Cohen,P. (2013) The anti-inflammatory drug BAY 11–7082 suppresses the MyD88-dependent signalling network by targeting the ubiquitin system. *Biochem. J.*, **451**, 427–437.
36. Krishnan,N., Bencze,G., Cohen,P. and Tonks,N.K. (2013) The anti-inflammatory compound BAY-11–7082 is a potent inhibitor of protein tyrosine phosphatases. *FEBS J.*, **280**, 2830–2841.
37. Jeon,K.I., Jeong,J.Y. and Jue,D.M. (2000) Thiol-reactive metal compounds inhibit NF-kappa B activation by blocking I kappa B kinase. *J. Immunol.*, **164**, 5981–5989.
38. Rauert-Wunderlich,H., Siegmund,D., Maier,E., Giner,T., Bargou,R.C., Wajant,H. and Stuhmer,T. (2013) The IKK inhibitor Bay 11–7082 induces cell death independent from inhibition of activation of NFkappaB transcription factors. *PLoS ONE*, **8**, e59292.
39. Mott,J.L., Kurita,S., Cazanave,S.C., Bronk,S.F., Werneburg,N.W. and Fernandez-Zapico,M.E. (2010) Transcriptional suppression of mir-29b-1/mir-29a promoter by c-Myc, hedgehog, and NF-kappaB. *J. Cell. Biochem.*, **110**, 1155–1164.
40. Davis,R.E., Brown,K.D., Siebenlist,U. and Staudt,L.M. (2001) Constitutive nuclear factor kappaB activity is required for survival of activated B cell-like diffuse large B cell lymphoma cells. *J. Exp. Med.*, **194**, 1861–1874.
41. Dweep,H., Sticht,C., Pandey,P. and Gretz,N. (2011) miRWalk–database: prediction of possible miRNA binding sites by 'walking' the genes of three genomes. *J. Biomed. Inform.*, **44**, 839–847.
42. Lewis,B.P., Burge,C.B. and Bartel,D.P. (2005) Conserved seed pairing, often flanked by adenosines, indicates that thousands of human genes are microRNA targets. *Cell*, **120**, 15–20.
43. Wang,X. (2008) miRDB: a microRNA target prediction and functional annotation database with a wiki interface. *RNA*, **14**, 1012–1017.
44. Di Lisio,L., Gomez-Lopez,G., Sanchez-Beato,M., Gomez-Abad,C., Rodriguez,M.E., Villuendas,R., Ferreira,B.I., Carro,A., Rico,D., Mollejo,M. *et al.* Mantle cell lymphoma: transcriptional regulation by microRNAs. *Leukemia*, **24**, 1335–1342.
45. Gerdes,J. (1990) Ki-67 and other proliferation markers useful for immunohistological diagnostic and prognostic evaluations in human malignancies. *Semin. Cancer Biol.*, **1**, 199–206.
46. Mosialos,G., Birkenbach,M., Yalamanchili,R., VanArsdale,T., Ware,C. and Kieff,E. (1995) The Epstein-Barr virus transforming protein LMP1 engages signaling proteins for the tumor necrosis factor receptor family. *Cell*, **80**, 389–399.
47. Zhang,B., Wang,Z., Li,T., Tsitsikov,E.N. and Ding,H.F. (2007) NF-kappaB2 mutation targets TRAF1 to induce lymphomagenesis. *Blood*, **110**, 743–751.
48. Ayllon,V. and O'Connor,R. (2007) PBK/TOPK promotes tumour cell proliferation through p38 MAPK activity and regulation of the DNA damage response. *Oncogene*, **26**, 3451–3461.
49. Homig-Holzel,C., Hojer,C., Rastelli,J., Casola,S., Strobl,L.J., Muller,W., Quintanilla-Martinez,L., Gewies,A., Ruland,J., Rajewsky,K. *et al.* (2008) Constitutive CD40 signaling in B cells selectively activates the noncanonical NF-kappaB pathway and promotes lymphomagenesis. *J. Exp. Med.*, **205**, 1317–1329.
50. Luftig,M., Yasui,T., Soni,V., Kang,M.S., Jacobson,N., Cahir-McFarland,E., Seed,B. and Kieff,E. (2004) Epstein-Barr virus latent infection membrane protein 1 TRAF-binding site induces NIK/IKK alpha-dependent noncanonical NF-kappaB activation. *Proc. Natl. Acad. Sci. U.S.A.*, **101**, 141–146.
51. Zhao,J., Liang,Q., Cheung,K.F., Kang,W., Lung,R.W., Tong,J.H., To,K.F., Sung,J.J. and Yu,J. Genome-wide identification of Epstein-Barr virus-driven promoter methylation profiles of human genes in gastric cancer cells. *Cancer*, **119**, 304–312.
52. Compagno,M., Lim,W.K., Grunn,A., Nandula,S.V., Brahmachary,M., Shen,Q., Bertoni,F., Ponzoni,M., Scandurra,M., Califano,A. *et al.* (2009) Mutations of multiple genes cause deregulation of NF-kappaB in diffuse large B-cell lymphoma. *Nature*, **459**, 717–721.
53. Xiao,C., Calado,D.P., Galler,G., Thai,T.H., Patterson,H.C., Wang,J., Rajewsky,N., Bender,T.P. and Rajewsky,K. (2007) MiR-150 controls B cell differentiation by targeting the transcription factor c-Myb. *Cell*, **131**, 146–159.
54. Rao,D.S., O'Connell,R.M., Chaudhuri,A.A., Garcia-Flores,Y., Geiger,T.L. and Baltimore,D. MicroRNA-34a perturbs B lymphocyte development by repressing the forkhead box transcription factor Foxp1. *Immunity*, **33**, 48–59.
55. Vigorito,E., Perks,K.L., Abreu-Goodger,C., Bunting,S., Xiang,Z., Kohlhaas,S., Das,P.P., Miska,E.A., Rodriguez,A., Bradley,A. *et al.* (2007) microRNA-155 regulates the generation of immunoglobulin class-switched plasma cells. *Immunity*, **27**, 847–859.